Regulation of Mitochondrial Autophagy by SUMO Proteases in Human Cells under Hypoxia

Alice Zhao

Department of Biomedical Science

The University of Sheffield

A thesis submitted in partial fulfilment of the requirements for the degree of

Doctor of Philosophy

February 2024

Dedication

This thesis is dedicated to my family and friends – for the boundless love and support that made completing this work possible.

To my parents, thank you for providing me with so many opportunities and for always believing in me.

Acknowledgements

The road to achieving this PhD has been both rewarding and challenging. I am deeply thankful for all the opportunities I have had during my education that have led me up to this point. The pursuit of knowledge is a lifelong endeavor. Although my PhD studies have drawn to a close, I feel as though I am still eternally a student at heart. Nonetheless, I have had the great privilege of being able to study my interests and complete this thesis.

I am tremendously grateful for my supervisor, Dr. Chun Guo. The way he approaches research with such enthusiasm and fervor always inspired me to persevere. I would like to express my deepest gratitude for all the guidance, encouragement, and support he has provided over the course of my PhD studies. I would not be where I am today without his dedication and sage advice. I am also grateful to my advisors, Dr. Steve Brown and Dr. Ivana Barbaric, whose guidance and insight were indispensable.

I would like to thank my family and friends for their support, understanding, and motivation throughout my studies, especially for when I complained too often about food. To my friends Kristie, Cevetta, Hubashia, and Enki: Thank you for all the fun times we shared while I was in the throes of my research and writing. Special thanks to Chris K. for the moral support and advice. This thesis was made possible by the immense dedication and support from my supervisor, family, and friends.

Abstract

Hypoxia is implicated in several conditions including ischemia and age-related diseases like neurodegenerative disorders and cancer. Mitochondrial dysfunction and disturbances in mitophagy accompany hypoxia and can ultimately lead to cell death. HIF-1 is the master transcription factor in regulating transcription of hypoxic response genes, including those involved in autophagy and mitophagy. Hypoxia-induced mitophagy (HIM) clears defective or excess mitochondria when the cell undergoes hypoxic cell stress. The reversible post-translational modification, SUMOylation, regulates the HIF-1 pathway. SUMOylation itself is regulated by deSUMOylation enzymes such as SENP1 and SENP3. While SENP1 and SENP3 regulate aspects of the HIF-1 pathway and hypoxic response, it is unknown whether they regulate HIM. Understanding the mechanisms that regulate HIM is crucial in developing therapeutics for diseases linked to hypoxia. To investigate the regulation of HIM through the activity of SENP1 and SENP3, we performed RNAi-mediated knockdowns of proteins of interest and utilized the dual-fluorescent probe, Mito-pHfluorin, in immunofluorescence microscopy to quantify and compare the levels of HIM in HeLa cells between different experimental conditions. In this thesis, we uncovered molecular mechanisms that provide evidence of a TBC1D17-mediated SENP3-Fis1 axis that regulates HIM. SENP3, but not SENP1, is required for HIM and deSUMOylates the mitochondrial fission protein Fis1. Furthermore, Fis1 is also necessary for HIM. The SUMOylation status of Fis1 regulates HIM levels: deSUMOylated Fis1 induces mitophagy under hypoxia, whereas Fis1 that cannot be deSUMOylated reduces HIM. SUMOylation overall, especially SUMO-2/3-ylation, suppresses HIM. TAK-981, a potent inhibitor of global SUMOylation, significantly increases HIM. The Rab-GAP TBC1D17 suppresses HIM likely through its interaction with Fis1. However, whether the mechanism behind TBC1D17-dependent Fis1-mediated HIM involves SUMO remains unknown. Additionally, this study uncovered the

capability of TAK-981 in upregulating mitophagy and MAM formation, leading to the discovery of a novel form of mitophagy, SUMOylation inhibition-induced mitophagy.

Table of Contents

Abbreviations

E1 – SUMO activating enzyme

E2 – SUMO conjugating enzyme

E3 – SUMO ligation enzyme

Fis1 – mitochondrial fission protein 1

FKBP8 – FK506-binding protein 8

HIF – hypoxia inducible factor

HIM – hypoxia-induced mitophagy

HRE – hypoxic response element

LC3 – microtubule-associated protein 1 light chain 3

LC3-I – non-lipidated LC3

LC3-II – lipidated LC3, phosphatidylethanolamine (PE)-conjugated LC3

MAM – mitochondria-associated membrane

OGD – oxygen glucose deprivation

PHD – proline hydroxylase domain

PTM – post-translational modification

Rab-GAP – Rab GTPase-activating protein

ROS – reactive oxygen species

SENP –SUMO/Sentrin-specific protease

Stx17 – syntaxin 17

SUMO – Small ubiquitin-like modifier

TBC1D15/17 – TBC1 domain family member 15/17

Chapter 1

Introduction

1. Introduction

Altered or defective mitochondrial turnover and function are believed to underpin pathological conditions such as ischemia and age-related diseases such as cancer and neurodegenerative disorders (Anding & Baehrecke, 2017). Mitochondria are major oxygen-consuming organelles in the cell and undoubtedly affected by hypoxia, which results from the imbalance between oxygen supply and consumption in tissues. Regulation of gene expression in response to hypoxia is mediated by the transcription factor hypoxia-inducible factor 1 (HIF-1). Hypoxic conditions induce HIF-1 stabilization through the conjugation of small ubiquitin-like modifier (SUMO), called SUMOylation (Ulrich, 2007). DeSUMOylating enzymes such as Sentrin-specific proteases 1 and 3 (Sentrin, another name for SUMO; SENP1 and SENP3) deconjugate SUMO from SUMOylated proteins and are known to be sensitive to hypoxia and regulate HIF-1 (Hickey et al., 2012; Kunz et al., 2016; Cui et al., 2017; Huang et al., 2009; Wang et al., 2012). HIF-activated transcription affects several different cellular processes under hypoxia including mitochondrial removal through mitophagy, which is the autophagic (lysosomal) degradation of mitochondria (Fu et al., 2020; Madhu et al., 2020), and mitochondrial regeneration by biogenesis mediated by peroxisome proliferator-activated receptor γ (PPARγ) coactivator 1α (PGC-1α) (Cai et al., 2012). However, how hypoxia coordinates HIF response, SUMOylation/deSUMOylation and mitophagy is not yet fully understood. To better understand the roles of hypoxia response in health and disease, with a central hypothesis that deSUMOylation enzymes are important for hypoxia-induced changes in mitochondrial removal, the aim of this PhD project is to investigate the roles of

deSUMOylation enzymes SENP1 and SENP3 in mitochondrial removal through mitophagy under hypoxia.

1.1 Hypoxia and Diseases

Hypoxia is implicated in several diseases. Notable examples of hypoxia in disease are ischemic diseases and age-related diseases like cancer and neurodegenerative disorders (Muz et al., 2015; Burtscher et al., 2021; Khan & Davies, 2008). Ischemia is the restricted or insufficient blood flow to tissues or organs that leads to inadequate oxygenation in the form of hypoxia (decreased oxygen) or anoxia (lack of oxygen) (S. Li et al., 2017).

1.1.1 Angiogenesis

Angiogenesis, the formation of new blood vessels from pre-existing vessels, accompanies tissue growth. In turn, cell proliferation increases oxygen consumption, leading to hypoxia. Hypoxic cells induce angiogenesis to increase blood flow to tissues in a HIF-1-dependent manner (Semenza, 2010). HIF-1 mediates transcription of vascular endothelial growth factor (VEGF) and other angiogenic cytokines and growth factors, along with their cognate receptors on vascular endothelial cells (ECs) (Forsythe et al., 1996; Manalo et al., 2005; Kelly et al., 2003; Semenza, 2010). Impairment of HIF-1-dependent gene expression during hypoxia reduces vascular responses associated with aging. Based on studies done with conditional knockout mice, it is confirmed HIF-1α and HIF-2α are both involved in modulation of EC tumor angiogenesis (Skuli et al., 2009; Tang et al., 2004).

1.1.2 Tumor Hypoxia

Hypoxia is commonly found in malignant tumors, exerting proteomic and genomic alterations in tumor cells and influencing tumor cells in a pro-death or pro-survival manner (Vaupel & Harrison,

2004). Hypoxia-induced processes stunt the cell cycle and promote cell death via apoptosis or necrosis in tumors (Koshiji et al., 2004; Vaupel, 2004). Alternatively, pro-survival mechanisms employed during hypoxia such as angiogenesis allow tumor cells to adapt to or escape their local environment (Goonewardene et al., 2002; Hanahan et al., 1996). Gene expression, post-transcriptional and post-translational changes can all result from hypoxic stress. HIF-1 regulates genes involved in tumor cell adaptation during hypoxic stress to favor survival, including those that play roles in angiogenesis, inhibition of programmed cell death, and cell metabolism (Semenza, 2000; Vaupel, 2004). In tumors, limited oxygen and high glucose consumption shift cell metabolism toward anaerobic glycolysis as the main source of adenosine triphosphate (ATP). HIF-1 upregulates expression of glycolytic enzymes and glucose transporters, assisting tumor cells in meeting energy requirements in hypoxia (Semenza et al., 1994; Vaupel, 2004). As a result of these adaptations, tumor hypoxia is associated with malignant tumor progression and enhanced resistance to cancer therapies (Vaupel, 2004).

1.1.3 Neurodegenerative Disorders

The connection between hypoxia and dementia is not fully understood. Hypoxia has been found to increase β-secretase activity, leading to processing of β-amyloid, the aggregative protein that forms plaques in Alzheimer's disease (Sun et al., 2006). Change in excitability and expression of ion channels may result from prolonged hypoxia and contribute to neurodegeneration. Formation of β-amyloid disrupts calcium homeostasis. In turn, this can worsen the neurotoxicity of β-amyloid (Kawahara & Kuroda, 2000). Hypoxia appears to elicit both detrimental and neuroprotective responses in the brain depending on the dose of exposure (Burtscher et al., 2021). Intermittent hypoxia conditioning (IHC), in which brief, repeated exposure to mild or moderate hypoxia increases an organism's resistance to subsequent hypoxic or ischemic encounters, has been suggested as an emergent strategy in treating diseases in the CNS (Burtscher et al., 2021;

Mayfield et al., 1994; Baillieul et al., 2017; Verges et al., 2015). Moderate IHC therapies have been reported to mitigate psychological stress and depression and improve cognition in older people (Navarrete-Opaza & Mitchell, 2014; Burtscher et al., 2021).

1.2 Hypoxia-Inducible Factors (HIFs)

When mammalian cells encounter hypoxic conditions, they increase the expression of various physiologically important proteins to adapt to the change in oxygen levels in their environment. At the cellular level, hypoxia is detected by intracellular molecular oxygen sensors. Signaling through specific promoter elements initiates downstream adaptations to hypoxia (Lutz & Prentice, 2002). The central pathway that maintains cellular hypoxic response is primarily governed by transcription factors known as HIFs. HIF activity is regulated by oxygen-regulated signals generated by prolyl-hydroxylase domain proteins (PHDs), which act as enzymatic oxygen sensors within the cell (Epstein et al., 2001; Hirsilä et al., 2003; Wilson et al., 2020).

In humans, there are three HIF isoforms (HIF-1~3), which are heterodimeric proteins each consisting of α and β subunits. These HIF subunits have non-redundant functions (Ratcliffe, 2007). Of the HIF-α isoforms, HIF-1α and HIF-2α are the most structurally similar and better characterized than HIF-3α (Majmundar et al., 2010). HIF-1 is a master regulator of cell response to hypoxia, prompting transcription of a myriad of genes including *VEGF* and *Epo*, which are involved in angiogenesis and erythropoiesis respectively, and those involved in glucose metabolism, cell proliferation and survival (Cheng et al., 2007; Semenza et al., 1994; Semenza, 2010; Vaupel, 2004). HIF-1 is comprised of a stable constitutively expressed HIF-1β subunit and the oxygen-regulated HIF-1α subunit (Ulrich, 2007). At physiological oxygen levels, or normoxia, HIF-1α is unstable and undergoes hydroxylation by PHDs, leading to the recognition of HIF-1α by ubiquitin ligase protein von Hippel-Lindau (VHL), and subsequent polyubiquitination and proteasomal degradation of HIF-1α (Ivan et al., 2001; Ulrich, 2007). Hydroxylation of proline

residues on HIF-1α by PHDs increases the affinity for HIF-1α binding to VHL more than 1000-fold (Illingworth et al., 2010; Wilson et al., 2020). Under hypoxia, HIF-1α is stabilized and translocates to the nucleus, where it can dimerize with HIF-1β and bind to hypoxic-response elements (HREs) in the genome, activating transcription of hypoxic response genes (Keith et al., 2011; Ulrich, 2007; **Figure 1.1**).

HIF-2α is similar to HIF-1α structurally, functionally and in its oxygen-dependent degradation, but it is only expressed in certain tissues whereas HIF-1α is ubiquitous (Loboda et al., 2010). HIF-3 is also heterodimeric with an oxygen-regulated α subunit and constitutive β subunit, but HIF-3α differs from HIF-1α and HIF-2α in structure and gene expression regulation (Yang et al., 2015). The *HIF-3α* gene gives rise to multiple HIF-3α splice variants due to different promoters, different transcription initiation sites and alternative splicing (Duan, 2016). Certain HIF-3α variants suppress HIF-1 and HIF-2- mediated gene expression by binding to HIF-1β or by disrupting HIF-1/2α interaction with HREs, but the roles of these variants are still unexplored (Duan, 2016; Yang et al., 2015).

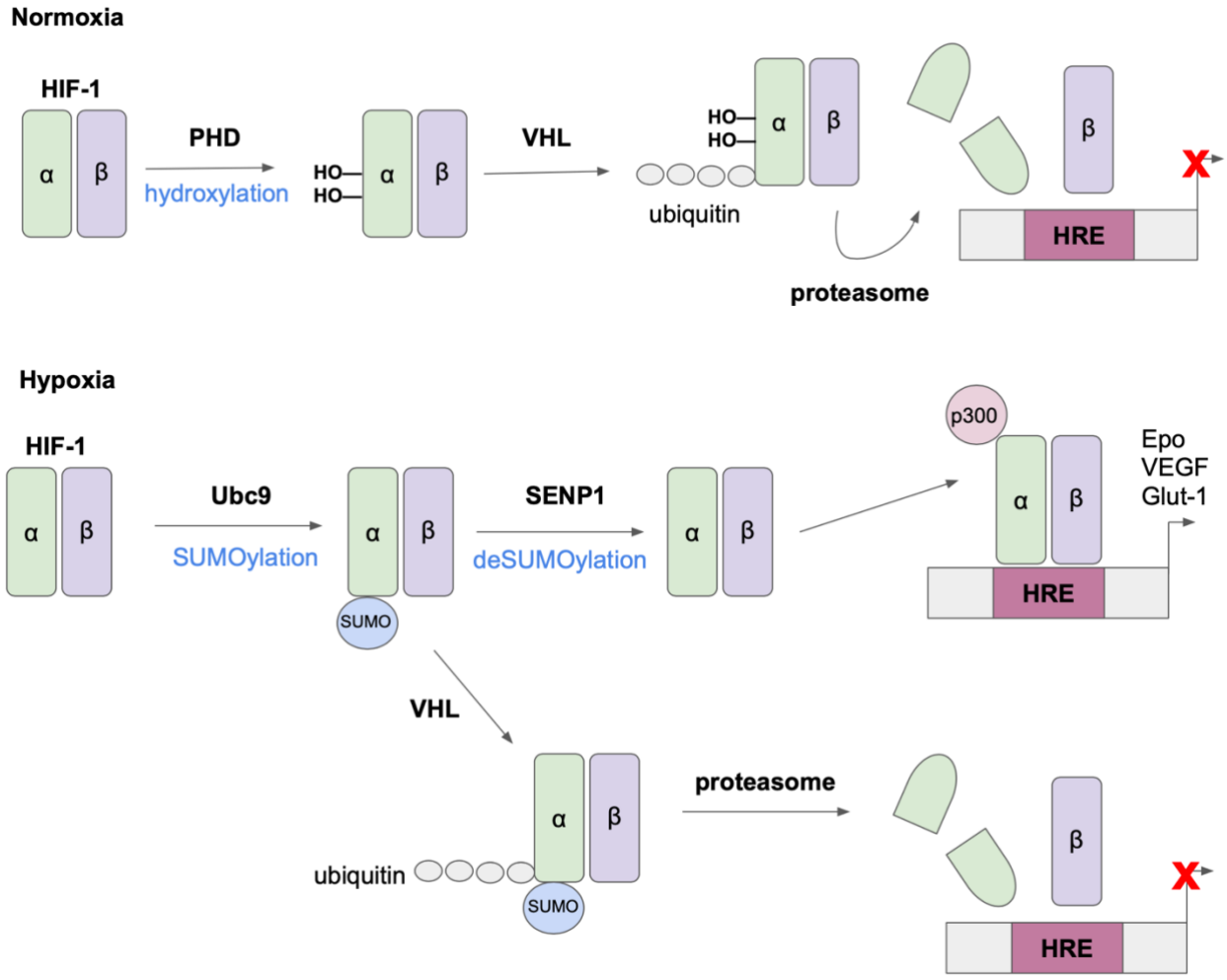

Figure 1.1: Coordination of the HIF-1 Pathway by Post-Translational Modifications of HIF-1α

HIF-1α stability is regulated through post-translational modifications. In normoxia, HIF-1α is unstable and targeted for proteasomal degradation via hydroxylation by prolyl hydroxylases domain proteins (PHDs). Hydroxylated HIF-1α is recognized by the ubiquitin ligase von Hippel-Lindau (VHL) and then polyubiquitinated and degraded. As a result, HIF-1α is unable to translocate to the nucleus and activate transcription of hypoxic response genes. Hypoxia induces SUMOylation of HIF-1α by the SUMO-conjugating E2 enzyme, Ubc9. VHL can recognize and ubiquitinate SUMOylated HIF-1α and target it for degradation as well (Cheng et al., 2007). When sentrin/SUMO-specific protease 1 (SENP1) is present, HIF-1α is deSUMOylated, escapes

degradation, and is able to activate transcription of genes such as those involved in angiogenesis (*VEGF*), erythropoiesis (*Epo*), and glucose metabolism (*Glut-1*). p300 is a coactivator of HIF-1α.

1.3 SUMO

1.3.1 SUMOylation

SUMO proteins are members of the ubiquitin-like protein (Ubl) family. There are five different SUMO protein variants in mammals, SUMO1-5. All variants are around 11 kDa and share an almost identical three-dimensional structure (Colnaghi et al., 2019). SUMO-1 was the first SUMO variant identified by Johnson et al. (1997). SUMO-2 and SUMO-3 were later discovered by homology screening and are often referred to as SUMO-2/3 since they differ by only 3 amino acids (Müller et al., 2001). Both SUMO-2 and SUMO-3 are ~47% identical to SUMO-1. SUMO-4 and SUMO-5 are newly proposed members of the SUMO family (Cappadocia & Lima, 2018; Liang et al., 2016). Precursor SUMO-4 cannot be processed into the mature active form due to the presence of Proline-90 in SUMO-4; Thus, formation of SUMO-4 conjugates is unlikely to occur (Owenbach et al., 2005). SUMO-5 is not expressed in HeLa cells (Liang et al., 2016).

At physiological conditions, most of SUMO-1 is conjugated while SUMO-2/3 is largely unconjugated. SUMO-1 is generally involved in homeostasis while SUMO-2/3 is associated with cell stress response (Guo & Henley, 2014). SUMOylation is a reversible post-translational modification in which SUMO is covalently attached to its target protein. SUMOylation was first observed by Mahajan et al. (1998) on RanGAP, targeting the nuclear pore protein to the nuclear pore complex. As shown in **Figure 1.2**, SUMO is conjugated to proteins in an ATP-dependent manner in three enzymatic steps similar to ubiquitin conjugation: 1) SUMO activation via formation of a thioester bond with E1 activating complex; 2) Transfer of SUMO to a catalytic cysteine on an E2 enzyme Ubc9; and 3) SUMO conjugation from Ubc9 to the substrate protein

catalyzed by a SUMO E3 ligase. Deconjugation of SUMO or deSUMOylation is mediated by SUMO proteases (Pichler et al., 2017).

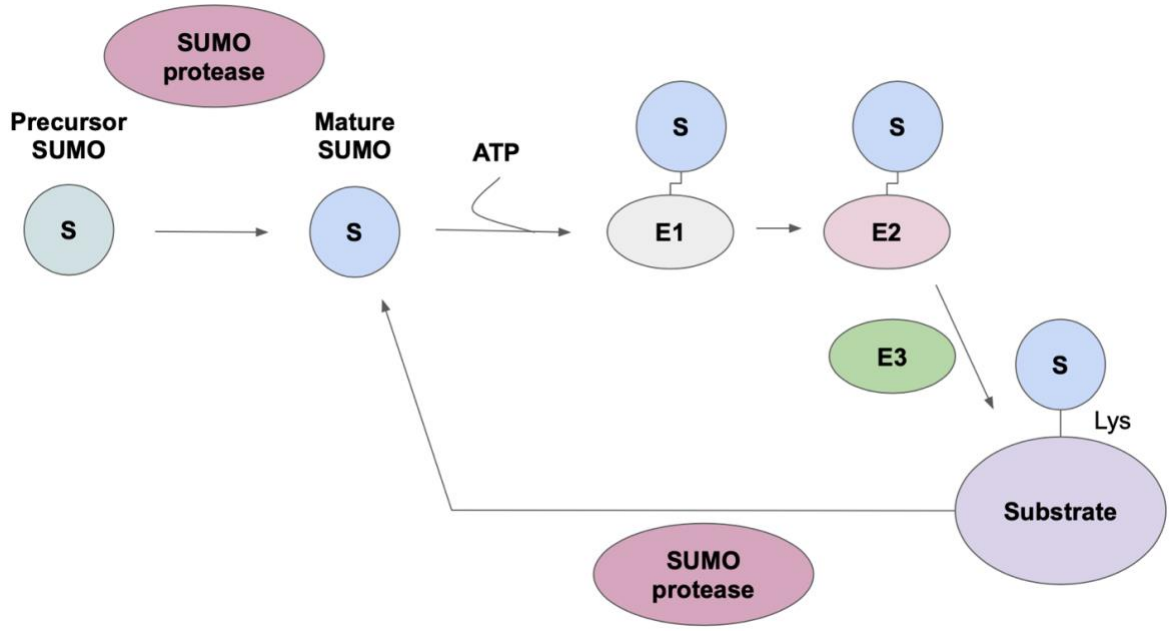

Figure 1.2: SUMOylation and deSUMOylation

SUMO maturation, activation, conjugation and deconjugation. A SUMO-protease will cleave precursor SUMO into its mature form that is ready for conjugation. Mature SUMO is then activated and conjugated to its target protein in an ATP-dependent manner. Conjugation involves three reactions catalyzed by the enzymes E1, E2 and E3 respectively (adapted from Hickey et al., 2012). SUMO deconjugation or deSUMOylation of a SUMOylated substrate protein is performed by a SUMO protease; Abbreviations: SUMO: small ubiquitin-like-modifier; E1: SUMO-activating enzyme E1; E2: SUMO- conjugating enzyme E2 or Ubc9; E3: SUMO ligase E3; Lys: lysine.

1.3.2 HIF and SUMO

HIF stability and activity are known to be controlled by SUMOylation. Under normoxia, HIF-1α is hydroxylated by PHDs and degraded by the proteasome. Hypoxia stabilizes HIF-1α, which can translocate to the nucleus, dimerize with HIF-1β, and activate transcription of target genes (Ulrich,

2007). Hypoxia increases SUMOylation of HIF-1α in the cytosol, but there are conflicting reports on the role of SUMO in HIF-1α stability in hypoxia. Cheng et al. (2007) reported that SUMO overexpression targets HIF-1α for ubiquitination and degradation in the cytoplasm. However, enhanced SUMO conjugation to HIF-1α has been shown to stabilize HIF-1α and rescue it from degradation (Bae et al., 2004; Carbia-Nagashima et al., 2007). DeSUMOylation of HIF-1α by SENPs prevents HIF-1α degradation, allowing its dimerization with HIF-1β in the nucleus after translocation (Ulrich, 2007; **Figure 1.1**).

Many mitochondrial adaptations to hypoxia are mitigated by HIF (Solaini et al., 2010; Zhang et al., 2007). Thus, to investigate the mechanisms underlying the regulation of SUMOylation in HIF-mediated hypoxic responses of mitochondria is a potential angle to explore when developing therapeutics for ischemia and age-related diseases. SUMOylation has been implicated in neurogenerative diseases, including Alzheimer's disease and Parkinson's disease, where autophagy or mitophagy are involved (Princz & Tavernarakis, 2020; Tran & Reddy, 2020; Lizama & Chu, 2021). Alteration of global SUMOylation levels and increase of SUMOylated target proteins such as α-synuclein have been observed in these age-related diseases (Rott et al., 2017; Maruyama et al., 2018). The underlying mechanisms responsible for altered SUMOylation in aging and disease are poorly understood and may be caused by changes in the activity of deSUMOylation enzymes under stress or disease conditions.

1.4 SENPs

1.4.1 deSUMOylation

There are three distinct classes of SUMO proteases: the UBL-specific protease (Ulp) and SENP class, the deSUMOylating isopeptidase (DESI) class, and the ubiquitin-specific protease-like (USPL1) class (Hickey et al., 2012; Schulz et al., 2012; Shin et al., 2012). SENPs are enzymes with two roles: SUMO maturation (C-terminal hydrolase precursor processing activity) and

SUMO deconjugation (isopeptidase activity) (Flotho & Melchior, 2013). There are six SENPs in mammals, SENP1-3 and SENP5-7, which vary in SUMO-specificity and localization (summarized in **Table 1**).

DeSUMOylating enzymes are regulated transcriptionally, post-translationally, and by cell stress. All SENPs except SENP6 exhibit heat-sensitivity, possibly explaining heat shock-induced increases in SUMOylation (Guo & Henley, 2014). SENP1 and HIF-1α engage in transcriptional positive feedback loops (Cui et al., 2017). Proteomic screens identified phosphorylation sites for several SENPs, but the role of phosphorylated SENPs is not yet understood. SENP3 levels are regulated by the ubiquitin-proteasome system (UPS) (Hickey et al., 2012).

1.4.2 HIF and SENPs

1.4.2.1 SENP1

HIF-1α deSUMOylation by SENP1 is necessary for HIF-1α activity and stability (Ulrich, 2007). *SENP1* was identified as a hypoxia responsive gene in humans. Heightened *SENP1* transcriptional response to hypoxia is observed in Andean individuals with chronic mountain sickness (CMS) (Zhou et al., 2013). This adaptation in life-long high altitude residents is protective against hypoxia and CMS (Cole et al., 2014). SENP1 regulates Epo production and consequently erythropoiesis by stabilizing HIF-1α. Knockout of SENP1 results in severe anemia and lethality in mouse embryos (Cheng et al., 2007). Hypoxia-induced hepatocellular cancer stemness is promoted by SENP1 through HIF-1α deSUMOylation, revealing a previously unknown positive feedback loop between SENP1 and HIF-1α that contributes to tumorigenesis (Cui et al., 2017). In cardiomyocytes, SENP1 protects against ischemia/reperfusion injury in a HIF-1α-dependent manner (Gu et al., 2014). Interestingly, SENP1 and SENP3 catalytic activity can be reversibly inhibited by hypoxia. This mechanism is speculated to be controlled by reactive oxygen species (ROS) accumulation (Kunz et al., 2016).

***Table 1*: Mammalian DeSUMOylating Enzymes**

Protein	SUMO-specificity	Role on SUMO	Localization
SENP1	SUMO-1, SUMO-2/3	Maturation, deconjugation	Nuclear pore, nuclear foci
SENP2	SUMO-2/3 > SUMO-1	Maturation, deconjugation	Nuclear pore + foci, cytoplasm
SENP3	SUMO-2/3	Deconjugation	Nucleolus
SENP5	SUMO-2/3	Maturation, deconjugation	Nucleolus, mitochondria
SENP6	SUMO-2/3	Deconjugation	Nucleoplasm
SENP7	SUMO-2/3	Deconjugation	Nucleoplasm
DESI1	SUMO-1, SUMO-2/3	Weak maturation, deconjugation	Cytoplasm, nucleus
DESI2	Unknown	No maturation	Cytoplasm
USPL1	SUMO-2/3> SUMO1	Weak maturation, deconjugation	Cajal bodies

DESI, deSUMOylating isopeptidase; SENP, sentrin/SUMO-specific protease; SUMO, small ubiquitin-like modifier; USPL1, ubiquitin-specific protease like-1 (Adapted from Hickey et al. 2012).

1.4.2.2 SENP3

SENP3 has been identified as a redox sensor (Huang et al., 2009; Wang et al., 2012). SENP3 regulates HIF-1 transcriptional activity under mild oxidative stress by deSUMOylating the HIF-1α coactivator p300. In physiological conditions, SENP3 is continuously degraded by the UPS. Modest ROS inhibits SENP3 degradation and regulates SENP3 localization to the nucleoplasm (Huang et al., 2009). DeSUMOylation of p300 by SENP3 increases p300 binding to HIF-1α and HIF-1α transactivation (Huang et al., 2009; Wang et al., 2012). SENP3 also undergoes degradation during oxygen and glucose deprivation (OGD) involving the activation of a protein RNA (PKR)-like ER kinase, PERK, an essential player in unfolded protein response (UPR) pathways (Guo et al., 2013). SENP3 is ubiquitinated by ubiquitin ligase CHIP (C-terminus of

HSP70-interacting protein) and degraded by the proteasome in normal conditions. In stress conditions, SENP3 escapes degradation by associating with heat-shock protein 90 (Hsp90) and deSUMOylates dynamin-related protein 1 (Drp1), a GTPase that regulates mitochondrial fission and cell death by cytochrome c release (Guo et al., 2013; Guo & Henley, 2014).

1.5 Autophagy

Autophagy is the cellular mechanism that regulates the degradation and recycling of cellular components. As shown in **Figure 1.3**, the first step of autophagy is the formation of the phagophore, a double membrane that engulfs cytoplasmic content including organelles. When edges of the phagophore fuse, a double-membrane vesicle called the autophagosome forms. The autophagosome later fuses with a lysosome into an autolysosome and the contents within are degraded and recycled (Mizushima, 2007).

1.5.1 Autophagy in Quality Control and Survival

Autophagy functions as a quality control program to ensure cell survival and defense against disease. It performs several roles in the cell including the removal of pathogens, degradation of long-lived and aggregative proteins, cell differentiation, adaptation to nutrient depletion, and organelle turnover (Mizushima, 2005). Autophagy recycles bulk elements in the cytoplasm for nutrients and is considered a non-selective process (Bento et al., 2016). Autophagy also selectively targets aggregation-prone proteins and organelles. Organelle clearance recycles organelle components, removing defective structures and toxic byproducts detrimental to cellular health. Maintenance of organelle quality and quantity is essential for homeostasis. Defects in autophagy are attributed to a plethora of human disorders like cancer and neurodegeneration (Anding & Baehrecke, 2017).

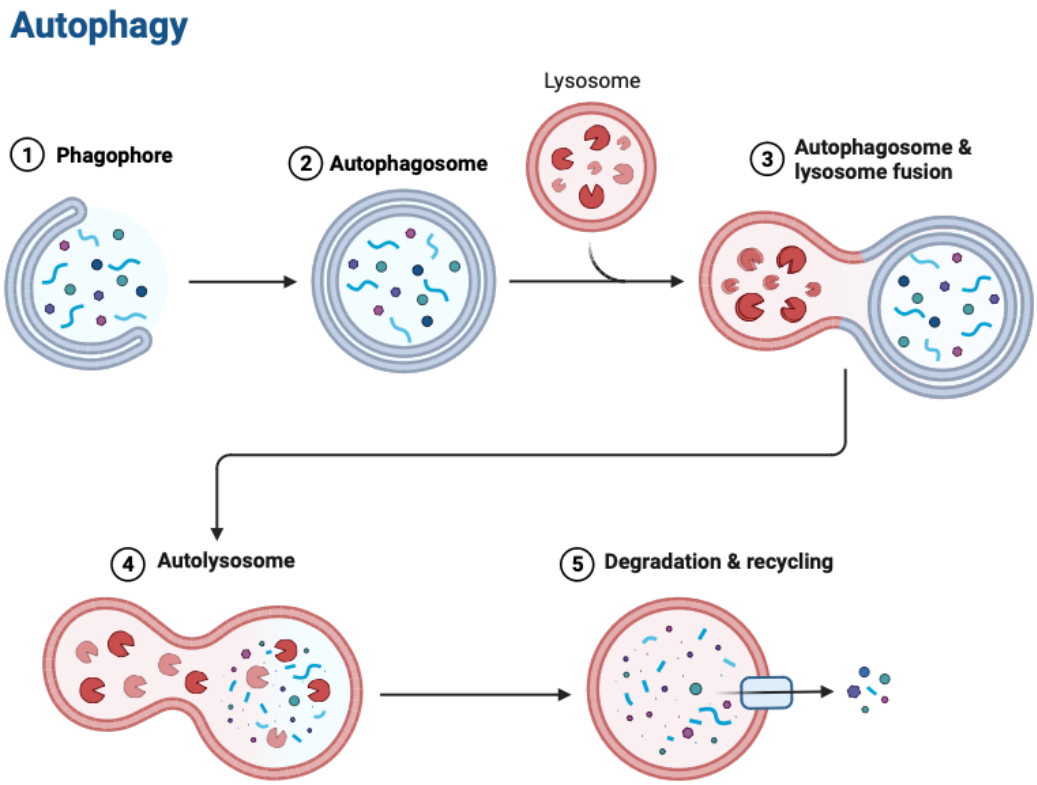

Figure 1.3: Summary of Autophagy

Schematic summarizing the process of autophagy. 1) A double membrane that engulfs cytoplasmic content including organelles called a phagophore forms. 2) Edges of the phagosome fuse, forming a closed double-membraned vesicle called the autophagosome. 3-4) The autophagosome later fuses with a lysosome into an autolysosome. 5) The contents within are degraded by hydrolytic enzymes and then recycled. Created with BioRender.com.

1.5.2 Mitochondrial Autophagy

Mitochondrial autophagy (mitophagy) is the selective degradation of mitochondria via autophagy (Lemasters, 2005). Mitochondria produce most of the cell's ATP. Therefore, damage and dysfunction to the mitochondria heavily impact cell metabolism and ROS production. Hypoxia, chemical uncouplers and ROS trigger mitophagy and programmed developmental changes in the cell. Thus, the cell has a mechanism to selectively clear defective mitochondria in the form of mitophagy (Anding & Baehrecke, 2017). The mechanism in which mitochondria are brought to

the phagophore begins with the accumulation of Pink1, a mitochondrial serine/threonine-protein kinase, on the mitochondrial surface. Pink1 phosphorylates ubiquitin and recruits E3 ubiquitin ligase Parkin (Koyano et al., 2014; Lazarou et al., 2015). Parkin ubiquitinates mitochondrial surface proteins recognized by cargo receptor proteins on the autophagosome like p62/sequestosome-1 (p62/SQSTM1), a multifunctional adaptor protein involved in signal transduction, cell transformation, and proteasomal and autophagic degradation of ubiquitinated proteins (Liu et al., 2016; Moscat et al., 2006). Mitochondria are then brought to autophagosomes for degradation.

The Parkin/Pink1 pathway is not responsible for all mitophagy. Emerging evidence suggests mitophagy can be enacted without Parkin. Hypoxia-induced mitophagy (HIM) as well as iron chelation induced mitophagy are considered Parkin-independent forms of mitophagy (Villa et al., 2018; Allen et al., 2013). One Parkin-independent pathway, outlined in **Section 1.6**, involves the BH3-only protein BNIP3 (Bcl-2/E1B 19 kDa-interacting protein 3) (Villa et al., 2018). Microtubule-associated protein 1 light chain 3 (LC3) is a 17 kDa autophagosome adaptor protein recruited to autophagosome membranes as a lipidated phosphatidylethanolamine (PE) conjugate, LC3-II, rather than the cytosolic and non-lipidated form, LC3-I (Tanida et al., 2008). Mitochondrial surface proteins also mediate phagophore recruitment by recognizing LC3, regardless of Parkin and p62 (Anding & Baehrecke, 2017), though p62 may also mediate autophagic clearance of protein aggregates since it can bind LC3 and ubiquitinated proteins (Bjorkoy et al., 2005; Pankiv et al., 2007).

1.6 The Effect of Hypoxia on Autophagy and Mitophagy Induction

In physiological conditions, mitophagy controls the quality and quantity of mitochondria. Due to hypoxic cell stress, mitophagy removes defective or excess mitochondria (Levine & Klionsky, 2004). Under prolonged hypoxia, mitophagy serves to prevent increased ROS and cell death

(Mazure & Pouysségur, 2010). Madhu et al. (2020) reported hypoxia and HIF-1α trigger mitophagy in nucleus pulposus cells through the translocation of BNIP3, an inducer of mitophagy, to the mitochondria. HIF-1α-BNIP3-mediated mitophagy has protective roles in acute kidney damage, inhibiting both apoptosis and ROS production (Fu et al., 2020). In mitophagy, LC3 binds BNIP3 on the outer mitochondrial membrane (OMM), initiating autophagosome formation. However, disrupting LC3-BNIP3 interactions only reduces but does not eliminate autophagy (Hanna et al., 2012). Severe hypoxia leads to heavy glucose and amino-acid restriction and inhibition of HIF-dependent pathways (Mazure & Pouysségur, 2010). Cells instead rely on HIF-independent mechanisms for autophagy such as the AMPK-mTOR (AMP-protein kinase; mammalian target of rapamycin) and UPR pathways. If the cell fails to adapt to extreme stress, autophagic cell death occurs (Mazure & Pouysségur, 2010).

1.7 Hypoxia and Mitochondria

1.7.1 ROS Production and Signaling

Mitochondria are major consumers of oxygen in the cell. Lowered oxygen levels heavily affect mitochondrial processes: mitochondrial fusion and fission, mitophagy, and oxidative phosphorylation (OXPHOS) (Fuhrmann & Brüne, 2017). The electron transport chain (ETC) and citric acid cycle (tricarboxylic acid cycle; TCA cycle) are both altered in hypoxic cells as metabolic adaptations. Electrons escape the ETC during the transfer to oxygen, producing ROS. Under hypoxia, mitochondria alter their ETC complex composition by exchanging subunits to prevent excess ROS production, mitochondrial damage and cell death (Fuhrmann & Brüne, 2017; Shadel & Horvath, 2015). ROS also contribute to cell signaling. PHDs sense oxygen levels and inhibit HIF under normoxia. Under hypoxic conditions, ROS inactivate PHDs, stabilizing HIF-1α, which then translocates to the nucleus, dimerizes with HIF-1β, and acts on its target genes

(Fuhrmann & Brüne, 2017). However, it is disputed whether ROS are necessary to activate HIF-1 (Solaini et al., 2010).

1.7.2 Mitochondrial Metabolism

HIF induction activates anaerobic glycolysis and inhibits mitochondrial aerobic metabolism, comprised of the TCA cycle and OXPHOS (Solaini et al., 2010). TCA cycle intermediates can coordinate PHD and HIF activity. Succinate accumulation inhibits PHD and promotes HIF stabilization (Pan et al., 2007). OXPHOS is the main source of ATP in cells. Decreasing OXPHOS strongly reduces energy availability. Cytochrome c oxidase (COXIV), the last ETC enzyme, converts oxygen to water via electron transfer. HIF-1 induces a switch in COXIV isoforms, increasing ATP levels in hypoxic COXIV-2 cells (Fukuda et al., 2007; Semenza, 2007).

1.7.3 Mitochondrial Biogenesis

Mitochondria are produced in response to cell division, mitophagy, and bioenergetic requirements (Gerhart-Hines et al., 2007; Palikaras et al., 2015; Shiota et al., 2015). PGC-1α is the master regulator of mitochondrial biogenesis and regulated by SENP1 and SUMOylation, wherein SENP1 promotes PGC-1α transcription by deSUMOylating PGC-1α and the transcription factor myocyte enhancer factor 2C (MEF2C) (Cai et al., 2012; Cai et al., 2015). Hypoxia and HIF generally cause reduced mitochondrial biogenesis and increased mitochondrial mass, though there are differences between the influence of HIF-1 and HIF-2 (Thomas & Ashcroft, 2019; Zhang et al., 2007). Translocase of the outer mitochondrial membrane 20 (Tom20) is an OMM protein in the TOM40 complex involved in mitochondrial protein import as an import receptor. Immunostaining for Tom20 is used to monitor mitochondrial mass and in Parkin-positive cells as a marker for loss of mitochondria from mitophagy (Ding & Yin, 2012; Yoshii et al., 2011). While much is known about the impact of hypoxia on autophagy and mitochondria, it remains

undetermined if deSUMOylation mediated by SENP1 or SENP3 has roles in regulated mitochondrial turnover (*i.e.*, mitochondrial removal by mitophagy and mitochondrial regeneration by biogenesis) under hypoxia.

1.8 Summary

Hypoxia is implicated in several conditions including ischemia and age-related diseases like neurodegenerative disorders and cancer. Since mitochondria are major oxygen-consuming organelles within the cell, altered or defective mitochondrial function is undoubtedly a cornerstone feature of hypoxic response in health and disease. HIF-1 is the master transcription factor for mediating cell stress response to hypoxia. The stability and function of the oxygen labile subunit of HIF-1, HIF-1α, is regulated by the reversible PTM, SUMOylation, which in turn is regulated by deSUMOylation enzymes. Under hypoxic conditions, the HIF-1 pathway upregulates transcription of hypoxic response genes involved in autophagy and mitophagy. HIM is a Parkin-independent form of mitophagy that serves to clear defective or excess mitochondria when the cell undergoes hypoxic cell stress. While the deSUMOylation enzymes SENP1 and SENP3 regulate aspects of the HIF-1 pathway and hypoxic response, it is unknown whether they are involved in the regulation of HIM. Since hypoxia has a profound impact on mitochondrial adaptations in human health and disease, understanding the mechanisms behind the regulation of SUMOylation in HIM is crucial in developing therapeutics for conditions ischemia and age-related diseases where hypoxia is implicated. This thesis explores the regulation of HIM through the activity of the SUMO proteases SENP1 and SENP3. Our preliminary data provides evidence of a TBC1D17-mediated SENP3-Fis1 axis that regulates HIM.

1.9 Aims of Thesis

Mitochondrial dysfunction is a critical feature of hypoxic stress response. In addition to its role in the HIF-1 pathway and regulation of hypoxic response, SUMOylation has an emergent role in neurodegenerative diseases such as Alzheimer's disease and Parkinson's disease wherein autophagy or mitophagy are involved (Princz & Tavernarakis, 2020; Tran & Reddy, 2020; Lizama & Chu, 2021). Changes in global SUMOylation levels have been observed in age-related diseases (Rott et al., 2017; Maruyama et al., 2018). The mechanisms behind altered SUMOylation in age-related diseases are poorly understood but may be linked to the activity of deSUMOylation enzymes under stress or disease conditions. SENP1 and SENP3 are deSUMOylation enzymes involved in mediating adaptations to hypoxic stress. However, it is unknown whether SUMOylation/deSUMOylation, SENP1 and SENP3 regulate HIM. In this thesis, we investigate the mechanisms underlying the roles of SUMOylation and the deSUMOylation enzymes SENP1 and SENP3 in the regulation of HIM.

The first aim of this thesis was to establish a hypoxia experimental system that induces hypoxia stress response in cultured cells using a SCI-tive Hypoxia Workstation to explore the protein profile of hypoxic cell response with Western blotting. Furthermore, we also aimed to optimize the use of the dual-fluorescent probe Mito-pHfluorin in immunofluorescence microscopy in order to visualize and quantify mitophagy in cells exposed to hypoxia. The experimental system and protocols we develop while achieving these aims allow us to further our investigation of the regulation of HIM by deSUMOylation enzymes in subsequent experiments.

The second aim of this thesis was to examine the roles of SUMO proteins, SUMO-1 and SUMO-2/3, and the deSUMOylation enzymes, SENP1 and SENP3, in the regulation of HIM. To do so, we utilized RNAi-mediated knockdown of the proteins of interest in HeLa cells and quantified and compared the levels of mitophagy indicated by the probe Mito-pHfluorin under different experimental conditions with immunofluorescence microscopy. Following our

preliminary data suggesting a crucial role for SENP3 in the induction of mitophagy under hypoxia, our third aim was to explore the role of downstream deSUMOylation targets of SENP3, FKBP8 and Fis1, in SENP3-mediated HIM. We investigated whether the SUMOylation status of these two proteins was important for regulating HIM.

Following the work in the previous aims that demonstrated that SUMOylation and deSUMOylation regulate HIM and that deSUMOylation status of Fis1 is important for this regulation, the final aim of this thesis was to elucidate potential mechanisms underlying Fis1-mediated HIM. Overall, exploration of these aims led to the discovery of a previously unknown SUMOylation-dependent HIM regulatory pathway mediated by TBC1D17.

Chapter 2

Materials and Methods

2.1 Cell culture

2.1.1 Principle

Human cell lines were used in a majority of the experiments in all chapters for this thesis. The HeLa cell line was originally derived from adenocarcinoma cells of the cervix from Henrietta Lacks, an African-American woman who underwent treatment for cervical cancer at John Hopkins hospital in 1951. Unbeknownst to Lacks and her family, cells from Lacks' cervical tumor biopsy were cultured by cell biologist Dr. George Otto Gey, giving rise to the first immortalized human cell line (Scherer et al., 1953; Callaway 2013). In this thesis, we investigate hypoxia-induced mitophagy, which is widely known to be a type of Parkin-independent mitophagy (Liu et al., 2012; Villa et al., 2018; Yoo & Jung 2018; Yuan et al., 2017). We use HeLa cells as a model for Parkin-independent mitophagy as they express little or no endogenous Parkin. This is due to the localization of the *Parkin* gene on FRA6E, a common fragile site in the human genome frequently mutated in ovarian tumors (Denison et al., 2003; Matsuda et al., 2010; Narendra et al., 2008). In addition to wild-type HeLa cells, we also utilized Fis1 knockout (KO) HeLa cells in this thesis, which were generated using CRISPR-Cas9 (Waters et al., 2022). HEK293 cells are immortalized human embryonic kidney cells originating from a cell line transformed with sheared adenovirus 5 (Ad5) DNA (Graham et al., 1977). The incorporation of Ad5 genes into the HEK genome led to the immortalization of the cell line, interfering with cell cycle control and preventing apoptosis (Berk 2005). HEK293 cells are commonly used in biochemical research since they exhibit high levels of recombinant protein production. SH-SY5Y cells are a cloned subline of the SK-N-SH neuroblastoma cell line, which was established in culture from a bone marrow biopsy of a

metastatic neuroblastoma of a 4-year-old female patient (Biedler et al., 1978). The SH-SY5Y line has been widely used as an in vitro model of Parkinson's disease (PD) and other neurodegenerative disorders (Xicoy et al., 2017). We utilized the aforementioned cell lines since they are well-known models for understanding human disease and easily used for transfection.

2.1.2 Procedure

Cell lines were maintained in Dulbecco's Modified Eagle Medium (DMEM) with 10% fetal bovine serum (FBS, Gibco), 1% glutamate and 1% penicillin/streptomycin at 37°C in humidified air supplemented with 5% CO_2 levels. Upon reaching appropriate confluency, cells were washed with 1x phosphate-buffered saline (PBS) and detached with trypsin-EDTA (1% w/v). Pre-warmed DMEM was used to stop the trypsinization. Cells were spun down (300x *g*, 2 min) and resuspended in fresh pre-warmed DMEM. The cell suspension was pipetted into a T75 flask containing fresh pre-warmed DMEM for passaging.

For immunofluorescence imaging, after cells were resuspended in DMEM, 6-12 µL of the cell suspension was diluted into 3 mL DMEM prior to passaging. The diluted cells were pipetted onto the center of 35 mm µ-dishes (ibidi) with ibi-Treated surfaces (400 µL per dish). IbiTreat is a physical surface modification to the dishes that improves cell adhesion to the dish. The surfaces are comparable to standard tissue culture-treated cell culture flasks (ibidi). The cells were incubated in an incubator (37°C, 5% CO_2 levels) for 1 h to allow for cell adhesion. Then, an additional 1.6 mL of DMEM was added to the dishes to a total of 2 mL per dish.

For freezing, after detachment the cells were resuspended in 90% FBS and 10% dimethyl sulfoxide (DMSO). The cell suspension was pipetted into a 1 mL plastic cryotube and frozen slowly overnight at -20°C before storage at -80°C. When thawing the cells, cryotubes were placed in a 37°C water bath for 2-3 min until contents were fully thawed. The cells were pipetted into a flask containing pre-warmed DMEM for subculture.

2.2 Transfection

2.2.1 Principle

Transfection is the introduction of foreign nucleic acids (DNA or RNA) into eukaryotic cells. The main purpose of transfection is to study gene function or protein expression by enhancing or inhibiting specific gene expression in the cell. In this thesis, we used Polyplus jetPRIME® transfection reagent to transfect DNA and siRNA into cells. Interaction of jetPRIME® transfection reagent with nucleic acids results in the formation of positively charged complexes that penetrate into the cell through endocytosis. The siRNA will remain in the cytoplasm while plasmid DNA is transported to the nucleus (Polyplus).

2.2.2 Procedure

Cells were seeded on 6-well plates or 35 mm µ-dishes 24 h prior to transfection. Transfection of DNA and siRNA was performed using Polyplus jetPRIME® transfection reagent according to the manufacturers' guidelines. DNA or siRNA was diluted in 200 µL of jetPRIME® buffer per well inside Eppendorf tubes and vortexed to mix the solution. 4 µL of jetPRIME® transfection reagent was added to the mixture, which was then briefly vortexed and spun down. The transfection solution was left to incubate at room temperature (RT) for 10-15 min and then added dropwise by pipet into the appropriate wells (200 µL/well). The plates or dishes containing cells were incubated at 37°C in humidified air with 5% CO_2 until further experimental use. In the event fluorescent proteins were expressed, the plates or dishes containing cells were covered with aluminum foil to prevent exposure to light. The DNA and siRNA used for transfection and their concentrations are listed in **Appendix 1**.

2.3 Site-directed mutagenesis

2.3.1 Principle

Site-directed mutagenesis is molecular biology technique used to introduce specific, targeted mutations on double-stranded plasmid DNA. Base substitution, insertion or deletion mutations can be created with this method. Site-directed mutagenesis uses polymerase chain reaction (PCR), with primers not fully complementary to template DNA in order to anneal and introduce the mutation after several cycles of amplification. The three steps of PCR are denaturation, primer annealing, and extension. In a PCR machine, the double-stranded DNA template are heated to 95°C to separate the strands. The temperature is reduced to 60°C in order to anneal the primers to complementary base pairs (bp) on the template strand. Then the temperature is raised to 72°C, the optimal temperature for the DNA polymerase to extend the DNA sequence with free dNTPs. This cycle is repeated approximately 15-40 times resulting in the PCR product. Optimal temperatures will vary depending on template length, primers, and guanine-cytosine (GC) content of the primers.

Site-directed mutagenesis was employed to generate plasmids encoding human SENP1 resistant to RNAi-mediated knockdown. RNAi-resistant (RNAi-R) GFP-SENP1 mutants were created to be used in future SENP1 knockdown and rescue experiments due to the possibility of SENP1 siRNA off-target effects and overexpression artifacts when knocking down or overexpressing SENP1 in cells. See **Appendix 2** for confirmation of RNAi-resistance of the GFP-SENP1 constructs.

2.3.2 Procedure

Primers were designed for the SENP1 siRNA target sequence: 5-GGACCAGCUUUCGCUUUCUdTdT-3', which corresponds to 108-126 nt of the cDNA encoding human SENP1 (5'-G GAC CAG CTT TCG CTT TCT-3'), as the original template for

introducing point mutations (Li et al., 2008). Primers with point mutations added to the original sequence were designed using Agilent QuikChange Primer Design. Up to 3 point mutations were introduced using this method while using the previously obtained GFP-SENP1 RNAi-R plasmid as the template for each additional point mutation.

All point mutations are listed below:

Original: 106 GAG GAC CAG CTT TCG CTT TCT 126

(R1) 1 mutation: 106 GAG GAC CA**A** CTT TCG CTT TCT 126

(R2) 2 mutations: 106 GAG GAC CA**A** CT**A** TCG CTT TCT 126

(R3) 3 mutations: 106 GAG GAC CA**A** CT**A** TCG CT**A** TCT 126

A 50 µL PCR reaction was set up in a small PCR tube using KOD Hot Start DNA Polymerase kit (supplied by EMD Millipore) following manufacturer's instructions (Toyobo). All PCR reaction components were kept on ice. The following was added to the PCR tube: 5 µL of 10x PCR buffer, 5 µL dNTPs (10 mM), 3 µL $MgSO_4$, 1 ng/µL of template GFP-SENP1, 1.5 µL forward primer (10 µM), 1.5 µL reverse primer (10 µM), 3 µL Quick solution containing DMSO, and 29.5 µL dH_2O. The primers for GFP-SENP1^{R1} cDNA constructs were: forward 5'-GGTTTTCCAGAGGACCAACTTTCGCTTTCTGACCA-3' and reverse 5'-TGGTCAGAAAGCGAAAGTTGGTCCTCTGGAAAACC-3'. The primers for GFP-SENP1^{R2} cDNA constructs were: forward 5'-GGTTTTCCAGAGGACCAACTATCGCTTTCTGACCA-3' and reverse 5'-TGGTCAGAAAGCGATAGTTGGTCCTCTGGAAAACC-3'. The primers for GFP-SENP1^{R3} cDNA constructs were: forward 5'-CCAGAGGACCAACTATCGCTATCTGACCAGCAG-3' and reverse 5'-CTGCTGGTCAGATAGCGATAGTTGGTCCTCTGG-3'. Lastly, 1 µL KOD polymerase was added before the start of the reaction. The PCR reaction mix was gently vortexed and spun down for 5 s. The PCR reaction was carried out to amplify the GFP-SENP1 RNAi-R plasmids with the following setup:

95°C 2 min

(95°C 20 s

55°C 20s

70°C x min)– repeat 34 cycles

70°C x min

4°C ∞ hold

*Extension time depends on length of fragment being amplified. Rate is 25 s/kb.

After the completion of PCR, the newly synthesized DNA plasmids were transferred into Eppendorf tubes and treated with DpnI to digest the template DNA. Then the plasmids underwent transformation into MAX Efficiency DH5α Competent bacteria cells (Invitrogen), inoculation, and DNA extraction and purification (see 2.4). The plasmids were also sequenced to confirm the identity of GFP-SENP1 (forward sequencing primer for SENP1: 5'-GGA TGA TAT TGC TGA TAG GAT GAG-3'). In subsequent experiments, the GFP-SENP1 RNAi-resistant mutants were transfected into HeLa cells with either non-specific siRNA (NSi) or SENP1-specific siRNA (SENP1i) to confirm whether the generated plasmids conferred resistance to siRNA-mediated knockdown with Western blotting (see **Appendix 2**).

2.4 Bacteria transformation and inoculation

2.4.1 Principle

Bacterial transformation is the process in which bacteria take up foreign genetic material from the environment. Transformation was first reported in *Streptococcus pneumoniae* in 1928 by Frederick Griffith (Griffith, 1928). In 1944, Avery et al. demonstrated that DNA was the transforming agent. Bacteria that are capable of transformation are known as competent cells. When bacteria transfer genetic material between each other in a process called conjugation, they attach to each other through a hair-like appendage known as a pilus. This allows a single strand

of plasmid DNA to enter the donor cell and a complementary strand is synthesized to form a double-stranded circular plasmid in both donor and recipient cells. The ability of bacteria to take up exogenous DNA from the environment and other cells has a variety of applications in molecular biology such as using transformed bacteria as host cells for cloning, creating multiple copies of DNA, and generating cDNA libraries. Here, we use competent bacteria cells to amplify DNA fragments obtained from PCR to make plasmid DNA. The plasmid DNA contains a selectable characteristic such as an antibiotic-resistant gene that can be detected when bacteria with the plasmid are grown on antibiotic-containing agar plates (**Table 2**).

2.4.2 Procedure

As briefly mentioned in 2.3, newly synthesized DNA products obtained from PCR were transferred into an Eppendorf tube and treated with 1 µL DpnI per sample to digest the template DNA. DpnI is an enzyme that cleaves methylated DNA; it degrades template plasmid DNA (which is methylated by bacterial DNA methyltransferases in competent cells during amplification) but not newly synthesized DNA from PCR. During the template digestion process, the DNA was placed on a heat block set to 37°C for 3 h. Each hour, the tube containing DNA product was vortexed and spun down for 1 min to facilitate the digestion process. 1 µL (for amplification) or 6 µL (for cloning or mutagenesis) of the DNA was pipetted into an Eppendorf tube containing 10-30 µL of competent bacterial cells (DN5α from Invitrogen for amplification, Trans5α from Biotech for cloning). The cells were left on ice for 30 min while a hot water bath set to 42°C and pre-warmed Luria-Bertani (LB, **Table 2**) broth were prepared.

The bacteria were placed in the hot water bath for heat shock treatment for 90 s. Afterward they were immediately placed on ice for 2 min. Using aseptic technique, 1 mL of LB broth was added to each tube, which were then placed in a shaker for 1 h (37.5°C, 220 rpm). The cells were spun down at 4000x *g* for 2 min. With aseptic technique, the liquid within the Eppendorf tubes

was decanted and the cells were resuspended in the remaining liquid. The cells were pipetted on to kanamycin or ampicillin agar plates and spread across the surface with a plastic spreader. The plates were placed in a 37°C shaker overnight. The next day, the plates were checked for successful colony growth. Colonies were picked and transferred into tubes with LB broth containing kanamycin (50 µg/µL) or ampicillin (50 µg/µL) with a sterile pipet tip. The tubes were placed in a shaker overnight set to 37°C and 250 rpm.

DNA was extracted using Mini or Midi prep kits according to manufacturer's instructions (Thermo Fisher Scientific). DNA concentration was determined with a Nanodrop 1000 Spectrophotometer (Thermo Fisher Scientific). All DNA was stored in -80°C refrigerators until further use.

Table 2: Materials Required for Transformation and Inoculation of Bacteria Cultures

Materials	**Components**
Luria-Bertani (LB) media	25 g/L in dH_2O (sterile) Addition of 50 µg/µL of ampicillin or kanamycin where needed
LB agar plate with antibiotic	25 g LB + 20 g agar per liter with 50 µg/µL of ampicillin or kanamycin prior to casting plate

2.5 Hypoxia induction

2.5.1 Procedure

Hypoxia treatment of the cells was performed within a SCI-tive Hypoxia Workstation (Baker Ruskinn) set to 1% (v/v) O_2 levels. DMEM was degassed in the hypoxia workstation to remove the oxygen dissolved in the medium at least 24 h prior to placing cells into the hypoxia chamber. As the cells were placed into the workstation, the media in the sample dishes was replaced with 1 mL of degassed DMEM. The cells were left in the hypoxia chamber for appropriate time durations. Control cells were cultured using a conventional incubator in normoxic conditions (on normal ambient O_2 levels: 20.9% (v/v)) for the same period of time. At the end of culture, cells were removed from the hypoxia chamber and used for either Western blotting or immunofluorescence-based imaging analysis.

2.6 Western blotting

2.6.1 Principle

Western blot is a technique used to detect and identify proteins based on their molecular weight as a means to examine protein expression levels and protein-protein interactions. Detection of proteins relies on specific antibody-antigen interactions and provides information about protein levels in the whole cell lysate. Western blotting was first established by Towbin et al. in 1979. The method is performed in the three following steps: separation of proteins by molecular weight with SDS-polyacrylamide gel electrophoresis (SDS-PAGE); transfer of proteins from the polyacrylamide gel to a polyvinylidene difluoride (PVDF) or nitrocellulose membrane; and detection of proteins through antibody-antigen interactions. Detection of proteins in the final step relies on the binding of the primary antibody to the specific target protein and the specificity of the enzyme-conjugated secondary antibody to the species the primary antibody was raised in, such as mouse or rabbit.

In this thesis, we modified our lysis buffer in the preparation of whole cell lysates for the detection of SUMOylation. SENP enzymes require cysteine residues for SUMO deconjugation. The activity of SENPs can be abolished by alkylating agents. Here we use *N*-ethylmaleimide (NEM) as an alkylating agent that interferes with SENP cysteine residues, preventing SUMO deconjugation of SENP substrate proteins. In experiments that require preservation of SUMOylation, 20 mM NEM was added to the lysis buffer along with cOmplete^{TM}, EDTA-free protease inhibitor cocktail (Roche).

2.6.2 Procedure

2.6.2.1 Cell lysate preparation for Western Blot

Prior to Western blotting, cells were seeded, underwent transfection, and were subjected to additional treatment such as hypoxia induction necessary to the experiment. 1× Triton X-100 lysis buffer (TLB) was prepared on ice with three additional reagents in order to detect SUMOylation: the Roche protease inhibitor cocktail (1:50 dilution), together with 0.1% SDS; and 20 mM NEM, were added to the buffer immediately before use (**Table 3**).

After the hypoxic treatment period elapsed, the cells were harvested and transferred into Eppendorf tubes, removed from the hypoxia chamber and spun down at 300x *g* for 2 min. Excess media was removed from the tubes and 250 µL Triton X-100 lysis buffer (TLB) was pipetted into each tube. The cells were allowed 15 min for lysis on ice. Samples were sonicated and spun down at 12,000x *g* for 15 min at 4°C. The lysates were transferred into new Eppendorf tubes and stored at -80°C until further use while the pellets formed from centrifugation were discarded.

Table 3: Recipes of Lysate Sample Preparation Buffers for Western blot

Buffer	Composition
2x TLB (store at 4°C)	40 mM Tris-HCl, pH 7.4, 274 mM NaCl, 4 mM $Na_4P_2O_7$ (sodium pyrophosphate), 4 mM EDTA, 2% Triton X-100 (Thermo Fisher Scientific), 50 mM β-glycerophosphate, 20% glycerol
1x TLB Lysis buffer with protease inhibitor	2x TLB buffer diluted 1:1 in dH_2O, 1:50 complete protease inhibitor cocktail (Roche tablet dissolved 1:1000 in dH_2O), 0.1% SDS, 20 mM *N*-ethylmaleimide (NEM)

2.6.2.2 Western blot

SDS-PAGE gels were prepared in order to separate proteins by molecular weight. Stacking (4% polyacrylamide) and resolving gels (7.5-15% polyacrylamide) were cast with glass plates from a Bio-Rad Mini Protean II electrophoresis system with 1.0 or 1.5 mm thickness depending on the volume of sample needed to be loaded into each well (**Table 4**). A comb was placed between the glass plates to create wells where the protein samples were loaded (10 or 15 wells). Reagents used for preparing and running SDS-PAGE gels are listed in **Table 5**. An electrophoresis chamber was assembled following manufacturer's instructions. Electrophoresis 1x running buffer was poured into the electrophoresis tank.

Cell lysate samples were thawed and prepared into aliquots with 6× Laemmli SDS sample buffer. Reducing agent Bond Breaker™ Tris(2-carboxyethyl)phosphine hydrochloride (TCEP) solution (Thermo Scientific) was added to the samples at 1:10 dilution as a reducing agent. The

samples were spun down for 30 s at 12,000x *g*, vortexed briefly, and denatured at 70°C on a heat block for 10 min. Samples loaded into the stacking gel alongside a Page Ruler Plus Molecular Weight Ladder (ThermoFisher Scientific). Electrophoresis was run at 100 V through the stacking gel and 150 V through the resolving gel. An ice pack was placed in the electrophoresis chamber to avoid over-heating the gels. The electrophoresis reaction was stopped when the proteins reached the bottom of the gel.

Upon completion of the gel electrophoresis, the gel was removed from the glass plates and soaked in transfer buffer (**Table 5**). Immun-Blot® PVDF membranes (Bio-Rad Laboratories, Inc.) were cut to appropriate sizes and incubated in 100% methanol for 10 s before being soaked in transfer buffer along with 4 pieces of Whatman 3MM filter paper per gel. A semi-dry transfer was performed with the Trans-blot Turbo blotting system (Bio-Rad Laboratories). Two pieces of transfer buffer-soaked Whatman filter paper were placed in the transfer chamber, followed by the PVDF membrane. The gel was placed on the stack next with two additional pieces of filter paper on top. Air bubbles between the gel and PVDF membrane were rolled out and the cassette was assembled. Transfer was performed at 15 V for 90 min.

Once the transfer was completed, the PVDF membrane was removed from the cassette and cut to appropriate sizes. The membrane was blocked in 5% (w/v) skimmed non-fat milk or 5% (w/v) bovine serum albumin (BSA) diluted in Tris-buffered saline (TBS) with 0.1% (v/v) Tween-20 (TBS-T) RT for 1 h to block for non-specific binding when the membrane is incubated with the primary antibody (**Table 5**). After this, the membrane was incubated with the primary antibody overnight at 4°C in 2% (w/v) skimmed non-fat milk diluted in TBS-T. The primary antibodies (Abs) used were: SENP1 (Mouse monoclonal Ab; Santa Cruz Biotechnology, 1:500 dilution), SENP2 (Rabbit polyclonal Ab; Novus Biologicals, 1:500 dilution), SENP3 (Rabbit monoclonal Ab; Cell Signaling, 1:10,000 dilution), SENP5 (Rabbit polyclonal Ab; ProteinTech, 1:2,000 dilution), SENP6 (Rabbit polyclonal Ab; Abcam, 1:2,000 dilution), SENP7 (Rabbit polyclonal Ab;

Assay BioTech, 1:1000 dilution), p62 (Rabbit polyclonal Ab; Cell Signaling, 1:1,000 dilution), LC3 (Rabbit polyclonal Ab; Cell Signaling, 1:1,000 dilution), GAPDH (Mouse monoclonal Ab; Santa Cruz Biotechnology, 1:1,000), HIF-1α (Mouse monoclonal Ab; BD Biosciences, 1:1,000 dilution), HIF-2α (Novus Biologicals, 1:2,000 dilution), Tom20 (Mouse monoclonal Ab; Santa Cruz Biotechnology, 1:2,000 dilution), COX-IV (Rabbit monoclonal Ab; Cell Signaling, 1:10,000 dilution), α-tubulin (Rabbit polyclonal Ab; ProteinTech, 1:1,000 dilution), Flag (DDDDK) tag (Mouse monoclonal Ab; ProteinTech, 1:1,000 dilution), Fis1 (Rabbit polyclonal Ab; ProteinTech, 1:1,000 dilution), FKBP8 (Mouse monoclonal Ab; Santa Cruz Biotechnology, 1:1,000 dilution), SUMO-1 (Mouse monoclonal Ab; Santa Cruz Biotechnology, 1:250 dilution), and SUMO-2/3 (Rabbit monoclonal Ab; Cell Signaling, 1:1,000 dilution).

Unbound primary antibody was removed by washing the membrane with TBST three times, 10 min each. Antibody complexes were detected with HRP-conjugated secondary antibodies (Sigma, 1:10,000) or donkey-anti mouse or -rabbit IgG (H+L) highly cross-absorbed secondary antibodies (Alexa-Fluor™ Plus 680 or 800; 1:12,000). The membrane was incubated with an appropriate secondary antibody diluted in 2% (w/v) skimmed non-fat milk diluted in TBST for 1 h for fluorescently-tagged secondary antibodies or 2 h for HRP-conjugated secondary antibodies at RT. Membranes incubated with fluorescently-tagged secondary antibodies were either covered with tin foil or incubated in a blacked-out box to prevent light from bleaching the fluorophore. The membrane was washed thrice in TBS-T for 10 min each to wash off unbound secondary antibody. The membrane was visualized using one of two methods based on the type of secondary antibody used.

When using HRP-conjugated secondary antibodies, the blots were developed by chemiluminescence using Luminata™ Forte Western HRP Substrate (Merck Millipore) or Amersham™ ECL™ Prime or Select Western Blotting Detection Reagent (GE Healthcare Life Sciences) on film (CL- XPosure™ Film, Thermo Scientific) following the manufacturer's

instructions. The ECL solution was prepared by mixing the two solutions provided in a 1:1 ratio. Volumes varied (300-500 µL) depending on the size of the blot. The membrane was incubated protein-side down in the ECL mixture at RT for 5 min. Excess ECL solution was gently removed by touching the membrane edge against a paper towel. The membrane was wrapped in cling film and taped securely inside the cassette. In the dark room, the CL-XPosure X-ray film was placed against the membrane within the cassette. Exposure times varied from 1 s to 20 min depending on the protein of interest. The film was passed through a developer in the dark room. The X-ray films were scanned. Quantification and analysis of protein levels was performed with ImageJ software. The proteins of interest were identified based on approximate molecular weight in reference to pre-stained protein ladders. Blots using fluorescent secondary antibodies were scanned with a Li-COR Odyssey imager. After the final TBST wash after secondary antibody incubation, the membrane was placed protein-side down in the imager and visualized with light corresponding to the wavelength that activates the fluorophore. The fluorescence antibody emits light that is captured on the imager. Quantification of protein levels was performed with Image Studio Lite software.

Table 4: Preparation of SDS-polyacrylamide gels for Western blot

Resolving Gels (1.0 mm-thick)

Reagents	**Volume (7.5 % T)**	**Volume (10% T)**	**Volume (12% T)**	**Volume (15% T)**
1.5 M Tris-HCl, pH 8.8	2.5 ml	2.5 ml	2.5 ml	2.5 ml
30% Bis acrylamide	2.5 ml	3.4 ml	4.0 ml	5.0 ml
Deionized H_2O	4.79 ml	3.89 ml	3.29 ml	2.29 ml
10% (w/v) SDS	100 µl	100 µl	100 µl	100 µl
10% (w/v) APS	100 µl	100 µl	100 µl	100 µl
TEMED	10 µl	10 µl	10 µl	10 µl
Total monomer	10 ml	10 ml	10 ml	10 ml

Stacking Gels (4%)

Reagents	**5ml**	**7.5ml**	**10ml**	**15ml**
1.0 M Tris-HCl, pH 6.8	1.25 ml	1.875 ml	2.5 ml	3.75 ml
30% Bis acrylamide	0.82 ml	0.93 ml	1.24 ml	1.86 ml
Deionized H_2O	2.82 ml	4.53 ml	6.04 ml	9.06 ml
10% (w/v) SDS	50 µl	75 µl	100 µl	150 µl
10% (w/v) APS	50 µl	75 µl	100 µl	150 µl
TEMED	10 µl	15 µl	20 µl	30 µl

Acronyms: SDS – sodium dodecyl sulfate; APS – ammonium persulfate; TEMED - tetramethylethylenediamine

Table 5: Buffers for Western Blot

Solution	Components
6x Laemmli reducing sample buffer	21 mL Tris pH 6.8, 10 mL glycerol, 3 mg bromophenol blue Aliquot to 1.5 mL tubes, freeze at -20°C Prior to heating samples on heat block add Bond Breaker™ TCEP solution 1:10
10x Running buffer	576 g glycine, 120 g Tris Add water to 4 L
1x Running buffer	1 L 10x running buffer, 100 mL of 10% SDS, 8.9 L water
Transfer buffer	400 mL 10x running buffer, 800 mL methanol, add water to 4 L
10x Tris-buffered saline (TBS)	350.7 g NaCl, 72.6 g Tris, add water to 4 L Adjust pH to 7.4
1x TBS-Tween (TBS-T)	100 mL 10x TBS, 1 mL Tween-20, add water up to 1 L
5% skimmed milk in TBS-T	2.5 g skim milk powder, add TBS-T to 50 mL
5% BSA in TBS-T	2.5 g BSA, add TBS-T to 50 mL

2.7 Co-Immunoprecipitation and His-Pulldown

2.7.1 Principle

Immunoprecipitation (IP) is a technique used to probe for a single protein that is the target antigen of an antibody and is widely used in modern cell biology. Co-immunoprecipitation (Co-IP) is the immunoprecipitation of a target protein that is also used to co-precipitate the protein's binding partners or associated protein complexes from the cell lysate. This method allows for the study of protein-protein interactions. Co-IP uses Protein A, Protein G or a mix of Protein A/G, bacterial proteins that strongly bind to antibodies and coat magnetic beads to capture the specific antibody targeting the protein of interest. Incubation of the cell lysate with the antibody-bound beads precipitates the target protein and protein complexes. The co-precipitated proteins are separated from the beads and are detected by immunoblotting.

Pulldown (PD) assays work similarly to IP and Co-IP but are not based on antigen-antibody interactions. Instead, pulldowns use tagged fusion proteins, or bait proteins, to capture binding partners, also called prey proteins, with tag-bound agarose or magnetic beads. Common tags on bait proteins include glutathione S-transferase (GST) and 6x histidine (His6). The basis of His-tag purification is immobilized metal ion affinity chromatography (IMAC), in which protein residues such as histidine have affinity for metal cations including nickel, cobalt, zinc, and iron that are immobilized by chelation to an insoluble matrix (Porath et al., 1975; Porath & Olin, 1983). A His-tag, also known as a polyhistidine tag, consists of a string of six to nine histidine residues on the N or C terminus of a recombinant protein. Recombinant proteins with a His-tag bind to metal ions like Ni^{2+} on a solid chelating resin and are then eluted and separated with SDS-PAGE gel electrophoresis. Interacting partner proteins of the recombinant protein are detected with Western blotting. His-SUMO-2 was used in His-PD assays to investigate SUMOylation of HA-FKBP8.

2.7.2 Procedure

2.7.2.1 Cell lysate preparation for Co-IP

HeLa cells were seeded and prepared ahead of time. After 48 h, insoluble material was removed from the lysate by first aspirating culture media from the cells. Cells were washed with 2 mL 1× PBS, which was then aspirated. 200 µL of ice cold TLB (**Table 3**) was pipetted into each well. Cells were scraped into a 1.5 mL tube and left on ice for 15 min. The tubes were centrifuged at 15,000x *g* at 4°C. The supernatant was transferred to a fresh 1.5 mL Eppendorf microcentrifuge tube and kept on ice.

2.7.2.2 Co-immunoprecipitation

While the cell lysate was in preparation, the antibody was pre-bound to protein G (for mouse monoclonal antibodies) or A-Sepharose beads (for rabbit polyclonal antibodies). 1-2 µg of antibody (HA rabbit polyclonal, ProteinTech; Flag mouse monoclonal, ProteinTech) was incubated in 1.5 mL microcentrifuge tube with 500 µL ice cold TLB. Then 30 µL of a 50% slurry of Protein G/A-Sepharose (Sigma) was pipetted into the tube. The microcentrifuge tubes were placed on a rotating platform for at least 1 h at 4°C for binding an antibody to the Sepharose beads.

The antibody-bound Protein G/A-Sepharose beads were washed three times with 1 mL TLB. Between washes, the Sepharose beads were collected at the bottom of the microcentrifuge tube by centrifugation for 30 s and the buffer was aspirated away. The clarified cell lysate was added to the antibody-bound Protein G/A-Sepharose, with additional TLB to a total of 500 µL. The microcentrifuge tubes were placed on a rotating platform for at least 3 h or overnight at 4°C. Parafilm was wrapped around the tubes to prevent potential leakage. A 40 µL aliquot of clarified lysate was saved for input and 15 µL of 6× Laemmli SDS sample buffer was added to it. This was kept on ice until the SDS-PAGE was ready to run. The Protein G/A-Sepharose beads were washed three times with 1 mL TLB. The beads were resuspended in 30 µL 6× Laemmli SDS sample buffer.

The samples were heated at 100°C for 5 min to denature the proteins and antibody and allow for the beads to be discarded. The IP and lysate samples were separated in SDS-PAGE gels and immunoblots was subsequently performed.

2.7.2.3 His-PD

HEK-293 cells grown on 6-well plates were transfected with His-SUMO-2 following the aforementioned transfection protocol. The media was aspirated and 200 µL of ice-cold PBS was added to each well. The cells were scraped, forming cell suspensions that were subsequently transferred into 1.5 mL Eppendorf tubes. 120 µL or 10% of the sample was saved for the input. After this, the samples were spun down at 200x *g* for 4 min at 4°C and the supernatant was removed. The cells were suspended in lysis buffer containing 6 M guanidinium-HCl (**Table 6**). The cells set aside for the input were suspended in 1x TLB lysis buffer with protease inhibitor (**Table 3**). 5 mM β-mercaptoethanol and 5 mM imidazole were added to the samples prepared for the His-PD assay. The samples were sonicated for 10 s at low power and centrifuged at 3000x *g* for 4 min at 4°C. The supernatant was removed without disrupting the pellet to prevent contamination of the beads in later steps.

1 mL of cell lysis buffer (**Table 6**) and 40 µL of Ni^{2+}-NITA agarose beads (Qiagen) were pipetted into a 1.5 mL microcentrifuge tube. The beads were washed by inverting the tube several times and spun down at 12,000x *g* for 1 min at RT. The beads were washed an additional three times with this method. The level of beads was monitored between experiments to maintain an equal level each time. The lysis buffer containing guanidium-HCl was removed and the cell lysate was added to the beads. The beads were incubated in the lysate overnight on a rotator at 4°C. 2x sample buffer was added to the input lysate and stored at -20°C.

After incubation, non-specific bound proteins were removed from the beads with a series of buffers, with all centrifugation steps performed at 12,000x *g* for 1 min at RT. For the first wash,

the beads were spun down and the supernatant was removed. 1 mL of wash buffer I (**Table 6**) as added to the beads, which were inverted to mix. The beads were spun down and the supernatant was removed again. A meniscus of roughly 20 µL was kept to prevent loss of beads during washing. The second wash was performed with 1 mL of wash buffer II (**Table 6**). The beads were once again spun down and the supernatant was removed. Two wash steps were performed, both using 1 mL of wash buffer III (**Table 6**). The final wash used 1mL PBS. After this series of washes, the beads were ready for elution.

The supernatant was aspirated and 40 µL of elution buffer (**Table 6**) was added to the beads. The beads were placed on a rotator and left to elute for 30 min at RT. After elution was completed, a portion of eluted protein was prepared for SDS-PAGE gel electrophoresis by boiling at 95°C for 3 min and spinning down in a table top centrifuge at 5000x *g* for 2 min. This portion was analyzed by Western blot (**2.6.2.2**) while the 10% lysate samples set aside previously were prepared as stated in **2.6.2.1**.

Table 6: Preparation of buffers for His-Purification

Buffer	Composition
Sodium phosphate buffer	0.2 M Na_2HPO_4 (disodium phosphate) and 0.2 NaH_2PO_4 (monosodium phosphate)
Cell lysis buffer I pH 8.0	6 M guanidium-HCl, 10 mM Tris, 100 mM sodium phosphate buffer pH 8.0
Wash buffer I pH 8.0	6 M guanidium-HCl, 10 mM Tris, 100 mM sodium phosphate buffer pH 8.0, 0.1% (v/v) Triton X-100 (Thermo Fisher Scientific), 5 mM β-mercaptoethanol
Wash buffer II pH 8.0	8 M Urea, 10 mM Tris, 100 mM sodium phosphate buffer pH 8.0, 0.1% (v/v) Triton X-100 (Thermo Fisher Scientific), 5 mM β-mercaptoethanol
Wash buffer III pH 6.3	8 M Urea, 10 mM Tris, 100 mM sodium phosphate buffer pH 6.3, 0.1% (v/v) Triton X-100 (Thermo Fisher Scientific), 5 mM β-mercaptoethanol
Elution buffer	200 mM imidazole, 5% (w/v) SDS, 150 mM Tris-HCl pH 6.7, 30% (v/v) glycerol, 720 mM β-mercaptoethanol, 0.0025% (w/v) bromophenol blue

2.8 Immuno-fluorescence microscopy

2.8.1 Principle

Fluorescence microscopy is an imaging technique used to visualize cells through the excitation of fluorophores and detection of fluorescence signals. When the fluorophore is excited by the light source from the fluorescence microscope, the light the fluorophore emits exhibits a longer wavelength, lower energy and different color due to the energy loss between absorption and emission. The instrument then detects the light emitted by the fluorophore to generate a digital image. Confocal microscopy was extensively used in this thesis to detect subcellular structures, the mitochondria in particular. Confocal microscopy achieves higher optical resolution and produces better quality images than standard light microscopes by utilizing a pinhole to block out of focus light.

Mito-pHfluorin was used extensively for the fluorescence microscopy experiments in this thesis. Mito-pHfluorin is a dual-fluorescent probe that detects mitophagic autophagosomes in cells. This probe is comprised of mCherry–SEP, a pH-sensitive GFP-variant, tagged to the mitochondrial targeting sequence of ActA protein from *Listeria monocytogenes* (sequence: LILAMLAIGVFSLGAFIKIIQLRKNN). In presence of low pH levels, the quenchable dual-fluorescent marker indicates areas where mitophagy occurs with red puncta (Waters et al. 2022).

2.8.2 Procedure

Preparation of 4% paraformaldehyde (PFA) in PBS 1x was performed under a fume hood. For every 100 mL of PBS 1x, 4 g of PFA (Sigma-Aldrich) was measured with a scale and added to a 50 mL falcon tube. The falcon tube was heated to 55°C in a water bath to dissolve the PFA into the solution. The PFA solution was filtered through a syringe filter and then divided in to aliquots in for easy usage. Aliquots were stored at -20°C until use. When needed, frozen aliquots of 4% PFA were thawed in a 37°C water bath and vortexed briefly.

Foil was used to cover all cells transfected with fluorescent proteins or stained with immunofluorescence. After undergoing appropriate treatments, HeLa cells seeded on 35 mm µ-dishes were fixed with pre-warmed 4% PFA for 10 min at RT. The PFA was aspirated from the dishes and the samples were washed thrice with 1x PBS for 3 min with gentle rocking. Cells that did not need to be stained with immunofluorescence were stored in 1x PBS at 4°C until use.

The samples that required immunofluorescence were incubated with 1 mL permeabilization buffer (**Table 7**) for 10 min. The cells were once again washed thrice with 1x PBS for 3 min. Cells were then incubated with blocking buffer for 1 h. Primary antibodies were diluted in blocking buffer (**Table 7**) at appropriate concentrations. . The primary antibodies used were: SENP1 (Recombinant monoclonal Ab; Abcam EPR3844, 1:200 dilution), SENP3 (rabbit monoclonal Ab; Cell Signaling #5591, 1:500 dilution), FKBP8 (mouse monoclonal Ab; Santa Cruz Biotechnology sc-166607, 1:200 dilution), HA-tag (rabbit polyclonal Ab; ProteinTech, 1:500 dilution), Flag-tag (mouse monoclonal Ab; ProteinTech, 1:500 dilution), Fis1 (rabbit polyclonal Ab; ProteinTech, 1:100 dilution), SUMO-1 (rabbit polyclonal Ab; Cell Signaling #4930, 1:250 dilution), SUMO-2/3 (rabbit monoclonal Ab; Cell Signaling #4971, 1:100 dilution), TBC1D15 (rabbit polyclonal Ab; ProteinTech, 1:100 dilution), TBC1D17 (rabbit polyclonal Ab; ProteinTech, 1:100 dilution), and Stx17 (ProteinTech 17815, 1:50). The cells were incubated with appropriate primary antibodies for 1 h and washed in 1× PBS three times with gentle rocking. Secondary antibodies for immunofluorescent staining were also diluted in blocking buffer at appropriate concentrations. The cells were incubated with appropriate secondary antibodies for 1 h. The secondary antibodies used were: Alexa Fluor 405 (A31553) and Alexa Fluor 680 (A32802) fluorescent secondary antibodies (ThermoFisher Scientific, 1:2,000). After incubation with the secondary antibody, the samples were washed thrice with 1× PBS. Fresh 1× PBS was added to the sample dishes. Samples were then kept at 4°C covered by foil until microscopy. All immunofluorescence microscopy was performed with a Zeiss LSM 880 Airyscan confocal

microscope within the Wolfson Light Microscope Facility at the University of Sheffield. Ibidi 35 mm imaging µ-dishes possess polymer coverslip bottoms. Cells fixed in ibidi µ-dishes were imaged directly with the confocal microscope after immersion oil was applied to the appropriate lens.

The mitochondria-associated membrane (MAM) is a subdomain of the endoplasmic reticulum (ER) that tethers to the mitochondrial outer membrane. In some experiments described in this thesis, the novel reporter MAMtracker Green created by Sakai et al. (2021) was employed to investigate potential links among MAM formation, SUMOylation/deSUMOylation and mitophagy induction. This reporter was transfected into HeLa cells and then subjected to different experimental conditions where MAM formation in living cells was monitored using confocal fluorescent microscopy (Zeiss LSM 880 Airyscan).

Hoechst dye and MitoTracker^{TM} Red CMXRos dye (ThermoFisher Scientific) were used to stain the nucleus and mitochondria respectively for live cell imaging experiments. Prior to live imaging, Hoechst (1: 10,000) and MitoTracker^{TM} Red (stock concentration 1 mM; working concentration 50 nM) were diluted in pre-warmed DMEM. Approximately 48 h post-transfection, the cell culture media in the samples was replaced with media containing the dyes. The cells were incubated with the dyes for 15 min at 37°C while covered in tin foil. Afterward, the media was replaced with fresh DMEM with or without further treatments and the cells were ready for live imaging.

TAK-981 is a SUMOylation inhibitor that targets SUMO-activating enzyme (SAE) used in cancer treatments (Langston et al., 2021). We used TAK-981 treatment in fluorescent microscopy experiments with both live and fixed cells to study the effect of global SUMOylation inhibition on MAM formation and mitophagy, respectively. For TAK-981 treatment, 10 mM stock TAK-981 solution was diluted to 100 nM in pre-warmed DMEM. DMSO at the same concentration was used as a control for TAK-981 treatment. For immunofluorescence imaging

with hypoxia-treated cells, right before placement of cells into the hypoxia chamber, the culture media was replaced with TAK-981-containing DMEM. Hypoxia treatment, fixation and immunostaining of cells after hypoxia treatment were carried out as previously described. In cases live cell imaging was needed and the cells could not be fixed, the culture media was replaced by TAK-981-containing media. The cells were placed in a 37°C incubator and imaged at the desired time intervals.

Table 7: Buffers for Immunofluorescence

Buffer	**Composition**
Permeabilization buffer	1x PBS, 0.3% Triton X-100 (Thermo Fisher Scientific)
Blocking buffer	1x PBS, 0.01% Triton X-100 (Thermo Fisher Scientific), 0.4% fish skin gelatin

2.8.3 Quantification of Mitophagy tagged by Mito-pHfluorin

A Macro program on ImageJ/Fiji automating the quantification of mitophagy as indicated by Mito-pHfluorin (**Appendix 3**) was written with the assistance of Dr. Darren Robinson from the University of Sheffield. Quantification of the red puncta is outlined in **Figure 2.1**. The average puncta per cell for each experimental condition is presented on histograms created with GraphPad Prism 10 software.

2.8.4 Quantification of Relative Fluorescence Intensity of MAMtracker Green

Fluorescence intensity (FI) of MAMtracker Green in cells was measured using Fiji/Image J program. Background intensity (BI) obtained by measuring the fluorescence intensity of a blank, non-fluorescent area that is the same size as the respective cell. Relative fluorescence intensity (RFI) of MAMtracker Green was calculated by subtracting the background intensity of an individual cell from fluorescence intensity and dividing this difference by the average RFI of the

control condition (*i.e.* in this case, the RFI of control refers to that of a DMSO-treated cell or cell transfected with Nsi). The formula for this calculation is as follows:

RFI = (FI – BI)/(average RFI of control condition)

2.8.5 Statistics

Data analysis was performed on GraphPad Prism 10 software. Histograms were generated with GraphPad Prism 10. Data was analyzed with appropriate statistical analysis methods.

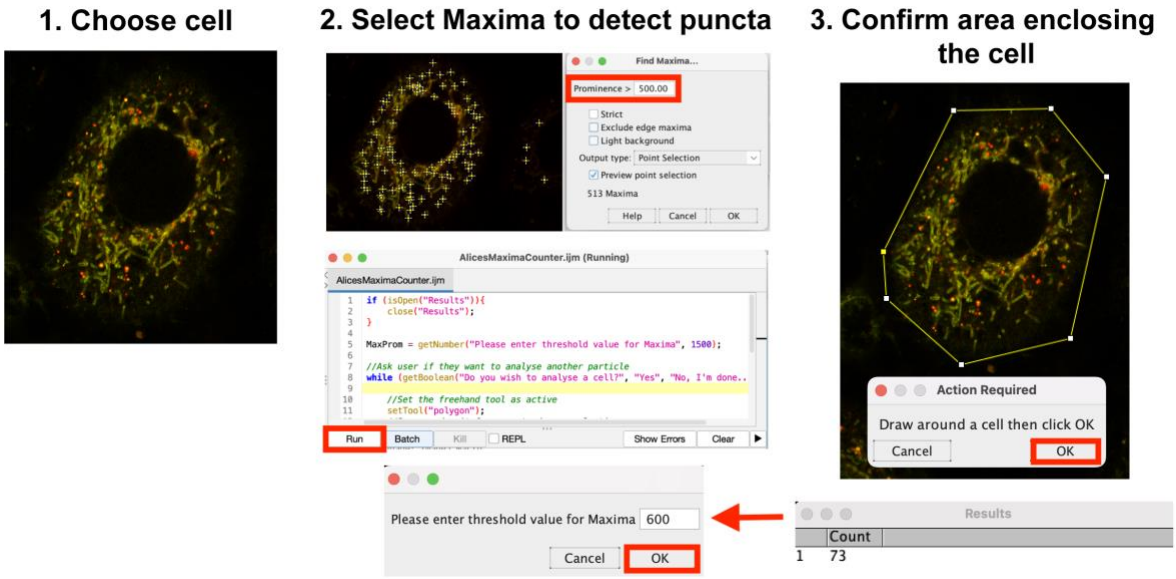

Figure 2.1: Overview of Mitophagy Quantification indicated by Mito-pHfluorin in Fiji

Step 1: Open microscopy image and choose appropriate cell.

Step 2: In Fiji, select the red channel of the image. Open Process > Find Maxima. Toggle the Maxima up to the value 1500 and preview the red puncta with "Preview point selection" until the majority of puncta appear selected in the preview. Close the "Find Maxima" menu and run the counting program, entering the Maxima value chosen.

Step 3: Using the polygon selection tool, draw around the area enclosing the cell to count the red puncta.

Chapter 3

Establishment of Experimental Systems for Characterization of Hypoxia-Induced Mitophagy (HIM)

3.1 Background

HIF-activated transcription affects a number of processes under hypoxia including mitochondrial removal through mitophagy, the autophagic degradation of mitochondria (Madhu et al., 2020; Fu et al., 2020), and mitochondrial regeneration by biogenesis mediated by peroxisome proliferator-activated receptor γ (PPARγ) coactivator 1α (PGC-1α) (Cai et al., 2012). However, how hypoxia coordinates HIF response, SUMOylation/deSUMOylation and mitochondrial turnover is not yet fully understood. In this chapter, we endeavor to establish a hypoxia experimental system wherein hypoxia stress response can be induced in cultured cells by using a SCI-tive Hypoxia Workstation (Baker Ruskinn) to expose HeLa cells to 1% (v/v) O_2 levels for set period of time. We then assess the effectiveness of the hypoxia treatment by comparing the level of HIF-1α expression between cells kept in hypoxic and normoxic conditions, with HIF-1α induction as an sign hypoxic stress response in cells. This acts as the first step in investigating the relationship between hypoxia-induced mitophagy and SUMOylation in this thesis.

From there, the rest of this chapter covers our investigation of the protein expression profile of hypoxia within our experimental system. In these experiments, we primarily use HeLa (model) cells because they express little or no Parkin and hypoxia-induced mitophagy is considered to be a form of Parkin-independent mitophagy. We also sparingly use SH-SY5Y and HEK293 cell lines as additional points of comparison for the differences in expression for certain

proteins. The levels of the autophagy marker LC3-II, autophagy-related proteins p62 and Tom20, SUMO-1 and SUMO-2/3, and the SENP family enzymes under hypoxia will be assessed in HeLa cells with Western blot.

3.1.1 Autophagy

LC3 is an autophagosome adaptor protein recruited to the autophagosome membrane as LC3-II, a lipidated form of LC3 that is conjugated to phosphatidylethanolamine (PE) (Tanida et al., 2008). LC3-II is generated from the conjugation of cytosolic unlipidated LC3-I to PE (Runwal et al., 2019). LC3-II is a marker for autophagy induced by various stress stimuli including starvation and hypoxia (Mizushima & Yoshimori 2007; Tanida et al., 2004). While LC3-II is not required in the initiation of autophagy, it mediates phagophore expansion and autophagosome formation. Degradation of LC3-II in the lumen of autophagosomes results in increased LC3-II turnover in hypoxia-induced autophagy (Rouschop et al., 2010). LC3-II induction serves to replenish turned over LC3-II under hypoxia-induced autophagy and indicates increased activation of autophagic processes from oxygen deprivation (Bellot et al., 2009; Roushop et al., 2010; Tanida et al., 2004). As a result, detection of LC3-II by immunoblotting can be used to monitor autophagy and autophagy-related processes (Tanida et al., 2008). LC3-II has migrates faster than LC3-I on SDS-PAGE due to its extreme hydrophobicity and thus appears below LC3-I in Western blot analysis (Mizushima & Yoshimori, 2007).

p62/sequestosome-1 (p62/SQSTM1) is a multifunctional adaptor protein involved in signal transduction, cell transformation, and proteasomal and autophagic degradation of ubiquitinated proteins (Liu et al., 2016; Moscat et al., 2006). Hypoxia and HIFs generally cause reduced mitochondrial biogenesis and increased mitochondrial mass, though there are differences between the effects of HIF-1 and HIF-2 (Thomas & Ashcroft 2019; Zhang et al., 2007). Translocase of the outer mitochondrial membrane 20 (Tom20) is an outer mitochondrial

membrane protein in the TOM40 complex involved in mitochondrial protein import as an import receptor. Immunostaining of Tom20 has been used to monitor mitochondrial mass in Parkin-positive cells as a marker for loss of mitochondria from mitophagy (Ding & Yin 2012; Yoshii et al., 2011).

3.1.2 SUMO and SENPs

HIF-1α stability and activity is known to be regulated by SUMOylation and its reverse process, deSUMOylation. Hypoxia has been reported to increase SUMOylation of HIF-1α in the cytosol; under hypoxia, deSUMOylation of HIF-1α by SENP1 in the nucleus stabilizes HIF-1α, rescuing HIF-1α from degradation via the proteasome (Cheng et al., 2007). In physiological conditions, most of SUMO-1 is conjugated while SUMO-2/3 is largely unconjugated (Saitoh & Hinchey, 2000). We examined levels of SUMO-1 and SUMO-2/3 under hypoxia in this chapter because SUMO-1-ylation and SUMO-2/3-ylation are reported to be altered in HeLa cells exposed to hypoxia (Kunz et al., 2016) and SUMO-1 and SUMO-2/3 are ubiquitously expressed as post-translational modifiers through SUMOylation (Hickey et al., 2012) and they are the most well-studied conjugatable SUMO proteins. However, whether SUMOylation participates in the regulation of hypoxia-mediated mitophagy remains unclear.

SUMO/Sentrin-specific proteases (SENPs) are a family of deSUMOylation enzymes that remove SUMO from target proteins. There are seven members of the mammalian SENP family: SENP1, SENP2, SENP3, SENP5, SENP6, SENP7 and SENP8. SENP8, specifically targets against ubiquitin-like protein Nedd8 and does not reverse SUMOylation (Mendoza et al., 2003; Mukhopadhyay & Dasso, 2007; Kunz et al., 2018). SENP1 has broad specificity for deSUMOylating SUMO-1 and SUMO-2/3 and the other SENP family members preferentially act on SUMO-2/3 (Hickey et al., 2012). SENP1 is encoded by the hypoxia response gene *SENP1* and participates in a positive feedback loop with HIF-1α under hypoxia, which has been shown to

promote cancer stemness in hepatocellular carcinoma cancer cells (Cui et al., 2017). While it is known SENP1 participates in the HIF-1 pathway, whether SENP1 contributes to HIF-1-dependent hypoxia-induced mitochondrial autophagy remains unknown. SUMO-2/3-ylation of the GTPase Drp1 is reported to play a cytoprotective role in the brain OGD model. SENP3 cleaves SUMO-2/3 from Drp1, promoting apoptosis (Guo et al., 2013). SENP3 is necessary for regulating Fis1-mediated DFP-induced mitophagy, a Parkin-independent form of mitophagy (Waters et al., 2022). Similarly, hypoxia-induced mitophagy is a Parkin-independent form of mitophagy. Though, it is unknown whether SENP3 or other SENP family members regulate hypoxia-induced mitophagy in a similar manner to SENP3-regulated DFP-induced mitophagy. SENP2 has been reported to have a protective effect on neuronal death, as disruption of SENP2 has been shown to induce neurodegeneration through dysregulated mitochondrial dynamics in mice (Fu et al., 2014). The effects of hypoxia on the levels and activity of other SENP family members in relation to the mitochondria and mitophagy has not been characterized.

In this chapter, the objective was to establish a hypoxia experimental system and confirm the robustness of its hypoxia induction by examining the protein expression profile of cells exposed to hypoxia. This will include the expression of hypoxic response transcription factors HIF-1α and HIF-2α; the autophagy marker LC3-II; autophagy-related proteins, p62 and Tom20; global SUMO-1 and SUMO-2/3 levels; and SENP family members SENP1 and SENP3. From there, a hypoxia time course was performed on HeLa cells transfected with Mito-pHfluorin to investigate the effect of hypoxia on mitophagy levels with fluorescence microscopy.

3.2 Results

3.2.1 Establishing the Hypoxic Experimental System

HIF-1 is known as the master transcription factor responsible for cell stress response to hypoxia and HIF-1α is the oxygen labile subunit of HIF-1. In order to study the effect of hypoxic exposure on cells, establishing a hypoxic experimental system that can induce HIF-1α expression is integral. In this thesis, we used the SCI-tive Hypoxia Workstation (Baker Ruskinn) to carry out experimental procedures in which hypoxia was necessary. To determine whether the hypoxia workstation could induce HIF-1α expression, a hypoxia time course was conducted on HeLa cells placed inside the inner chamber of the workstation. The HeLa cells were exposed to 1% O_2 for different durations of time (2, 4, 6, 8, 12 or 24 h). Control cells were exposed to atmospheric levels of oxygen. Subsequently, the cells were harvested for cell lysate preparation and HIF-1α induction was assessed by Western blot analysis. Induction of a HIF-1α antibody reactive band at 120 kDa was observed in cells exposed to hypoxia for 2 to 24 h (**Figure 3.1a**). While solid bands for HIF-1α were present in cells exposed to normoxia, the HIF-1α bands from hypoxic cells were larger and more prominent, denoting an increase of HIF-1α expression under hypoxia. This was quantified against the loading control α-tubulin, the levels of which were unchanged throughout treatment conditions (**Figure 3.1b**). The increase of HIF-1α expression under hypoxia confirms use of the hypoxia workstation can induce HIF-1α induction and hypoxic cell response. The calculated molecular weight of HIF-1α is 93 kDa, while the observed molecular weight is 120 kDa. The discrepancy between calculated and observed molecular weights of HIF-1α is likely attributed to protein modification, as the HIF-1α sequence contains multiple sites for phosphorylation (Wang et al., 1995). HIF-1 DNA-binding activity has been shown to require phosphorylation (Wang & Semenza, 1993).

In addition to HIF-1α induction, the induction of HIF-2α under hypoxia up to 24 h was also assessed through Western blotting (**Figure 3.2a**). HIF-2α levels under normoxia increased

over time, while under hypoxia HIF-2α levels did not change. At 24 h, there was a significant difference in HIF-2α levels between normoxia and hypoxia conditions (**Figure 3.2b**). Similar to HIF-1α, HIF-2α possesses an observed molecular weight of approximately 120 kDa. The poor quality of the Western blots (**Figure 3.2**) made it difficult to determine the expression pattern of HIF-2α under hypoxic conditions. Thus, we were unable to reach any conclusion regarding HIF-2α induction in our experimental system.

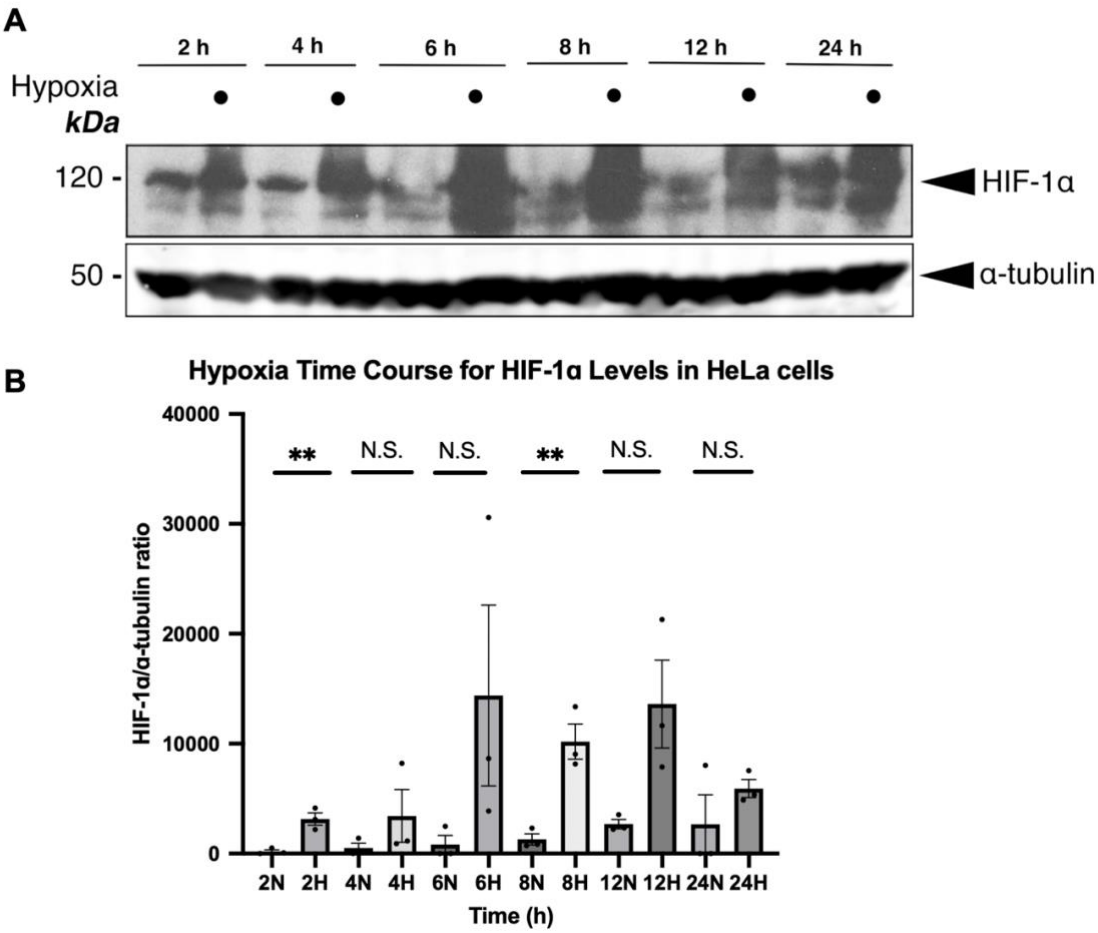

Figure 3.1: HIF-1α Induction under Hypoxia in HeLa cells

A) HeLa cells were exposed to normoxia or hypoxia (1% O_2) for 2 to 24 h. Whole cell lysate samples were prepared and blotted for HIF-1α as indicated. B) Histogram shows relative HIF-1α levels in HeLa cells exposed to normoxia (N) or hypoxia (H) for 2 to 24 h. (n = 3; N.S., non-significant; **$p < 0.01$; Student's unpaired t-test).

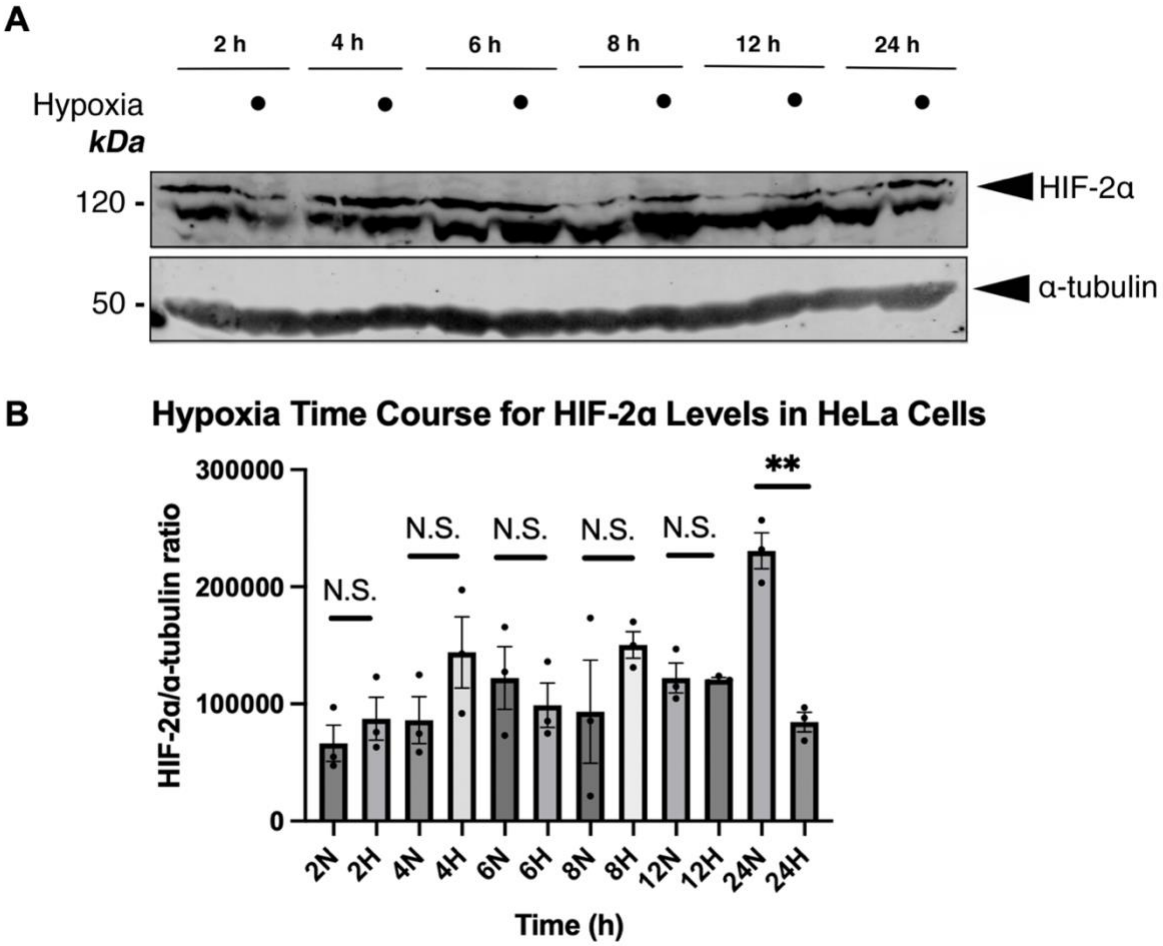

Figure 3.2: HIF-2α Induction under Hypoxia in HeLa cells

A) HeLa cells were exposed to normoxia or hypoxia (1% O_2) for 2 to 24 h. Whole cell lysate samples were prepared and blotted for HIF-2α as indicated. B) Histogram shows relative HIF-2α levels in HeLa cells exposed to normoxia (N) or hypoxia (H) for 2 to 24 h. (n = 3; N.S., non-significant; **$p < 0.01$; Student's unpaired t-test).

3.2.2 Induction of Autophagy by Hypoxia

In order to determine whether the hypoxic experimental system established in **Section 3.2.1** can induce general autophagy with hypoxic conditions, we assessed the level of LC3-II induction in HeLa and SH-SY5Y cells exposed to hypoxia. HeLa cells were exposed to hypoxia for 2 to 24 h (**Figure 3.3a**) in a hypoxia time course and Western blotting was performed to detect LC3-II. In the hypoxia time course, the general trend was that LC3-II levels under hypoxia increased after 2 to 12 h of exposure and decreased at 24 h (**Figure 3.3b**). Because of the change in relative LC3-II levels between 12 and 24 h of hypoxia exposure observed in the hypoxia time course, additional Western blotting for LC3-II was performed on HeLa cells exposed to hypoxia for 12 and 24 h (**Figure 3.3c**). When HeLa cells were exposed to hypoxia for 12 h, LC3-II levels significantly increased compared to the normoxia control (**Figure 3.3d**). There was no significant difference in LC3-II levels in HeLa cells exposed to hypoxia at 24 h compared to the normoxia control (**Figure 3.3d**). In SH-SY5Y cells, LC3-II levels significantly increased under hypoxia compared to normoxia at both 12 and 24 h of exposure (**Figure 3.4**). The increase of LC3-II levels under hypoxia in HeLa cells and SH-SY5Y cells suggests that hypoxia exposure can lead to autophagy induction.

3.2.3 The Effect of Hypoxia on the Expression of Autophagy-Related Proteins

After determining the hypoxia experimental system was capable of inducing general autophagy in cells, we examined the levels of the following proteins related to autophagy and mitophagy under hypoxia: p62 and Tom20. Both p62 levels and Tom20 levels significantly decreased in cells exposed to hypoxia for 24 h (**Figure 3.5, Figure 3.6**).

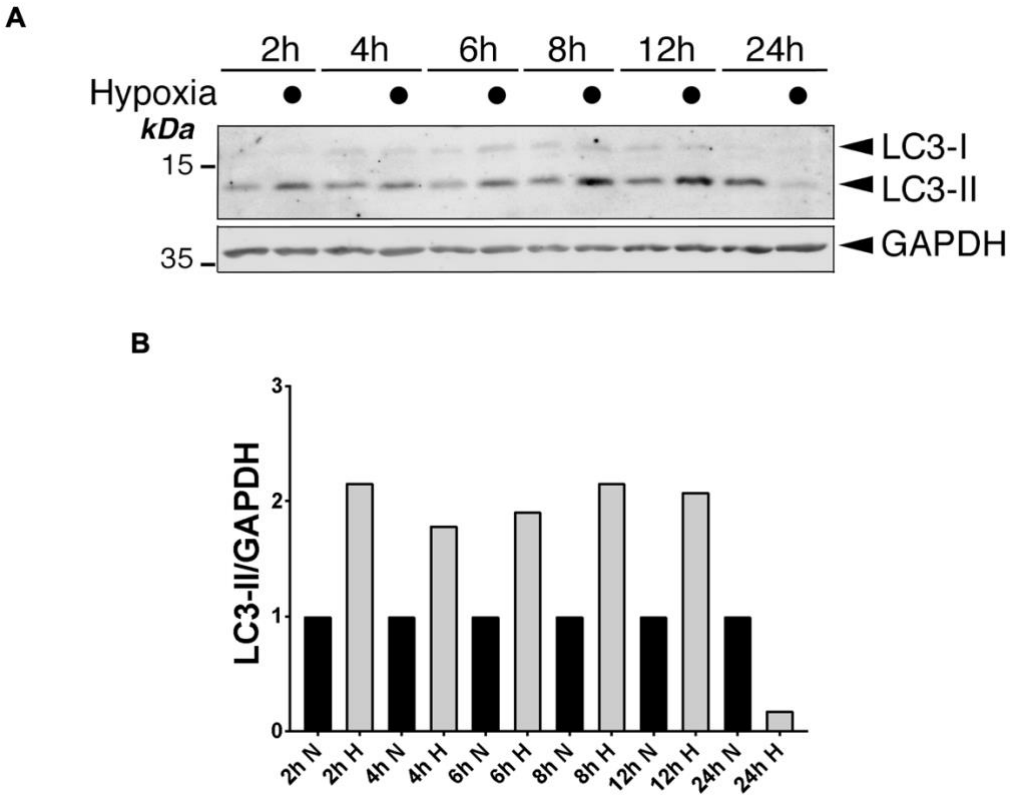
A
2h
4h
6h
8h
12h
24h
Hypoxia
kDa
15
35
LC3-I
LC3-II
GAPDH
B
LC3-II/GAPDH
3
2
1
0
2h N
2h H
4h N
4h H
6h N
6h H
8h N
8h H
12h N
12h H
24h N
24h H
C
12h
24 h
Normoxia
Hypoxia
15 kDa
35 kDa
LC3-I
LC3-II
GAPDH
LC3-II Levels in HeLa Cells
D
LC3-II/GAPDH ratio
1.5
1.0
0.5
0.0
*
N.S.
12N
12H
24N
24H
Treatment Time

Figure 3.3: Induction of Autophagy Marker LC3-II by Hypoxia in HeLa cells

A) Immunoblotting analysis of LC3-II levels in normoxic HeLa cells and HeLa cells exposed to hypoxia (1% oxygen) for 2 to 24 h. B) Quantification of the experiment in Figure 3.3a comparing LC3-II levels between normoxic (N) and hypoxic (H) cells incubated for the same duration. C) Immunoblotting analysis of LC3-II levels in normoxic HeLa cells and HeLa cells exposed to 12 or 24 h of hypoxia. D) Quantification of the experiment in Figure 3.3c comparing LC3-II levels between normoxic and hypoxic cells (n = 3; N.S. non-significant, *$p < 0.05$; Student's unpaired t-test).

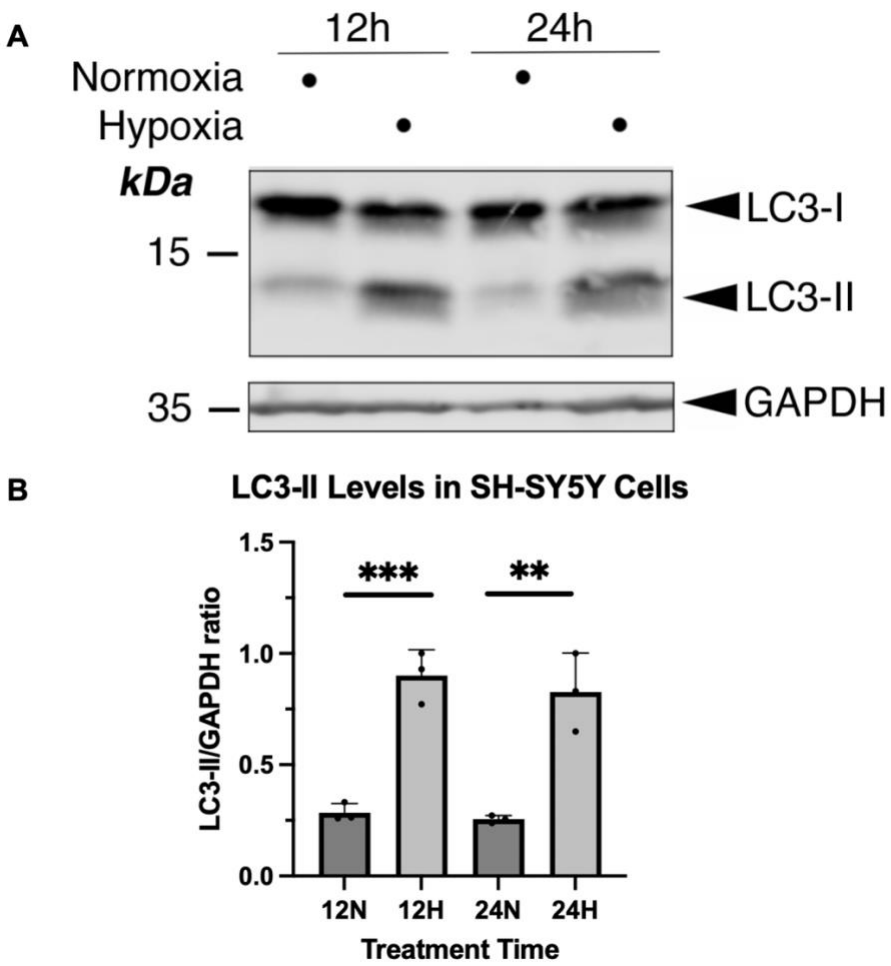

Figure 3.4: Induction of Autophagy Marker LC3-II by Hypoxia in SH-SY5Y cells

A) SH-SY5Y cells were exposed to normoxia or hypoxia (1% O_2) for 12 or 24 h. Whole cell lysate samples were prepared and blotted as indicated. B) Histogram shows relative LC3-II levels in SH-SY5Y cells comparing normoxic (N) and hypoxic (H) cells after 12 and 24 h of incubation respectively (n = 3; **p < 0.01, ***p <0.001; Student's unpaired t-test).

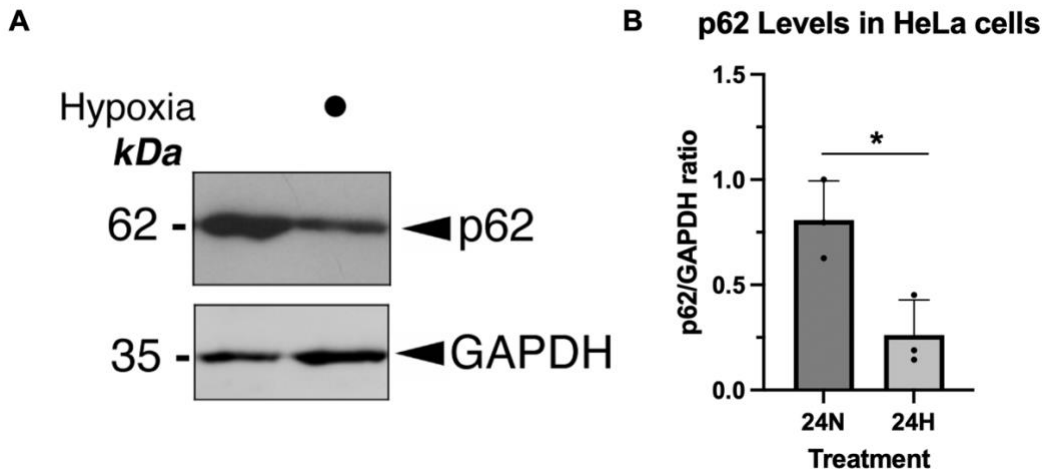

Figure 3.5: p62 levels decrease under hypoxia in HeLa cells

A) HeLa cells were exposed to normoxia or hypoxia (1% O_2) for 24 h. Whole cell lysate samples were prepared and blotted for p62 as indicated. B) Histogram shows relative p62 levels in HeLa cells exposed to normoxia (N) or hypoxia (H) for 24 h. (n = 3; *p < 0.05; Student's unpaired t-test).

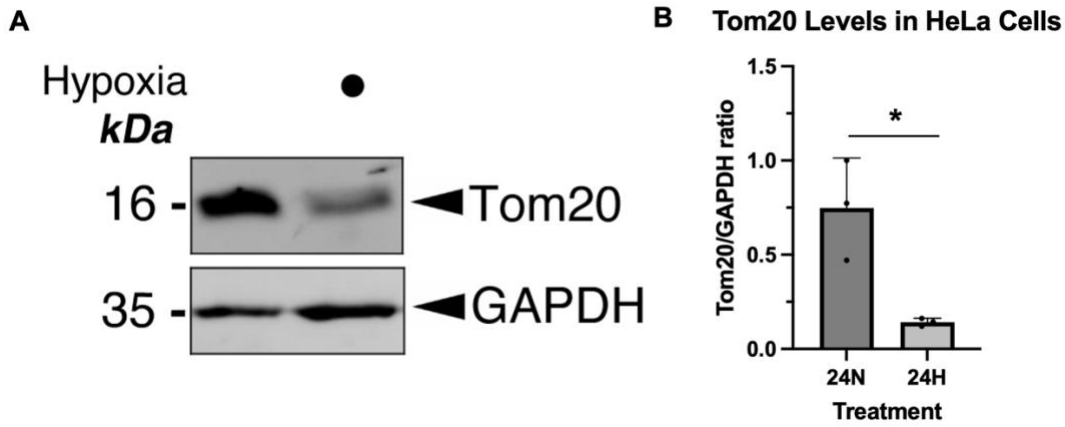

Figure 3.6: Tom20 levels decrease under hypoxia in HeLa cells

A) HeLa cells were exposed to normoxia or hypoxia (1% O_2) for 24 h. Whole cell lysate samples were prepared and blotted for Tom20 as indicated. B) Histogram shows relative Tom20 levels in HeLa cells exposed to normoxia (N) or hypoxia (H) for 24 h. (n = 3; *p < 0.05; Student's unpaired t-test).

3.2.4 The Effect of Hypoxia on Global SUMOylation

Hypoxia reportedly increases SUMOylation of HIF-1α in the cytosol, stabilizing HIF-1α and rescuing it from degradation by the proteasome (Cheng et al., 2007). Here, we examined the effect of hypoxia on global SUMO-1 (**Figure 3.7**) and SUMO-2/3 (**Figure 3.8**) levels in HeLa cells using Western blotting. Western blot analysis for SUMO-1 showed that exposure of HeLa cells to 24 h hypoxia decreased the level of both SUMO-1 conjugates and free SUMO-1 protein compared to levels in cells exposed to normoxia (**Figures 3.7b, 3.7c**). Knockdown of SUMO-1 abolished free SUMO-1 levels in both normoxic and hypoxic conditions, while decreasing but not depleting levels of SUMO-1 conjugates. SUMO-1 knockdown led to a depletion of SUMO-1 conjugates larger than approximately 40 kDa in cells exposed to hypoxia (**Figure 3.7**). This was quantified against the loading control β-actin, the levels of which were unchanged throughout treatment conditions (**Figures 3.7b, 3.7c**). Free SUMO-2/3 levels decreased under hypoxic conditions (**Figure 3.8c**). With the exception of 250 kDa SUMO-2/3 conjugates, levels of conjugated SUMO-2/3 were low under normoxia and near undetectable under hypoxia in both NSi and SUMO-2/3i cells (**Figure 3.8b**). These results, in contrast to the findings from a previous study by Kunz et al. (2016) in which hypoxia appeared to promote SUMO-1-ylation and SUMO-2/3-ylation in HeLa cells, suggest that exposure of the model cells to hypoxia for 24 h decreased SUMO conjugation likely from either downregulation of *SUMO-1* and *SUMO-2/3* gene expression or reduction of free SUMO-1 and SUMO-2/3 protein levels. While the observations from these Western blots offer interesting information regarding SUMO protein expression under hypoxia, they are still preliminary due to the lack of experimental repeats. Further investigation beyond this experiment is warranted to substantiate what we have gleaned from these findings.

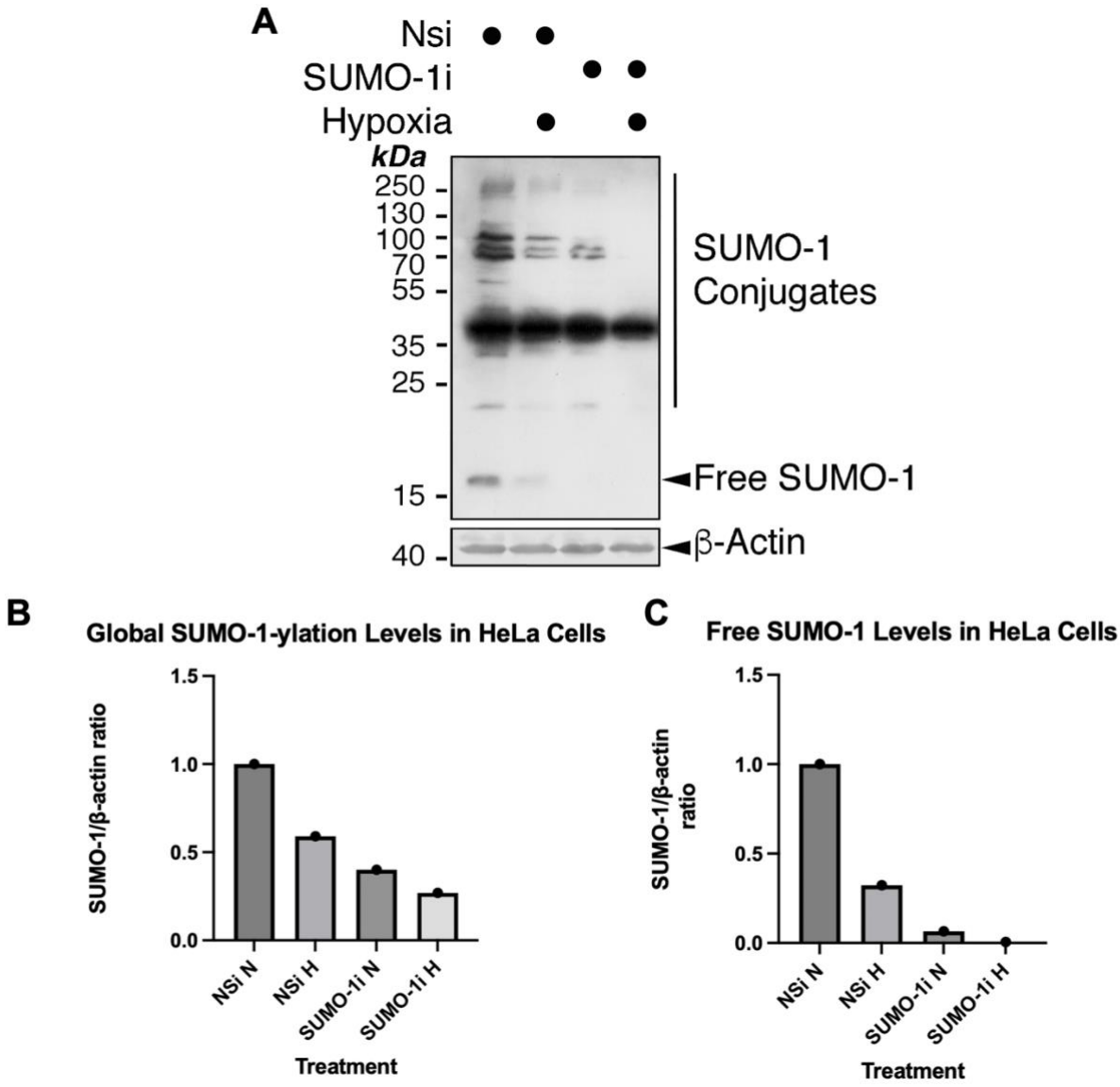

Figure 3.7: The Effect of Hypoxia on SUMO-1-ylation in HeLa cells

A) HeLa cells were transfected with either Nsi or SUMO-1-specific siRNA (SUMO-1i). 48 h post-transfection the cells were exposed to normoxia or hypoxia (1% O_2) for a further 24 h. Whole cell lysate samples were prepared and blotted as indicated. B) Histogram shows relative levels of global SUMO-1 conjugation in HeLa cells exposed to normoxia (N) or hypoxia (H) for 24 h. C) Histogram shows the levels of free SUMO-1 in HeLa cells exposed to N or H for 24 h.

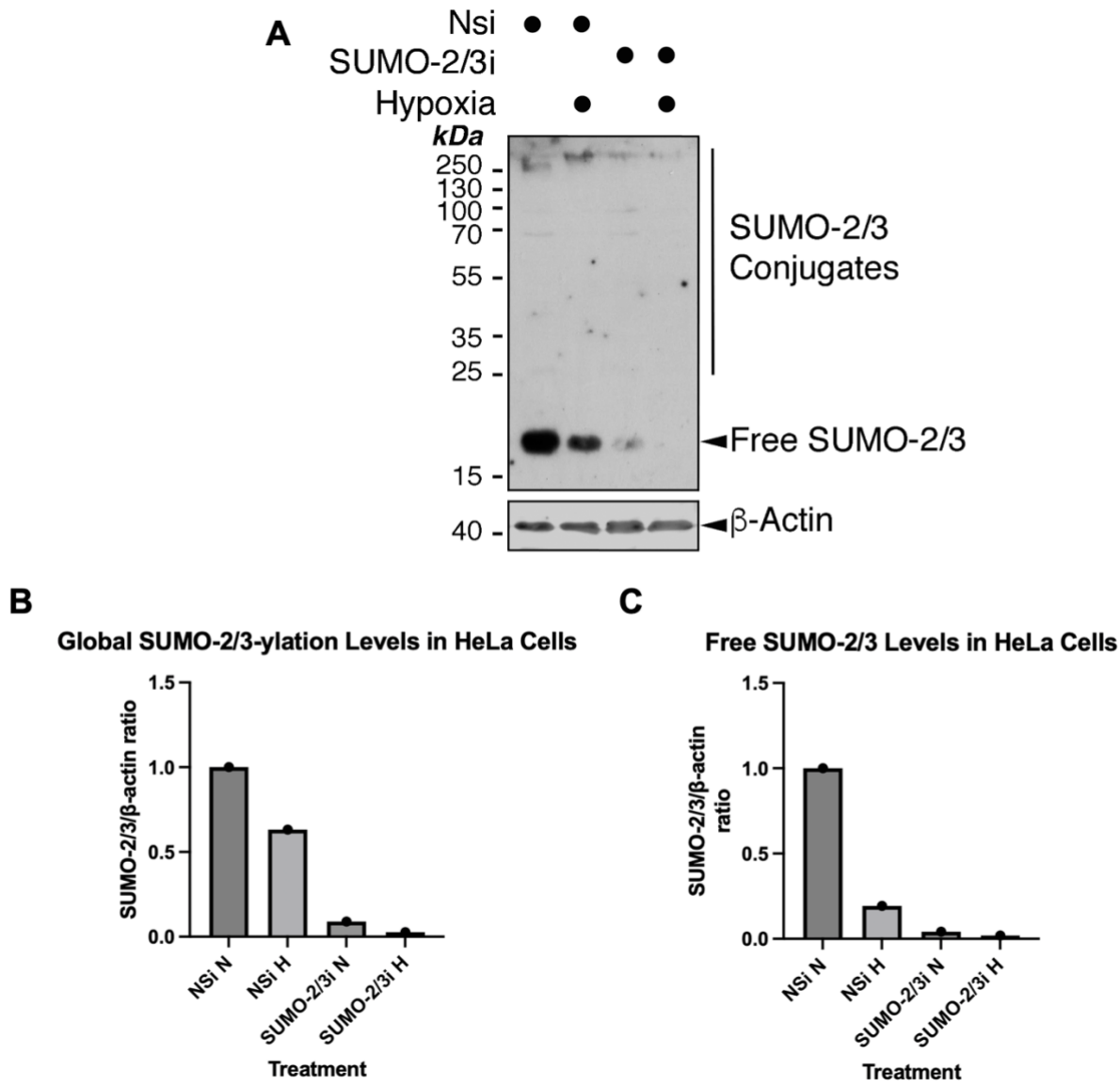

Figure 3.8: The Effect of Hypoxia on SUMO-2/3-ylation in HeLa cells

A) HeLa cells were transfected with either Nsi or SUMO-2/3-specific siRNA (SUMO-2/3i). 48 h post-transfection the cells were exposed to normoxia or hypoxia (1% O_2) for a further 24 h. Whole cell lysate samples were prepared and blotted as indicated. B) Histogram shows relative levels of global SUMO-2/3 conjugation in HeLa cells exposed to normoxia (N) or hypoxia (H) for 24 h. C) Histogram shows the levels of free SUMO-2/3 in HeLa cells exposed to N or H for 24 h.

3.2.5 The Effect of Hypoxia on the Expression of SENPs

There are six known mammalian SUMO-specific proteases (SENPs): SENP1-3 and SENP5-7, which vary in SUMO-specificity and cellular localization. DeSUMOylating enzymes are regulated transcriptionally, post-translationally and by cell stress (Guo & Henley, 2014). Here we investigated the effect of hypoxia on SENP expression levels in cells with Western blotting to determine which SENP family members may potentially have roles in regulating HIM. A hypoxia time course was performed where HeLa cells were exposed to 1% O_2 for 2, 4, 6, 8 or 10 h. From there, cell lysates were prepared for Western blot analysis of SENP1 (**Figure 3.9a**). SENP1 levels did not seem to be affected by hypoxia for up to 10 h in our experimental system (**Figure 3.9b**). Another hypoxia time course to assess SENP1 levels was performed from 2 to 24 h (**Figure 3.9c**) where it appeared SENP1 levels under hypoxia fluctuated over time but ultimately increased after 24 h (**Figure 3.9d**). Unfortunately, due to the poor quality of the blot in **Figure 3.9c** and the lack of repeats, we could not determine whether there was a pattern in SENP1 expression due to hypoxia exposure.

Similarly, a hypoxia time course was also performed on HeLa cells for 2 to 24 h to analyze SENP3 levels under hypoxia (**Figure 3.10**). Due to the quality of the Western blot shown in **Figure 3.10a**, it was difficult to determine a pattern of SENP3 levels under hypoxia over time. The results were inconclusive for the 24 h time point (**Figure 3.10b**), so additional Western blotting was performed on HeLa cells exposed to hypoxia for 12 and 24 h to assess SENP3 levels (**Figure 3.10c**). No significant changes in SENP3 levels were detected in lysate samples from HeLa cells exposed to hypoxia for both 12 and 24 h compared to control cells exposed to normoxia (**Figure 3.10d**). SENP3 levels in HeLa cells that underwent prolonged exposure (24 and 48 h) to hypoxia were also assessed (**Figure 3.11a**). Similar to the previously stated results, no changes in SENP3 levels were observed at 24 h of hypoxia exposure compared to normoxia (**Figure 3.11b**). However, after 48 h, SENP3 levels declined drastically under hypoxia compared to normoxia (**Figure 3.11b**).

Hypoxia time courses were conducted in HeLa cells to assess SENP2, SENP5, and SENP7 levels at different durations of exposure to hypoxia (**Figures 3.12-3.14**). Briefly, there were no general trending patterns for these SENPs under hypoxia. We examined SENP6 levels with Western blot as well. However, SENP6 could not be detected and thus the results were inconclusive. It should be noted that these Western blot experiments were single experiments. Ideally, subsequent repeat experiments should be performed to obtain more data to determine if there are any expression patterns for these SENPs under hypoxia.

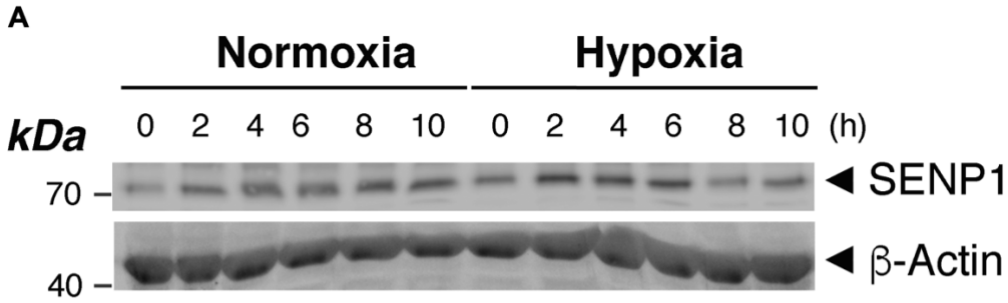
A
Normoxia
Hypoxia
kDa
0 2 4 6 8 10 0 2 4 6 8 10 (h)
70
40
SENP1
β-Actin

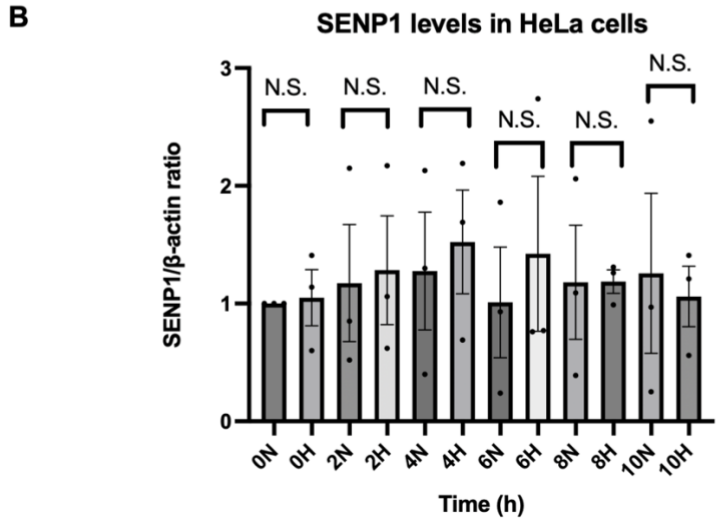
B
SENP1 levels in HeLa cells
SENP1/β-actin ratio
N.S.
Time (h)
0N 0H 2N 2H 4N 4H 6N 6H 8N 8H 10N 10H

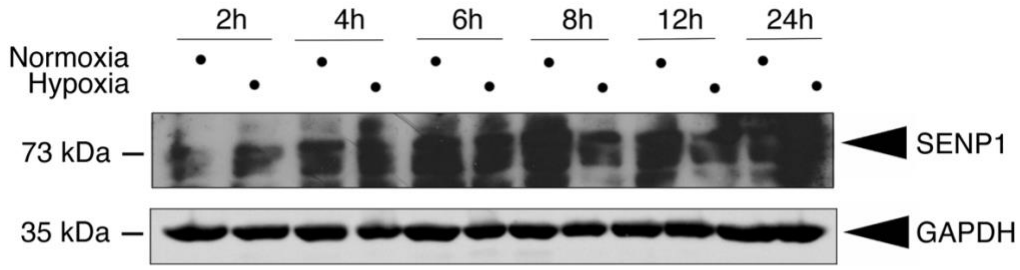
C
2h 4h 6h 8h 12h 24h
Normoxia
Hypoxia
73 kDa
35 kDa
SENP1
GAPDH

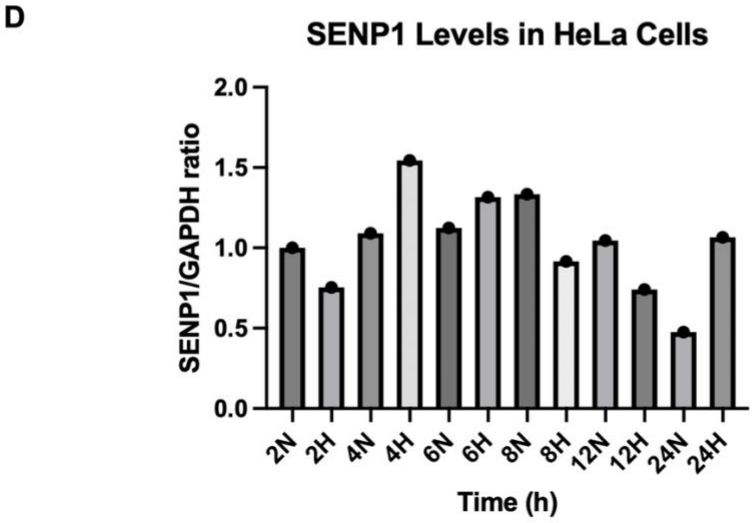
D
SENP1 Levels in HeLa Cells
SENP1/GAPDH ratio
Time (h)
2N 2H 4N 4H 6N 6H 8N 8H 12N 12H 24N 24H

Figure 3.9: The Effect of Hypoxia on SENP1 Levels in HeLa cells

A) HeLa cells were exposed to normoxia or hypoxia (1% O_2) for 0 to 10 h. Whole cell lysate samples were prepared and blotted for SENP1 as indicated. B) Histogram shows relative SENP1 levels in HeLa cells exposed to normoxia (N) or hypoxia (H) for 0 to 10 h. (n = 3; N.S., non-significant; Student's unpaired t-test). C) HeLa cells were exposed to normoxia or hypoxia (1% O_2) for 2 to 24 h. Whole cell lysate samples were prepared and blotted for SENP1 as indicated. D) Histogram shows relative SENP1 levels in HeLa cells exposed to N or H for 2 to 24 h. (n = 1).

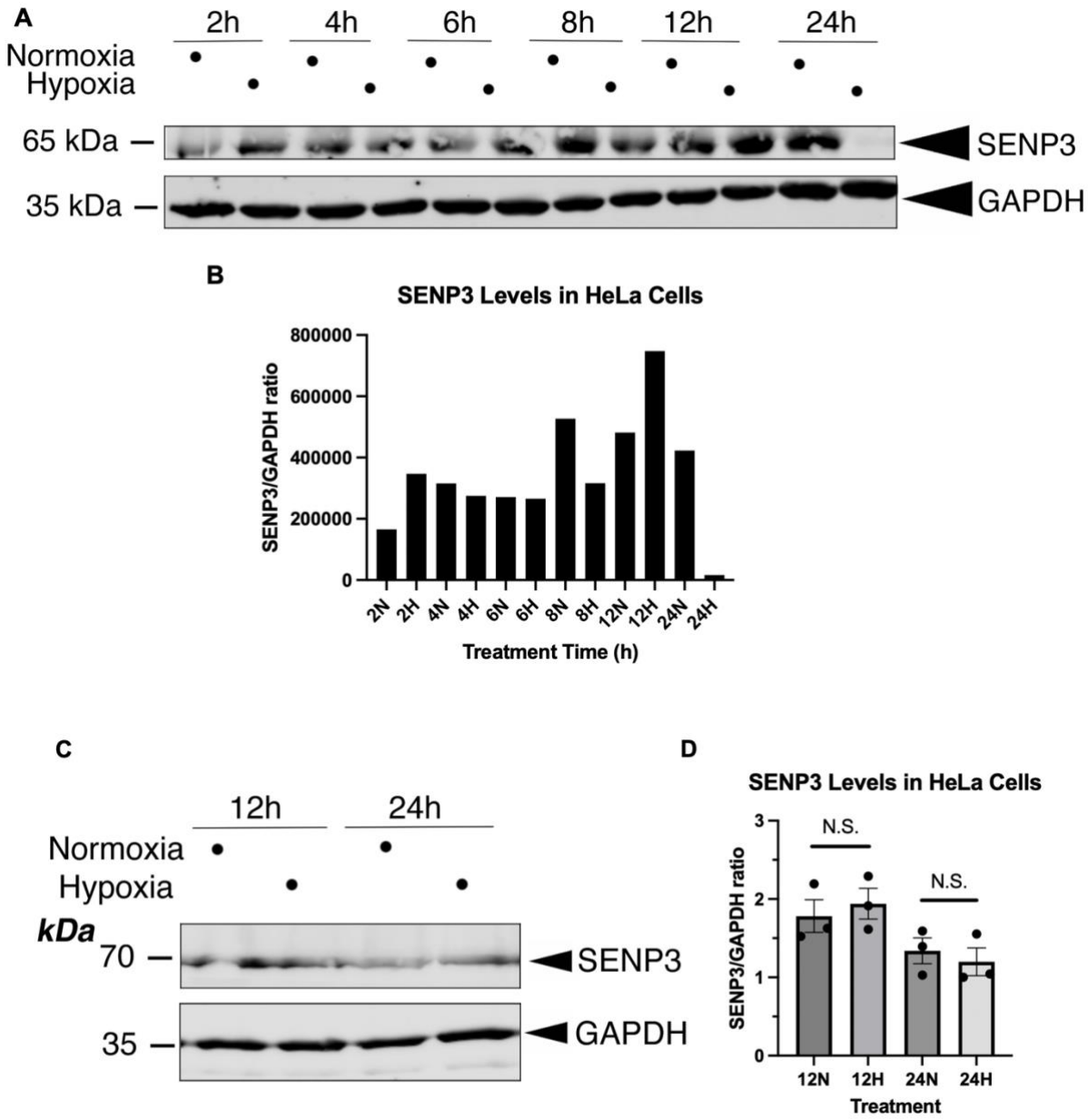

Figure 3.10: The Effect of Hypoxia on SENP3 Levels in HeLa cells

A) HeLa cells were exposed to normoxia or hypoxia (1% O_2) for 2 to 24 h. Whole cell lysate samples were prepared and blotted for SENP3 as indicated. B) Histogram shows relative SENP3 levels in HeLa cells exposed to N or H for 2 to 24 h. (n = 1). C) HeLa cells were exposed to normoxia or hypoxia (1% O_2) for 12 or 24 h. Whole cell lysate samples were prepared and blotted for SENP3 as indicated. D) Histogram shows relative SENP3 levels in HeLa cells exposed to N or H for 2 to 24 h. (n = 3; N.S., non-significant; Student's unpaired t-test).

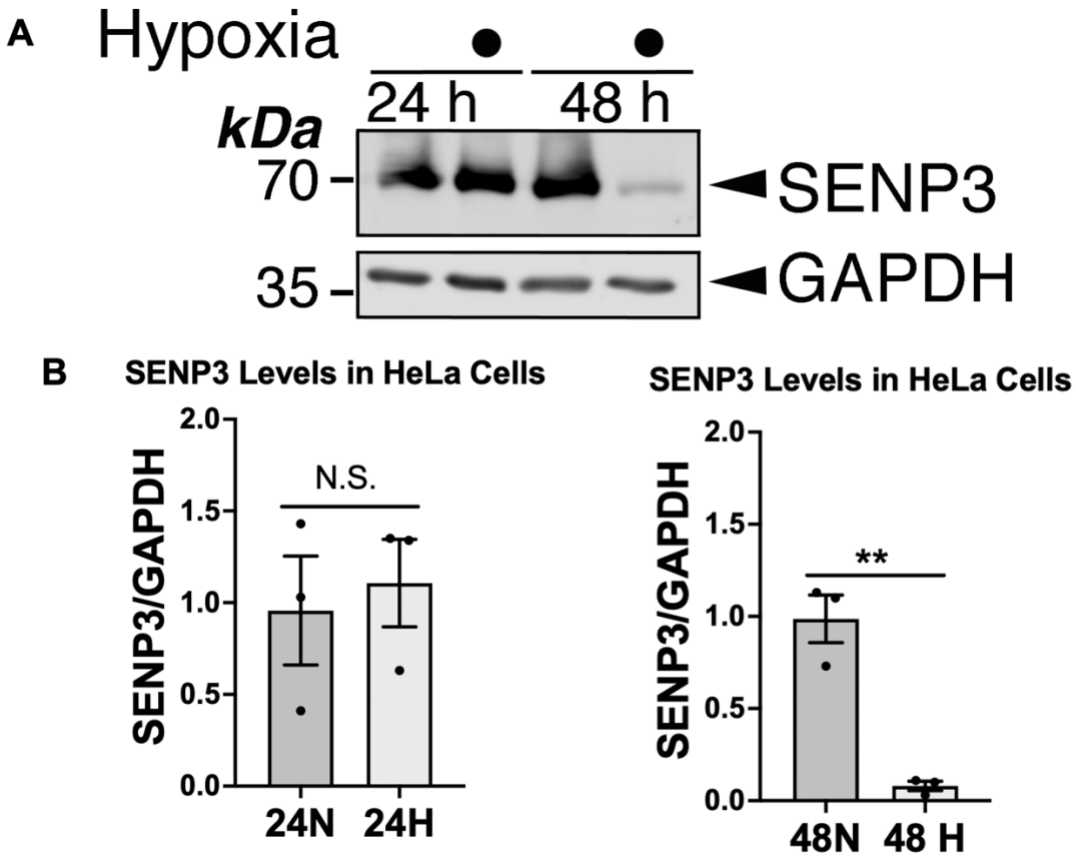

Figure 3.11: SENP3 Levels under Prolonged Hypoxia

A) HeLa cells were exposed to normoxia or hypoxia (1% O_2) for 24 or 48 h. Whole cell lysate samples were prepared and blotted for SENP3 as indicated. B) Histograms of relative SENP3 levels in HeLa cells exposed to N or hypoxia H for 24 h (left) or 48 h (right). (n = 3; N.S., non-significant, **$p < 0.01$; Student's unpaired t-test).

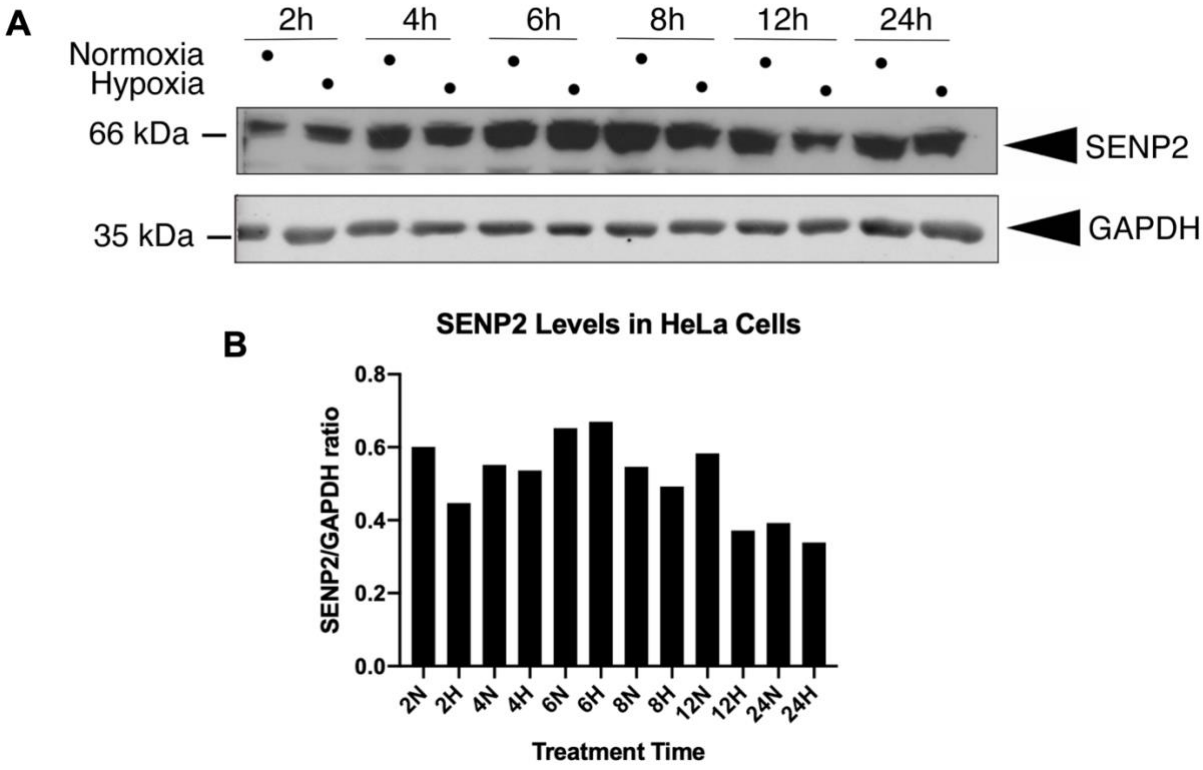

Figure 3.12: The Effect of Hypoxia on SENP2 Levels in HeLa cells

A) HeLa cells were exposed to normoxia or hypoxia (1% O_2) for 2 to 24 h. Whole cell lysate samples were prepared and blotted for SENP2 as indicated. B) Histograms of relative SENP2 levels in HeLa cells exposed to normoxia (N) or hypoxia (H) for 2 to 24 h. (n = 1).

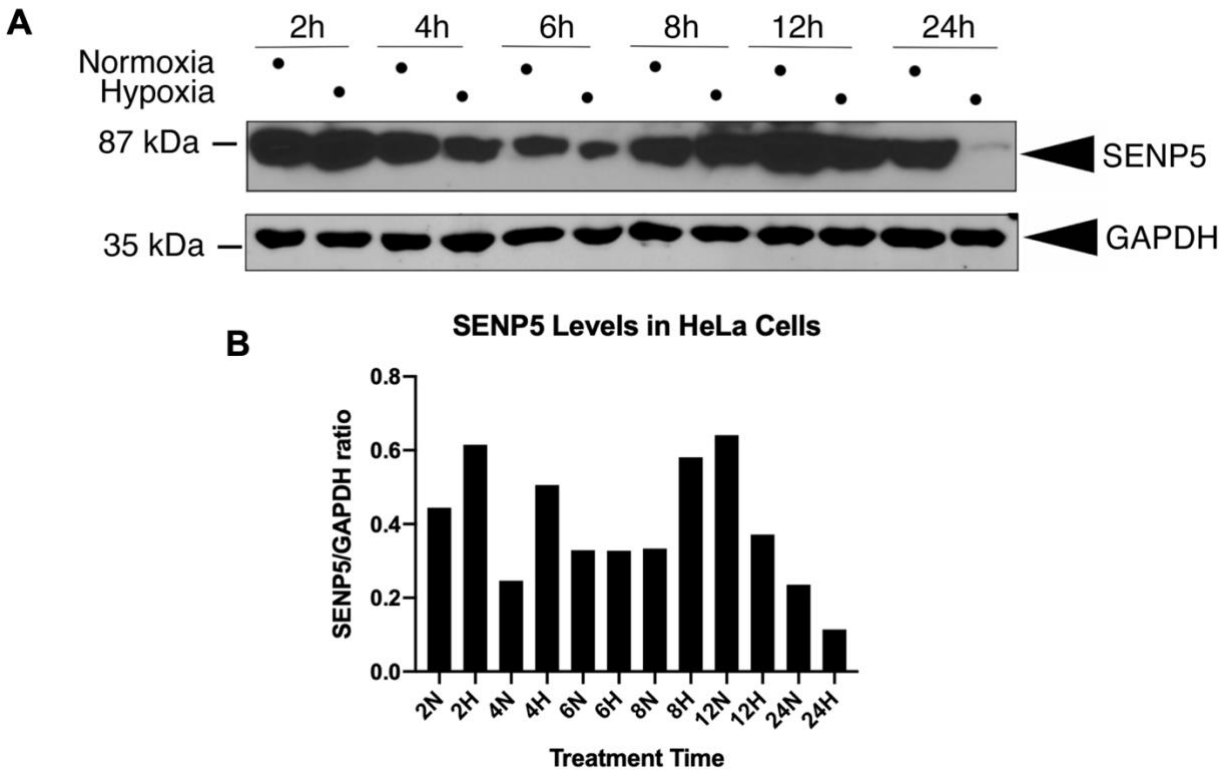

Figure 3.13: The Effect of Hypoxia on SENP5 Levels in HeLa cells

A) HeLa cells were exposed to normoxia or hypoxia (1% O_2) for 2 to 24 h. Whole cell lysate samples were prepared and blotted for SENP5 as indicated. B) Histograms of relative SENP5 levels in HeLa cells exposed to normoxia (N) or hypoxia (H) for 2 to 24 h. (n = 1).

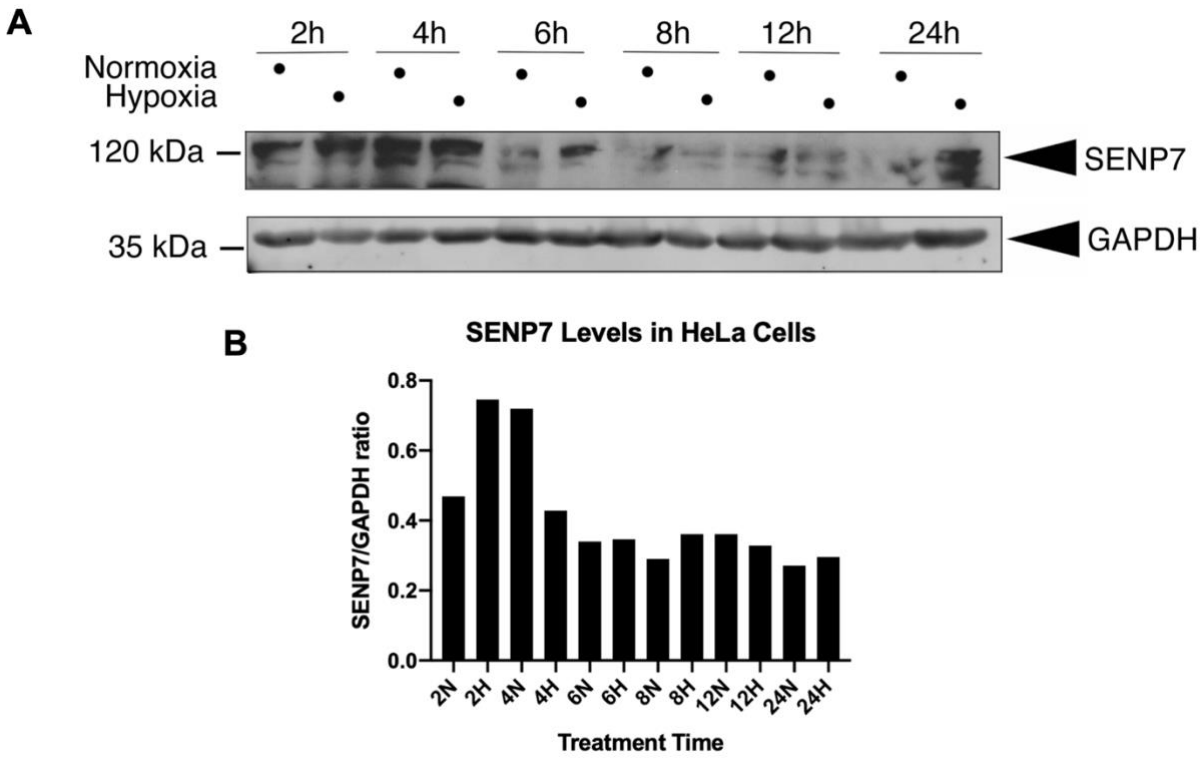

Figure 3.14: The Effect of Hypoxia on SENP7 Levels in HeLa cells

A) HeLa cells were exposed to normoxia or hypoxia (1% O_2) for 2 to 24 h. Whole cell lysate samples were prepared and blotted for SENP7 as indicated. B) Histograms of relative SENP7 levels in HeLa cells exposed to normoxia (N) or hypoxia (H) for 2 to 24 h. (n = 1).

3.2.6 The Effect of Knockdown of deSUMOylation Enzymes on Hypoxia-Induced Autophagy

SENP1 and SENP3 knockdowns were performed in HeLa cells exposed to hypoxia to address the roles of the deSUMOylation enzymes on hypoxia-induced autophagy. HeLa cells were transfected with NSi or SENP1-specific siRNA (SENP1i) and then exposed to normoxia or hypoxia (1% O_2) for 8 h. LC3-II and SENP1 levels were assessed with Western blotting. Knockdown of SENP1 appeared to prevent LC3-II induction under hypoxia (**Figure 3.15**), suggesting SENP1 is may be important for phagophore expansion and autophagosome formation induced by hypoxia. Similarly, HeLa cells were transfected with NSi or SENP3-specific siRNA (SENP3i) and then exposed to normoxia or hypoxia (1% O_2) for 8 h. LC3-II and SENP3 levels were assessed with Western blotting. SENP3 KD did to seem to not affect LC3-II induction by hypoxia. There was no significant change in LC3-II levels between cells transfected with NSi and SENP3-specific siRNA under both normoxia and hypoxia conditions (**Figure 3.16**). These results suggest that decreasing SENP3 levels may not directly affect phagophore expansion and autophagosome formation induced by hypoxia. Both of these Western blot experiments were single experiments, thus further repeat experiments should be performed to substantiate the preliminary data presented.

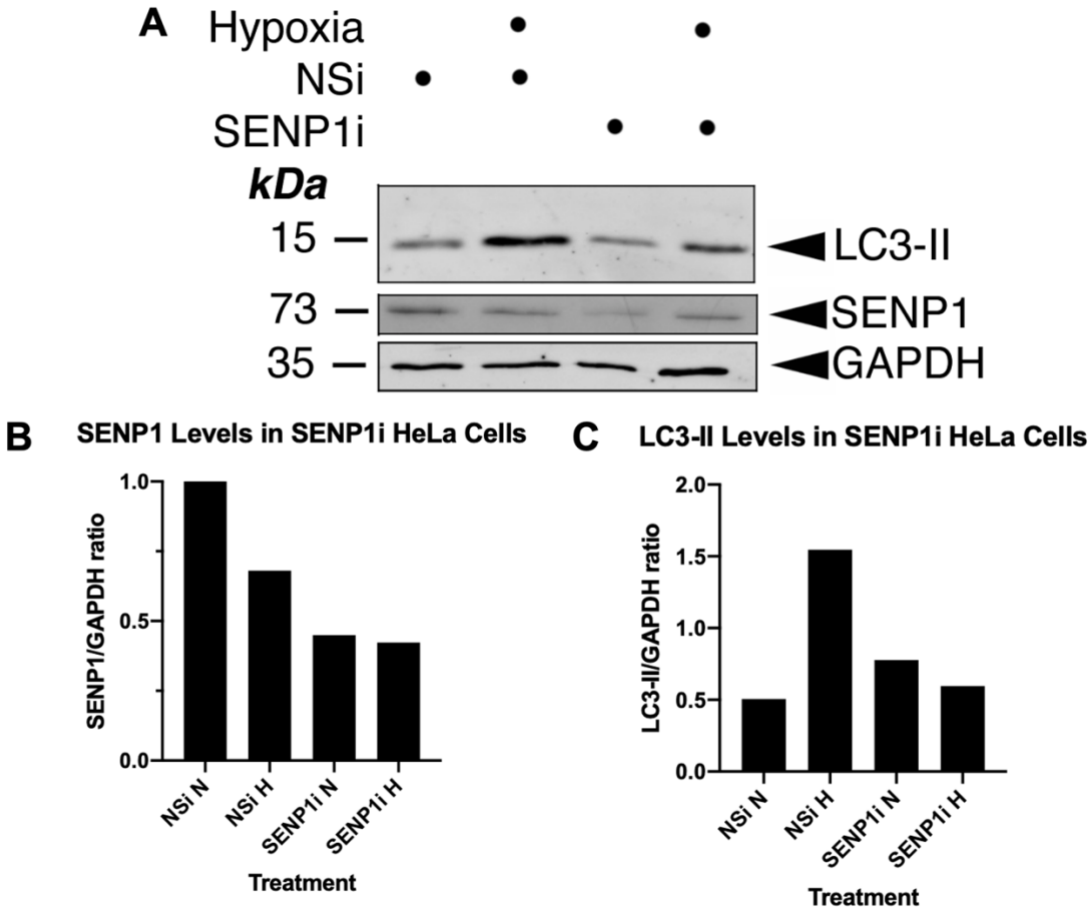

Figure 3.15: Effect of siRNA-mediated Knockdown of SENP1 on LC3-II Induction by Hypoxia in HeLa cells

A) HeLa cells were transfected with Nsi or SENP1i. Post-transfection 48 h, the cells were exposed to 8 h hypoxia. Levels of SENP1 or LC3-II were examined using immunoblotting with the appropriate antibodies. B-C) Histograms showing relative SENP1 or LC3-II levels in normoxic (N) and hypoxic (H) cells are shown in histograms (n = 1).

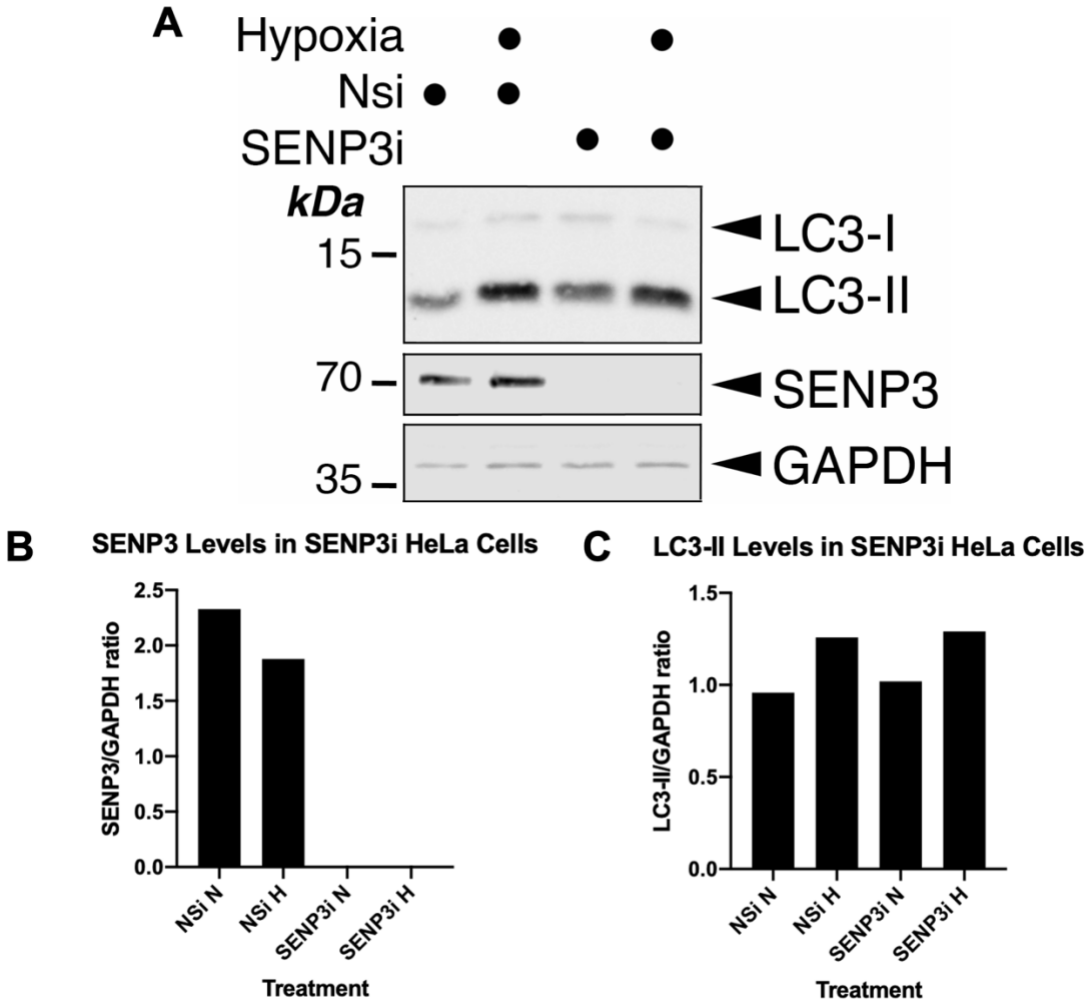

Figure 3.16: Effect of siRNA-mediated Knockdown of SENP3 on LC3-II Induction by Hypoxia in HeLa cells

A) HeLa cells were transfected with Nsi or SENP3i. 48 h post-transfection, the cells were exposed to 8 h hypoxia. Levels of SENP3 or LC3-II were examined using immunoblotting with the appropriate antibodies. B-C) Histograms showing relative SENP3 and LC3-II levels in normoxic (N) and hypoxic (H) cells are shown in histograms (n = 1).

3.2.7 Effect of SENP1 overexpression on LC3-II Induction in HeLa cells

In order to determine whether overexpression of SENP1 affects LC3-II levels, we overexpressed SENP1 in HeLa cells and assessed LC3-II levels with Western blotting (**Figure 3.17**). pcDNA3 or Flag-SENP1 were transfected into HeLa cells under normoxic conditions. Cell lysate samples were prepared and Western blots were performed to assess relative levels of SENP1 and LC3-II (**Figure 3.17a**). SENP1 OE does not seem to increase LC3-II levels (**Figure 3.17b**). This Western blot experiment was performed only once, thus further repeat experiments should be performed to substantiate the preliminary data presented.

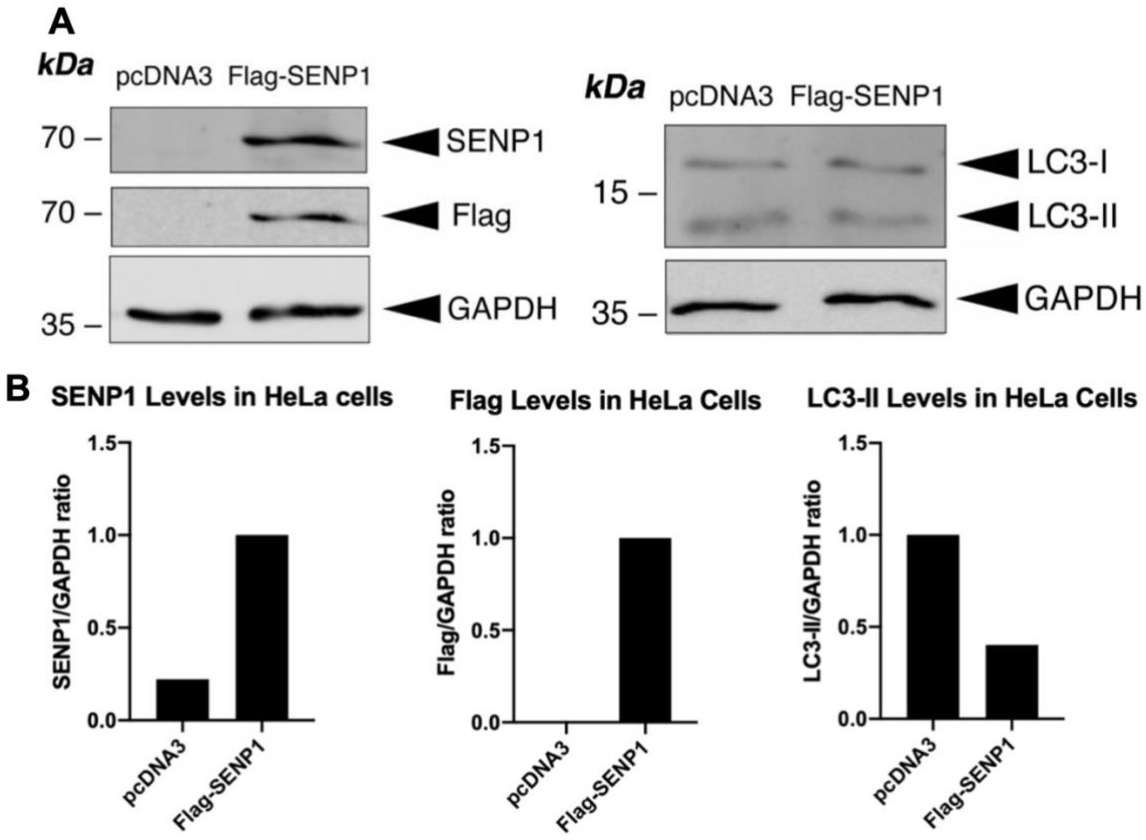

Figure 3.17: The Effect of SENP1 Overexpression on Autophagosome Formation

HeLa cells were transfected with either pcDNA3 or Flag-SENP1. Whole cell lysates were collected and blotted as indicated. A) Western blots for Flag-SENP1 and LC3-II with pcDNA3 as the negative control. B) Histograms showing relative levels of SENP1, Flag-tag; and LC3-II in the cell lysate samples in the Western blots. (n = 1).

3.2.8 Detection of Hypoxia-Induced Mitophagy with Mito-pHfluorin

The experimental results in this chapter suggest that the hypoxia experimental system was capable of inducing autophagy in cells. The next step in characterizing the hypoxia experimental system is to determine whether the hypoxia can induce mitophagy. In order to visualize and quantify the level of mitophagy occurring in the cell under hypoxia, we utilized the dual-fluorescent probe Mito-pHfluorin and fluorescence microscopy. A hypoxia time course was performed on HeLa cells transfected with Mito-pHfluorin. Cells were fixed with 4% PFA after 4, 8, 16, or 24 h exposure to 1% (v/v) O_2 levels. Images were analyzed with Fiji software. A semi-automated program written jointly by Dr. Darren Robinson of the University of Sheffield and myself was used to quantify the number of red puncta per cell in cells containing Mito-pHfluorin, which indicate the occurrence of mitophagy in mitochondria-containing autolysosomes. Representative images of HeLa cells exposed to hypoxia for each duration of time are shown in **Figure 3.18a** along with control cells exposed to normoxia. The average number of puncta per cell increased with exposure time to hypoxia. In comparison to cells exposed to normoxia, cells exposed to hypoxia for 4, 8, 16, or 24 h possessed significantly increased numbers of red puncta (**Figure 3.18b**), which suggests that our hypoxia experimental system can induce mitophagy in HeLa cells.

In subsequent microscopy experiments utilizing hypoxia and Mito-pHfluorin, HeLa cells were exposed to hypoxia for 24 h as the optimal time point to quantify levels of mitophagy. In HeLa cells transfected with Mito-pHfluroin and Nsi, hypoxia treatment significantly increased the average number of puncta per cell compared to normoxic conditions (**Figure 3.19**), providing further evidence that our hypoxia experimental system is capable of inducing mitophagy through hypoxia.

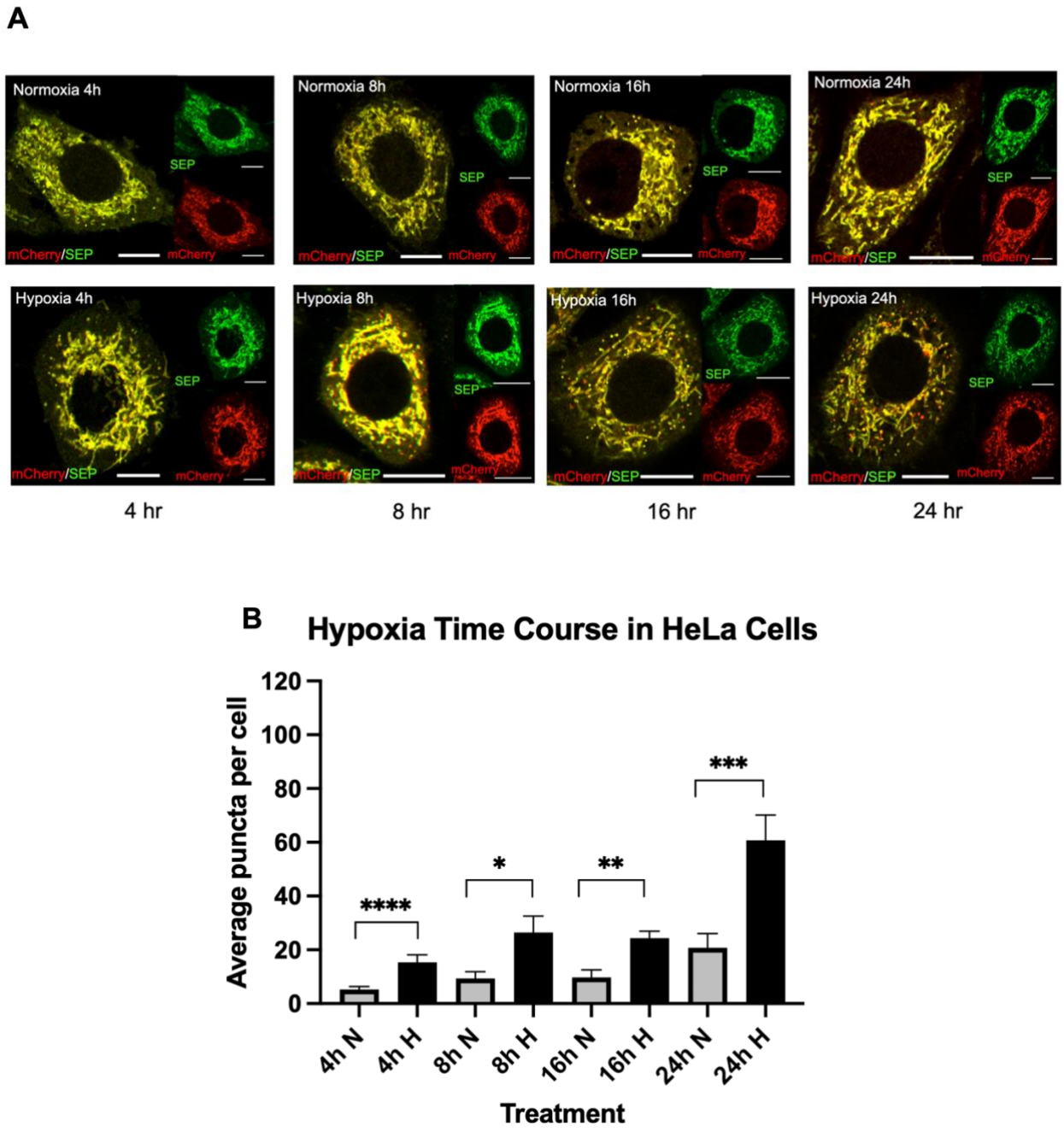

Figure 3.18: Hypoxia Time Course with Mito-pHfluorin

A) HeLa cells were transfected with 0.25 µg Mito-pHfluorin per dish. 48 h post-transfection , the cells were exposed to (1% O_2) hypoxia for 4, 8, 16, or 24 h. Scale bar: 10 µm. b) Histogram shows quantifications of the average number of puncta per cell. Quantifications were performed with Fiji software cell counter. (n = 19-51; *p < 0.05; **p < 0.01; ***p < 0.001; ****p < 0.0001; Student's unpaired t-test). The data presented are from a single experiment. n refers to the number of cells from one µ-dish used to quantify the average number of puncta per experimental condition.

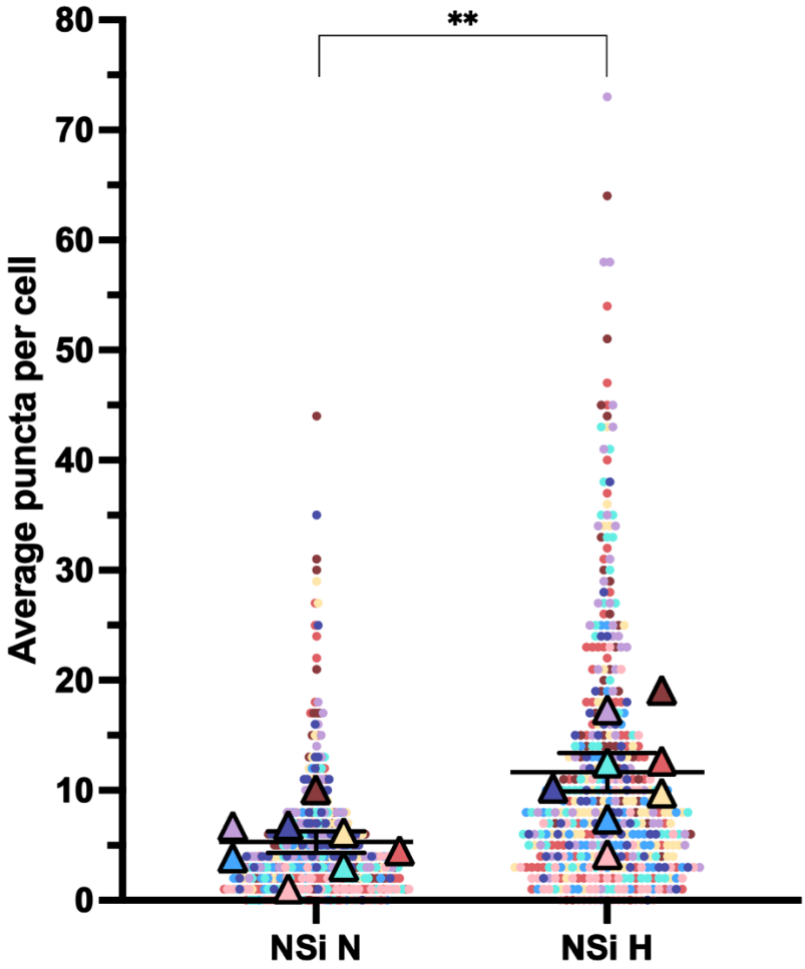

Figure 3.19: Hypoxia induces mitophagy in HeLa cells

HeLa cells transfected with Mito-pHfluorin and Nsi. 48 h post-transfection the cells were exposed to normoxia (N) or hypoxia (H; 1% O_2) for 24 h. The cells were fixed with PFA 4% and then imaged with confocal microscopy. The plot shows colored triangles representing the average number of Mito-pHfluorin red puncta per cell for cells exposed to N or H for 24 h for each experimental repeat. The beeswarm plot shows the number of puncta per cell as individual data points color-coded by experiment. Quantifications were performed with Fiji software cell counter. (n = 8; **p < 0.01; Student's unpaired t-test). n refers to the number of biological replicates.

3.3 Discussion

3.3.1 Induction of HIF-1 and HIF-2 by Hypoxia

HIF-1 is the master transcription factor for hypoxia cell response. HIF-1α, the oxygen labile subunit of HIF-1, controls expression of genes involved in mitochondrial turnover in cells exposed to hypoxia. HIF-1α and HIF-2α are the most studied isoforms of the subunits of HIFs. HIF-1α and HIF-2α are structurally similar to one another and share similar functions and sensitivity to oxygen-dependent degradation. However, HIF-1α is ubiquitously expressed across all cells whereas HIF-2α is expressed in only certain tissues (Wiesener et al., 2003; Patel & Simon, 2008; Loboda et al., 2010). For these reasons, we focused on the expression of HIF-1α under hypoxia in determining whether our hypoxia workstation induces hypoxic cell response. The hypoxia workstation yielded robust induction of HIF-1α as seen through Western blotting, confirming our experimental setup as suitable for further use in hypoxia-based experiments. The increase of HIF-1α levels under hypoxia was consistent with previous reports of HIF-1α induction by hypoxia (Wiener et al., 1996; Bergeron et al., 1999).

HIF-2α levels in our model HeLa cells varied under different lengths of exposure to hypoxic conditions but overall did not change. Given the poor quality of the Western blots for HIF-2α, it was difficult to determine any trend in HIF-2α expression over the hypoxia time course, so our data here may be inconclusive. Aside from issues in the quality of the HIF-2α Western blots, the difference in expression patterns between HIF-1α and HIF-2α can be attributed to the tissue-specific expression of HIF-2α (Patel & Simon, 2008; Loboda et al., 2010). The “HIF switch” model proposed by Koh & Powis (2012) describes the relationship between the diverging roles of HIF-1 and HIF-2 in hypoxic response as non-redundant and complementary. Koh & Powis (2012) outlined that HIF-1α drives initial response to hypoxia (< 24 h) whereas HIF-2α deals with chronic hypoxia response (> 24 h). This HIF switch may partly account for our results regarding HIF-2α

levels under hypoxia where the switch toward a HIF-2 response had not fully occurred at 24 h of exposure.

3.3.2 Effect of Hypoxia on Autophagy and Mitophagy-related proteins

To address the effects of hypoxia on autophagy, we assessed the levels of the autophagic marker LC3-II in HeLa and SH-SY5Y cells in hypoxic conditions. Additionally, we also investigated the levels of p62 and Tom20 in HeLa cells under hypoxia. Significant LC3-II induction was observed in HeLa cells exposed to hypoxia for 12 h and in SH-SY5Y cells exposed to hypoxia for 12 and 24 h, suggesting that our hypoxia experimental system was capable of inducing autophagosome formation. The differences observed in LC3-II induction between HeLa and SH-SY5Y cells may be attributed to Parkin expression in SH-SY5Y cells, since prolonged 24 h exposure to hypoxia induced LC3-II expression in SH-SY5Y cells but not in HeLa cells. This may be partly attributable to the potential role of Parkin in preserving autophagic capacity as part of cell survival response (Bernardini et al., 2019). Autophagy induction by hypoxia differ between the cell types due to HeLa cells expressing little or no Parkin as they originate from a cervical cancer cell line, whereas SH-SY5Y cells are neuronal in origin. Cancer cells have other mechanisms to enhance cell survival under stress conditions. HeLa cells may use such survival methods in addition to autophagy in response to hypoxic stress, which could result in a weaker induction of LC3-II by hypoxia than what was observed in SH-SY5Y cells. Alternatively, HeLa cells may undergo higher basal levels of autophagy, leading to more autophagosome formation marked by LC3-II at physiological conditions. Our results show that hypoxia as induced by our experimental setup elicits a robust hypoxic cell response in cells, as evidenced by induction of the HIF-1 pathway and general autophagy under hypoxia. This step in establishing an experimental system that elicits hypoxia-induced autophagy in cells is crucial for investigating hypoxia-induced mitophagy in further experimental procedures.

In addition to LC3-II induction, hypoxia lead to a significant decrease in the levels of the following autophagy- or mitophagy-related proteins: p62 and Tom20. This evidence suggests hypoxia leads to degradation of p62, which indicates induction of hypoxia-activated autophagy (Pursiheimo et al., 2008). Decreased Tom20 levels under hypoxia may indicate a reduction of mitochondrial mass due to Parkin-independent mitophagy (Ding & Yin, 2012; Yoshii et al., 2011). These findings further support that the hypoxia experimental system we established induces autophagy and likely also mitophagy in HeLa cells.

3.3.3 Hypoxia decreases SUMO-1 and SUMO-2/3 levels in HeLa cells

After establishing the hypoxic experimental system, the next step was to investigate the expression pattern of SUMO proteins under hypoxia, since SUMOylation plays a key role in regulating the HIF-1 pathway. Western blot analysis was used to examine global levels of SUMO-1 and SUMO-2/3 in cells exposed to hypoxia. Hypoxia appeared to decrease the level of SUMO-1 conjugates larger than 40 kDa, including SUMO-1-ylated HIF-1α. Levels of larger SUMO-1 conjugates are depleted under hypoxia when SUMO-1 was knocked down. Decrease of conjugated SUMO-1 levels under hypoxia are consistent with deSUMOylation of HIF-1α by SENP1 under hypoxia, which stabilizes HIF-1α and allows for its translocation to the nucleus and subsequent binding to HIF-1β (Azad et al., 2016; Cui et al., 2017; Xu et al., 2010). Conjugated SUMO-2/3 levels appeared low under normoxia, which is consistent with SUMO-2/3 remaining largely unconjugated at physiological conditions (Saitoh & Hinchey, 2000). Free SUMO-2/3 levels decreased under hypoxia and knocking down SUMO-2/3 in cells exposed to hypoxia completely depleted both free and conjugated SUMO-2/3 levels. SUMO-2/3 is associated with cell stress response (Guo & Henley, 2014). Conjugation of SUMO-2/3 has been suggested to be an endogenous neuroprotective stress response to oxygen glucose deprivation (OGD). Silencing SUMO-2/3 in neurons undergoing prolonged OGD led to severe cell loss (Datwyler et al., 2011).

In OGD conditions, SENP3 levels have been reported to decrease while levels of SUMO-2/3 conjugates increase due to the degradation of SENP3 under OGD (Guo et al., 2013). The reduction of free and conjugated SUMO-2/3 levels combined with the lack of change in SENP3 levels we observed in HeLa cells exposed to hypoxia suggest that cell response to OGD and hypoxia may diverge in their effect on SUMO-2/3 and SENP3 levels. Downregulation of the *SUMO-2/3* gene expression or degradation of free SUMO-2/3 protein may result in the decrease of both free and conjugated SUMO-2/3 under hypoxia.

Overall, our results suggest that in our hypoxia experimental system, hypoxia seems to decrease both free and conjugated SUMO-1 and SUMO-2/3 in HeLa cells. Hypoxic cell response may utilize SUMO-1 and SUMO-2/3 in concert to regulate different aspects stress response since SENP1 has a specificity for cleaving off both SUMO-1 and SUMO-2/3, whereas other SENP family members preferentially act on SUMO-2/3 (Hickey et al., 2012). Thus, levels of free and conjugated SUMO-1 and SUMO-2/3 are perhaps downregulated under hypoxia by SENPs or other deSUMOylation enzymes to enact changes in integral cellular processes such as autophagy or mitophagy. Since SUMOylation is reversible, it is difficult to determine what cellular processes SUMOylation or deSUMOylation affect with only Western blotting of SUMO proteins.

3.3.4 Effect of Hypoxia on SENP Expression

As mentioned in the previous section, in our model HeLa cells, levels of free and conjugated SUMO-1 and SUMO-2/3 appear to decrease under hypoxia, suggesting that hypoxia affects global SUMO and SUMOylation levels. By extension, deSUMOylation of proteins by SENPs, or SUMO-specific proteases, and SENP expression levels may also be affected by low oxygen levels. Due to the direct relationship between SUMO and the deSUMOylation enzymes SENPs, we examined the effect of hypoxia on the levels of the following SENP proteins in cells with Western blot: SENP1, SENP3, SENP2, SENP5, and SENP7. Our findings showed SENP1 levels in our

model HeLa cells did not change between 0 and 10 h of exposure to hypoxia but appeared to increase at 24 h. These findings for SENP1 levels at 24 h of hypoxia exposure are consistent with reports of SENP1 expression increasing in cells exposed to hypoxia for 24 h (Zhou et al., 2013; Cui et al., 2017) albeit in other cell types. Our data for up to 10 h of hypoxia exposure contradict the general consensus that SENP1 increases under hypoxia since *SENP1* is a hypoxic response gene in the HIF-1 pathway and engages in a transcriptional positive feedback loop with HIF-1α (Zhou et al., 2013; Cui et al., 2017). However, Kunz et al. (2016) did not detect significant changes in SENP1 levels in cells kept under hypoxic conditions at various time points up to 24 h, which provide a similar SENP1 expression pattern to our own data.

We found that SENP3 levels did not significantly change in HeLa cells exposed to hypoxia for 12 and 24 h but significantly decreased after prolonged (48 h) exposure. These results were consistent with previous reports of SENP3 levels under hypoxia for up to 24 h of exposure (Kunz et al., 2016). Kunz et al. (2016) also reported SENP2, SENP5, and SENP7 levels did not significantly change under hypoxia at different time points, suggesting that the decrease of SUMO-1 and SUMO-2/3 conjugation in hypoxic cells was not due to changes in protein levels of SENP family members. Given this, hypoxia may not directly affect SENP3 expression levels, though ROS accumulation generated in the mitochondria may increase SENP3 stability and expression, affecting SUMO-2/3-ylation levels (Huang et al., 2009; Kunz et al., 2016). Prolonged hypoxic exposure, however, can affect cell viability (Azad et al., 2008). The loss of SENP3 in cells after 48 h of exposure to hypoxia we observed could be attributed to cell death due to prolonged hypoxia rather than a change in protein expression levels. SENP3 has been identified as a redox sensor and SENP3 activity is regulated by oxygen levels. SENP3 regulates HIF-1 transcriptional activity under mild oxidative stress by deSUMOylating the HIF-1α coactivator p300, increasing p300 binding to HIF-1α and HIF-1α transactivation. Modest ROS also inhibits SENP3 degradation and regulates SENP3 localization to the nucleoplasm (Huang et al., 2009;

Wang et al. 2012). SENP3 also undergoes degradation during OGD in a process involving protein RNA(PKR)-like ER kinase (PERK), an essential player in unfolded protein response (UPR) pathways (Guo et al., 2013).

Many of our Western blots examining the effect of hypoxia on SENP levels were performed without replicates. In addition, the quality of Western blots among these experiments varied. Data from low quality blots were difficult to interpret and at times inconclusive or incomplete. So while some data for certain SENPs such as SENP3 show a more distinct pattern of expression under hypoxia, our findings are preliminary and more thorough investigation is required to conclude whether hypoxia treatment within our experimental setup affects the levels of different SENPs. With regard to SENP2, SENP5 and SENP7, our results showed that SENP5 levels in hypoxic conditions fluctuated over time, but SENP2 and SENP7 levels exhibited little or no change under hypoxia compared to under normoxia. SENP2 represses glycolysis and regulates glucose metabolism (Tang et al., 2013). Overexpression of SENP2 significantly decreases hypoxia-induced glycolysis (Agbor et al., 2011). Stable SENP2 levels under hypoxia may be necessary to regulate levels of SUMOylation involved in glycolytic flux that occurs in hypoxia. Currently there is a lack of information in the literature about SENP5, so whether SENP5 has a role in hypoxia or hypoxia-induced mitophagy remains unknown. SENP7 overexpression has been shown to protect cancer cells from OGD and is associated with poor prognosis in colon cancer (Gallardo-Chamizo et al., 2022). After examining the levels of SENP family members under hypoxia, we decided to focus on determining whether SENP1 and SENP3 have roles in hypoxia-induced autophagy and mitophagy in subsequent experiments. SENP1 and SENP3 are the best characterized out of the SENP family in relation to hypoxic cell stress, given SENP1's involvement with the HIF-1 pathway and SENP3's role in OGD response.

3.3.5 Roles of SENP1 and SENP3 in LC3-II induction by Hypoxia

As previously stated, SENP1 and SENP3 became the main proteins of interest in this chapter after examining how hypoxia affected the levels of SENP family proteins. SENP1 and SENP3 knockdowns were performed in HeLa cells to address the roles of the deSUMOylation enzymes on hypoxia-induced autophagy. Immunoblotting for LC3-II was performed after SENP1 or SENP3 KD to determine whether siRNA-mediated depletion of SENP1 and SENP3 affected autophagosome formation under hypoxia. Knockdown of SENP1 led to lack of LC3-II induction by hypoxia. Meanwhile, SENP3 KD led to no change in LC3-II induction under hypoxia. These results suggest that SENP1 may be necessary for LC3 lipidation, the phagophore expansion, and autophagosome formation upon general autophagy induced by hypoxia. They also suggest that the level of SENP3 may not directly affect those intracellular processes upon autophagy induction by hypoxia. This does not rule out SENP3 role(s) in the regulation of hypoxia-induced autophagy because LC3 is not required in the initiation of autophagy but rather mediate autophagosome formation (Rouschop et al., 2010) and SENP3 may be involved in other intracellular events essential for autophagy induction. It should be noted that these experiments were performed without replicates, and thus the results, while interesting, are preliminary and warrant follow-up experiments to corroborate our initial data. More investigation is needed to elucidate the roles of SENP1 and SENP3 in hypoxia-induced autophagy and hypoxia-induced mitophagy.

3.3.6 SENP1 overexpression does not increase LC3-II induction

Overexpression of SENP1 does not seem to increase LC3-II levels under normoxic conditions, implying that increase of SENP1 levels alone may not be responsible for LC3-II induction and perhaps stress conditions are necessary for such induction. Interestingly, findings from Kunz et al. (2016) that suggested that hypoxia inhibits the enzymatic activity of SENP1 in a reversible process, though the same group also suggested this hypoxic inactivation of SENP1 may serve to limit HIF-

1α accumulation in prolonged hypoxia (Kunz et al., 2016). The positive feedback loop between SENP1 and HIF-1α during hypoxia described by Cui et al. (2017) may explain why SENP1 overexpression under normoxia did not lead to LC3-II induction in our experimental system: HIF-1α induction by hypoxia and SENP1 may be required for LC3 lipidation. This experiment was performed without repeats, thus the findings presented here are preliminary. Further investigation is needed to determine if and how SENP1 affects LC3-II levels.

3.3.7 Detection of Hypoxia-induced Mitophagy with Mito-pHfluorin

Lastly, we were able to confirm hypoxia induces mitophagy in HeLa cells within our hypoxia experimental system with the use of fluorescence microscopy and the Mito-pHfluorin dual fluorescent probe. The levels of mitophagy in HeLa cells exposed to hypoxia were significantly increased compared to cells exposed to normoxia for the same duration of time. Longer durations of exposure to hypoxia led to increased levels of hypoxia-induced mitophagy as indicated by Mito-pHfluorin. Given these data, we chose 24 h as the optimal time point to examine hypoxia-induced mitophagy levels in future experimental procedures using immunofluorescence microscopy and Mito-pHfluorin in order to assess the role of proteins of interest such as SENP1 and SENP3 in hypoxia-induced mitophagy. This method will allow for detection of the presence a protein of interest or lack thereof (under siRNA-mediated KD) in fixed cells with immunostaining and reliable visualization of quantifiable levels of mitophagy in the cell between normoxia and hypoxia conditions.

In conclusion, this chapter highlights the protein expression profile of hypoxic cell response within the context of the HIF-1 pathway, SUMOylation and SENPs, and general autophagy. By examining the hypoxic protein expression profile with our hypoxia experimental system, we confirm that our experimental setup could elicit genuine hypoxic cell response in HeLa cells, the

cell line we primarily use in the rest of this thesis. Based on the preliminary results from our experiments that examined the effect of SENP1 and SENP3 KD on hypoxia-induced autophagy, we will further investigate SENP1 and SENP3 as possible proteins of interest in the regulation of hypoxia-induced mitophagy in this thesis. A hypoxia time course was performed on HeLa cells transfected with Mito-pHfluorin to visualize and quantify hypoxia-induced mitophagy in cells exposed to hypoxia for various durations of time with fluorescent confocal microscopy. We confirmed that within our experimental system, mitophagy was induced by hypoxia in HeLa cells significantly more than at basal, normoxic conditions. Not only did our data further support that the hypoxia induction in our experimental setup was genuine and robust, but it also showed that Mito-pHfluorin is a reliable marker for visualizing hypoxia-induced mitophagy with fluorescence microscopy. Equipped with these tools for inducing, visualizing, and quantifying hypoxia-induced mitophagy, we are able to delve further into investigating the role of SENP1, SENP3, and SUMOylation in regulating hypoxia-induced mitophagy with these tools in Chapter 4 and beyond.

Chapter 4

Regulation of Hypoxia-Induced Mitophagy by SUMOylation and DeSUMOylation Enzymes

4.1 Background

In this chapter, we investigated the roles of SUMO-1 and SUMO-2/3 proteins and deSUMOylation enzymes SENP1 and SENP3 in regulating HIM. We utilized siRNA-mediated knockdown of proteins of interest, transfection of Mito-pHfluorin, hypoxia induction, and immunofluorescence microscopy to compare the average number of red puncta per cell in each experimental condition, as an indication the levels of mitophagy occurring in the cells.

Hypoxia-induced mitochondrial dysfunction is associated with various human diseases including cancer, Alzheimer's disease and cardiac ischemia/reperfusion injury (He et al., 2020). The conjugation of SUMO-1 and SUMO-2/3 has been reported to increase under hypoxia (Comerford et al., 2003; Agbor et al., 2011; Kunz et al., 2016). SUMOylation plays a regulatory role in cardiovascular diseases such as cardiac hypertrophy, hypertension, atherosclerosis and cardiac ischemia-reperfusion injury (Xiao et al., 2022). SUMOylation regulates mitochondrial dysfunction and mitophagy (Kim et al., 2021; He et al., 2020), which contribute to the development and progression of cardiovascular diseases (Kim et al., 2021; Huynh et al., 2021; Vasquez-Trincado et al., 2016; Silveirinha et al., 2013). SUMOylation appears to have a protective function under hypoxia. Dynamin-related protein 1 (Drp1) is a key regulator of mitochondrial fission and a SUMO-1 target protein (Harder et al., 2004; Figueroa-Romero et al., 2009). SUMOylation of Drp1 is involved in regulating mitochondrial fission (Harder et al., 2004; Zunino et al., 2007). Accumulation of SUMO-1 was reported to protect endogenous Drp1 from lysosomal degradation by stabilizing Drp1, which results in increased mitochondrial fragmentation (Harder

et al., 2004). The level of SUMO-1 modification of proteins in hypoxia/reoxygenation has been reported to be regulated by zinc in order to protect cardiomyocytes from ischemia/reperfusion injury (Bian et al., 2019). Bian et al. (2019) found that SUMOylation of Drp1 induced by zinc regulates mitophagy and contributes to the protective effect of zinc on hypoxia/reoxygenation injury. In mouse models of cerebral or cardiac ischemia and cellular models of ischemia, an increase of SUMOylation is associated with tolerance against hypoxia (Yang et al., 2008; Loftus et al., 2009; Guo et al., 2013). SUMO-2/3-ylated Drp1 inhibits mitochondrial fission and cytochrome c release (Guo et al., 2013; He et al., 2020). The interaction between mitofusins (MFNs) and SUMO-2 through SUMOylation promotes lysosomal degradation of mitochondria (Kim et al., 2021; Juncker et al., 2021). While it is known that SUMOylation is regulated by hypoxia and has roles in regulating mitochondrial dynamics, the specific pathways that SUMOylation participates in to regulate HIM remain unknown.

TAK-981 is an inhibitor of SUMO-activating enzymes (SAEs, SAE1 and SAE2) used in the treatment of cancer (Langston et al., 2021). SUMOylation of proteins occurs in an enzymatic cascade, the first step of which involves activation of SUMO through an ATP-dependent process catalyzed by SAEs (Desterro et al., 1999). TAK-981 inhibits SAEs by forming a SUMO-TAK-981 adduct as the inhibitory species within the SAE enzyme catalytic site (Langston et al., 2021). In the present study, TAK-981 was used in microscopy experiments as an alternative method of SUMOylation inhibition to siRNA-mediated knockdown of SUMO-1 and SUMO-2/3. Preventing SUMOylation with TAK-981 treatment could provide supporting evidence to confirm the effect of SUMOylation inhibition on HIM in HeLa cells. In theory, TAK-981 treatment may elicit a similar effect on mitophagy as the knockdown of both SUMO-1 and SUMO-2/3. TAK-981 interferes with SUMO protein conjugation that would mimic reduced SUMO-1-ylation and SUMO-2/3-ylation due to the depletion of conjugatable SUMO moieties (*i.e.* SUMO-1 and SUMO-2/3) by RNAi-mediated silencing of gene expression through the RISC complex, which

uses the siRNA as a template to recognize complementary mRNA encoding for the protein of interest and activates RNase to cleave the RNA (Hammond et al., 2000; Tuschl et al., 1999; Elbashir et al., 2001a; Elbashir et al., 2001b).

SENP1 and SENP3 activity are both affected by hypoxia (Kunz et al., 2016). In Chapter 3, our results suggested that SENP1 but not SENP3 may regulate the formation of autophagosomes during hypoxia-induced autophagy. In this chapter, we performed RNAi-mediated knockdown of SENP1 and SENP3 in HeLa cells transfected with Mito-pHfluorin and exposed to hypoxia to investigate the effect of the deSUMOylation enzymes on HIM.

4.2 Results

4.2.1 The Effects of RNAi-mediated Depletion of SUMO-1 or SUMO-2/3 on Hypoxia-induced Mitophagy

HeLa cells were transfected with Mito-pHfluorin and Nsi or SUMO-1-specific siRNA or SUMO-2/3-specific siRNA for 48 h, and then exposed to normoxia or hypoxia for a further 24 h (**Figures 4.1** and **4.2**). As shown in **Figure 4.1b**, SUMO-1 knockdown (KD) in HeLa cells did not change the levels of mitophagy under normoxia. SUMO-1 KD did reduce but not abolish the induction of mitophagy by hypoxia, since there was still a non-significant increase in levels of mitophagy in SUMO-1 KD cells exposed to hypoxia compared to those exposed to normoxia.

As shown in **Figure 4.2b**, mitophagy levels in SUMO-2/3 KD cells were significantly higher than the levels in cells transfected with Nsi under both normoxic and hypoxic conditions. SUMO-2/3 KD also did not prevent induction of mitophagy by hypoxia. There was a significant increase of levels of mitophagy in SUMO-2/3 KD cells exposed to hypoxia compared to those exposed to normoxia.

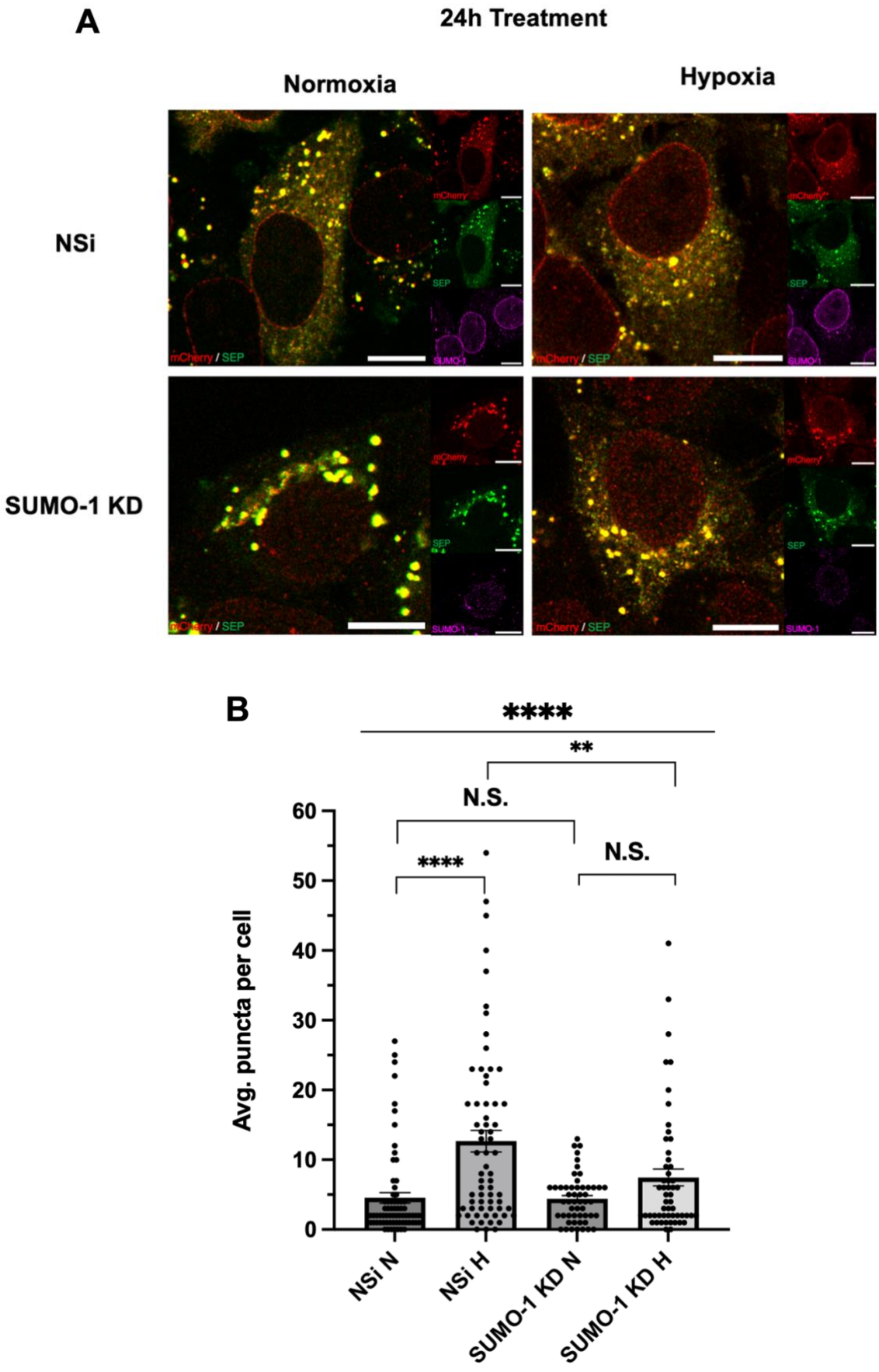
A
24h Treatment
Normoxia
Hypoxia
NSi
SUMO-1 KD
mCherry / SEP
mCherry
SEP
SUMO-1
B
****
**
N.S.
N.S.
****
Avg. puncta per cell
60
50
40
30
20
10
0
NSi N
NSi H
SUMO-1 KD N
SUMO-1 KD H

Figure 4.1: The Effect of SUMO-1 KD on Hypoxia-induced Mitophagy in HeLa cells

A) HeLa cells were transfected with Mito-pHfluorin and Nsi or SUMO-1-specific siRNA (50 nM). 48 h post-transfection the cells were exposed to normoxia or hypoxia (1% O_2) for 24 h. The cells were fixed with PFA 4% and stained for SUMO-1 and then imaged with confocal microscopy. B) Histogram shows average number of Mito-pHfluorin red puncta per cell for cells exposed to N or H for 24 h. (n = 52-71, N.S. non-significant; **p < 0.01; ****p < 0.0001, Ordinary one-way ANOVA). Scale bar 10 μm. The data presented are from a single experiment. n refers to the number of cells from one μ-dish used to quantify the average number of puncta per experimental condition.

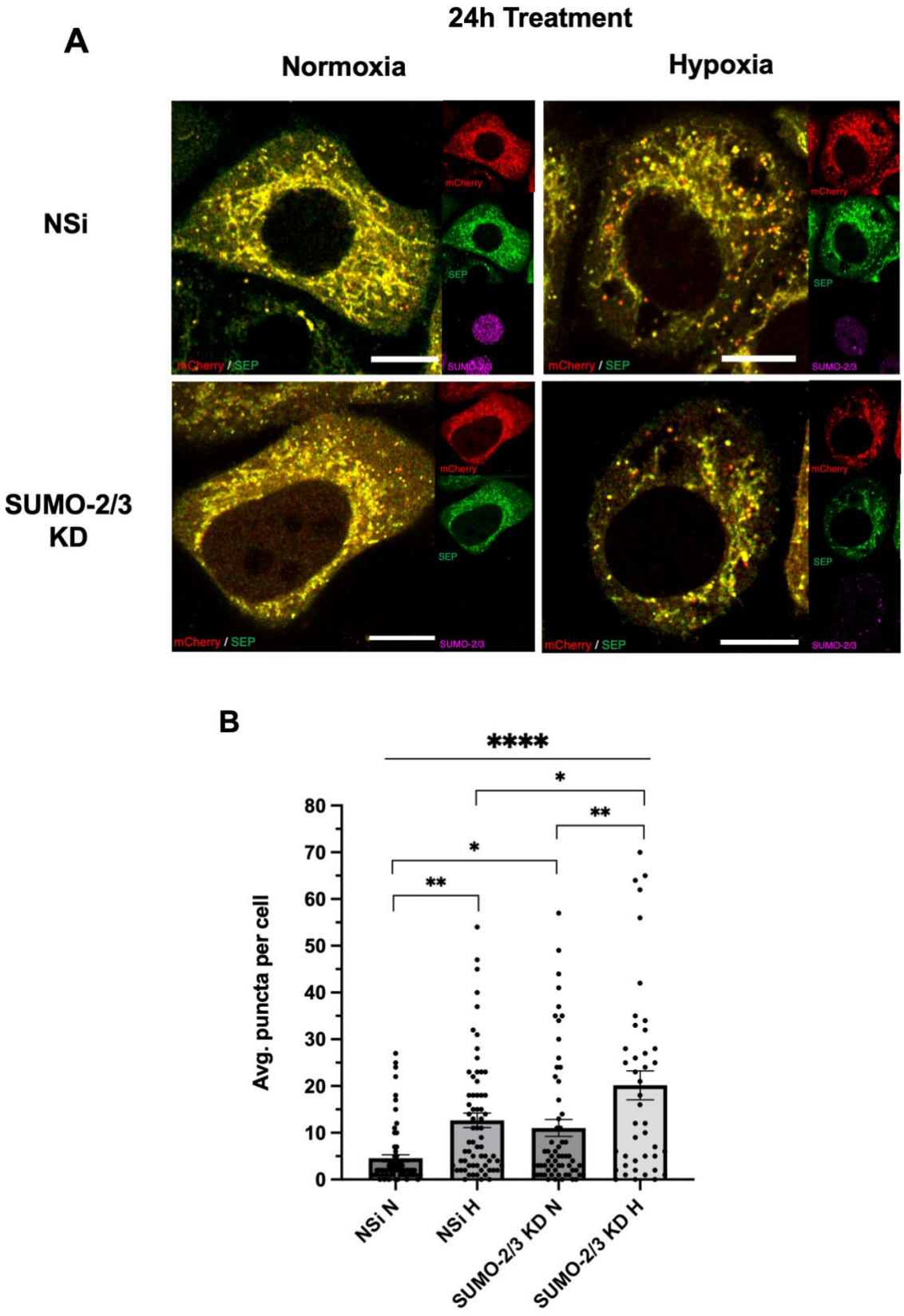
A
24h Treatment
Normoxia
Hypoxia
NSi
SUMO-2/3 KD
mCherry
SEP
SUMO-2/3
mCherry / SEP
B
Avg. puncta per cell
0
10
20
30
40
50
60
70
80
****
*
**
*
**
NSi N
NSi H
SUMO-2/3 KD N
SUMO-2/3 KD H

Figure 4.2: The Effect of SUMO-2/3 KD on Hypoxia-induced Mitophagy in HeLa cells

A) HeLa cells were transfected with Mito-pHfluorin and Nsi or SUMO-2/3-specific siRNA (50 nM). 48 h post-transfection the cells were exposed to normoxia or hypoxia (1% O_2) for 24 h. The cells were fixed with PFA 4% and stained for SUMO-2/3 and then imaged with confocal microscopy. B) Histogram shows average number of Mito-pHfluorin red puncta per cell for cells exposed to N or H for 24 h. (n = 42-71, *p < 0.05; **p < 0.01; ****p < 0.0001, Ordinary one-way ANOVA). Scale bar 10 μm. The data presented are from a single experiment. n refers to the number of cells from one μ-dish used to quantify the average number of puncta per experimental condition.

4.2.2 The Effect of TAK-981-mediated SUMOylation Inhibition on Hypoxia-induced Mitophagy

HeLa cells were transfected with Mito-pHfluorin for 48 h, and treated with DMSO or TAK-981 and then exposed to normoxia or hypoxia for a further 24 h (**Figure 4.3**). As shown in **Figure 4.3b**, mitophagy levels in TAK-981-treated cells were significantly higher than those in DMSO-treated cells under both normoxic and hypoxic conditions. TAK-981 treatment did not prevent induction of mitophagy under hypoxia. There was a significant increase in the levels of mitophagy in TAK-981-treated cells exposed to hypoxia compared to cells exposed to normoxia.

To confirm the effect of TAK-981 treatment on the inhibition of SUMO-1 and SUMO-2/3-ylation in HeLa cells, cells were treated with increasing concentrations of TAK-981 (0 to 1000 nM) for 4 h. Whole cell lysates were collected and Western blots were performed to detect SUMO-1 and SUMO-2/3 levels (**Figure 4.4a-b**). As TAK-981 concentrations were increased, both SUMO-1 and SUMO-2/3 conjugates decreased while levels of free SUMO-1 and SUMO-2/3 increased.

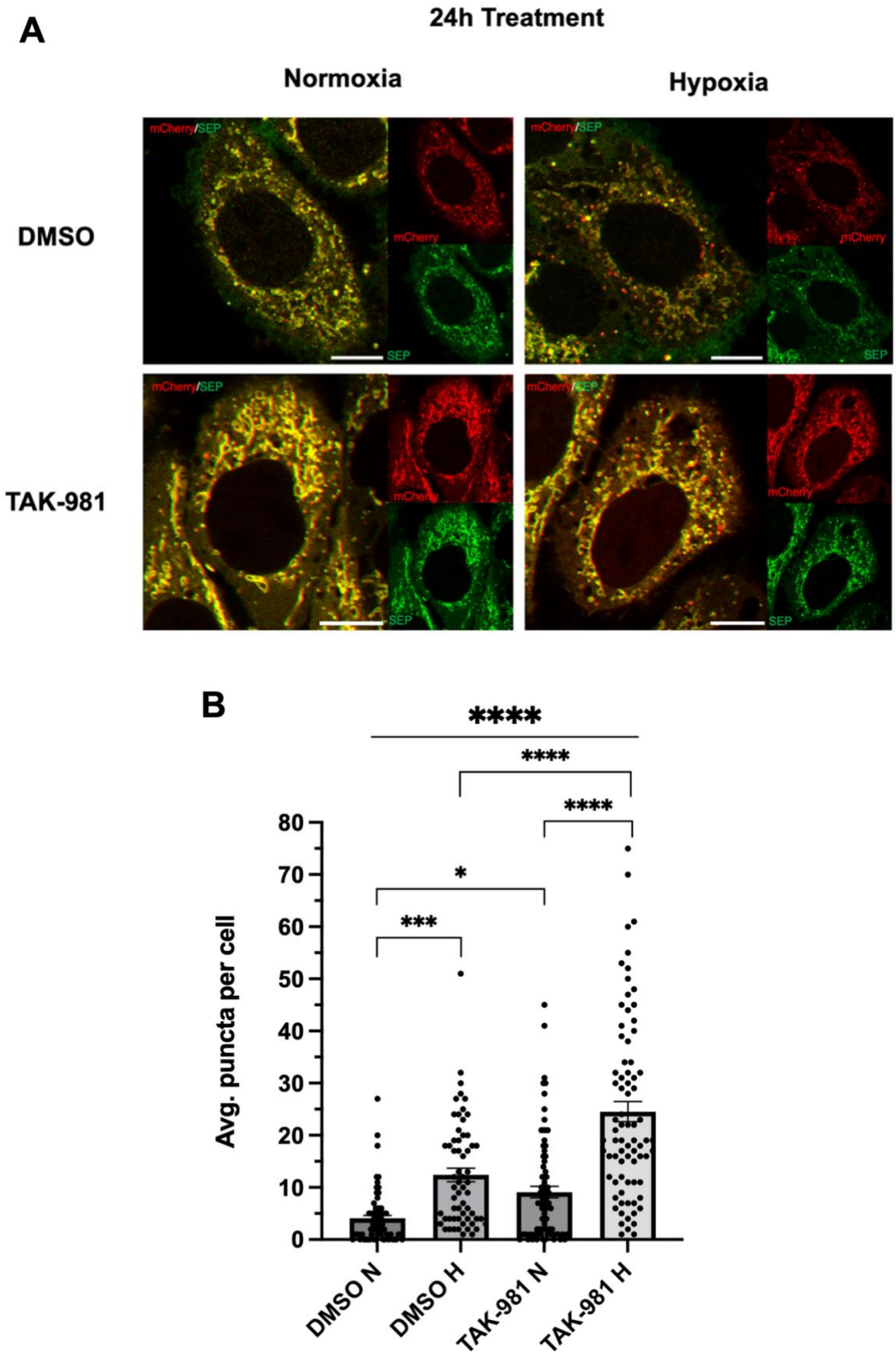
A
24h Treatment
Normoxia
Hypoxia
DMSO
TAK-981
mCherry/SEP
mCherry
SEP
B
****
****
****
*
***
Avg. puncta per cell
80
70
60
50
40
30
20
10
0
DMSO N
DMSO H
TAK-981 N
TAK-981 H

Figure 4.3: The Effect of TAK-981 Treatment on Hypoxia-induced Mitophagy in HeLa cells

A) HeLa cells were transfected with Mito-pHfluorin. 48 h post-transfection the cells were treated with DMSO or TAK-981 (100 nM) and exposed to normoxia or hypoxia (1% O_2) for 24 h. The cells were imaged with confocal microscopy. B) Histogram shows average number of Mito-pHfluorin red puncta per cell for cells treated with DMSO or TAK-981 under and exposed to N or H for 24 h. (n = 62-81, *p < 0.05; ***p < 0.001; ****p < 0.0001, Ordinary one-way ANOVA). Scale bar 10 μm. The data presented are from a single experiment. n refers to the number of cells from one μ-dish used to quantify the average number of puncta per experimental condition.

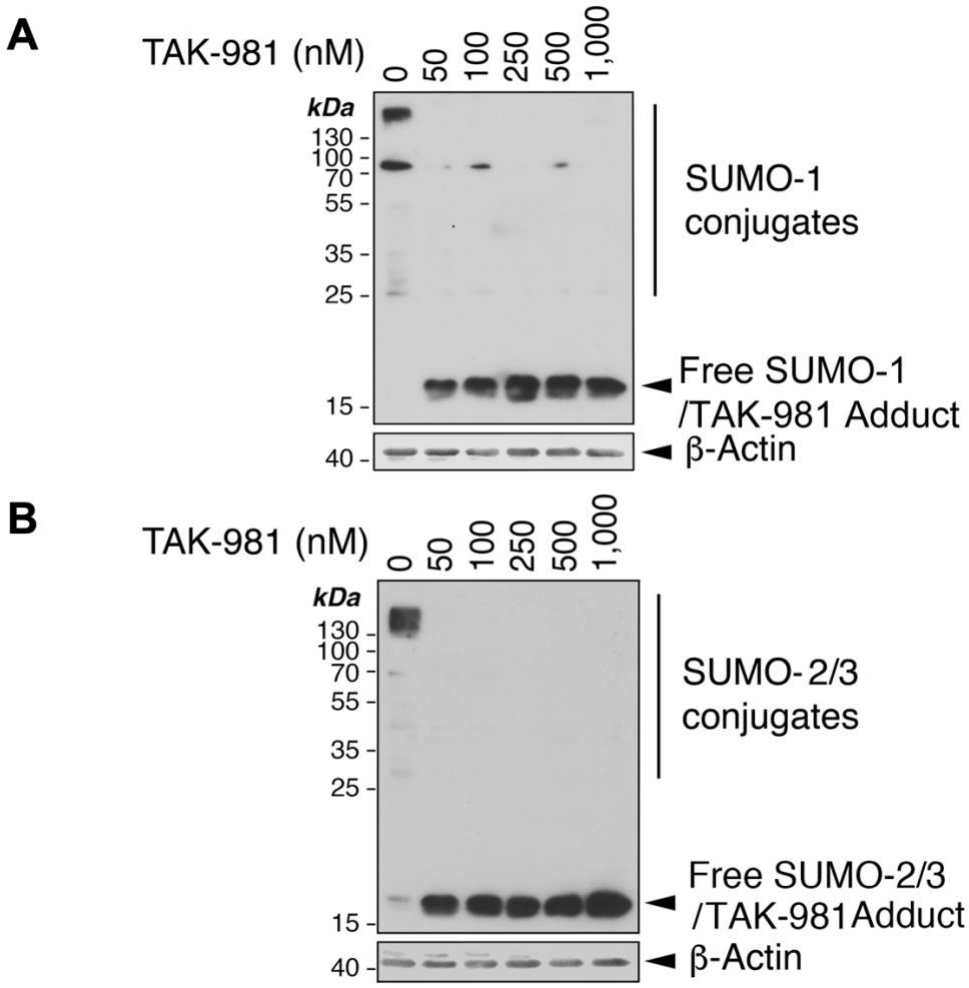

Figure 4.4: TAK-981 Treatment inhibits SUMO-1 and SUMO-2/3 conjugation and increases free SUMO-1 and SUMO-2/3 levels

Immunoblots for SUMO-1 (A) and SUMO-2/3 (B) in HeLa cells treated with increasing concentrations of TAK-981 (0-1000 nM) for 4 h.

4.2.3 The Role of SENP1 in Hypoxia-Induced Mitophagy

In Chapter 3, our results suggested that SENP1 is important for LC3-II induction by hypoxia, which may indicate that SENP1 regulates autophagosome formation under hypoxia through an unknown mechanism. In order to investigate the effect of SENP1 on HIM, we knocked down SENP1 in HeLa cells transfected with Mito-pHfluorin and then exposed the cells to hypoxia for 24 h. The cells were fixed with 4% PFA and stained for SENP1. Finally, the cells were visualized with a confocal microscope (**Figure 4.5**). Unexpectedly, SENP1 knockdown did not lead to significant changes in the average number of red puncta quantified (**Figure 4.5b**), suggesting that SENP1 levels may not be involved in regulating HIM in HeLa cells.

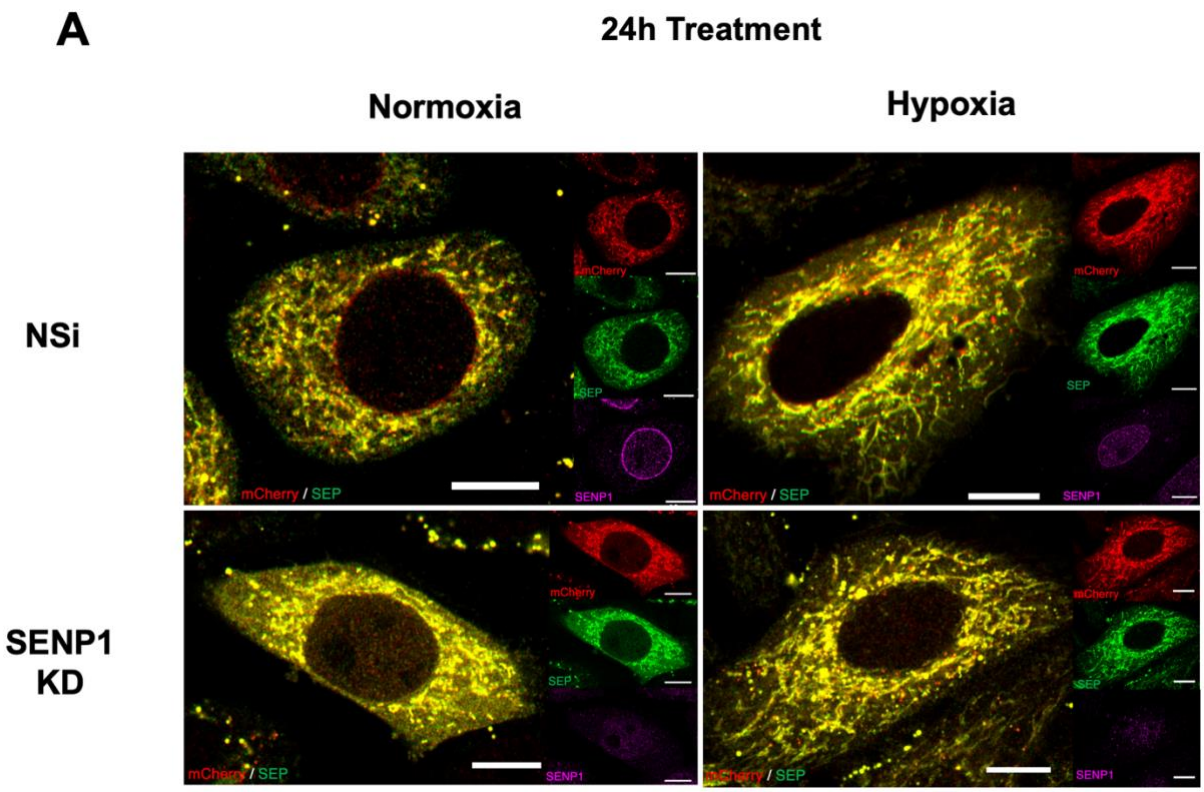
A
24h Treatment
Normoxia
Hypoxia
NSi
SENP1 KD
mCherry / SEP
SENP1
mCherry
SEP

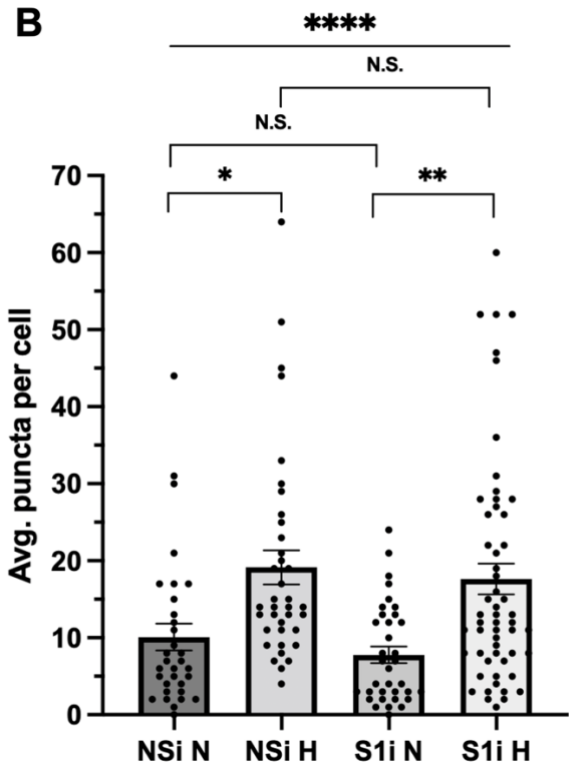
B
****
N.S.
N.S.
*
**
Avg. puncta per cell
0
10
20
30
40
50
60
70
NSi N
NSi H
S1i N
S1i H

Figure 4.5: The Effect of SENP1 KD on Hypoxia-Induced Mitophagy in HeLa cells

A) HeLa cells were transfected with Mito-pHfluorin and Nsi or SENP1-specific siRNA (50 nM). 48 h post-transfection the cells were exposed to normoxia or hypoxia (1% O_2) for 24 h. The cells were fixed with PFA 4% and stained for SENP1 and then imaged with confocal microscopy. B) Histogram shows average number of Mito-pHfluorin red puncta per cell for cells exposed to N or H for 24 h. (n = 32-55, N.S. non-significant; *p < 0.05; **p < 0.01; ****p < 0.0001, Ordinary one-way ANOVA). Scale bar 10 μm. The data presented are from a single experiment. n refers to the number of cells from one μ-dish used to quantify the average number of puncta per experimental condition.

4.2.4 The Role of SENP3 in Hypoxia-Induced Mitophagy

Our data in Chapter 3 suggested that SENP3 levels do not directly affect the formation of autophagosomes through LC3-II induction by hypoxia. However, it has been reported that SENP3 activity is affected by hypoxia (Kunz et al., 2016) and that Fis1, a target of deSUMOylation for SENP3, is involved in a form of Parkin-independent mitophagy (Waters et al., 2022). Therefore, we investigated the role of SENP3 in HIM by performing a SENP3 knockdown in HeLa cells transfected with Mito-pHfluorin. The cells were then exposed to normoxia or hypoxia for 24 h, fixed with 4% PFA, stained for SENP3 and visualized with a confocal microscope (**Figure 4.6**). Knocking down SENP3 in cells led to a significant decrease in mitophagy levels under hypoxic conditions and a non-significant decrease in mitophagy levels under normoxic conditions compared to cells transfected with Nsi. There was no significant difference in the levels of mitophagy between SENP3 KD cells exposed to normoxia and hypoxia, indicating that SENP3 KD may prevent induction of mitophagy by hypoxia (**Figure 4.6b**).

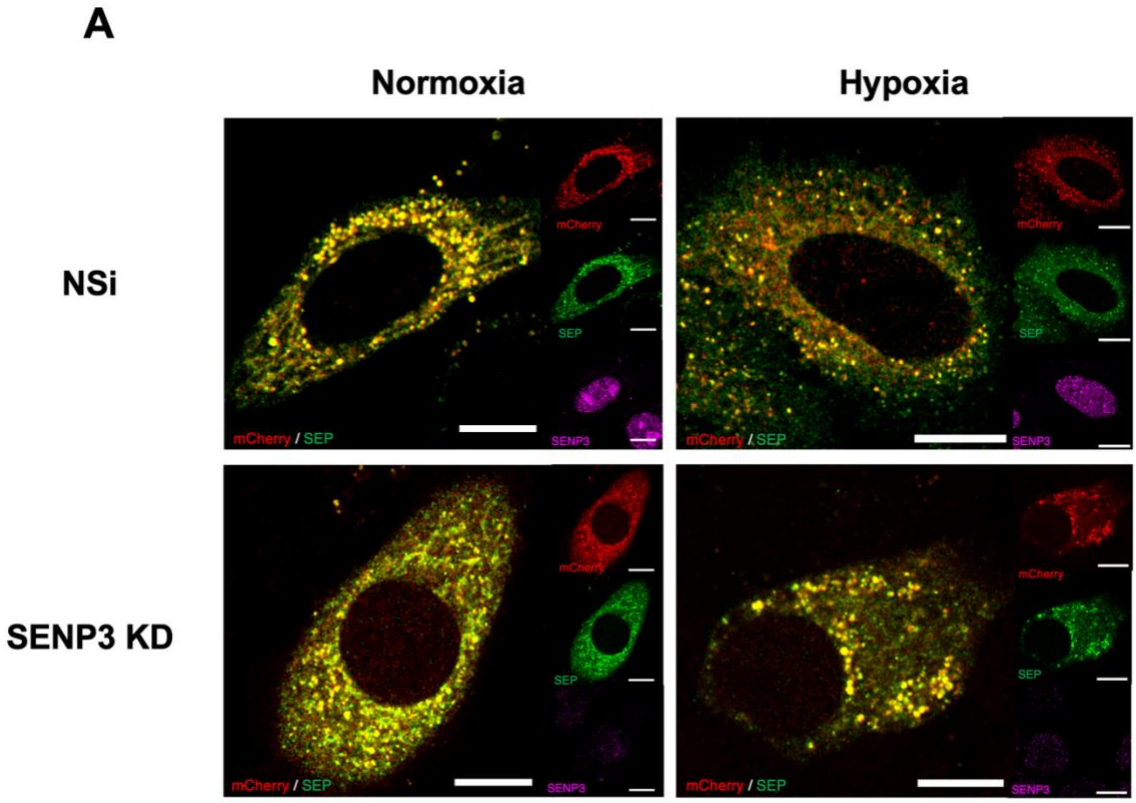
A
Normoxia
Hypoxia
NSi
SENP3 KD
mCherry
SEP
SENP3
mCherry / SEP

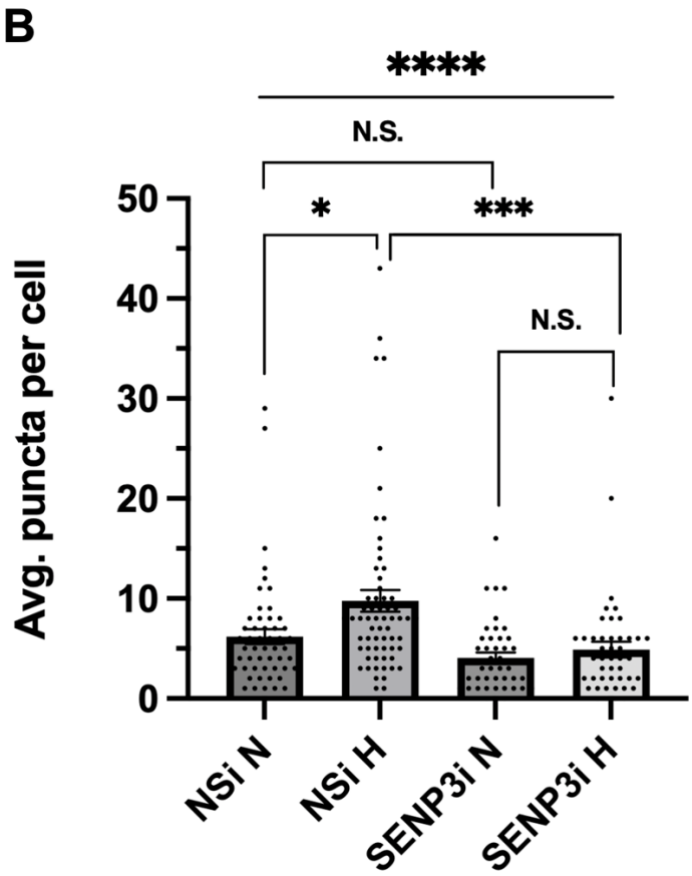
B
****
N.S.
*
***
N.S.
Avg. puncta per cell
50
40
30
20
10
0
NSi N
NSi H
SENP3i N
SENP3i H

Figure 4.6: The Effect of SENP3 KD on Hypoxia-induced Mitophagy in HeLa cells

A) HeLa cells were transfected with Mito-pHfluorin and Nsi or SENP3-specific siRNA (50 nM). 48 h post-transfection the cells were exposed to normoxia or hypoxia (1% O_2) for 24 h. The cells were fixed with PFA 4% and stained for SENP3 and then imaged with confocal microscopy. B) Histogram shows average number of Mito-pHfluorin red puncta per cell for cells exposed to N or H for 24 h. (n = 42-63, N.S. non-significant; *p < 0.05; ***p < 0.001; ****p < 0.0001, Ordinary one-way ANOVA). Scale bar 10 µm. The data presented are from a single experiment. n refers to the number of cells from one µ-dish used to quantify the average number of puncta per experimental condition.

4.3 Discussion

Figure 4.7 summarizes the main findings covered in Chapter 4 along with proposed mechanisms of HIM regulation to be discussed in the current section, **4.3**.

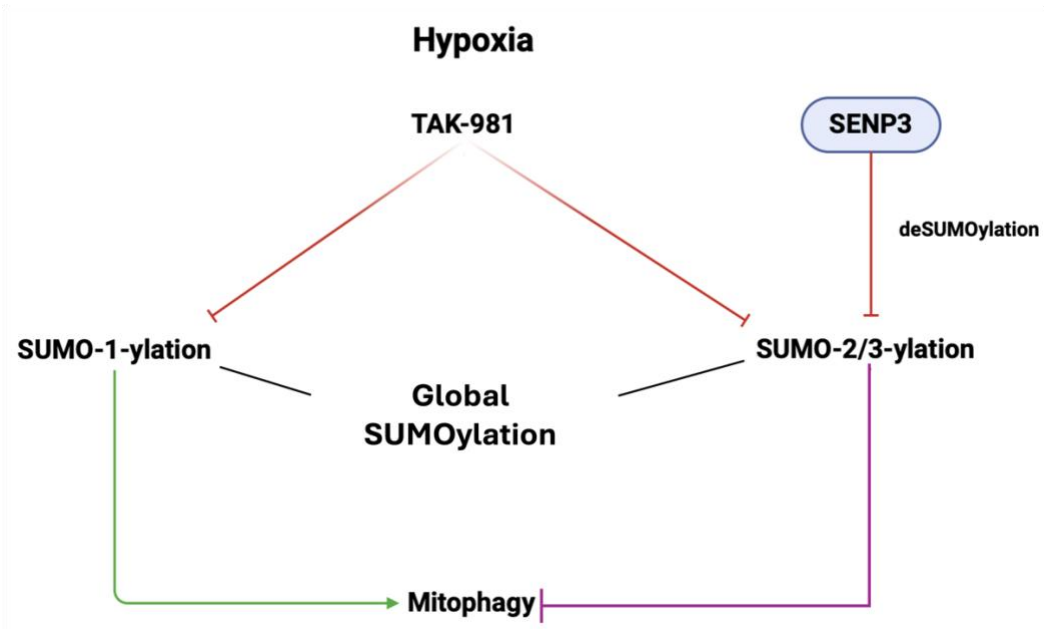

Figure 4.7: Summary of Chapter 4 Findings

Global SUMOylation suppresses hypoxia-induced mitophagy (HIM). Inhibition of SUMOylation through TAK-981 treatment promotes HIM. SUMO-1-ylation appears to positively regulates HIM,

while SUMO-2/3-ylation suppresses it. Based on these findings, the effect of global SUMOylation on HIM skews in favor of SUMO-2/3 rather than SUMO-1. SENP3, which preferentially deSUMOylates SUMO-2/3 conjugates, appears to be important for inducing mitophagy under hypoxic conditions.

4.3.1 SUMO Depletion and SUMOylation Inhibition

Hypoxia enhances SUMO modification of a subset of target proteins (Kunz et al., 2016). SUMOylation is known to regulate mitochondrial dysfunction and mitophagy (Kim et al., 2021; He et al., 2020). Here, we investigated whether SUMO-1 and SUMO-2/3 have roles in regulating hypoxia-induced mitophagy. Interestingly, RNAi-mediated SUMO-1 depletion does not appear to affect basal mitophagy levels under normoxic conditions but significantly reduces HIM, suggesting the importance of SUMO-1 and likely SUMO-1-ylation in maintaining the levels of mitophagy under hypoxic conditions. In contrast, RNAi-mediated SUMO-2/3 depletion significantly increases mitophagy levels under both normoxic and hypoxic conditions, suggesting the importance of SUMO-2/3 and likely SUMO-2/3-ylation in suppressing the levels of mitophagy under the two conditions. These findings from our SUMO KD experiments suggest that SUMO paralogues may have specific functions in regulating mitophagy in different experimental settings.

Similar to RNAi-mediated SUMO-2/3 depletion, TAK-981 treatment, which inhibits the levels of global SUMO-1-ylation and SUMO-2/3-ylation, significantly increases mitophagy levels under normoxic and hypoxic conditions. Altogether, these results indicate a collective role for SUMOylation in regulating HIM, especially in suppressing mitophagy in model HeLa cells. These results are consistent with previous findings by Princz et al. (2020) in *C. elegans* where reduced SUMO (encoded by *smo-1* in *C. elegans*) resulted in induction of mitophagy in neurons.

It should be noted that SUMO might regulate mitophagy in a tissue-specific manner as the group also found that reduced SUMO inhibited mitophagy in muscle cells (Princz et al., 2020).

Mitophagy is a key process in the homeostasis of mitochondria, but mitophagy may also exert deleterious effects on cells if it is defective or excessive. In our hypoxia model, SUMO-2/3-ylation may suppress harmful excess levels of mitophagy. Thus, significantly increased mitophagy in HeLa cells following RNAi-mediated depletion of SUMO-2/3 and reduction of SUMO-2/3-conjugates by TAK-981 treatment is most likely due to the loss of inhibitory regulation of SUMOylation under both normoxic and hypoxic conditions.

4.3.2 SENP1 knockdown does not affect HIM levels

We have shown in this chapter that RNAi-mediated depletion of SUMO-1 reduces the levels of hypoxia-induced mitophagy. Because SENP1 is primarily responsible for deSUMOylation of SUMO-1 conjugates (Sharma et al., 2013), SENP1 knockdown would enhance SUMO-1-ylation to promote HIM. Unexpectedly, we found that RNAi-mediated knockdown of SENP1 in HeLa cells did not cause significant changes in the level of HIM or mitophagy under normoxia. In addition to SENP1, other SENP family members (*i.e.* SENP2, SENP3, and SENP5) are also capable of deconjugating SUMO-1 from SUMOylated proteins (Alegre & Reverter, 2011). One explanation for the unexpected finding is that other SENP family members may compensate for the siRNA-mediated depletion of SENP1 in HeLa cells and deSUMOylate SUMO-conjugates that SENP1 would normally target.

The effect of RNAi-mediated depletion of SENP1 on HIM in HeLa cells also seems to contradict what we have shown. In Chapter 3, we showed that RNAi-mediated depletion of SENP1 prevents induction of LC3-II in HeLa cells exposed to hypoxia. This implies that SENP1 somehow regulates phagophore elongation or autophagosome formation under hypoxia since LC3-II mediates those processes, and that LC3-II induction under hypoxia may not be essential

for induction of mitophagy by hypoxia. Another possibility is that basal levels of LC3-II in HeLa cells might be sufficient for mitophagic phagophore elongation or autophagosome formation required for HIM. In this respect, further investigation is needed to explore mechanism(s) and functional consequences of SENP1-dependent LC3-II induction by hypoxia.

4.3.3 SENP3 knockdown reduces HIM levels

We have shown in this chapter that RNAi-mediated depletion of SUMO-2/3 enhances the levels of mitophagy under normoxic and hypoxic conditions. Because SENP3 is primarily responsible for deconjugating SUMO-2/3 from SUMOylated proteins (Guo et al., 2013), SENP3 knockdown would enhance SUMO-2/3-ylation to suppress hypoxia-induced mitophagy. As expected, our results show that RNAi-mediated depletion of SENP3 led to a lack of induction of mitophagy under hypoxia, indicating an important role for SENP3 in HIM. In Chapter 3, when we knocked down SENP3 to assess the effect of SENP3 depletion on LC3-II levels, we did not find a significant difference in LC3-II levels between HeLa cells transfected with SENP3i and Nsi under normoxia or hypoxia. This suggests that SENP3 is not required for induction of LC3-II by hypoxia. Therefore, SENP3-dependent regulation of HIM seems to be independent of LC3-lipidation induced by hypoxia but dependent on mito-autolysosome formation as evidenced by our results based on Mito-pHfluorin.

The possible mechanism for SENP3-mediated regulation of HIM may involve deSUMO-2/3-ylation of OMM proteins such as FKBP8 or Fis1. FKBP8 is known to regulate Parkin-independent mitophagy (Yoo et al., 2020). In the present study, we have validated FKBP8 has a genuine target for SUMOylation and identified the key lysine (i.e., K335) for SUMO conjugation. However, unfortunately our results do not support a major role for FKBP8 SUMOylation in HIM regulation (see Chapter 5). Moreover, SENP3 has been reported to deSUMOylate Fis1 in regulating Parkin-independent mitophagy (Waters et al. 2022). Since DFP- and hypoxia-induced

mitophagy are both Parkin-independent forms of mitophagy, Fis1 may potentially regulate HIM in a similar manner as it does in DFP-induced mitophagy. SENP3 is necessary for Fis1-mediated DFP-induced mitophagy and the K149 residue on the C-terminus of Fis1 is required for Fis1 SUMOylation (Waters et al., 2022). DFP treatment downregulates CHIP, preventing degradation of SENP3, which enhances SENP3-mediated deSUMOylation of Fis1. DeSUMOylation of Fis1 or the prevention of Fis1 SUMOylation enhances localization of Fis1 to the mitochondria to participate in stress-induced mitophagy (Waters et al., 2022).

In summary, we have evidence that SUMOylation plays an inhibitory role in regulating hypoxia-induced mitophagy. SENP1 does not appear to have a direct effect on levels of HIM but may instead act on hypoxia-induced autophagy, namely autophagosome formation, because it is involved in induction of LC3-II under hypoxia. SENP3 appears to have an important role in the induction of mitophagy under hypoxia because SENP3 KD under hypoxia prevented induction of mitophagy. In the next chapter, we investigate FKBP8- and Fis1-mediated regulation of HIM.

Chapter 5

FKBP8- and Fis1-mediated Regulation of Hypoxia-Induced Mitophagy

5.1 Background

5.1.1 FKBP8

FKBP8 (aka FKBP38) is a protein anchored on the OMM and a member of the FKBP family. Proteins in the FKBP family possesses a FK506 binding domain and peptidyl isomerase activity, but only the peptidyl isomerase activity of FKBP8 is activated upon binding to calmodulin (Edlich et al., 2005). FKBP8 is a co-chaperone protein for the cystic fibrosis transmembrane conductance regulator (CTFR) in cystic fibrosis (Banasavadi-Siddegowda et al., 2011). FKBP8 also anchors the proteasome to the mitochondria and inhibits apoptosis by binding to Bcl-2 (Shirane & Nakayama, 2003; Nakagawa et al., 2007). FKBP8 is recruited to the site of mitochondria undergoing mitophagy in stress conditions and plays a role in mitochondrial fragmentation and mitophagy under hypoxia (Yoo et al., 2020). Yoo et al. (2020) found that FKBP8 has an LC3-interacting region (LIR) motif-like sequence (LIRL) and a LIR motif on the N-terminus of FKBP8 that are necessary for inducing mitochondrial fragmentation. The study suggested that FKBP8 has an essential role in mitochondrial fragmentation through LIRL during mitophagy and that FKBP8 together with LIR is needed for mitophagy under stress conditions including hypoxia (Yoo et al., 2020). In a mass spectrometry (MS)-based proteomics investigation for endogenous SUMO-2/3-ylation sites, FKBP8 was reported to have multiple SUMO-2/3-ylation sites including at K335 (Hendriks et al., 2018). Whether the SUMOylation of FKBP8 regulates hypoxia-induced mitophagy remained unknown. In this chapter, we investigated whether FKBP8 levels were affected by hypoxia in HeLa cells and then explored the effect of FKBP8 on HIM levels. To

address whether SUMOylation of FKBP8 regulates HIM, we first validated whether FKBP8 is a *bona fide* SUMOylation target with histidine pulldown (His-PD) and then tested whether changes to the SUMOylation status of FKBP8 affected levels of HIM.

5.1.2 Mitochondrial dynamics and Fis1

Mitochondrial fusion is the merging of two distinct mitochondria, while mitochondrial fission is the separation of one mitochondrion into two mitochondria (Sebastian & Zorzano, 2018). Fusion and fission counterbalance one another, controlling the fate of mitochondrial structure (Scorrano, 2013; Y. J. Liu et al., 2020). In mammalian cells, fusion is coordinated by fusion proteins, MFN1 and MFN2 on the OMM and optic atrophy 1 (OPA1) on the IMM, in distinct sequential events (Malka et al., 2005; Song et al., 2009). MFN1 and MFN2 are dynamin-like GTPases anchored to the OMM and GTP hydrolysis drives the fusion of OMMs, which causes a conformational change that brings opposing membranes in contact with each other (Wai & Langer, 2016; Chen et al., 2003; Cao et al., 2017; Y.J. Liu et al., 2020). Similarly, OPA1 is a dynamin-like GTPase anchored to the IMM and mediates the fusion of IMMs (Delettre et al., 2000). Loss of fusion proteins results in mitochondrial fragmentation (Y.J. Liu et al., 2020). Mitofusion degradation is regulated by ubiquitylation and phosphorylation, while mitofusin synthesis is regulated transcriptionally and post-transcriptionally. OPA1 is regulated both post-transcriptionally and post-translationally (Wai & Langer, 2016).

Fission involves recruitment of the ER to a constriction site, where the mitochondrion will be separated. Initiation of fission begins with replication of mtDNA in the mitochondrial matrix, which marks the site of recruitment of the ER (Y.J. Liu et al., 2020). In mammalian cells, OMM-bound proteins including the mitochondrial fission 1 protein (Fis1), Mff, MID49 and MID50 recruit the large GTPase Drp1 to the mitochondrial surface to aid in ER-mediated constriction (Losón et al., 2013; Y.J. Liu et al., 2020). Fis1 has been reported to promote mitochondrial

fragmentation both through activating fission and inhibiting fusion. In humans, Fis1 regulates mitochondrial dynamics by inhibiting fusion machinery, specifically through preventing the GTPase activity of fusion proteins MFN1, MFN2, and OPA1 (Yu et al., 2019). Findings from a study by Twig et al. (2008) suggest that mitochondrial fission events segregate damaged or dysfunctional daughter mitochondria from metabolically healthy ones, enabling the subsequent removal of the damaged daughter organelle through mitophagy.

Fis1 mediates fission upstream of mitophagy and also has roles in mitophagy (Shen et al., 2014; Ihenacho et al., 2021). Fis1 aids in limiting autophagosome formation by recruiting GTPase activating proteins (GAPs) TBC1D15 and TBC1D17 to sites of mitophagy (Yamano et al., 2014). Recently, more evidence has emerged describing the role of Fis1 in mitophagy induced by stressors such as antimycin A, paraquat or deferiprone (DFP) (Shen et al., 2014; Yamano et al., 2014; Waters et al., 2022; Wilkinson & Guo, 2022). Iron chelation caused by DFP leads to Parkin-independent mitophagy and SENP3 is essential for DFP-induced mitophagy (Waters et al., 2022). Fis1 was identified in a proteomic screen as a target for SUMOylation *in vivo* (Tirard et al., 2012). Waters et al. (2022) demonstrated that Fis1 was a novel SUMO target deSUMOylated by SENP3 and necessary for DFP-induced mitophagy. The K149 residue on the C-terminus of Fis1 is required for Fis1 SUMOylation (Waters et al., 2022). Mitochondrial fission has been reported to be involved in mitophagy (Twig et al., 2008; Mao et al., 2013). Given that Fis1 is a mitochondrial fission protein that is regulated by SUMOylation in a Parkin-independent form of mitophagy, in this chapter we first investigated whether Fis1 levels were affected by hypoxia in HeLa cells. Then we explored the effect of Fis1 knockout (KO) and knockdown on levels of hypoxia-induced mitophagy in HeLa cells. Lastly, we investigated the role the SUMOylation status of Fis1 has in HIM.

5.2 Results

5.2.1 The Effect of Hypoxia on SENP3 deSUMOylation of Target Proteins FKBP8 and Fis1

To explore whether FKBP8 and Fis1 are involved in regulating HIM, we first examined the effects of hypoxia on the levels of both proteins in HeLa cells with Western blotting. As expected, we found that the levels of either protein significantly decreased in HeLa cells exposed to hypoxia for 24 h (**Figures 5.1** and **5.2**). Because the two proteins are mainly localized in the mitochondria, their decreased levels in cells exposed to hypoxia support the possibility of their degradation due to mitophagy.

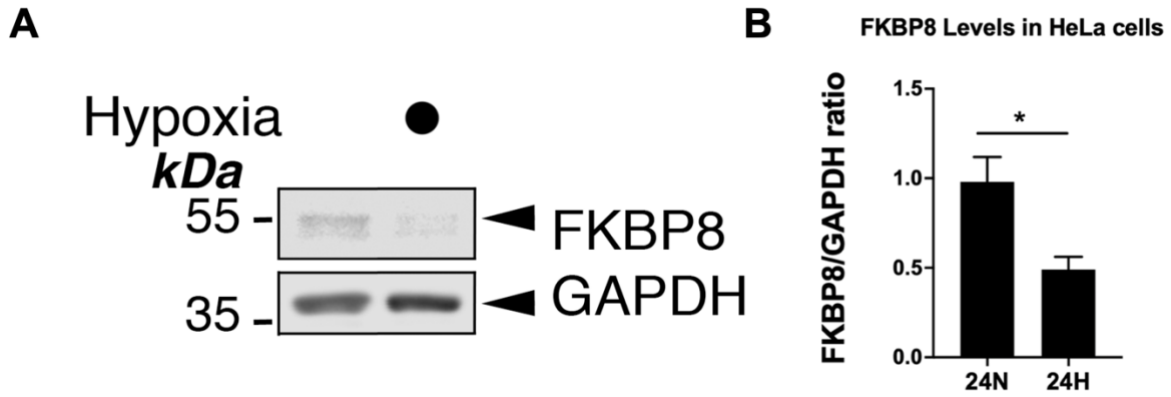

Figure 5.1: Hypoxia decreases FKBP8 levels in HeLa cells

A) HeLa cells were exposed to normoxia or hypoxia (1% O_2) for 24 h. Whole cell lysate samples were prepared and blotted as indicated. B) Histogram shows relative levels of FKBP8 in HeLa cells exposed to N or H for 24 h. (n = 3, *p < 0.05, Student's unpaired t-test).

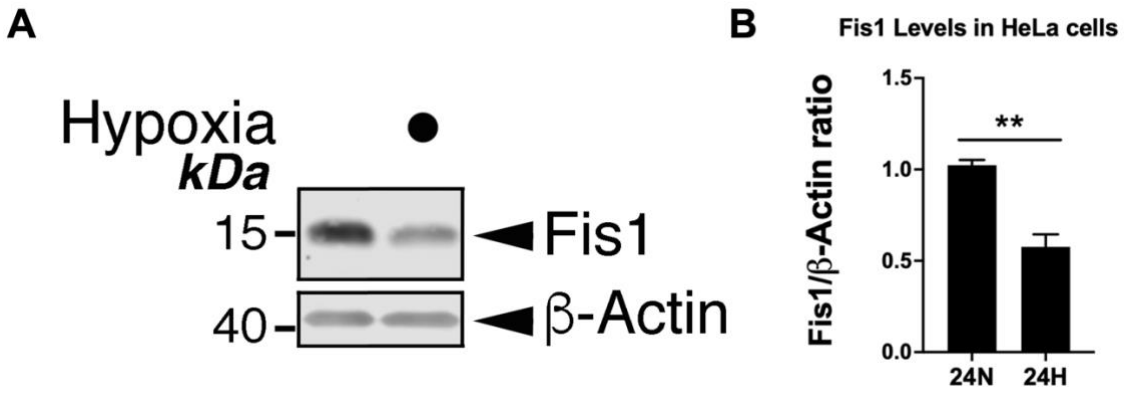

Figure 5.2: Hypoxia decreases Fis1 levels in HeLa cells

A) HeLa cells were exposed to normoxia or hypoxia (1% O_2) for 24 h. Whole cell lysate samples were prepared and blotted as indicated. B) Histogram shows relative levels of Fis1 in HeLa cells exposed to N or H for 24 h. (n = 3, **p < 0.01, Student's unpaired t-test).

5.2.2 The Role of FKBP8 in Hypoxia-induced Mitophagy

Because we found that the levels of FKBP8 were affected by hypoxia, we investigated whether FKBP8 has a role in regulating hypoxia-induced mitophagy in our experimental system. HeLa cells were transfected with Mito-pHfluorin and Nsi or FKBP8-specific siRNA. 48 h post-transfection, the cells were exposed to hypoxia for 24 h. The cells were fixed with 4% PFA and stained for FKBP8. The samples were then imaged with a confocal microscope (**Figure 5.3a**). When FKBP8 was knocked down, levels of average red puncta per cell indicating areas of mitophagy non-significantly decreased under normoxia compared to cells transfected with Nsi, suggesting that the protein does not have a role in regulating basal levels of mitophagy. Unexpectedly, FKBP8 knockdown did not lead to a significant decrease in the levels of mitophagy in cells exposed to hypoxia (**Figure 5.3b**) in contrast to the finding from a previous study (Yoo et al., 2020). This discounts the importance of FKBP8 in regulating HIM.

Furthermore, we investigated whether SUMOylation of FKBP8 has a role in the regulation of mitophagy under normoxic and hypoxic conditions. To validate whether FKBP8 is a *bona fide*

SUMOylation target, a histidine pulldown (His-PD) was performed. HEK293 cells were transfected with either *pcDNA3* or His-SUMO-2 and HA-FKBP8 to enrich and purify His-SUMO-2 and its conjugates. Samples were analyzed by Western blot and immunoblotted for HA tag to determine whether HA-tagged FKBP8 is modified by His-SUMO-2. There was no immunoreactive band for SUMO-2-ylated HA-FKBP8 detected in the His-PD in the absence of His-SUMO-2, which acted as a negative control (**Figure 5.4**, lane 1). An immunoreactive band was detected in the His-PD samples in the cell lysates prepared from cells expressing His-SUMO-2 and HA-FKBP8 together (**Figure 5.4**, lane 2), indicating that FKBP8 can be SUMO-2-ylated. This band appeared below 100 kDa, matching with the estimated molecular weight (~72 kDa, the sum of ~18 kDa for His-SUMO-2 and ~54 kDa for HA-FKBP8) for His-SUMO-2-ylated HA-FKBP8.

Next, to identify which lysine residue in human FKBP8 is modified by SUMO, we performed site-directed mutagenesis. As predicted by GPS-SUMO (Zhao et al., 2014), FKBP8 contains one high-probability consensus lysine residue (K335), which was mutated to an arginine (R) to prevent potential SUMO conjugation. His-PD was performed with HA-FKBP8 WT and HA-FKBP8 K335R mutant. HEK293 cells were transfected with either *pcDNA3* or His-SUMO-2 and HA-FKBP8 WT or HA-FKBP8 K335R to purify His-SUMO-2 and its conjugates. Samples were analyzed by Western blot and immunoblotted for His tag to determine whether HA-FKBP8 K335R mutant could be SUMO-2-ylated. There was no immunoreactive band for His-SUMO-2 detected in the His-PD in the absence of His-SUMO-2, which was included as a negative control (**Figure 5.5**, lane 1). An immunoreactive band between 70 and 100 kDa was detected in the His-PD samples in the cell lysates prepared from cells expressing His-SUMO-2 and HA-FKBP8 WT together (**Figure 5.5**, lane 2), indicating the conjugation of His-SUMO-2 to HA-FKBP8 WT that was also seen in the 2nd lane of **Figure 5.4**. There was no immunoreactive band detected in the His-PD samples from cells expression His-SUMO-2 and HA-FKBP8 K335R together (**Figure 5.5**,

lane 3), in contrast to the finding from the MS studies by Hendriks et al. (2018) in which three residues K119, K273 and K335 of FKBP8 were identified as potential SUMO conjugation sites, indicating that the K335 is the conjugation site for His-SUMO-2 on HA-FKBP8.

After validating HA-FKBP8 as a genuine target for SUMOylation and identifying K335 as the site for SUMOylation, we tested whether changes in SUMOylation status of HA-FKBP8 could affect the level of HIM in HeLa cells. To do this, we overexpressed HA-FKBP8 WT and the non-SUMOylatable mutant (HA-FKBP8 K335R) in HeLa cells expressing Mito-pHfluorin and exposed the cells to hypoxia for 24 h. After the cells were fixed with 4% PFA, immunostaining was performed on the cells for HA-tag and the cells were visualized with confocal microscopy (**Figure 5.6**). The overexpression of HA-FKBP8 WT but not HA-FKBP8 K335R in HeLa cells increased the levels of mitophagy under hypoxia compared to the control cells transfected with *pcDNA3*, suggesting that switching overexpressed FKBP8 to non-SUMOylatable status may abolish its ability to promote mitophagy under hypoxia. However, no significant difference between the average puncta per cell was observed between cells overexpressing HA-FKBP8 WT and HA-FKBP8 K335R in both normoxia and hypoxia, though levels of mitophagy in cells overexpression HA-FKBP8 are slightly but not significantly increased, suggesting that the SUMOylation of HA-FKBP8 may not play a major role in regulating hypoxia-induced mitophagy in HeLa cells (**Figure 5.6b**).

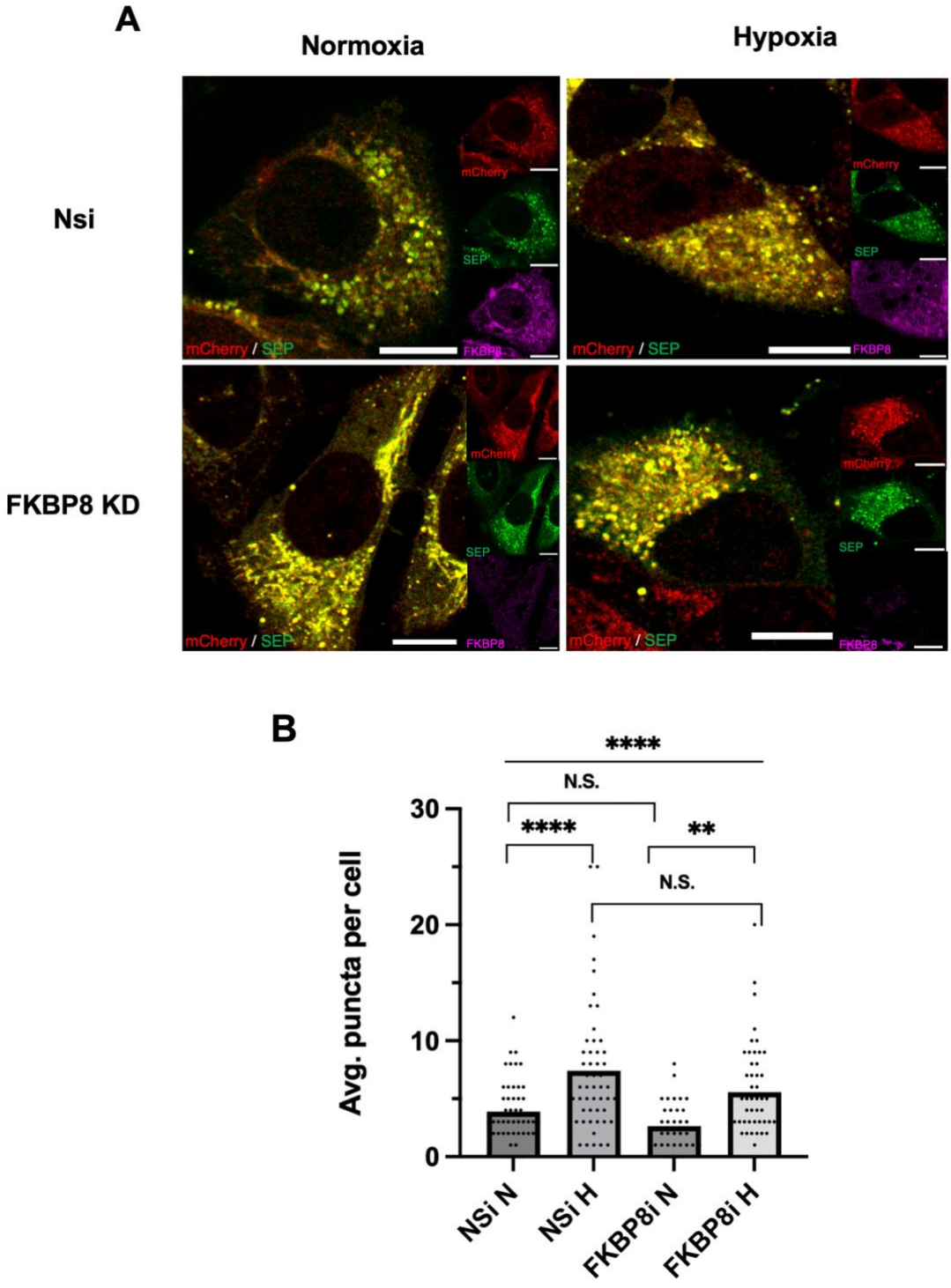

Figure 5.3: The Effect of FKBP8 KD on Hypoxia-induced Mitophagy in HeLa cells

A) HeLa cells were transfected with Mito-pHfluorin and Nsi or FKBP8-specific siRNA (50 nM). 48 h post-transfection the cells were exposed to normoxia or hypoxia (1% O_2) for 24 h. The cells were fixed with PFA 4% and stained for FKBP8 and then imaged with confocal microscopy. B) Histogram shows average number of Mito-pHfluorin red puncta per cell for cells exposed to N or

H for 24 h. (n = 34-51, N.S. non-significant; **p < 0.01; ****p < 0.0001; Ordinary one-way ANOVA followed by Sidak's multiple comparisons test). Scale bar 10 µm. The data presented are from a single experiment. n refers to the number of cells from one µ-dish used to quantify the average number of puncta per experimental condition.

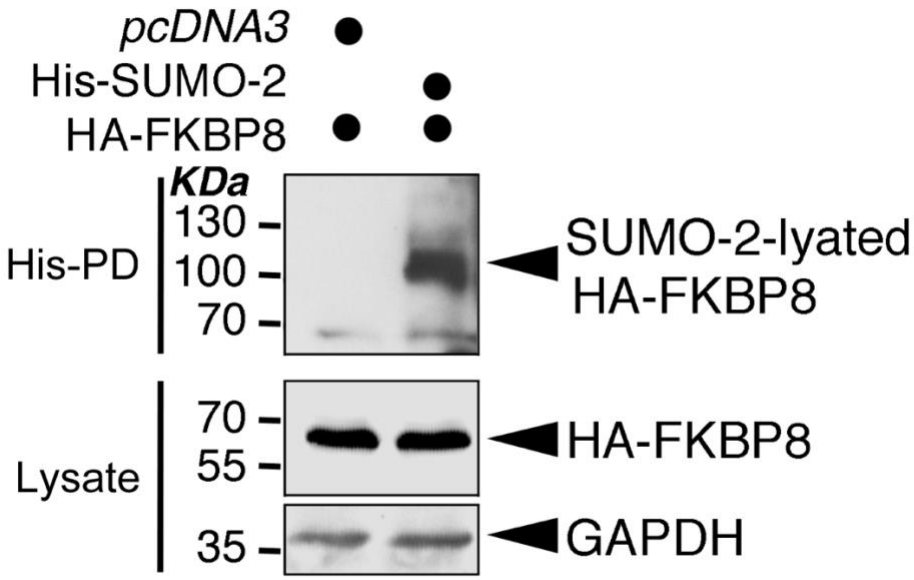

Figure 5.4: FKBP8 is a target for SUMO-2-ylation in HEK293 cells

HA-FKBP8 and pcDNA3 or His-SUMO2 were transfected into HEK293 cells for 48 h. 48 h post-transfection, cells were lysed and His-tagged proteins were enriched through His-pulldown (His-PD). Lysate (input) and His-PD samples were immunoblotted for HA tag (HA-FKBP8) and GAPDH.

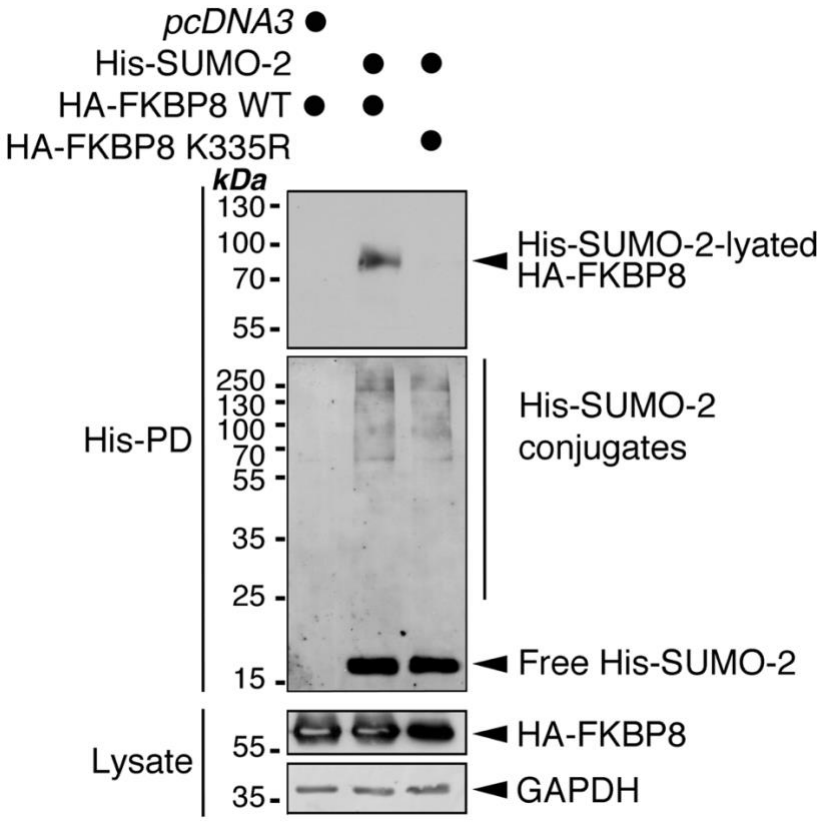

Figure 5.5: K335 is the major site for His-SUMO-2 conjugation of FKBP8 in HEK293 cells

His-SUMO-2 and HA-FKBP8 WT or HA-FKBP8 K335R were transfected into HEK293 cells for 48 h. pcDNA3 was used as a control for His-SUMO-2. 48 h post-transfection, cells were lysed and His-tagged proteins were enriched through His-pulldown (His-PD). His-PD samples were immunoblotted for His tag. Lysate (input) samples were immunoblotted for HA tag (HA-FKBP8) and GAPDH.

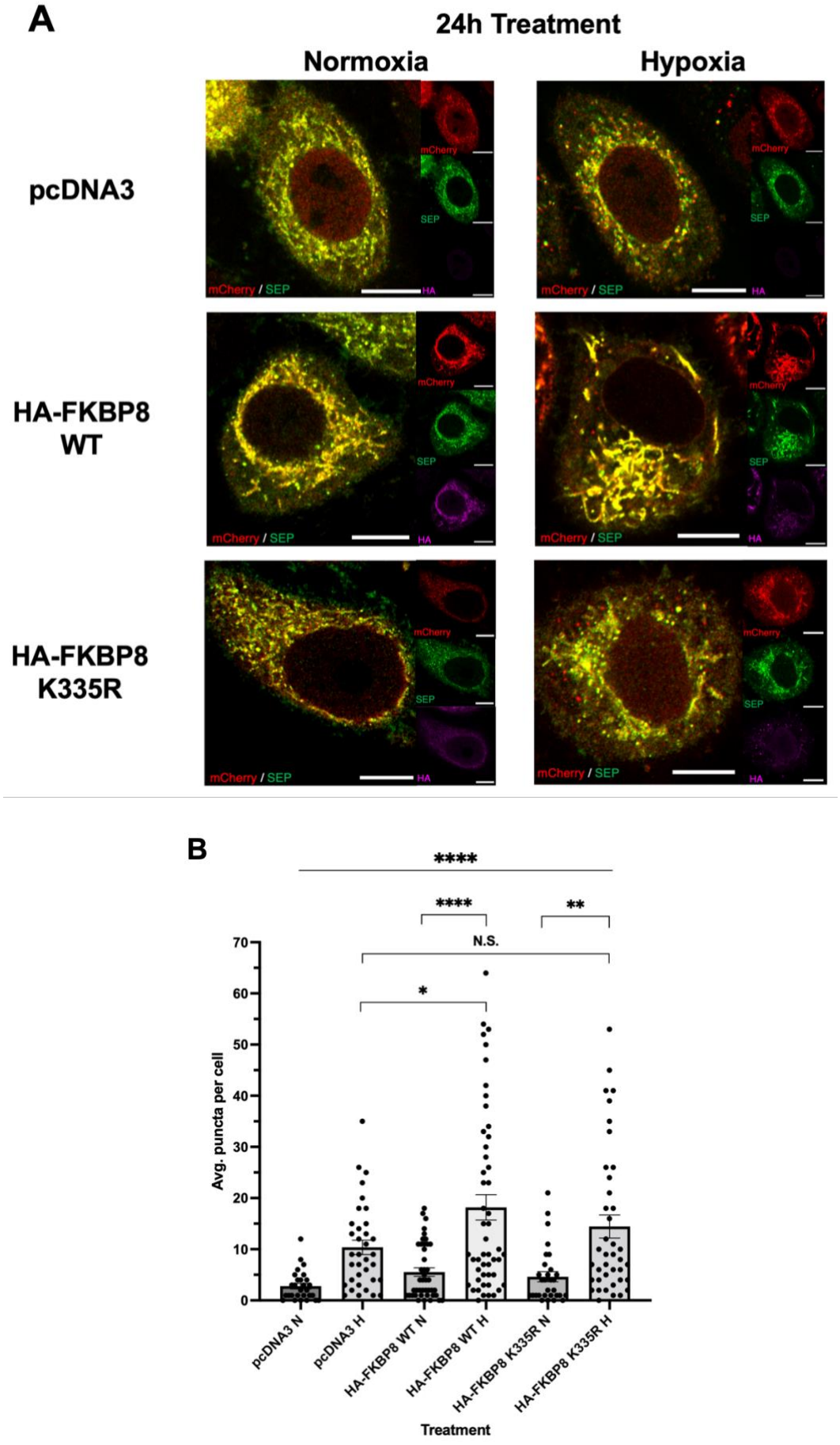
A
24h Treatment
Normoxia
Hypoxia
pcDNA3
HA-FKBP8 WT
HA-FKBP8 K335R
mCherry
SEP
HA
mCherry / SEP
B
****
****
**
N.S.
*
Avg. puncta per cell
0
10
20
30
40
50
60
70
pcDNA3 N
pcDNA3 H
HA-FKBP8 WT N
HA-FKBP8 WT H
HA-FKBP8 K335R N
HA-FKBP8 K335R H
Treatment

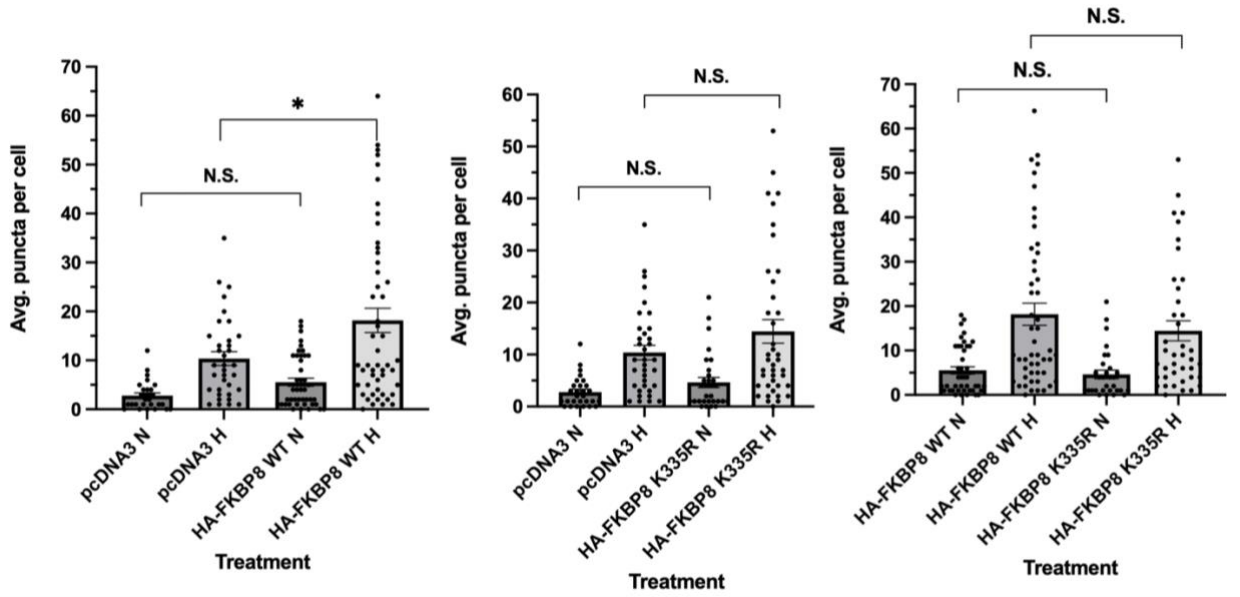

Figure 5.6: The Effect of Overexpressing of HA-FKBP8 WT or K335R on Hypoxia-induced Mitophagy in HeLa cells

A) HeLa cells were transfected with Mito-pHfluorin and pcDNA3, HA-FKBP8 WT or HA-FKBP8 K335R (0.25 µg/well). 48 h-post transfection, the cells were exposed to normoxia or hypoxia (1% O_2) for 24 h. The cells were fixed and stained for HA-tag and imaged with confocal microscopy. B) Histograms comparing the average number of Mito-pHfluorin red puncta per cell between different conditions as indicated. (n = 28-50, N.S. non-significant; *p < 0.05; ***p < 0.001; ****p < 0.0001; Ordinary one-way ANOVA followed by Sidak's multiple comparisons test). Scale bar 10 µm. The data presented are from a single experiment. n refers to the number of cells from one µ-dish used to quantify the average number of puncta per experimental condition.

5.2.3 The Role of Fis1 in Hypoxia-induced Mitophagy

Because we found that the levels of Fis1 were affected by hypoxia, we investigated whether Fis1 has a role in regulating hypoxia-induced mitophagy in our experimental system. Fis1 knockout (KO) HeLa cells were generated with CRISPR/Cas9-mediated gene editing (Waters et al., 2022). The Fis1 KO HeLa cells were transfected with Mito-pHfluorin and 48 h post-transfection, the cells were exposed to hypoxia for 24 h. The cells were fixed with 4% PFA and the samples were then imaged with a confocal microscope (**Figure 5.7a**). Fis1 KO abolished HIM and led to a non-significant decrease of mitophagy under normoxia (**Figure 5.7b**). This suggests that Fis1 is crucial for HIM and may contribute to basal levels of mitophagy. Additionally, we performed RNAi-mediated depletion of Fis1 in HeLa cells transfected with Mito-pHfluorin to assess the effect of Fis1 KD on levels of HIM. 48 h post-transfection, the cells were exposed to hypoxia for 24 h, fixed with 4% PFA and stained for Fis1. The samples were then imaged with a confocal microscope as shown in **Figure 5.8a**. Similar to our Fis1 KO results, Fis1 KD significantly decreased but did not abolish HIM levels (**Figure 5.8b**). Fis1 KD did not change levels of mitophagy under normoxia (**Figure 5.8b**). While these findings are preliminary and further research is needed to confirm that Fis1 is essential for HIM and its regulation, the data from our experiments provide evidence that support the importance of Fis1 in HIM.

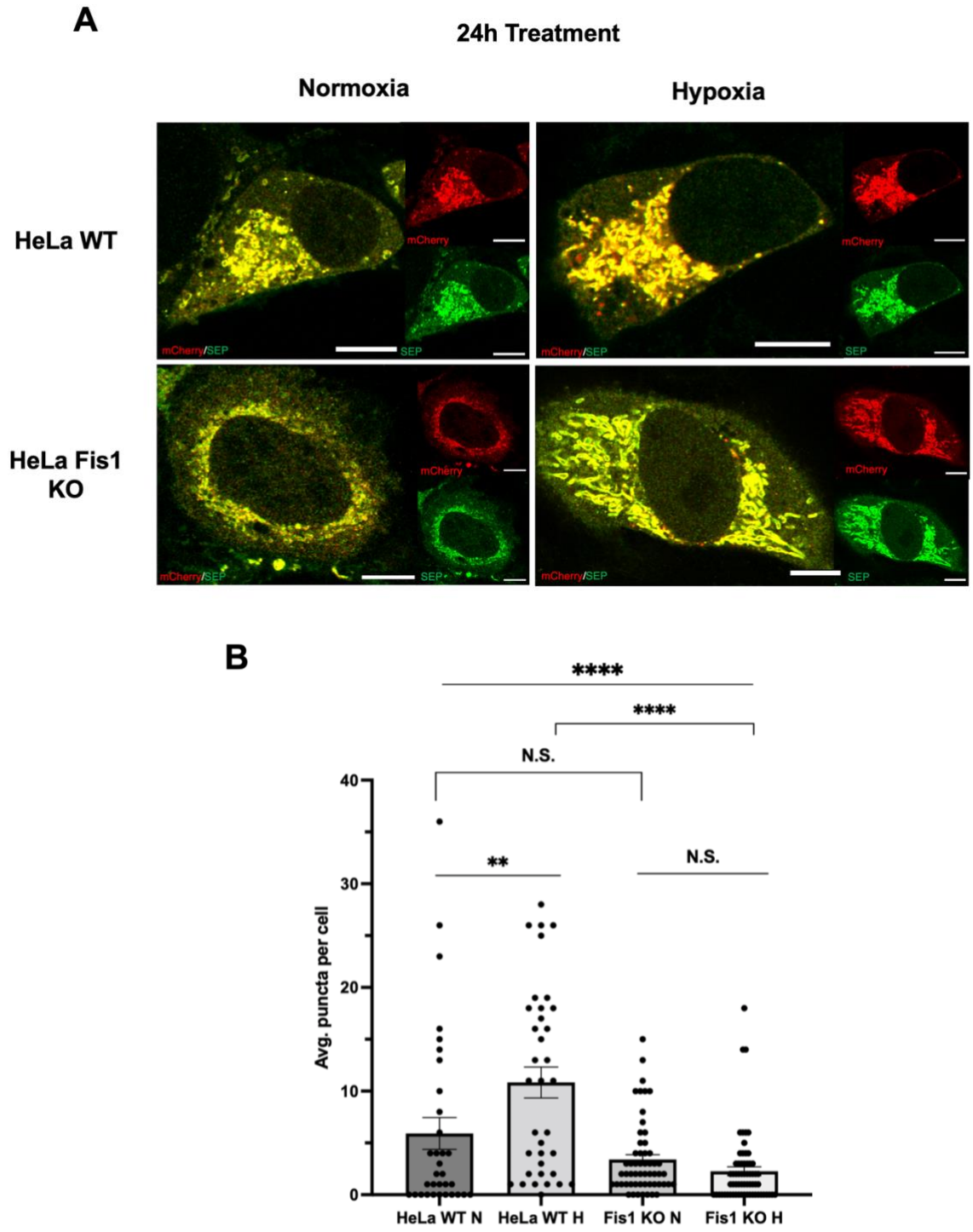

Figure 5.7: Fis1 KO abolishes mitophagy induced by hypoxia in HeLa cells

A) Fis1 KO HeLa cells were transfected with Mito-pHfluorin. 48 h post-transfection the cells were exposed to normoxia or hypoxia (1% O_2) for 24 h. The cells were fixed with PFA 4% and then imaged with confocal microscopy. B) Histogram shows average number of Mito-pHfluorin red puncta per cell for cells exposed to N or H for 24 h. (n = 33-64, N.S. non-significant; **p <

0.01; ****p < 0.0001; Ordinary one-way ANOVA followed by Sidak's multiple comparisons test). Scale bar 10 µm. The data presented are from a single experiment. n refers to the number of cells from one µ-dish used to quantify the average number of puncta per experimental condition.

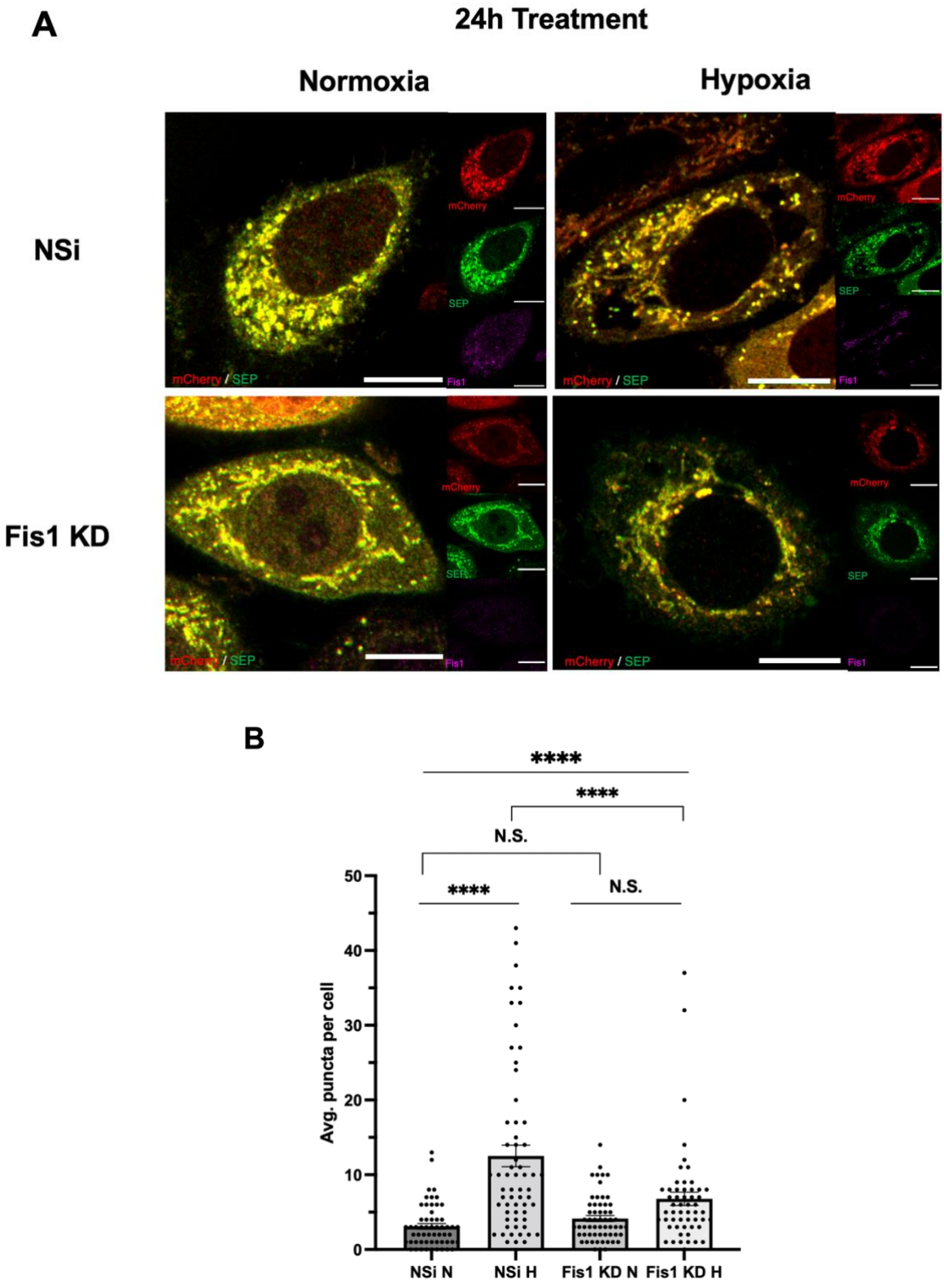

Figure 5.8: Fis1 KD decreases hypoxia-induced mitophagy in HeLa cells

A) HeLa cells were transfected with Mito-pHfluorin and Nsi or Fis1-specific siRNA (55 μM). 48 h post-transfection the cells were exposed to normoxia or hypoxia (1% O_2) for 24 h. The cells were fixed with PFA 4% and stained for Fis1 and then imaged with confocal microscopy. B) Histogram shows average number of Mito-pHfluorin red puncta per cell for cells exposed to N or H for 24 h. (n = 54-61, N.S. non-significant; ****p < 0.0001; Ordinary one-way ANOVA followed by Sidak's multiple comparisons test). Scale bar 10 μm. The data presented are from a single experiment. n refers to the number of cells from one μ-dish per experimental condition.

5.2.4 The Role of Fis1 SUMOylation on Hypoxia-induced Mitophagy

5.2.4.1 Fis1 K149R Mutant Rescues Hypoxia-induced Mitophagy in SENP3i HeLa cells

In our previous experiments described in Chapter 4, RNAi-mediated SENP3 KD significantly decreased levels of hypoxia-induced mitophagy. In this chapter, data from our model cells suggest that Fis1 is important for HIM. Moreover, Waters et al. (2022) demonstrated that Fis1 is a novel target of SENP3 for deSUMOylation and that the K149 site is required for Fis1 SUMOylation. Fis1 K149R is a SUMOylation site mutant generated by PCR-based mutagenesis that reduces the SUMOylation of Fis1 by ~90% (Waters et al., 2022). To investigate the effect of Fis1 SUMOylation status on HIM levels, we transfected Mito-pHfluorin and CFP-Fis1 or CFP-Fis1 K149R in SENP3 knockdown HeLa cells. 48 h post-transfection, the cells were exposed to hypoxia for 24 h, fixed with 4% PFA and then imaged with a confocal microscope (**Figure 5.9a**). We found that CFP-Fis1 K149R rescued induction of mitophagy by hypoxia in SENP3i HeLa cells while CFP-Fis1 WT did not (**Figure 5.9b**). This suggests that deSUMOylation of Fis1 is important for HIM.

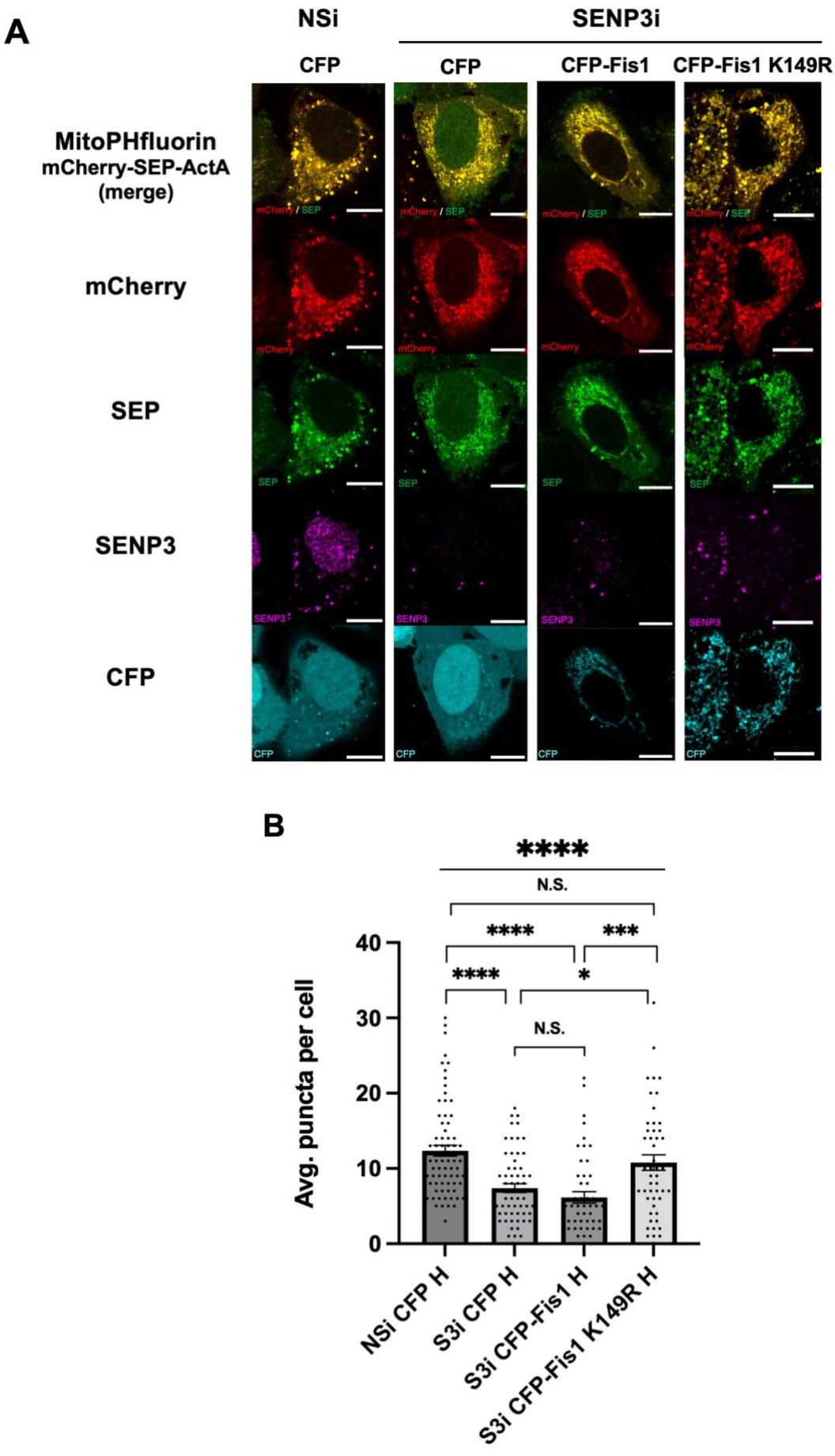
A
NSi
SENP3i
CFP
CFP
CFP-Fis1
CFP-Fis1 K149R
MitoPHfluorin
mCherry-SEP-ActA
(merge)
mCherry
SEP
SENP3
CFP
B
****
N.S.
****
***
****
*
N.S.
Avg. puncta per cell
40
30
20
10
0
NSi CFP H
S3i CFP H
S3i CFP-Fis1 H
S3i CFP-Fis1 K149R H

Figure 5.9: Fis1 K149R mutant rescues HIM in SENP3i HeLa cells

A) HeLa cells were transfected with Mito-pHfluorin, Nsi or SENP3-specific siRNA (50 nM), and CFP, CFP-Fis1 (0.25 µg/well) or CFP-Fis1 K149R (0.3 µg/well). 48 h post-transfection the cells were exposed to hypoxia (1% O_2) for 24 h. The cells were fixed with PFA 4% and stained for SENP3 and then imaged with confocal microscopy. B) Histogram shows average number of Mito-pHfluorin red puncta per cell. (n = 48-74, N.S. non-significant; *p < 0.05; ***p < 0.001; ****p < 0.0001; Ordinary one-way ANOVA followed by Sidak's multiple comparisons test). Scale bar 10 µm. The data presented are from a single experiment. n refers to the number of cells from one µ-dish used to quantify the average number of puncta per experimental condition.

5.2.4.2 Fis1-SUMO-2 fusion mutant reduces hypoxia-induced mitophagy

After investigating the role of deSUMOylated Fis1 on hypoxia-induced mitophagy in absence of SENP3, next we utilized CFP-Fis1-SUMO-$2^{\Delta GG}$, a mutant mimicking constitutively SUMOylated form of Fis1, to investigate the role of Fis1 that cannot be deSUMOylated in HIM. HeLa cells were transfected with Mito-pHfluorin and CFP-Fis1 or CFP-Fis1-SUMO-$2^{\Delta GG}$ and 48 h post-transfected they were exposed to hypoxia for 24 h. The cells were fixed with 4% PFA and the samples were then imaged with a confocal microscope (**Figure 5.10a**). As shown in **Figure 5.10b**, CFP-Fis1-SUMO-$2^{\Delta GG}$ but not CFP-Fis1 significantly reduced levels of HIM. Additionally, there was no significant difference in levels of mitophagy between cells expressing CFP-Fis1-SUMO-$2^{\Delta GG}$ under hypoxia and the control cells expressing CFP under normoxia (**Figure 5.10b**). These data imply that fully SUMOylated Fis1 may have a suppressive effect on HIM.

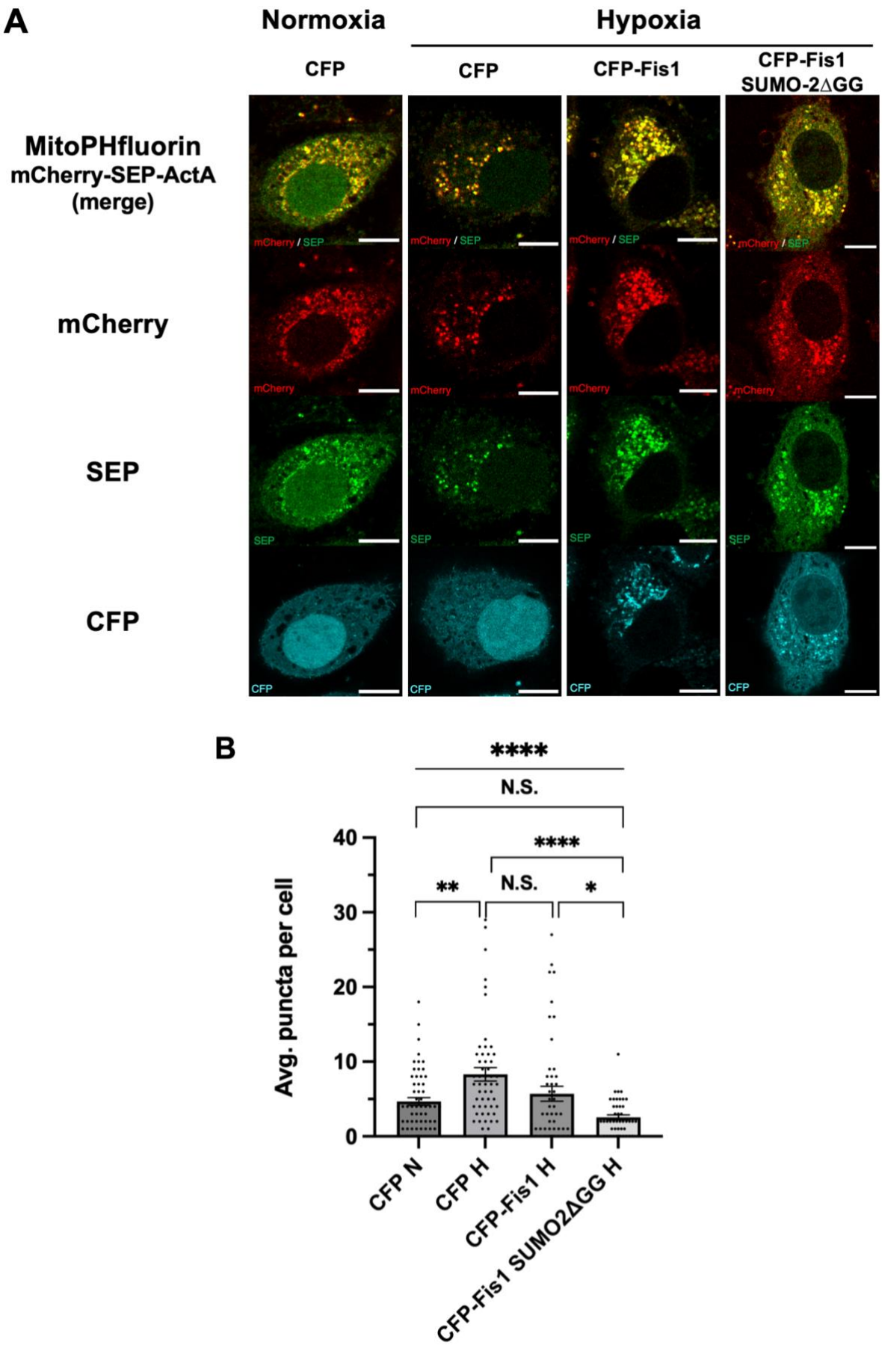
A
Normoxia
Hypoxia
CFP
CFP
CFP-Fis1
CFP-Fis1
SUMO-2ΔGG
MitoPHfluorin
mCherry-SEP-ActA
(merge)
mCherry
SEP
CFP
mCherry / SEP
mCherry
SEP
CFP
B
****
N.S.
****
**
N.S.
*
Avg. puncta per cell
40
30
20
10
0
CFP N
CFP H
CFP-Fis1 H
CFP-Fis1 SUMO2ΔGG H

Figure 5.10: Expressing Fis1-SUMO-2 fusion mutant reduces HIM levels in HeLa cells

A) HeLa cells were transfected with Mito-pHfluorin and CFP, CFP-Fis1 or CFP-Fis1-SUMO-$2^{\Delta GG}$ (0.25 µg/well). 48 h post-transfection the cells were exposed to normoxia or hypoxia (1% O_2) for 24 h. The cells were fixed with PFA 4% and then imaged with confocal microscopy. B) Histogram shows average number of Mito-pHfluorin red puncta per cell. (n = 46-58, N.S. non-significant; *p < 0.05; **p < 0.01; ****p < 0.0001; Ordinary one-way ANOVA followed by Sidak's multiple comparisons test). Scale bar 10 µm. The data presented are from a single experiment. n refers to the number of cells from one µ-dish used to quantify the average number of puncta per experimental condition.

5.2.4.3 TAK-981 treatment in Fis1 KO HeLa cells

Since we found that Fis1 KO abolished hypoxia-induced mitophagy in HeLa cells and SUMOylation inhibition by TAK-981 treatment significantly increased mitophagy under both normoxia and hypoxia, we investigated the effect of inhibition of global SUMOylation on mitophagy levels in the absence of Fis1 in HeLa cells. Fis1 KO HeLa cells were transfected with Mito-pHfluorin for 48 h and treated with DMSO or TAK-981 for 24 h. The cells were fixed with 4% PFA and imaged with a confocal microscope (**Figure 5.11a**). TAK-981 treatment caused a significant increase of mitophagy levels in Fis1 KO HeLa cells (**Figure 5.11b**). This suggests that SUMOylation suppresses mitophagy in absence of Fis1. While the SUMOylation status of Fis1 is important in regulating HIM, it appears that there is also an unknown Fis1-independent mechanism for suppressing of mitophagy involving SUMOylation.

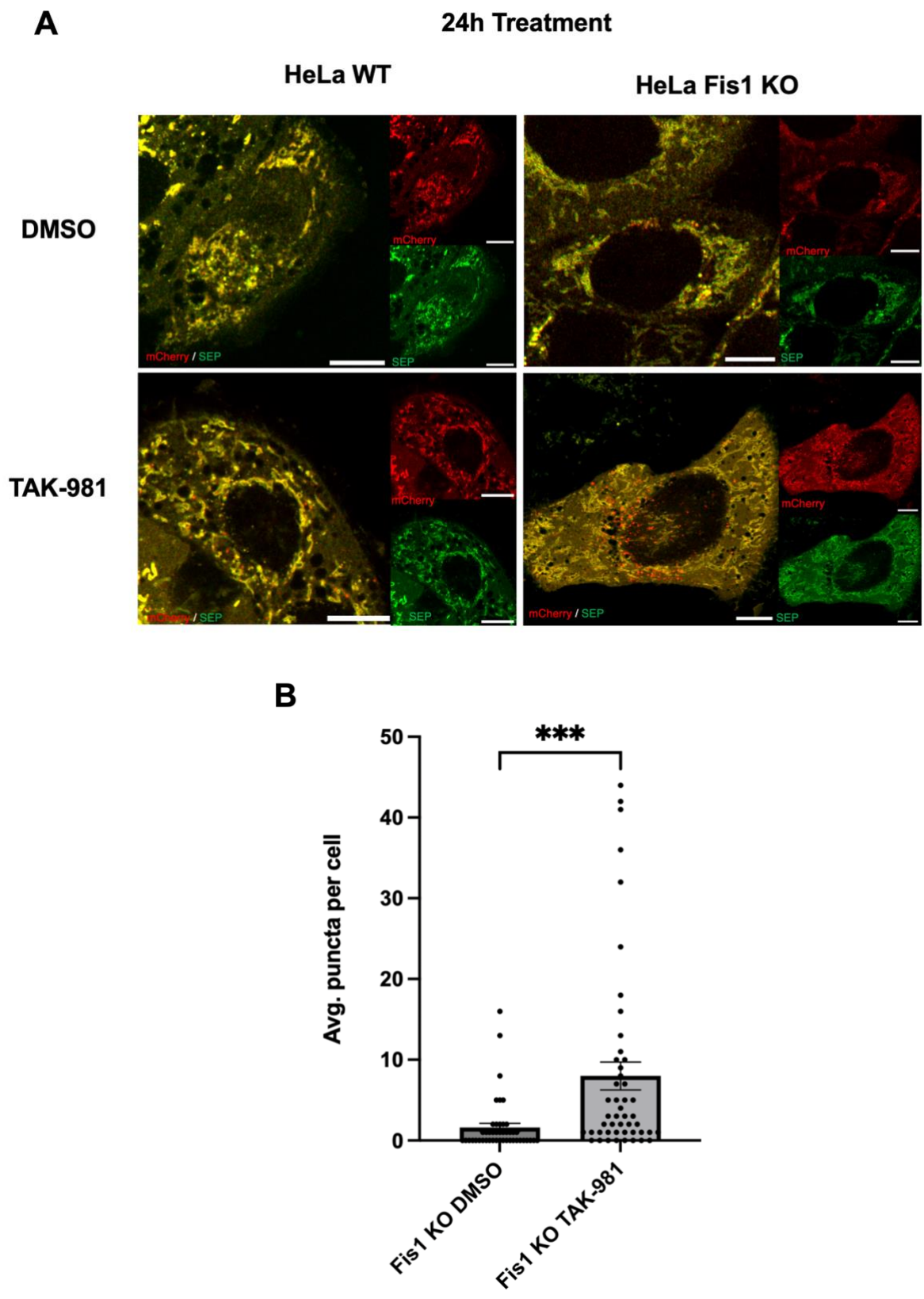
A
24h Treatment
HeLa WT
HeLa Fis1 KO
DMSO
TAK-981
mCherry / SEP
mCherry
SEP
B
***
Avg. puncta per cell
50
40
30
20
10
0
Fis1 KO DMSO
Fis1 KO TAK-981

Figure 5.11: The effect of SUMOylation inhibition on mitophagy levels in absence of Fis1

A) HeLa WT or Fis1 KO HeLa cells were transfected with Mito-pHfluorin. 48 h post-transfection the cells were treated with DMSO or TAK-981 (100 nM) for 24 h. The cells were fixed with PFA 4% and then imaged with confocal microscopy. B) Histogram shows average number of Mito-pHfluorin red puncta per cell. (n = 44-48, N.S. non-significant; ***p < 0.001; Unpaired Student's t-test). Scale bar 10 μm. The data presented are from a single experiment. n refers to the number of cells from one μ-dish used to quantify the average number of puncta per experimental condition.

5.3 Discussion

Figure 5.12 summarizes the main findings and proposed mechanisms from Chapter 5.

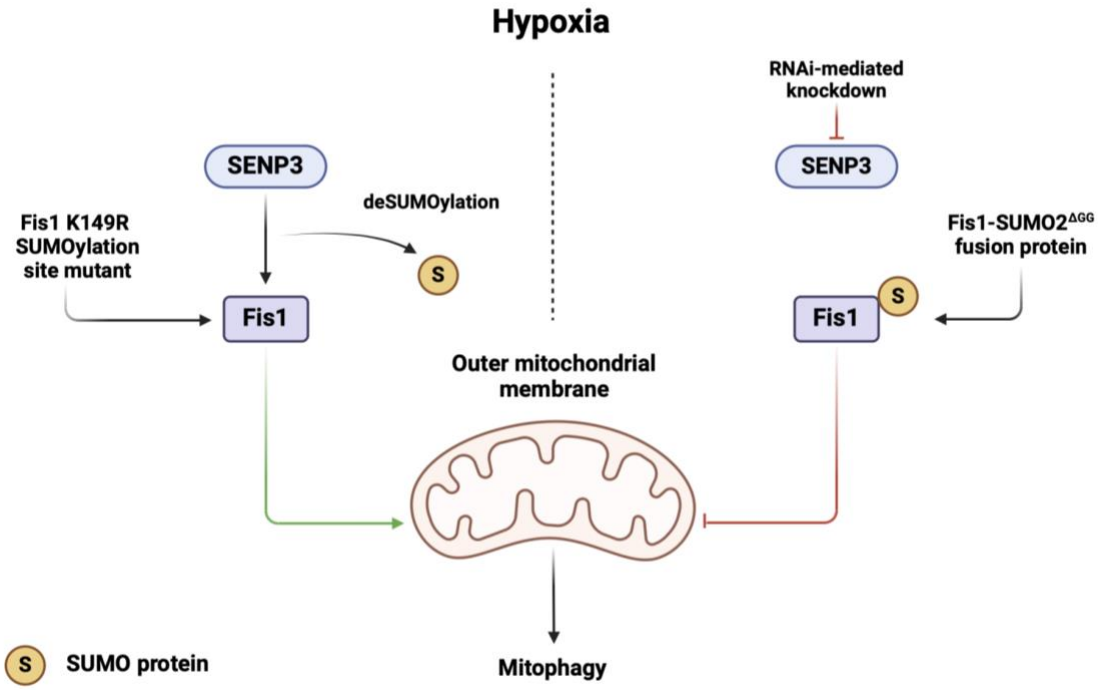

Figure 5.12: Summary of Chapter 5 Findings

Under hypoxia, the SUMOylation status of Fis1 regulates the level of mitophagy. SENP3 deSUMOylates Fis1. deSUMOylated Fis1 or the SUMOylation site mutant Fis1 K149R promotes HIM. SENP3 KD leads to more SUMOylated Fis1 protein. SUMOylated Fis1 suppresses HIM

levels. Additionally, a Fis1 fusion protein, Fis1-SUMO2$^{\Delta GG}$, which cannot be deSUMOylated, also decreases HIM levels.

5.3.1 FKBP8 Levels under Hypoxia

In the present study, we have found that 24 h exposure of cells to hypoxia leads to the decrease in FKBP8 levels in HeLa cells. Given that hypoxia increases the level of mitophagy in HeLa cells and FKBP8 is anchored to the OMM, this result would be consistent with increased clearance of mitochondria with FKBP8 on the OMM under hypoxia (Shirane & Nakayama, 2003; Yoo et al., 2020). Studies have shown that FKBP8 regulates Parkin-independent mitophagy (Yoo et al., 2020; Bhujabal et al., 2017; Lim & Lim, 2017). Since FKBP8 is reported to be necessary for Parkin-independent mitophagy under stress conditions such as hypoxia (Yoo et al., 2020), we knocked down FKBP8 in HeLa cells transfected with Mito-pHlufluorin to determine whether FKBP8 is needed hypoxia-induced mitophagy in our model cells. FKBP8 KD in HeLa cells did not affect mitophagy levels under normoxia and hypoxia. This suggests that FKBP8 may not have roles in regulating the level of basal mitophagy and HIM. However under hypoxia, loss of FKBP8 already occurs as our Western blot for FKBP8 levels under hypoxia showed. Reduced FKBP8 levels under hypoxia may result from HIM, but FKBP8 itself may not contribute significantly to changing levels of mitophagy induced by hypoxia. Another possibility is that the depletion of FKBP8 by RNAi is not sufficient to block HIM. Knocking out FKBP8 with CRISPR/Cas9 would be required to uncover the role of FKBP8 in HIM.

5.3.2 FKBP8 SUMOylation

Whether SUMOylation of FKBP8 plays a role in regulating hypoxia-induced mitophagy has previously not been characterized. Our His-PD experimental results provide evidence that FKBP8 is SUMO-2-ylated and that the conjugation site for SUMOylation is K335. In order to determine

whether SUMOylation of FKBP8 regulates HIM, we performed immunofluorescence microscopy on HeLa cells expressing empty plasmid *pcDNA3* (as a control), HA-FKBP8 WT or HA-FKBP8 K335R and Mito-pHfluorin exposed to normoxia or hypoxia for 24 h. Overexpression of HA-FKBP8 WT caused an increase of mitophagy compared to the *pcDNA3* control cells under hypoxia, while overexpression of HA-FKBP8 K335R did not. This suggests that while overexpression of HA-FKBP8 that can be SUMOylated in HeLa cells promotes mitophagy under HIM, the K335R mutation abolishes this promoting effect, which implies that FKBP8 SUMOylation may play a role in mitophagy regulation. However, our results from FKBP8 KD experiments do not support an important role for endogenous FKBP8 in regulating the levels of HIM. Additionally, the lack of significant difference in the levels of HIM or mitophagy under normoxia when comparing between cells expressing HA-FKBP8 WT and the SUMOylation site mutant HA-FKBP8 K335R does not support a major role for FKBP8 deSUMOylation in regulating HIM.

5.3.3 Fis1 Levels under Hypoxia

In our current study, we have found that 24 h exposure of hypoxia leads to the decrease of Fis1 levels in HeLa cells. The reduction of Fis1 may be due to hypoxia-mitophagy, as Fis1 is located mainly on the OMM (Mozdy et al., 2000). Lower levels of Fis1 under hypoxia may result from the increased degradation of mitochondria that Fis1 proteins are anchored to during mitophagy induced by hypoxic stress conditions. In contrast to our findings, Fis1 as well as Drp1 are upregulated in murine cardiomyocytes that have undergone hypoxia-reperfusion *in vitro* and *in vivo,* resulting in excessive mitochondrial fragmentation (Zhou et al., 2018; Ihenacho et al., 2021). Fis1 levels were reportedly increased in an animal model for hypoxic-ischemic brain damage (HIBD) from neonatal rats after 24 h of HIBD (M. X. Li et al., 2017). While these studies report that low oxygen levels lead to the increase of Fis1, mitophagy induced by hypoxia may serve to clear the increased mitochondrial fragmentation and disruption to mitochondrial function

associated with the hypoxic stress, leading to the decrease of Fis1 levels under hypoxia in our Western blotting experiments. Additionally, Fis1 levels under hypoxia may vary between cell types. Furthermore, Fis1 involvement in mitochondrial fragmentation and mitophagy may contribute to its own reduction.

5.3.4 Effect of Fis1 KO and KD on HIM

We found that Fis1 KO in HeLa cells abolished hypoxia-induced mitophagy and Fis1 KD significantly decreased but did not completely abolish HIM, suggesting that Fis1 has an important role in HIM. These data are similar to the findings from Waters et al. (2022), which demonstrated that Fis1 was required in a form of Parkin-independent mitophagy induced by DFP. Because SUMOylation of Fis1 is involved in the regulation of DFP-induced mitophagy, there may be a similar or parallel mechanism responsible for Fis1-mediated regulation of HIM, which is also a Parkin-independent form of mitophagy.

Reduction of Fis1 levels affects both mitophagy and mitochondrial fragmentation. Twig et al. (2008) reported that knockdown of Fis1 decreased mitophagy levels and lead to the accumulation of oxidized mitochondrial proteins. Furthermore, Kim et al. (2011) reported that reduced expression of Fis1 significantly decreased hypoxia-mediated mitochondrial fragmentation in NIH 3T3 mouse fibroblast cells. Mitochondrial fission has been proposed to be necessary but not sufficient for mitophagy. Mitochondrial fission facilitates the segregation of depolarized mitochondria from the mitochondrial network, enabling their subsequent engulfment by autophagosomes (Twig et al., 2008; Ma et al., 2020). Similarly, knockout of Fis1 has also been reported to negatively affect mitophagy. In male germ cell-specific Fis1 KO mice, the disruption of *Fis1* gene led to accumulation of mitochondria with aberrant structures and mitophagic and autophagic intermediates, indicating defective mitophagy (Varuzhanyan et al., 2021). This aligns with our findings where Fis1 KO decreased the level of mitophagy in basal conditions. Here, we

present evidence from our model cells that Fis1 is important for HIM. However, whether the SUMOylation of Fis1 regulates this process remained unknown.

5.3.5 Fis1 SUMOylation mutants (Fis1 K149R, Fis1-SUMO-2$^{\Delta GG}$)

We investigated how the SUMOylation status of Fis1 affects hypoxia-induced mitophagy by expressing the Fis1 K149R (SUMOylation deficient) mutant or Fis1-SUMO-2$^{\Delta GG}$ mutant (mimicking constitutive Fis1 SUMOylation). In the absence of SENP3, Fis1 K149R but not Fis1 WT rescued HIM, indicating that deSUMOylating or ablating SUMOylation of Fis1 is likely needed for induction of mitophagy under hypoxia. When Fis1 cannot be deSUMOylated, in the case of Fis1-SUMO-2$^{\Delta GG}$, the level of HIM decreased. This suggested that SUMOylation of Fis1 negatively regulates HIM. Our results regarding the role of Fis1 SUMOylation in HIM regulation are similar to the findings by Waters et al. (2022), which described regulation of DFP-induced mitophagy by Fis1 SUMOylation. Waters et al. (2022) found that expressing Fis1 K149R in SENP3-depleted HeLa cells rescues DFP-induced mitophagy and that expressing Fis1-SUMO-2$^{\Delta GG}$ but not Fis1 WT reduced DFP-mediated induction of LC3-II (Waters et al. 2022). The SUMOylation status of Fis1 has been suggested to regulate Fis1 mitochondrial localization and the induction of mitophagy by Waters et al. (2022). Fis1 with the K149R mutation displays increased mitochondrial localization, while Fis1-SUMO-2$^{\Delta GG}$ to relocate to the cytosol (Waters et al., 2022). It is possible that the distribution of Fis1 to the mitochondria is regulated by SUMOylation under HIM. In the previous chapter, we found that inhibition of global SUMOylation by TAK-981 treatment increased HIM levels, indicating that overall SUMOylation likely suppresses mitophagy. Our experimental data also revealed that SUMO-2/3 appears to suppress HIM while SUMO-1 promotes it. Iron chelation by DFP induces protein deSUMO-2/3-ylation but not deSUMO-1-ylation (Waters et al., 2022). This further supports SUMO-2/3 conjugation having a suppressive effect on Parkin-independent forms of mitophagy, which may

explain the effect of Fis1 SUMOylation status on HIM. However, the exact mechanism of this remains unknown.

5.3.6 Effect of TAK-981 treatment on mitophagy in Fis1 KO HeLa cells

We found that TAK-981-mediated inhibition of SUMOylation in Fis1 KO HeLa cells increased mitophagy levels under normoxia. This suggests that SUMOylation in absence of Fis1 has an overall suppressive effect on mitophagy under normoxic conditions. As we previously found, deSUMOylation or the prevention of SUMOylation of Fis1 increases hypoxia-induced mitophagy and TAK-981 treatment of HeLa WT cells exposed to hypoxia led to increased HIM. Although, our previous results also showed that Fis1 is likely important for the induction of mitophagy by hypoxia since Fis1 KO decreased levels of mitophagy under both normoxia and hypoxia, induction of mitophagy by TAK-981 treatment may present an additive effect on the levels of mitophagy in Fis1 KO HeLa cells. Currently, there is no literature available about the effect of TAK-981 on mitochondria function or mitophagy. TAK-981-induced mitophagy is a potentially novel form of mitophagy.

In summary, we found that hypoxia led to the decrease of both FKBP8 and Fis1 levels in HeLa cells. Overall, our data suggest that FKBP8 is SUMO-2-ylated at K335 and likely does not regulate hypoxia-induced mitophagy even when its SUMOylation is prevented. On the other hand, as outlined in **Figure 5.12**, our findings suggest that Fis1 is crucial for the regulation of hypoxia-induced mitophagy and that Fis1 SUMOylation status affects levels of hypoxia-induced mitophagy in HeLa cells. In Chapter 6, we investigate a potential mechanism underlying Fis1-mediated regulation of hypoxia-induced mitophagy.

Chapter 6

Regulatory Mechanism of Fis1-mediated Hypoxia-induced Mitophagy

6.1 Background

6.1.1 TBC1 Domain Family Members 15 and 17 (TBC1D15 and TBC1D17)

TBC1D15 is a mitochondrial Rab GTPase-activating protein (Rab-GAP) that is required for the formation of the mitophagic autophagosome downstream of Parkin activation (Yamano et al., 2014). Yamano et al. (2014) showed that TBC1D15 and Fis1 work together to control autophagosome morphology in Parkin-mediated mitophagy. TBC1D15 binds mitochondria through Fis1 and the C-terminus of Fis1 is essential for Fis1-TBC1D15 interaction (Onoue et al., 2013). TBC1D15, in concert with Fis1, inhibits Rab7 activity in order to prevent excessive growth of autophagosome by binding to damaged mitochondria while the autophagosome grows around the mitochondria (Yamano et al., 2014). Rab7 itself is necessary for the maturation of early endosomes and transport from late endosomes to lysosomes (Bento et al., 2013) and has also been shown to have roles in autophagosome biogenesis (Gutierrez et al., 2004; Jager et al., 2004). TBC1D17 is also a GAP protein and the member of the TBC family that forms homodimers and heterodimers with TBC1D15 and interacts with Fis1 (Yamano et al, 2014). Together, TBC1D15 and TBC1D17 mediate mitophagy through regulation of Rab7 (Yamano et al., 2014; Jimenez-Orgaz et al. 2018). TBC1D17 is also needed for normal morphology of mitochondria and peroxisomes (Yamano et al., 2014). Because TBC1D15 and TBC1D17 interact with Fis1 during Parkin-mediated mitophagy (Yamano et al., 2014), we hypothesized that there may be a similar mechanism involving TBC1D15, TBC1D17 and Fis1 in Fis1-mediated hypoxia-induced Parkin-

independent mitophagy. If so, we also pose the question of whether SUMOylation and deSUMOylation are involved.

6.1.2 Syntaxin 17 (Stx17)

Stx17 is a SNARE (soluble *N*-ethylmaleimide-sensitive factor attachment protein receptor) protein located in the mitochondria-associated membrane (MAM) and mitochondria. Stx17 was identified by Hamasaki et al. (2013) in a screen for ER-resident SNARE proteins involved in autophagy. Stx17 localizes at the MAM after starvation induces autophagy and activates autophagosome formation by recruiting Atg14, an autophagosome marker, to the MAM (Hamasaki et al., 2013). Stx17 has also been reported to interact with Drp1 at MAMs and promote mitochondrial fission by regulating Drp1 localization and activity (Arasaki et al., 2015). Starvation conditions disrupt the interaction between Stx17 and Drp1 and increases mitochondrial elongation during mitophagy (Arasaki et al., 2015). Furthermore, Stx17 is required for fusion of autophagosomes with the endosome/lysosome during autophagy (Itakura et al., 2012; Takats et al., 2013). Xian et al. (2019) found that Stx17 interacts with Fis1 via proteomics analysis. Within the same study, Xian et al. (2019) indicated that the interaction between Stx17 and Fis1 is responsible for controlling the shuffling of Stx17 between the ER and mitochondria. Overexpression of Stx17 in Fis1-depleted (Fis1 KO) HeLa cells leads to Stx17 accumulation on the mitochondria and promotes Parkin-independent mitophagy (Xian et al., 2019). In addition, Stx17 has also been reported to participate in Parkin-mediated mitophagy (Sugo et al., 2018). Because Stx17 has roles in the mitochondria-associated membranes (MAMs), autophagy, and mitophagy, along with its interactions with Fis1, here we investigate whether Stx17 is involved in HIM.

6.1.3 MAM Formation and Hypoxia

In Chapter 4, we demonstrated that SUMO inhibition by TAK-981 treatment or RNAi-mediated knockdown of SUMO-1 or SUMO-2/3 affect mitophagy levels in HeLa cells under normoxia and hypoxia, indicating involvement of de/SUMOylation in regulating mitophagy. In Chapter 5, our findings suggest that there is a SENP3-Fis1 axis that regulates HIM and the SUMOylation status of Fis1 appears to serve as a molecular switch for HIM. Fis1 has been proposed to be involved in the formation of MAMs (Ihenacho et al., 2021; Wilson et al., 2021). MAMs are the portions of the ER reversibly tethered to the mitochondria at mitochondria-ER contact sites (MERCs). The dynamic MERCs consist of the OMM, ER-subdomain and a series of proteins (Yang et al., 2020). MAMs are involved in calcium ion transport between the ER to mitochondria (Rizzuto et al., 1998), lipid metabolism (Rusinol et al., 1994; Vance 2014), regulating mitochondrial shape and motility (van Vliet et al., 2014) and autophagy (Tooze & Yoshimori, 2010; Hamasaki et al., 2013). MAMs have a critical role in initiating autophagosome formation during general autophagy (Matsunaga et al., 2010; Hamasaki et al., 2013) and are regarded as the origin site of autophagy (Yang et al., 2020). The MAM is essential for mitochondrial fission before the engulfment of mitochondria by the autophagosome during mitophagy (Friedman et al., 2011; Murphy et al., 2013). In addition, there is emerging evidence that the MAM is responsive to hypoxia (Wu et al., 2016; Chai et al., 2021). Yang et al. (2019) demonstrated that MAM formation increased under hypoxic conditions in human pulmonary artery endothelial cells. Therefore, we investigate if SUMOylation/deSUMOylation has a role in regulating MAM formation and if there is a link between the potential effects of SUMOylation/deSUMOylation on MAM formation and their effects on mitophagy induction as shown in Chapter 4: TAK-981-induced SUMOylation inhibition (to mimic deSUMOylation) and SENP3 KD (known to induce SUMO-2/3-ylation; Guo et al., 2013). To visualize changes in MAM formation in HeLa cells, we utilize MAMtracker-

Green, a novel reporter for MAMs generated by Sakai et al. (2021) that is suitable to track reversible changes in the MAM in cultured living cells.

Techniques that have been used to monitor and analyze MAM status include electron microscopy, proximity ligation assay (PLA), fluorescence microscopy, and bimolecular fluorescence complementation (BiFC). Recently, there have been MAM reporters developed using split green fluorescent protein (split GFP), a molecule used in BiFC, in order to detect ER-mitochondria contact sites in live cells (Yang et al., 2018; Kakimoto et al., 2018; Cieri et al., 2018). However, the disadvantage of split GFP-based BiFC in detecting MAM is that the interactions between the split GFP components are irreversible and may lead to artifacts of MAM structure. In contrast, MAMtrackers are suitable for detecting dynamic changes in MAM than BiFC-based detection because the interactions between the components of MAMtracker-Green are reversible due to its high dissociation constant (K_d = 9 μM) (Sakai et al., 2021).

6.2 Results

6.2.1 Roles of TBC1D15 and TBC1D17 in Hypoxia-induced Mitophagy

HeLa cells were transfected with Mito-pHfluroin and Nsi, TBC1D15-specific siRNA or TBC1D17 siRNA. 48 h post-transfection the cells were exposed to 24 h normoxia or hypoxia. Subsequently, the cells were fixed with 4% PFA and stained for TBC1D15 or TBC1D17 as appropriate. The cells were imaged as shown in **Figures 6.1** and **6.2** with a confocal microscope. Knockdown of TBC1D15 in HeLa cells led to no significant change in HIM or mitophagy under normoxic conditions (**Figure 6.1b**). On the other hand, knockdown of TBC1D17 in HeLa cells significantly increased levels of HIM (**Figure 6.2b**). These results do not support a role for TBC1D15 in regulating HIM and suggest that TBC1D17 suppresses HIM. Consistent with these results, we also found that TBC1D15 levels do not significantly change while TBC1D17 levels

decrease in HeLa cells exposed to hypoxia for 24 h with Western blotting (**Figure 6.1c-d**; **Figure 6.2c-d**), raising the possibility of TBC1D17 degradation by HIM.

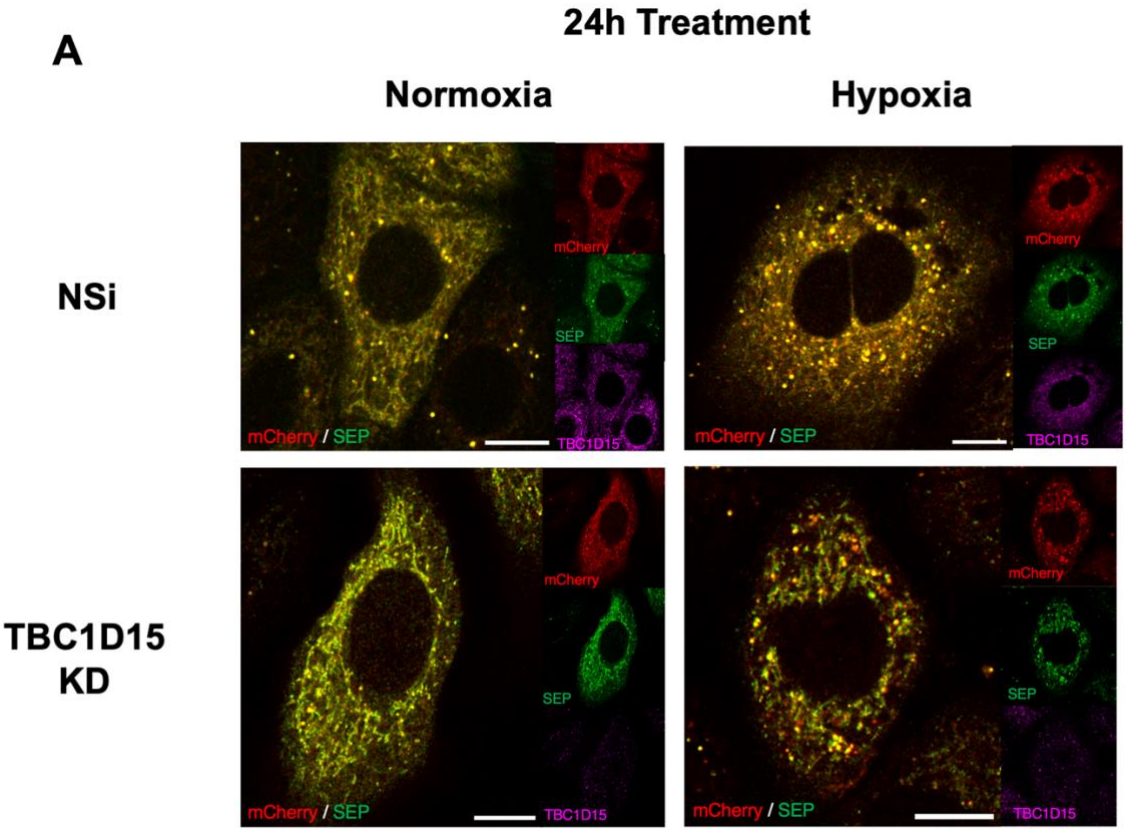

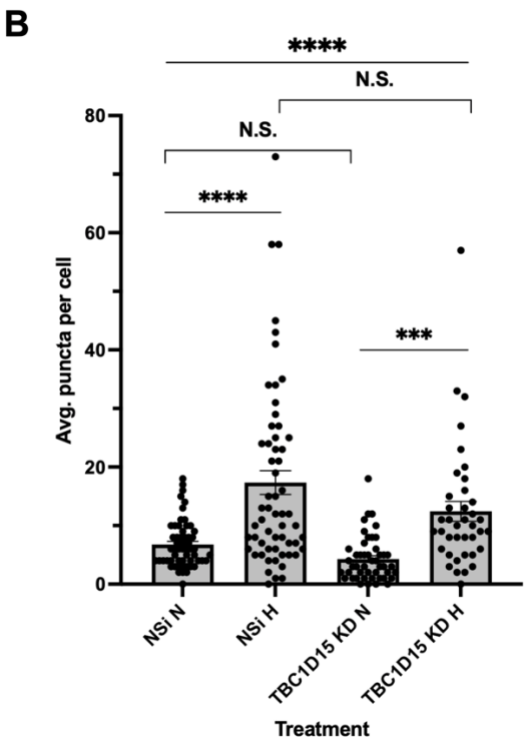

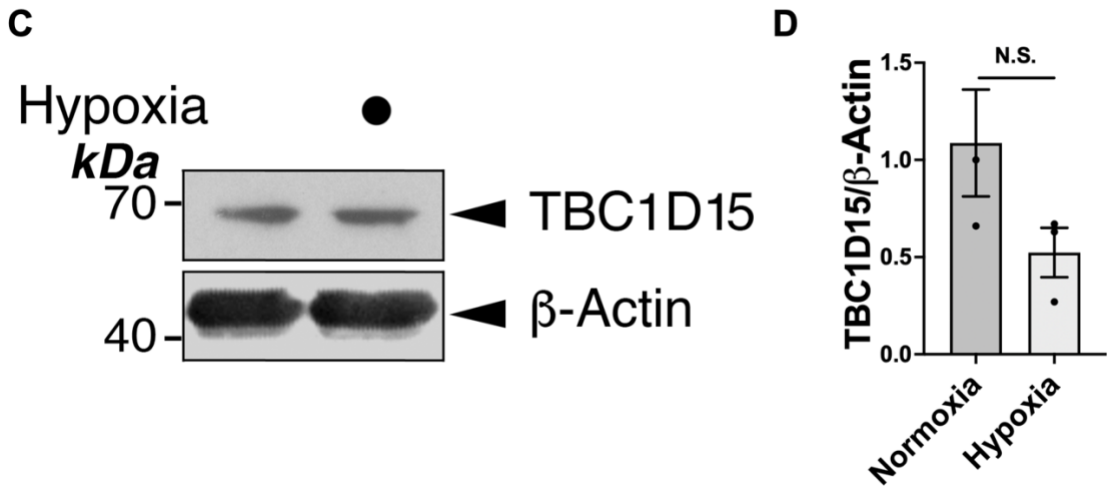

Figure 6.1: The Effect of TBC1D15 KD on Hypoxia-Induced Mitophagy in HeLa cells

A) HeLa cells were transfected with Mito-pHfluorin and Nsi or TBC1D15-specific siRNA (20 nM). 48 h post-transfection the cells were exposed to normoxia or hypoxia (1% O_2) for 24 h. The cells were fixed with PFA 4% and stained for TBC1D15 and then imaged with confocal microscopy. B) Histogram shows average number of Mito-pHfluorin red puncta per cell for cells exposed to N or H for 24 h. (n = 39-59, N.S. non-significant; ***$p < 0.001$; ****$p < 0.0001$; Ordinary one-way ANOVA followed by Sidak's multiple comparisons test). The data presented in 6.1A-B are from a single experiment. n refers to the number of cells from one µ-dish used to quantify the average number of puncta per experimental condition. C) HeLa cells were exposed to normoxia or hypoxia (1% O_2) for 24 h. Whole cell lysate samples were prepared and blotted as indicated. D) Histogram shows relative levels of TBC1D15 in HeLa cells exposed to normoxia or hypoxia for 24 h. (n = 3, N.S. non-significant; $p > 0.05$; Unpaired Student's t-test). Scale bar 10 µm.

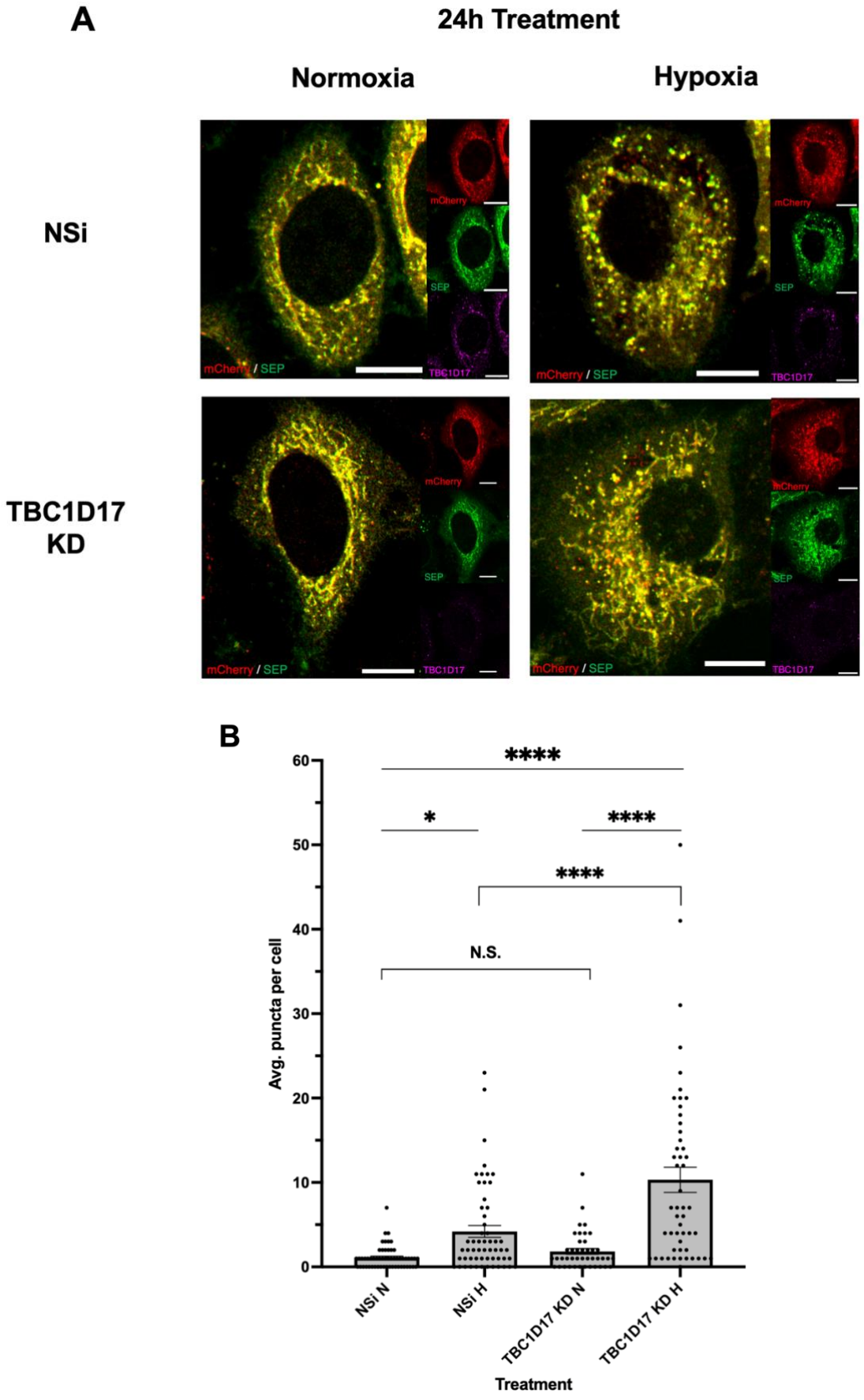
A
24h Treatment
Normoxia
Hypoxia
NSi
TBC1D17 KD
mCherry
SEP
TBC1D17
mCherry / SEP
B
Avg. puncta per cell
0
10
20
30
40
50
60
****
*
****
****
N.S.
NSi N
NSi H
TBC1D17 KD N
TBC1D17 KD H
Treatment

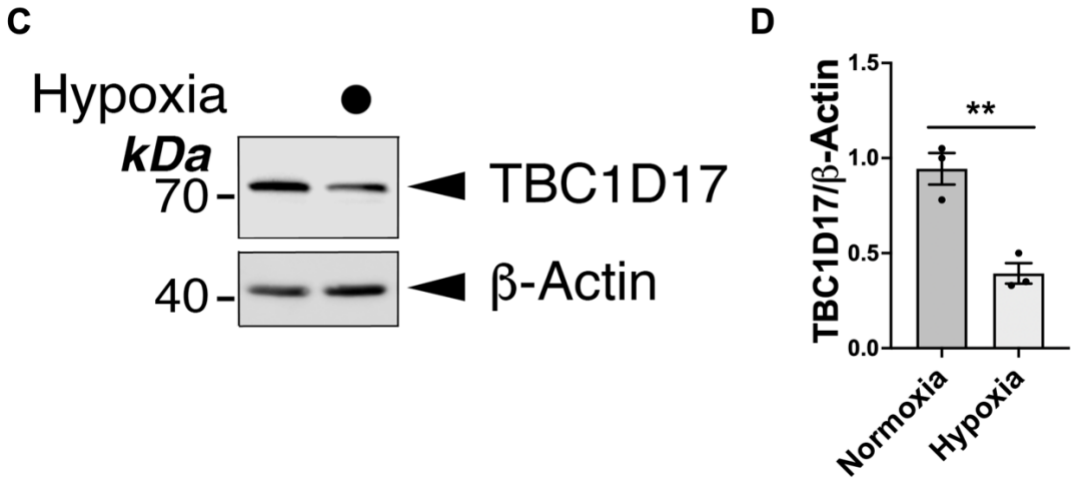

Figure 6.2: The Effect of TBC1D17 KD on Hypoxia-Induced Mitophagy in HeLa cells

A) HeLa cells were transfected with Mito-pHfluorin and Nsi or TBC1D17-specific siRNA (20 nM). 48 h post-transfection the cells were exposed to normoxia or hypoxia (1% O_2) for 24 h. The cells were fixed with PFA 4% and stained for TBC1D17 and then imaged with confocal microscopy. B) Histogram shows average number of Mito-pHfluorin red puncta per cell for cells exposed to N or H for 24 h. (n = 42-56, N.S. non-significant; *p < 0.05; ****p < 0.0001; Ordinary one-way ANOVA followed by Sidak's multiple comparisons test). The data presented in 6.2A-B are from a single experiment. n refers to the number of cells from one µ-dish used to quantify the average number of puncta per experimental condition. C) HeLa cells were exposed to normoxia or hypoxia (1% O_2) for 24 h. Whole cell lysate samples were prepared and blotted as indicated. D) Histogram shows relative levels of TBC1D17 in HeLa cells exposed to normoxia or hypoxia for 24 h (n = 3, **p < 0.01; Unpaired Student's t-test). Scale bar 10 µm.

6.2.2 Suppression of hypoxia-induced mitophagy by TBC1D17 depends on Fis1-TBC1D17 interaction

Both exogenously expressed TBC1D15 and TBC1D17 have been shown to interact with Fis1 to mediate mitophagy (Yamano et al., 2014). Because the results from our TBC1D15 and TBC1D17 knockdown experiments suggest that TBC1D17 but not TBC1D15 regulates levels of HIM in HeLa cells, we next investigated whether TBC1D17 works with Fis1 to mediate this regulation. Thus, we performed a double knockdown of Fis1 and TBC1D17 in HeLa cells that were co-transfected with Mito-pHfluorin. 48 h post-transfection, the cells were subjected to hypoxia for 24 h and fixed with 4% PFA. The cells were stained for Fis1 and TBC1D17 and imaged with a confocal microscope as shown in **Figure 6.3a**. It appears that TBC1D17 and Fis1 co-localized to the mitochondria (**Figure 6.3a, c**). Interestingly, in absence of Fis1, loss of TBC1D17 did not increase levels of HIM (**Figure 6.3b**), suggesting that Fis1 is a downstream interacting partner of the Rab-GAP protein in regulating HIM and that suppression of HIM by TBC1D17 is dependent on TBC1D17 interaction with Fis1. As shown in **Figure 6.3c**, hypoxia appears to increase colocalization between TBC1D17 and Fis1 in the Nsi/Nsi control samples compared to normoxic conditions. Consistent with our Western blotting results (**Figure 5.2, Figure 6.2c-d**), Fis1 and TBC1D17 levels decreased under hypoxia in these samples. Our colocalization analysis was also, to the best of our knowledge as of this study, the first evidence of potential endogenous interaction between Fis1 and TBC1D17 under normoxia (**Figure 6.3c**). However, future investigation is needed to substantiate these preliminary observations.

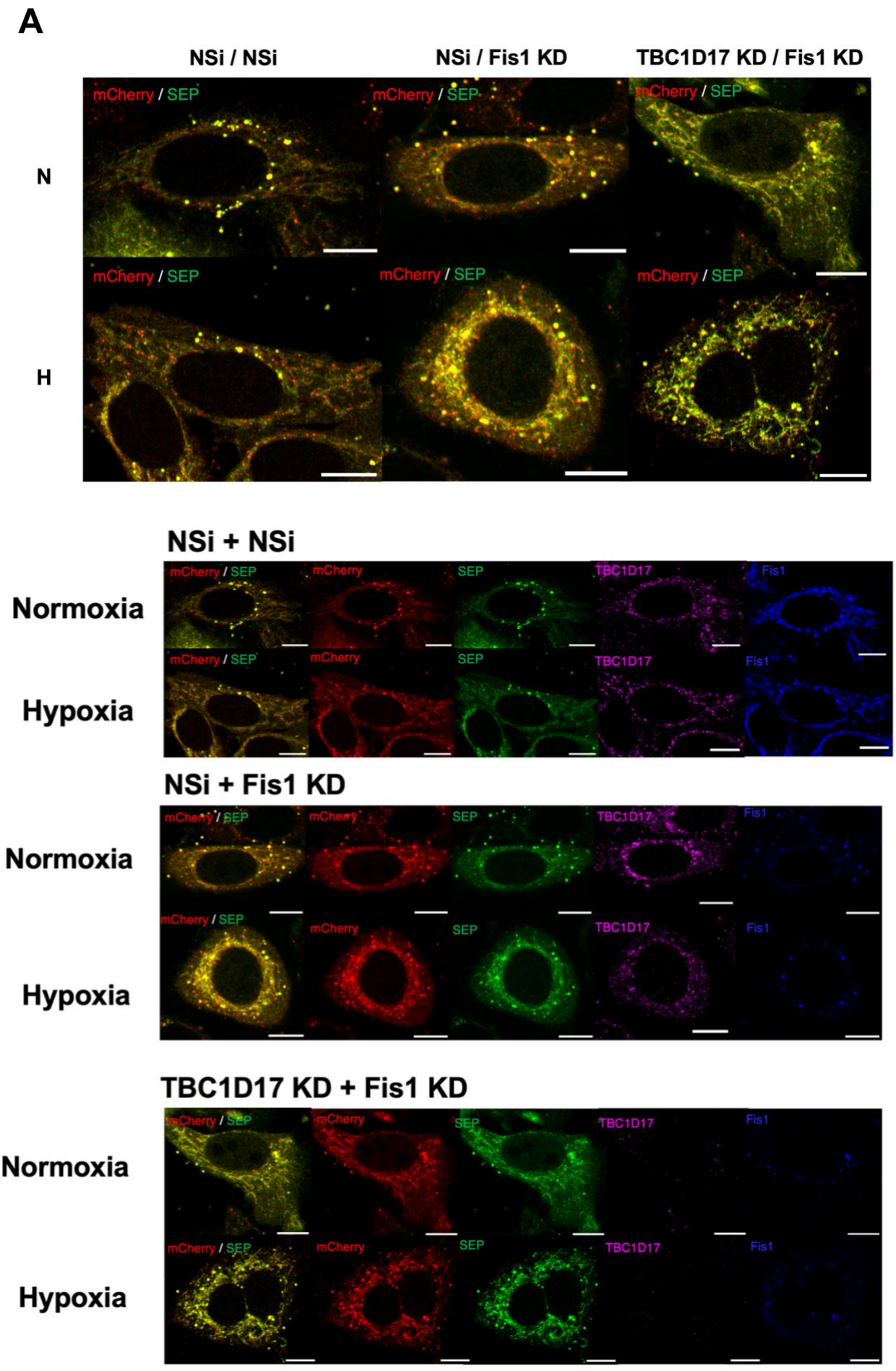
A
NSi / NSi
NSi / Fis1 KD
TBC1D17 KD / Fis1 KD
N
H
mCherry / SEP
NSi + NSi
Normoxia
Hypoxia
mCherry
SEP
TBC1D17
Fis1
NSi + Fis1 KD
TBC1D17 KD + Fis1 KD

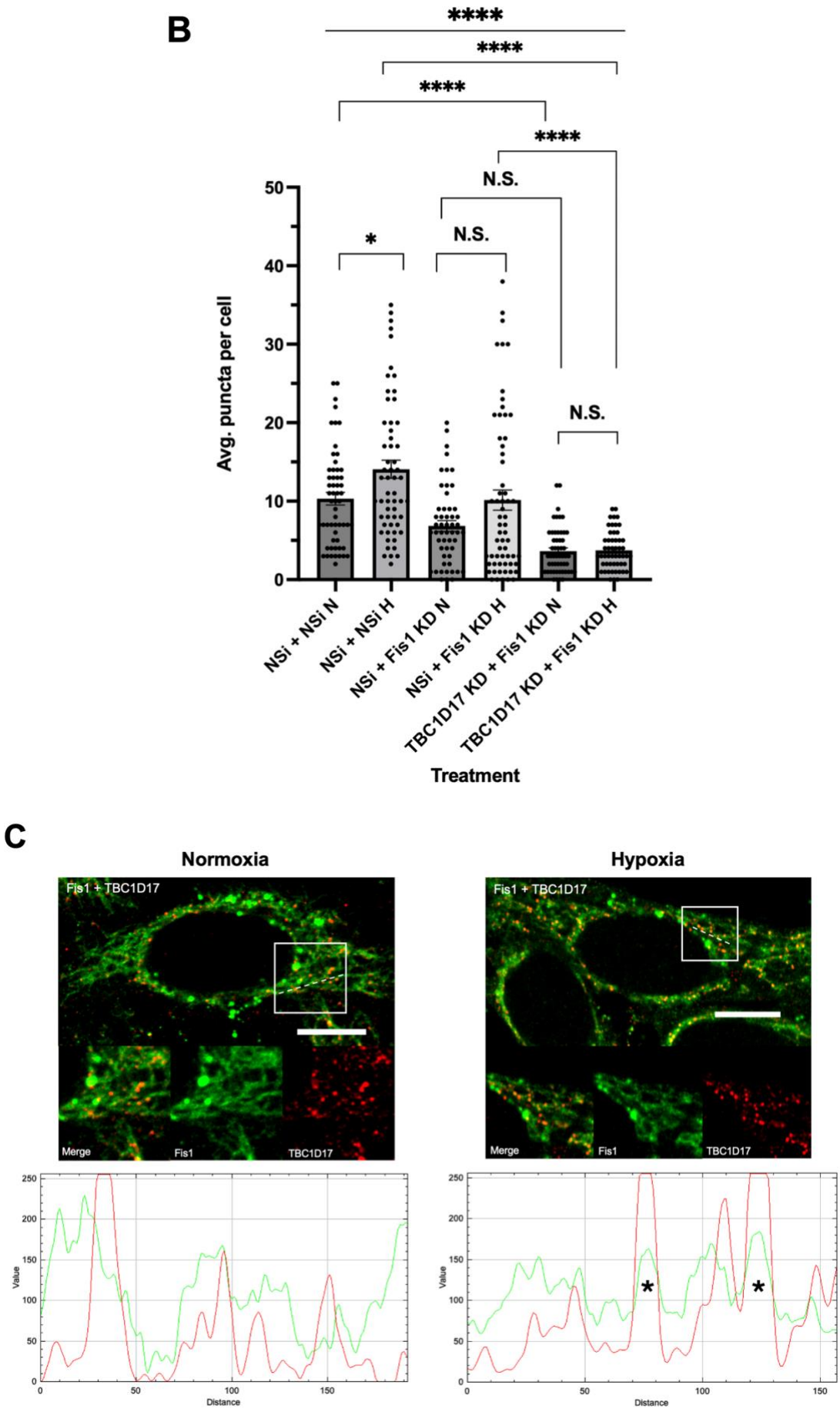
B
****
****
****
****
N.S.
N.S.
N.S.
*
Avg. puncta per cell
0
10
20
30
40
50
NSi + NSi N
NSi + NSi H
NSi + Fis1 KD N
NSi + Fis1 KD H
TBC1D17 KD + Fis1 KD N
TBC1D17 KD + Fis1 KD H
Treatment
C
Normoxia
Hypoxia
Fis1 + TBC1D17
Merge
Fis1
TBC1D17
Value
Distance
0
50
100
150
200
250
*
*

Figure 6.3: TBC1D17-mediated suppression of hypoxia-induced mitophagy depends on TBC1D17-Fis1 interaction

A) HeLa cells were transfected with Mito-pHfluorin and a combination of Nsi, TBC1D17-specific siRNA (20 nM), and/or Fis1-specific siRNA (50 nM) as indicated. 48 h post-transfection the cells were exposed to normoxia (N) or hypoxia (H, 1% O_2) for 24 h. The cells were fixed with 4% PFA and stained for TBC1D17 and Fis1 and then imaged with confocal microscopy. B) Histogram shows average number of Mito-pHfluorin red puncta per cell for cells exposed to N or H for 24 h. (n = 54-79, N.S. non-significant; *p < 0.05; ****p < 0.0001; Ordinary one-way ANOVA followed by Sidak's multiple comparisons test). The data presented are from a single experiment. n refers to the number of cells from one µ-dish used to quantify the average number of puncta per experimental condition. C) Hypoxia increases colocalization between TBC1D17 (red) and Fis1 (green) in the Nsi/Nsi samples shown in Figure 6.3a. Relative fluorescence intensity of each channel as points along the white dotted line shown in the lower graphs for normoxia and hypoxia conditions. Asterisks (*) on the graph indicate areas of potential colocalization. Scale bar 10 µm.

6.2.3 Role of Stx17 in Mitophagy

HeLa cells were transfected with Mito-pHfluorin and Nsi or Stx17-specific siRNA. 48 post-transfection, the cells were exposed to normoxia or hypoxia for 24 h and then fixed with 4% PFA. The cells were imaged with a confocal microscope as shown in **Figure 6.4a**. Stx17 KD significantly decreased levels of mitophagy under normoxic conditions and abolished HIM (**Figure 6.4b**). These data imply that Stx17 plays an important role in controlling basal mitophagy levels as well as HIM.

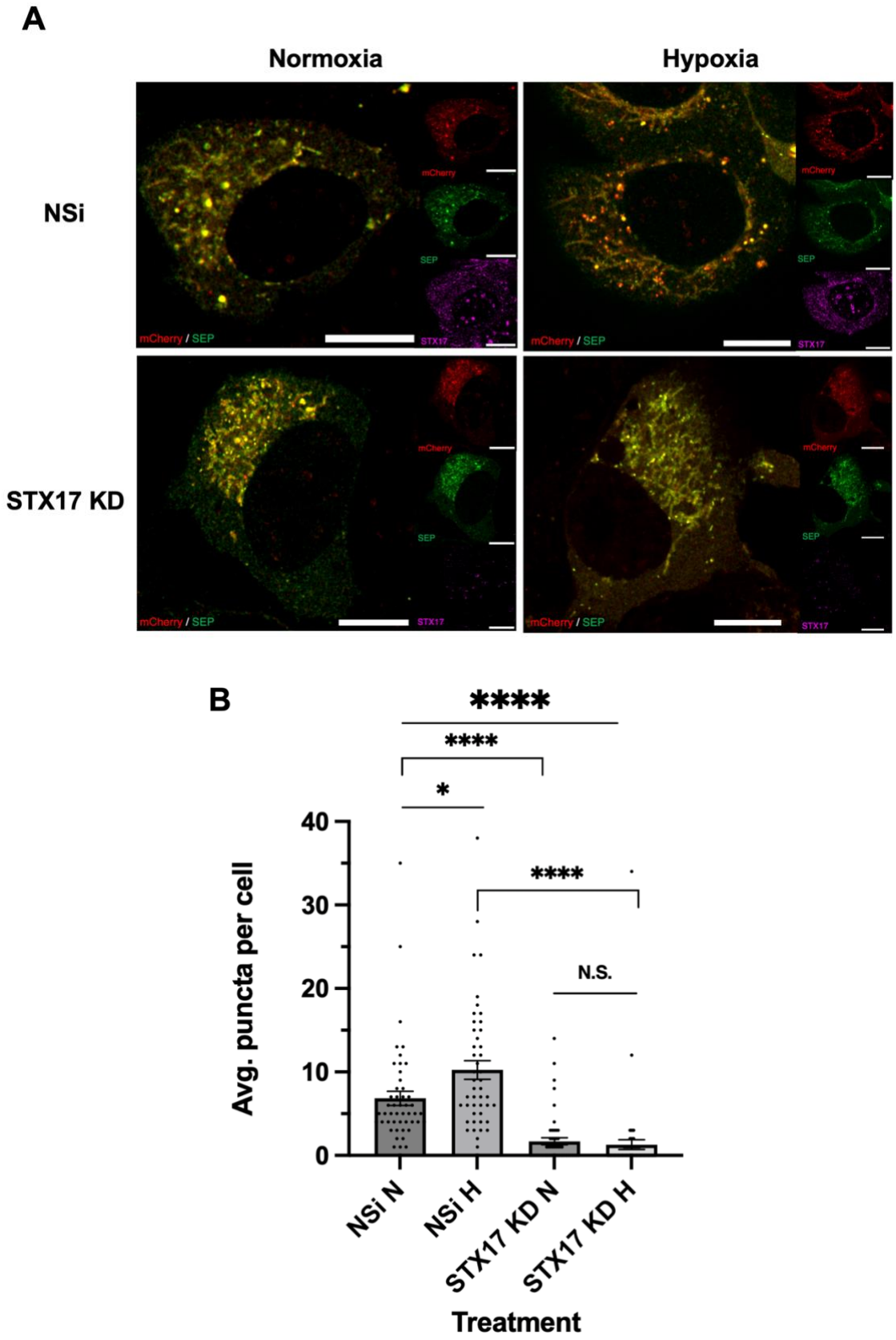
A
Normoxia
Hypoxia
NSi
STX17 KD
mCherry
SEP
STX17
mCherry / SEP
B
****
****
*
****
N.S.
Avg. puncta per cell
40
30
20
10
0
NSi N
NSi H
STX17 KD N
STX17 KD H
Treatment

Figure 6.4: The Effect of Stx17 KD on Hypoxia-Induced Mitophagy in HeLa cells

A) HeLa cells were transfected with Mito-pHfluorin and Nsi or Stx17-specific siRNA (20 nM). 48 h post-transfection the cells were exposed to normoxia or hypoxia (1% O_2) for 24 h. The cells were fixed with PFA 4% and stained for Stx17 and then imaged with confocal microscopy. B) Histogram shows average number of Mito-pHfluorin red puncta per cell for cells exposed to N or H for 24 h. (n = 47-61, N.S. non-significant; *p < 0.05; ****p < 0.0001; Ordinary one-way ANOVA followed by Sidak's multiple comparisons test). Scale bar 10 µm. The data presented are from a single experiment. n refers to the number of cells from one µ-dish used to quantify the average number of puncta per experimental condition.

6.2.4 The Effect of SUMOylation on MAM Formation

MAMtracker-Green was generated by Sakai et al. (2021) to monitor changes in MAM status in living cells. In the experiments that were performed to determine the effect of SUMOylation inhibition by TAK-981 treatment or SENP3 knockdown on the level of MAM formation, we imaged live HeLa cells that were transfected with MAMtracker-Green, which stains for the sites of ER-mitochondria contact. To quantify the level of MAM-formation, we compared the relative fluorescence intensity (RFI) of MAMtracker-Green between cells of different conditions. Relative fluorescence intensity was calculated by subtracting the background intensity of an individual cell from fluorescence intensity and dividing the difference by the average RFI of the control condition (*i.e.* in this case, the RFI of control refers to that of a DMSO-treated cell or cell transfected with Nsi).

To investigate the role of SUMOylation on MAM formation, we used TAK-981 to inhibit SUMOylation in HeLa cells. Briefly, HeLa cells were transfected with MAMtracker-Green. 48 post-transfection, the cells were treated with DMSO or TAK-981 for up to 24 h. The cells were imaged at 0 h, 4 h and 24 h time points as shown in **Figure 6.5a**. TAK-981 treatment for 4 h and

24 h appears to significantly increase the level of MAM formation compared to cells treated with DMSO (**Figure 6.5b**). These data suggest that SUMOylation may have a regulatory role in MAM formation under normoxic conditions, but future investigation is needed to support these this idea.

In a similar vein, we also investigated the role of SENP3 in MAM formation because SENP3 suppresses SUMO-2/3-ylation levels by functioning as a deSUMO-2/3-ylating enzyme. We performed SENP3 knockdown in HeLa cells to determine the effect of SENP3 on MAM formation levels. HeLa cells were transfected with MAMtracker-Green and Nsi or SENP3-specific siRNA. 48 h post-transfection, Mitotracker Red was added to the cells to stain for the mitochondria and the cells were then imaged as shown in **Figure 6.6a**. Unexpectedly, knockdown of SENP3 led to no significant change in MAM formation (**Figure 6.6b**). This does not support a role for SENP3 in the regulation of MAM formation in HeLa cells under normoxic conditions.

Note: (RFI = (Fluorescence intensity – background intensity)/average of control relative fluorescence intensity)

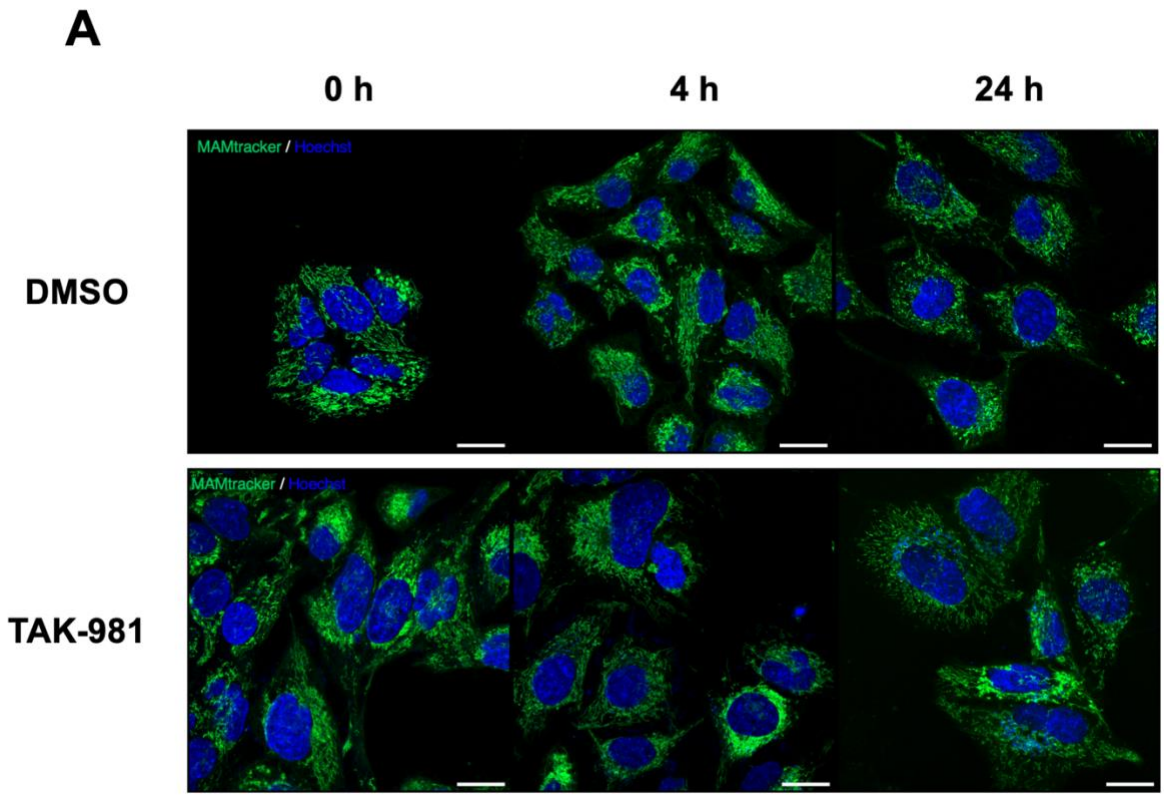

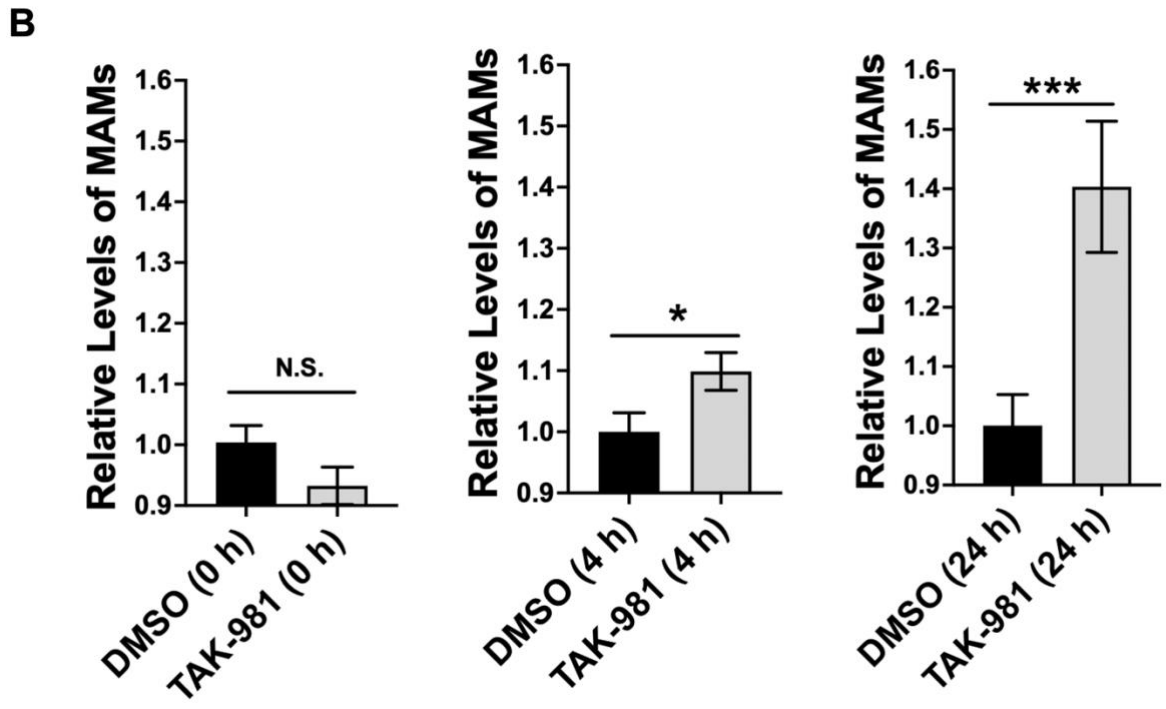

Figure 6.5: TAK-981 treatment increases MAM formation in HeLa cells

A) HeLa cells were transfected with MAMtracker-Green (1 µg/well). 48 h post-transfection the cells were treated with DMSO or TAK-981 (100 nM) for up to 24 h. Nuclei were stained with Hoechst (1:10,000). The cells were imaged with confocal microscopy at 0, 4 and 24 h time points. B) Histograms show the relative levels of MAMs between cells treated with DMSO v. TAK-981 for 0, 4, or 24 h (left, center, right, respectively). Relative levels of MAMs were obtained by normalizing the average relative fluorescence intensity (RFI) of MAMtracker-Green of each condition to the average RFI of cells treated with DMSO for the respective time point. For 0 h, n = 52-59. For 4 h, n = 57. For 24 h, n = 33-43. (N.S. non-significant; *$p < 0.05$; ***$p < 0.001$; Unpaired Student's t-test). Scale bar 20 µm. The data presented are from a single experiment. n refers to the number of cells from one µ-dish used to quantify the average number of puncta per experimental condition.

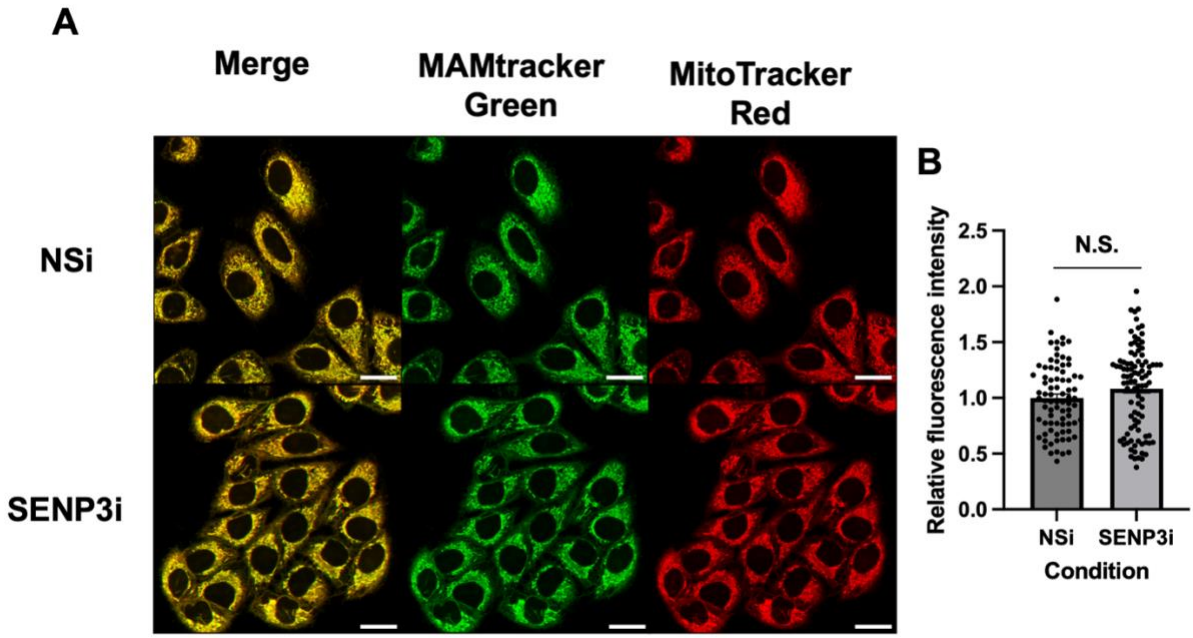

Figure 6.6: SENP3 KD does not change levels of MAM formation in HeLa cells

A) HeLa cells were transfected with MAMtracker-Green (1 µg/well) and Nsi or SENP3-specific siRNA (50 nM). 48 h post-transfection the cells were stained with MitoTracker Red (50 nM). The cells were imaged with confocal microscopy. B) Histogram shows the average relative fluorescence intensity (RFI) of MAMtracker-Green. (n = 80-94, N.S. non-significant; Unpaired Student's t-test). Scale bar 20 µm. The data presented are from a single experiment. n refers to the number of cells from one µ-dish used to quantify the average number of puncta per experimental condition.

6.3 Discussion

Figure 6.7 summarizes the main findings and proposed mechanisms from Chapter 6. The left side covers discussion sections **6.3.1-6.3.3**, while the right side covers sections **6.3.5**.

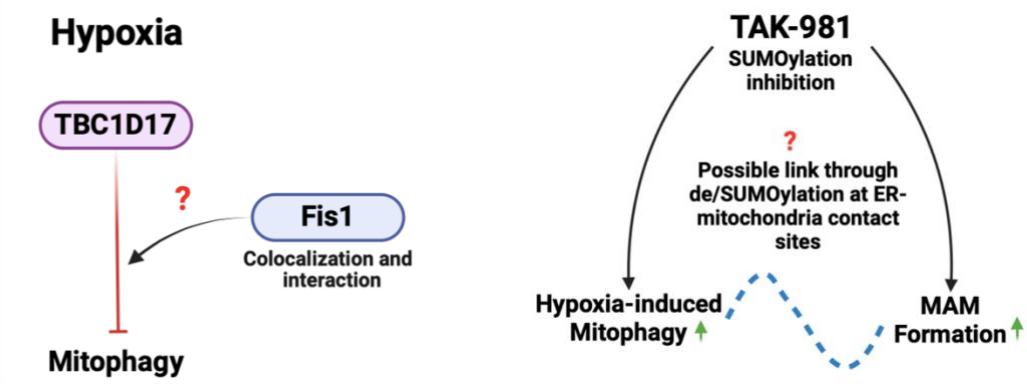

Figure 6.7: Summary of Chapter 6 Findings

(Left) TBC1D17 suppresses HIM levels. TBC1D17-Fis1 interactions seem important for TBC1D17-mediated suppression of HIM. (Right) TAK-981 increases both HIM levels and MAM formation. There may be a link between HIM and MAM formation based on de/SUMOylation events at the ER-mitochondria contact sites.

6.3.1 The role of TBC1D15 KD in regulating mitophagy induced by hypoxia in cells lacking Parkin

We found that knockdown of TBC1D15 in HeLa cells did not lead to changes in levels of HIM and mitophagy under normoxia while knockdown of TBC1D17 increased HIM. These results suggest that TBC1D15 is less likely to be involved in HIM and that TBC1D17 plays an inhibitory role in HIM. However, more research is needed to elucidate what the roles of TBC1D15 and TBC1D17 are in HIM and how they differ. One possible reason for why TBC1D15 knockdown did not affect levels of HIM is that we performed these experiments in HeLa cells, which express little or no Parkin. In Parkin-expressing HCT116 cells, Yamano et al. (2014) reported that TBC1D15 works downstream of Parkin activation for autophagosome biogenesis and morphology.

In absence of Parkin, TBC1D15 may not exhibit the same role in mitophagy compared to when Parkin is present in cells. Since HIM is a Parkin-independent form of mitophagy, depletion of TBC1D15 may not strongly affect the level of autophagosome formation during mitophagy. Consistent with our findings under normoxic conditions, Xian et al. (2019) found that loss of TBC1D15 in HeLa cells did not impact mitophagy. In contrast, Rojansky et al. (2016) described that TBC1D15 KD reduced oxidative phosphorylation-induced mitophagy in mouse embryonic fibroblasts (MEFs), which express Parkin. Yamano et al. (2014) reported that the interaction between Fis1 and TBC1D15 is not essential for Parkin-mediated mitophagy induced by valinomycin, which dissipates mitochondrial inner membrane potential, but deletion of either Fis1 or TBC1D15 hinders the clearance of damaged mitochondria and that TBC1D15 escapes degradation during mitophagy while Fis1 does not. This is supported by our findings that showed no change in TBC1D15 levels in HeLa cells exposed to hypoxia for 24 h. While these findings highlight important but non-essential roles for Fis1 and TBC1D15 in Parkin-mediated mitophagy, based on our findings, Fis1 is likely necessary for Parkin-independent HIM. Therefore, it is possible that the role of TBC1D15 in mitophagy varies between cell types and mitophagic activation pathways. In a Parkin-free system, TBC1D15 does not seem to majorly affect levels of basal mitophagy or HIM despite its interactions with Fis1.

6.3.2 The role of TBC1D17 KD in regulating mitophagy induced by hypoxia in cells lacking Parkin

As stated above, to the best of our knowledge, we for the first time provide evidence that TBC1D17 regulates HIM, specifically, by suppressing it. TBC1D15 and TBC1D17 can heterodimerize with each other or homodimerize to mediate mitophagy (Yamano et al., 2014). TBC1D17 may act as the limiting factor in a Fis1-mediated regulatory pathway for HIM, given that TBC1D15 knockdown did not change the levels of HIM while endogenous TBC1D17 was

still present in cells and available to form homodimers with itself. This is a novel finding since as of this thesis, as there are currently no reports of TBC1D17 regulating mitophagy in cells lacking Parkin under hypoxia. We also found that TBC1D17 levels decrease in HeLa cells exposed to hypoxia for 24 h. From this, the decrease of TBC1D17 levels under hypoxia appears to correlate with increase of HIM, further supporting the idea of a suppressive role for TBC1D17 in HIM. TBC1D17 has been reported to regulate the inhibition of endocytic recycling by inhibiting colocalization of Rab8 and transferrin receptors (TFR) in HeLa cells (Vaibhava et al., 2012). Interestingly, the TBC1D17-mediated pathway appears to be independent of Parkin activation (Vaibhava et al., 2012). In a study investigating glaucoma-causing mutations in *OPTN*, the gene encoding the protein optineurin, Chalasani et al. (2014) found that knockdown of TBC1D17 rescued cells from the inhibition of autophagy mediated by the E50K mutation in retinal cells. The E50K mutation induces retinal cell death through impaired autophagy and results in defective endocytic recycling of TFR mediated by TBC1D17-dependent inactivation of Rab8 (Chalasani et al., 2007; Vaibhava et al., 2012). The inhibitory roles of TBC1D17 in autophagy and endocytic recycling are interesting to note, especially when compared to our findings that suggest TBC1D17 has a suppressive or inhibitory effect on HIM in HeLa cells.

6.3.3 The role of Fis1 in TBC1D17-mediated mitophagy induced by hypoxia in cells lacking Parkin

Because our findings suggested that Fis1 is important for HIM and that TBC1D17 has a suppressive effect on HIM levels in HeLa cells, we performed knockdowns of both Fis1 and TBC1D17 to determine if the two proteins work together to regulate HIM. Interestingly, knockdown of both proteins together abolished HIM in HeLa cells. As of this thesis, there are no other studies exploring the role and mechanism(s) of TBC1D17 under hypoxia or HIM. To the best of our knowledge, while preliminary, our findings are the first to provide evidence of a role

for Fis1 in the inhibition of HIM mediated by TBC1D17 in HeLa cells and the endogenous interaction of TBC1D17 with Fis1 under normoxic conditions. Further investigation on the role TBC1D17-Fis1 interactions potentially have in HIM could provide novel insights on HIM regulation. Yamano et al. (2014) identified TBC1D17 as a binding partner for Fis1 and TBC1D15 and detected the mitochondrial colocalization of exogenously expressed Fis1 and TBC1D17. Consistent with the aforementioned study by Yamano and colleagues (2014), our findings suggest that Fis1-TBC1D17 interaction may be a prerequisite for TBC1D17-mediated inhibition of HIM. Our colocalization analysis of Fis1-TBC1D17 interaction in Nsi control samples appears to show that TBC1D17 colocalization with Fis1 increases under hypoxic conditions, suggesting that HIM is potentially accompanied by an endogenous level of TBC1D17-mediated suppression to prevent excess induction of mitophagy under hypoxic conditions.

6.3.4 The role of Stx17 in mitophagy regulation in cells lacking Parkin under normoxia and hypoxia

In the present study, we found that RNAi-mediated depletion of Stx17 significantly decreased the levels of mitophagy under both normoxic and hypoxic conditions, suggesting an important role for Stx17 in both types of mitophagy. Our findings in cells exposed to normoxia are consistent with a previous study that showed depletion of Stx17 inhibited mitophagy under normoxia (Sugo et al., 2018). In a previous study by Hamasaki et al. (2013), Stx17 KD was found to decrease autophagy through various intracellular molecular events such as the degradation of p62 and long-lived proteins, which depend on autophagic clearance. Hamasaki et al. (2013) also reported that Stx17 knockdown lead to an accumulation of isolation membranes and a lack of autolysosomes, indicating that Stx17 KD prevents autophagosome maturation. In Stx17 KO cells, fusion of autophagosomes with lysosomes was defective, which could be rescued by the introduction of Stx17 WT but not an autosome-lysosome defective mutant Stx17 (Wang et al., 2019). Thus, Stx17

contributes to the formation of functional autophagosomes and our knockdown of Stx17 decreased mitophagy under normoxia and hypoxia most likely by preventing autophagosome maturation. Xian et al. (2019) reported that Stx17 interacts with Fis1, and interestingly only in absence of Fis1 does Stx17 overexpression appear to promote Stx17 accumulation on the mitochondria and the initiation of Parkin-independent mitophagy. The same study also noted that in contrast to Fis1, TBC1D15 is not involved in Stx17 overexpression-mediated mitophagy (Xian et al., 2019). So although Stx17 interacts with Fis1 and regulates Parkin-independent mitophagy, it may not necessarily participate in the Fis1-dependent HIM pathway demonstrated in this study, which are mediated by both Fis1 and TBC1D17 to regulate HIM. Currently, there are no published studies directly showing the function(s) of Stx17 in hypoxia or HIM. To the best of our knowledge, we provide evidence of the role of Stx17 on HIM for the first time, though the mechanism behind this remains unclear and warrants further investigation.

6.3.5 MAM formation and mitophagy induction mediated by SUMOylation/deSUMOylation

In the present study, we found that inhibition of SUMOylation by TAK-981 treatment increases MAM formation while knockdown of SENP3 did not affect MAM levels, suggesting that deSUMOylation may contribute to MAM formation. There are currently no studies discussing the role of SUMOylation on MAM formation under normoxia, so these findings, while preliminary, are novel. In chapter 4, we found that SUMOylation inhibition by TAK-981 treatment, which mimics deSUMOylation, leads to an increase of HIM in HeLa cells and SENP3 KD, which is known to enhance SUMO-2/3-ylation, significantly decreases mitophagy under both normoxic and hypoxic conditions. From these results, it appears deSUMOylation affects both MAM formation and HIM levels. Furthermore, SENP3 KD, which enhances SUMO-2/3-ylation, does not significantly change levels of MAM formation but, as we discussed in Chapter 4, suppresses

mitophagy under normoxia and hypoxia. In addition, MAMs are reported to be responsive to hypoxia (Wu et al., 2016; Chai et al., 2021). Therefore, SUMOylation/deSUMOylation may serve as mechanistic links between MAM formation and SUMO-mediated mitophagy where deSUMOylation increases HIM possibly by affecting the formation of MAMs, which are considered the sites of origin for autophagy (Matsunaga et al., 2010; Hamasaki et al., 2013). SUMO-2/3-ylation may fit into this paradigm by suppressing mitophagy levels but perhaps not by affecting the level MAM formation. Our SENP3 KD experiments have been focused on assessing the effect of SENP3 on HIM. Unfortunately, due to technical constraints we were unable perform imaging experiments assessing MAM formation under hypoxia, so we currently cannot determine whether TAK-981-mediated SUMOylation inhibition and SENP3 KD impact MAM formation under hypoxia.

While MAMtracker-Green is a powerful tool for monitoring MAM status in live cells, we unfortunately could not utilize MAMtracker-Green in fixed cells or on live cells exposed to hypoxia unless they are imaged while still under hypoxic conditions. This placed limitations on the type of experiments we could perform pertaining to MAM formation. Theoretically, hypoxia experiments can be performed with MAMtracker-Green if the cells used were imaged while still within the same hypoxic environment as the hypoxia workstation. Realistically, it would be difficult achieve this setup due to the size and availability of the Airyscan confocal microscope. To overcome the technical constraints, we consider detecting MAM formation in fixed cells can be achieved by using alternative fluorescent probes for protein components of the MAM on the mitochondrial outer membrane and ER (such as FKBP8 and cytochrome b5 or KDEL peptide, respectively) and monitoring the overlap of these proteins. To explore the link between MAM formation and HIM, we consider using Mito-pHfluorin as we have previously described and demonstrated in this thesis in combination with the approach for MAM detection under hypoxic conditions.

Chapter 7

General Discussion

7.1 Summary of Main Findings

7.1.1 Chapter 3 – Establishment of Experimental Systems for Characterization of Hypoxia-Induced Mitophagy (HIM)

Mitophagy is a homeostatic process that selectively clears out damaged or dysfunctional mitochondria by the autophagic pathway. Both hypoxia and defects in mitophagy have been linked to various human diseases including cancer, neurodegeneration and inflammatory disease (Muz et al., 2015; Burtscher et al., 2021; Biddelstone et al., 2015; Vara-Perez et al., 2019; Palikaras & Tavernarakis, 2012; Gkikas et al., 2018). Hypoxic cell response is controlled by the master transcription factor HIF-1 and is regulated by the reversible PTM SUMOylation (Bae et al., 2004; Cheng et al., 2007; Carbia-Nagashima et al., 2007). Under hypoxia, the HIF-1 pathway upregulates genes involved with autophagy and mitophagy (Fu et al., 2020; Mazure & Pouysségur, 2010). This thesis investigates the role of deSUMOylation enzymes on the regulation of HIM. The primary aim of the work carried out in Chapter 3 was to establish a hypoxia experimental system that induces hypoxia stress response in cultured cells using a SCI-tive Hypoxia Workstation (Baker Ruskinn) in order to explore the protein profile of hypoxic cell response with Western blotting. Additionally, we optimize our usage of the dual-florescent probe Mito-pHfluorin in fluorescence microscopy to visualize and quantify mitophagy in cells exposed to hypoxia. This is the first step in our investigation of how HIM is regulated by deSUMOylation enzymes.

First, HIF-1α and HIF-2α levels were assessed under hypoxia in model (HeLa) cells to ensure that the hypoxia workstation induces hypoxic cell response. As expected, the hypoxic environment within the workstation yielded robust and significant induction of HIF-1α in HeLa

cells, as confirmed with Western blotting. Hypoxic conditions stabilize HIF-1α, rescuing it from hydroxylation by PHDs and subsequent proteasomal degradation (Ulrich, 2007). Induction of HIF-1α levels under hypoxia is consistent with previous reports (Wiener et al., 1996; Begeron et al., 2008). This confirms cell response to hypoxia occurs within our hypoxia experimental system and that our setup is suitable for further use in hypoxia-based experiments. However, we observed that HIF-2α levels in our model cells fluctuated at different lengths of hypoxic exposure and significantly decreased after 24 h of exposure to hypoxia. Due to the poor quality of the Western blots for HIF-2α, we could not determine a clear pattern of HIF-2α expression under hypoxia from our data. Similar to HIF-1α, HIF-2α is reported to be stabilized under hypoxia and increases with prolonged exposure to hypoxia (Holmquist-Mengelbier et al., 2006). Aside from the Western blot quality, a possible reason why our Western blot results contradict this is that according to the HIF switch model, HIF-2 hypoxic response occurs with prolonged hypoxia. In our experiment, at 24 h of hypoxic exposure the cells may have not yet switched from an acute hypoxia response driven by HIF-1 to a chronic hypoxia response driven by HIF-2 (Koh & Powis, 2012). Because HIF-1 is expressed in nearly all cell types while HIF-2 is expressed in certain tissues (Loboda et al., 2010; Wiesener et al., 2003), we primarily rely on HIF-1α induction by hypoxia to confirm the effectiveness of our hypoxia induction.

Induction of autophagy by hypoxia was monitored with the detection of the autophagic marker LC3-II. In HeLa cells, LC3-II levels significantly increased after exposure to hypoxia for 12 h but not 24 h. In SH-SY5Y cells, LC3-II levels significantly increased after both 12 and 24 h of exposure to hypoxia. Although LC3 does not seem to be required for autophagy initiation, it mediates phagophore expansion and formation of autophagophores (Rouschop et al., 2010). However, increase of LC3-II alone does not indicate an increase of autophagosome formation. Whether the induction of LC3-II levels by hypoxia is caused by upregulation of autophagosome formation or blockage of autophagic degradation can be investigated with the treatment of cells

with lysosomal protease inhibitors such as chloroquine or bafilomycin A1 (Mizushima & Yoshimori, 2007). Levels of p62 and Tom20 both significantly decreased in HeLa cells exposed to hypoxia for 24 h. Degradation of p62 under hypoxia indicates induction of hypoxia-activated autophagy (Pursiheimo et al., 2008). Decreased Tom20 levels suggest a reduction in mitochondrial mass in Parkin-independent mitophagy (Ding & Yin, 2012; Yoshii et al., 2011). Altogether, these findings regarding LC3-II, p62 and Tom20 levels under hypoxia provide evidence that our hypoxia experimental system is capable of inducing autophagosome formation.

Unexpectedly, our Western blotting data showed that exposure of HeLa cells to hypoxia for 24 h decreased free SUMO-1 and SUMO-2/3 levels. SUMO-1 and SUMO-2/3 conjugates also decreased under hypoxia with the exception of 250 kDa SUMO-2/3 conjugates. These results may indicate the potential shut down of the SUMO pathway, leading to global deSUMOylation. The decrease of free SUMO levels may be caused by downregulation of *SUMO* gene transcription. Examination of *SUMO-1*, *SUMO-2* and *SUMO-3* gene expression levels by qPCR would elucidate whether downregulation of *SUMO* genes is behind reduction of free SUMO under hypoxia. Decreased availability of SUMO molecules due to potential downregulation of *SUMO* genes may result in the reduction of SUMO conjugation in our findings. Another explanation for reduced SUMO conjugation, though less likely, would be an upregulation of deSUMOylation enzymes. These results contradict findings from studies that show hypoxia enhances SUMO-1-ylation and SUMO-2/3-ylation (Shao et al., 2004; Carbia-Nagashima et al., 2007; Kunz et al., 2016). The discrepancies in SUMOylation levels may be attributed to differences in experimental settings, including exposure durations, equipment, and model cell lines used between the studies. Reduction of free SUMO levels and SUMOylation under hypoxic conditions in our model HeLa cells may signify the relevance of SUMO in regulating cell survival mechanisms under hypoxia. Moreover, our results indicate that TAK-981, as a potent SUMOylation inhibitor that activates robust anti-tumor immune response (Nakamura et al., 2019; Nakamura et al., 2020; Langston et

al., 2021) and a drug currently being evaluated in clinical trials in cancer patients (Khattar et al., 2019), is a powerful experimental tool in studying the role of deSUMOylation in autophagy or mitophagy induction.

SENP1 levels did not appear to be affected by hypoxia by our experimental system. SENP3 levels did not significantly change in HeLa cells exposed to hypoxia for 12 and 24 h but drastically declined in HeLa cells exposed to prolonged hypoxia (48 h). Because prolonged hypoxic exposure affects cell viability (Azad et al., 2008), the loss of SENP3 we observed at 48 h of exposure to hypoxia may be caused by cell death due to prolonged hypoxia instead of a change in protein expression levels. Briefly, we conducted hypoxia time courses on HeLa cells to assess levels of SENP2, SENP5 and SENP7 at different lengths of exposure to hypoxia. Levels of these SENPs fluctuated over time but with no discernible pattern correlating with length of exposure to hypoxia. Consistent with our findings, Kunz et al. (2016) reported that exposure of HeLa cells to various lengths of hypoxia up to 24 h did not yield significant changes in SENP1, SENP3, SENP2, SENP5, or SENP7 levels. We did not directly assess the deSUMOylation activity of the SENP proteins under hypoxia. Thus, we cannot determine how hypoxia affects activity of SENPs in our experimental settings in comparison to findings by Kunz et al. (2016), which showed hypoxia reduces SENP1 and SENP3 catalytic activity, in order to explain the decline of free and conjugated SUMO-1 and SUMO-2/3 levels we observed under hypoxia. Based on this, upon continuing our exploration of the role of SUMO proteases in HIM regulation, we narrow our focus to only SENP1 and SENP3 for the remainder our investigation because the roles of SENP1 and SENP3 in hypoxic cell response are the most extensively studied of the SENP family proteins. After observing that hypoxia could induce LC3-II levels within our hypoxia experimental system, we tested whether SENP1 or SENP3 affect LC3-II induction under hypoxia by knocking down SENP1 or SENP3 and performing Western blots to assess LC3-II levels under hypoxic conditions. SENP1 KD seemed to lead to a lack of LC3-II induction under hypoxia.

SENP3 KD did not seem to affect LC3-II levels under either normoxia or hypoxia. These results suggest that SENP1 but not SENP3 may be important for phagophore expansion and autophagosome formation induced by hypoxia. However, overexpression of SENP1 did not increase LC3-II levels under normoxia, suggesting that SENP1 alone is not responsible for LC3-II induction and hypoxic stress itself is perhaps needed for SENP1-mediated LC3-II induction. SENP1 and SENP3 display different preferences with respect to deconjugating SUMO isoforms, with SENP1 being capable of deconjugating all SUMO isoforms with a preference for SUMO-1 while SENP3 preferentially targets SUMO-2 and SUMO-3 conjugates (Hickey et al., 2012; Gareau & Lima, 2010; **Table 1**). Therefore, SENP1 and SENP3 likely would not regulate the same aspects of autophagy or mitophagy under hypoxia if at all.

To test for successful induction of mitophagy by hypoxia and optimize the duration of hypoxic exposure on cells for subsequent immunofluorescence experiments, a hypoxia time course (for 4, 8, 16, and 24 h) was performed on HeLa cells transfected with Mito-pHfluorin. Mito-pHfluorin was previously used by Waters et al. (2022) to study DFP-induced mitophagy. Here we confirm that Mito-pHfluorin can indicate where mitophagy induced by hypoxia occurs in the cell visualized by red puncta. For every time point tested in the hypoxia time course, there was significantly more mitophagy in Hela cells exposed to hypoxia compared to normoxia, indicating successful induction of mitophagy by hypoxia in our experimental system. Based on our results and in reference to the findings previously described (Liu et al., 2012; Wu et al., 2014; Chen et al., 2016), the optimal length of hypoxia exposure to visualize mitophagy with Mito-pHfluorin was determined to be 24 h. In the following chapters of this thesis, we use Mito-pHfluorin probe and RNAi-mediated knockdown and/or CRISPR-Cas9-mediated knockout of proteins of interest to study the effect of these proteins on HIM.

7.1.2 Chapter 4 – Regulation of Hypoxia-Induced Mitophagy by SUMOylation and DeSUMOylation Enzymes

The aim of Chapter 4 of this thesis was to study the roles of SUMO proteins, SUMO-1 and SUMO-2/3, and the deSUMOylation enzymes, SENP1 and SENP3, on the regulation of HIM. To do so, we performed RNAi-mediated knockdown of the proteins of interest in HeLa cells and quantified and compared the levels of mitophagy indicated by the probe Mito-pHfluorin under different experimental conditions with immunofluorescence microscopy.

Based on our results from our SUMO-1 KD experiment in HeLa cells expressing Mito-pHfluorin, we found that while SUMO-1 KD did not change mitophagy levels under normoxia, SUMO-1 KD significantly reduces but does not abolish HIM levels. These findings suggest that SUMO-1 and SUMO-1-ylation are important for maintaining the level of mitophagy under hypoxic conditions. In contrast, SUMO-2/3 KD significantly increased mitophagy levels under both normoxia and hypoxia, suggesting that SUMO-2/3 has an important suppressive role in regulating mitophagy. Altogether, our findings point toward the SUMO paralogues having specific functions in regulating mitophagy under hypoxia. The drug TAK-981, which is a global SUMOylation inhibitor and mimics global deSUMOylation, was used to assess the role of SUMOylation on HIM levels. TAK-981 treatment significantly increased mitophagy levels under both normoxic and hypoxic conditions. The efficiency of TAK-981 to reduce SUMOylation in HeLa cells was confirmed by Western blotting. TAK-981 treatment lead to decreased SUMO-1 and SUMO-2/3 conjugates and increased levels of free SUMO-1 and SUMO-2/3 (in the form of TAK-981 adduct). Given these results, it appears the overall effect of SUMOylation is to inhibit HIM, while individually SUMO-1 promotes HIM and SUMO-2/3 suppresses HIM. The significant increase of HIM induced either by the knockdown of SUMO-2/3 or by TAK-981 treatment of cells most likely reflects the loss of inhibitory regulation on HIM by SUMOylation, especially SUMO-2/3-ylation.

After investigating how global SUMOylation/deSUMOylation (*i.e.*, SUMOylation inhibition) regulates HIM, we examined the role of the deSUMOylation enzymes SENP1 and SENP3 in the regulation of HIM. Knock down of SENP1 did not lead to significant changes in levels of HIM or mitophagy under normoxia in HeLa cells, suggesting that the level of SENP1 may not regulate HIM levels. These results were unexpected, since loss of SENP1 is embryonic lethal (Cheng et al., 2007) and SENP1 deSUMOylates HIF-1α, which is known to be essential for the induction of Parkin-independent mitophagy (including iron chelation-induced and hypoxia-induced mitophagy) (Allen et al., 2013; Zhao et al., 2020; Mazure & Pouysségur, 2010). Our results here appear also to be contradictory to our results in Chapter 3, where we observed that SENP1 KD seems to prevent induction of LC3-II in HeLa cells under hypoxia. Our combined findings regarding SENP1 suggest that SENP1 levels do not directly regulate HIM levels, but it is possible SENP1 may regulate phagophore elongation or autophagosome formation (for general autophagy or other types of autophagy) under hypoxia due to the influence that SENP1 has on LC3-II induction under hypoxia. Allen et al. (2013) observed that high levels of HIF-1α do not always correlate with high levels of hypoxia-induced and iron chelation-induced mitophagy, suggesting HIF-1α stabilization may be important but may not be sufficient to drive mitophagy. SENP1 may function in line with this since SENP1 stabilizes HIF-1α through deSUMOylation under hypoxia (Cheng et al., 2007), but, based on our results, may not be sufficient to drive HIM levels. Another possibility is that other SENP family proteins deSUMO-1-ylate SUMO-1 conjugates to compensate for RNAi-mediated depletion of SENP1, causing HIM levels in SENP1 KD cells to remain unchanged compared to the control cells.

As for SENP3, we found that SENP3 KD significantly decreased levels of HIM and prevented induction of mitophagy by hypoxia, suggesting that SENP3 has an important role in HIM regulation. One possible mechanism behind SENP3-mediated regulation of HIM involves deSUMO-2/3-ylation of OMM proteins such as FKBP8 or Fis1, since SENP3 is known to regulate

Parkin-independent mitophagy induced by DFP through a SENP3-Fis1 axis (Waters et al., 2022). SENP1 has specificity for deconjugating SUMO-1 from SUMOylated proteins, whereas SENP3 primarily removes SUMO-2/3 from SUMO conjugates (Sharma et al., 2013; Guo et al., 2013). Based on our results obtained from hypoxia immunofluorescence experiments with Mito-pHfluorin probe, SENP3 and SUMO-2/3 display stronger influence on HIM levels than SENP1 and SUMO-1. Because our findings suggested that SENP1 does not have a direct role in regulating the levels of HIM while SENP3 does, we chose to focus mainly on SENP3-mediated regulation of HIM in the following chapters of this thesis. Our findings regarding the effect of SENP3 on HIM are consistent with the findings from out SUMO-2/3 KD immunofluorescence microscopy experiments. If SUMOylation, especially SUMO-2/3-ylation, has an inhibitory effect on HIM, then deSUMOylation mediated by SENP3 should restore levels of HIM. These data support each other since SENP3 preferentially deSUMOylates SUMO-2/3-ylated proteins (Guo et al., 2013).

SENP3 may help mediate the formation of autophagosomes through a mechanism induced by oxidative stress during hypoxia. Hypoxia is known to increase reactive oxygen species (ROS) formation and cause oxidative stress and SENP3 is sensitive to oxidative stress (Azad et al., 2009; Yan et al., 2010). SENP3 is stabilized under mild oxidative stress by interacting with Hsp90, which protects SENP3 from CHIP-mediated ubiquitination and degradation (Yan et al., 2010). SENP3 accumulates to the cytoplasm during starvation conditions in a ROS-dependent manner, resulting in increased interacting between SENP3 and BECN1 (K. Liu et al., 2020). BECN1 plays a role in the initiation of autophagy by forming the BECN1-PIK3C3 complex, which is important for the localization of autophagic proteins to the phagophore assembly site and also autophagosome formation (Liang et al., 2006; Kang et al., 2011). K. Liu et al. (2020) found that deSUMOylation of BECN1 by SENP3 that has been stabilized by increased generation of ROS led to inhibited autophagy induction under basal and starvation conditions. However, our immunofluorescence microscopy results do not align with the findings of these studies that

suggest that ROS-dependent accumulation of SENP3 ultimately aids in inhibiting excess autophagy (K. Liu et al., 2020; Zhou et al., 2022). If SENP3 regulated HIM levels within this framework, then knockdown of SENP3 would have increased the level of HIM compared to cells transfected with Nsi that were exposed to hypoxia. Given our results, SENP3 appears to positively regulate HIM levels rather than inhibit it.

SUMO-2/3 appears to contribute to inhibition of mitophagy levels more so than SUMO-1. Enhancement of SUMOylation has been suggested to play a protective role in hypoxia, especially with SUMO-2/3 in ischemia models (Yang et al., 2008; Loftus et al., 2009; Guo et al., 2013). During ischemic stress and OGD, SENP3 is degraded by lysosomal enzyme, resulting in prolonged SUMOylation of Drp1. SUMOylation of Drp1 reduces Drp1-mediated release of cytochrome *c* from the mitochondria, allowing cells to escape programmed cell death (Guo et al., 2013). Findings from Princz et al. (2020) revealed a direct link between SUMO and regulation of ageing in *C. elegans,* wherein SUMO promotes longevity and mitochondrial homeostasis during ageing. Interestingly and importantly, this evidence from the present study suggests that SENP3 and SUMO-2/3-ylation maintain a balanced level of HIM, possibly to promote mitophagy-mediated cell survival.

7.1.3 Chapter 5 – FKBP8- and Fis1-mediated Regulation of Hypoxia-Induced Mitophagy

The aim of Chapter 5 of this thesis was to explore the roles of FKBP8 and Fis1 in the regulation of HIM and whether the SUMOylation status of these two proteins are important for HIM in HeLa cells. FKBP8 has been identified as a potential target for SUMOylation through mass spectrometry (Hendriks et al., 2018) and regulates mitophagy induced by hypoxia (Yoo et al., 2020). Fis1 is a validated target protein for SUMOylation and SENP3-mediated deSUMOylation (Waters et al., 2022). FKBP8 and Fis1 are both reported to be required for Parkin-independent

mitophagy (Bhujabal et al., 2017; Yoo et al., 2020; Waters et al., 2022) and thus are potential downstream targets for SENP3 during HIM.

Our findings regarding FKBP8 in this study are as follows: The level of FKBP8 is significantly decreased under hypoxic conditions. Unexpectedly, we found that the knockdown of endogenous FKBP8 does not affect HIM levels, suggesting that FKBP8 is not involved in regulating HIM in contrast to findings reported by Yoo et al., (2020). Additionally, we verified that FKBP8 is a *bona fide* target SUMO-2-ylation target and the key site of SUMOylation is K335. Overexpression of SUMOylatable FKBP8 (WT) but not the non-SUMOylatable mutant FKBP8 K335R appeared to promote HIM. Given these findings, SUMOylation of FKBP8 may contribute to regulation of mitophagy but perhaps not when FKBP8 is expressed at endogenous levels in HeLa cells. This may also be explained as an overexpression artifact. Due to this, we conclude that the results of our study do not support a role for FKBP8 in the regulation of HIM.

Yoo et al. (2020) found that FKBP8 induces mitochondrial fragmentation independent of other mitophagy mediators Drp1, BNIP3, and NIX. The increase of HIM caused by overexpression of HA-FKBP8 WT may be due to the overexpression HA-FKBP8 (as exogenous FKBP8) inadvertently compensating for the loss of endogenous FKBP8 in HeLa cells under hypoxia. If changes in SUMOylation status of FKBP8 does indeed contribute to HIM, that effect may be minor. There have not yet been studies exploring how SUMOylation of FKBP8 affects cellular processes. However, Lee et al. (2022) identified FKBP8 as a novel dual lysine kinase (DLK)-interacting protein that induces degradation of DLK, a key regulator of axon regeneration, via the ubiquitin-dependent protein degradation pathway. The kinase domain of DLK contains a major site for ubiquitination and SUMOylation at lysine residue 271, which is responsible for regulating FKBP8-mediated proteasomal degradation involving autophagy. Lee et al. (2022) suggested that competition between ubiquitination and SUMOylation may occur at the K271 site of DLK and that this site is required for ubiquitin-dependent degradation of DLK. SUMOylation

of proteins that FKBP8 regulates during mitophagy could possibly affect HIM rather than the SUMOylation of endogenous FKBP8 itself. More research is needed to understand whether SUMOylation and FKBP8 together regulate HIM and other cellular processes.

As for Fis1, we found that Fis1 levels significantly decrease under hypoxia in HeLa cells. Knockout of Fis1 in HeLa cells abolishes HIM and knockdown of Fis1 significantly decreases HIM. Based on these results, we propose that Fis1 is important, if not essential, for the induction of mitophagy under hypoxia. Since Fis1 is a validated target for deSUMOylation by SENP3 and involved in regulating Parkin-independent (DFP-mediated) mitophagy (Waters et al., 2022), we investigated whether the SUMOylation status of Fis1 is important for regulating HIM. In SENP3 knockdown HeLa cells, which exhibit decreased HIM, the expression of Fis1 K149R, a SUMOylation site mutant that reduces Fis1 SUMOylation, rescues HIM levels. The Fis1-SUMO-2 fusion mutant Fis1-SUMO-2$^{\Delta GG}$, which mimics constitutively SUMOylation of Fis1, significantly reduces HIM in SENP3 knockdown HeLa cells. Together, these findings suggest that deSUMOylation of Fis1 promotes HIM while SUMOylation of Fis1 exerts a suppressive effect on HIM. Thus, in addition to the importance of Fis1 in HIM, the de/SUMOylation status of Fis1 also seems to play a key role in regulating HIM.

In addition to the role of Fis1 SUMOylation status in HIM regulating, we also explored whether SUMOylation in absence of Fis1 affects mitophagy under normoxia. TAK-981 treatment of Fis1 KO HeLa cells significantly increased mitophagy levels, indicating that SUMOylation in the absence of Fis1 suppresses mitophagy under normoxic conditions. Therefore, it appears that SUMOylation regulates mitophagy through both Fis1-dependent and Fis1-independent mechanisms. TAK-981-induced mitophagy independent of Fis1 appears to be a novel form of Parkin-independent mitophagy that we, to the best of our knowledge, have demonstrated for the first time.

Interestingly, Yamano et al. (2014) reported that loss of Fis1 caused LC3 accumulation during Parkin-mediated mitophagy. In our experimental system with Parkin-free cells, we found that hypoxia increased the levels of LC3-II in HeLa cells in the absence of autophagy or lysosomal inhibition at the time point examined prior to 24 hours as shown in Chapter 3 and decreased Fis1 levels in Chapter 5. Yamano et al. (2014) also demonstrated loss of TBC1D15 led to LC3 accumulation in Parkin-mediated mitophagy. Mitochondrial fission has been reported to be involved in mitophagy, so defects, loss or reduction of Fis1 may contribute to the regulation of mitophagy (Twig et al., 2008; Mao et al., 2013). Yamano et al. (2014) suggested that Fis1 along with TBC1D15 regulate autophagosome biogenesis during mitophagy. The Rab-GAPs TBC1D15 and TBC1D17, which both interact with Fis1 on the OMM and form heterodimers with each other, may be the relevant proteins in the regulation of HIM due to their interactions with Fis1 in Parkin-mediated mitophagy (Yamano et al. 2014). Due to the interactions of TBC1D15 and TBC1D17 with Fis1, it would be worthwhile to investigate the roles of these proteins in Parkin-free mitophagy.

7.1.4 Chapter 6 – Regulatory Mechanism of Fis1-mediated Hypoxia-Induced Mitophagy

The aim of the final Results chapter of this thesis was to explore potential mechanisms underlying Fis1-mediated hypoxia-induced mitophagy, following the work in previous chapters that provided evidence that SUMOylation and deSUMOylation regulate HIM and that deSUMOylation status of Fis1 is important for this regulation. TBC1D15 and TBC1D17 are Rab-GAPs that interact with Fis1 to regulate mitophagy. In this study, we found that TBC1D17 but not TBC1D15 suppresses HIM levels in HeLa cells and that Fis1-TBC1D17 interaction is likely a prerequisite for TBC1D17-mediated inhibition of HIM. We also found that hypoxia appears to increase TBC1D17 colocalization with Fis1 and that endogenous interactions likely occur between Fis1 and TBC1D17 under normoxia. Altogether, as of this thesis, these findings to our knowledge are the

first to describe a relationship between TBC1D17 and Fis1 specifically in the regulation of Parkin-independent HIM and to demonstrate potential endogenous interaction between Fis1 and TBC1D17 in normoxic conditions. Our findings suggest that Fis1 is a downstream interacting partner of TBC1D17 in the HIM regulatory process. Both exogenously (Yamano et al., 2014) and endogenously (**Figure 6.3a, c**) expressed Fis1 and TBC1D17 co-localize to the mitochondria. Yamano et al. (2014) identified TBC1D17 as a Fis1- (and TBC1D15-) binding protein. Based on our findings, decreased TBC1D17 levels correlate with increased levels of HIM. Indeed, we also found that endogenous TBC1D17 levels significantly decrease under hypoxic conditions in HeLa cells (**Figure 6.2c-d**). Although hypoxic conditions increase mitophagy, TBC1D17 appears to keep that increase in check. Our colocalization analysis of Fis1 and TBC1D17 (**Figure 6.3c**) suggests that hypoxia potentially increases the colocalization of TBC1D17 with Fis1, providing further evidence that HIM is accompanied by an endogenous level of TBC1D17-mediated suppression that prevents excess mitophagy induction during hypoxia. Interestingly, decreased levels of endogenous TBC1D17 under hypoxia may lessen the suppressive effect of TBC1D17 on HIM, indicating that TBC1D17 itself may be regulated during HIM.

In comparison to TBC1D15, TBC1D17 may be a limiting factor in regulating Fis1-mediated HIM because only knockdown of TBC1D17 and not TBC1D15 led to significant changes in HIM levels. Whether this is due to the absence of Parkin in HeLa cells, redundancy of the function(s) of these Rab-GAPs, combination specificity of the TBC1D15/17 dimers, or another mechanism in regulation of Fis1-mediated HIM remains unknown. A possible mechanism controlling whether TBC1D17 suppresses Fis1-mediated HIM is the SUMOylation status of Fis1. Since we have evidence that SUMO-2/3 has an inhibitory effect on HIM levels similar to TBC1D17 and both global inhibition of SUMOylation and the deSUMOylation status of Fis1 increase HIM, we propose that interaction of TBC1D17 with SUMOylated Fis1 leads to the suppression of HIM while deSUMOylated Fis1 reduces this TBC1D17-dependent suppression,

thereby increasing HIM (**Figure 7.1**). To verify this, future experiments would be conducted to determine whether the SUMOylation status of Fis1 affects Fis1-TBC1D17 binding interactions under hypoxic conditions.

Beyond investigating how SUMOylation or deSUMOylation of Fis1 regulates TBC1D17-dependent suppression of HIM, the questions of how exactly TBC1D17 mechanistically suppresses HIM remains. Our findings suggest that the SENP3-Fis1 axis is crucial for promoting HIM and imply a potentially important role for the axis in cell death & survival mediated by HIM (Mazure & Pouysségur, 2010). TBC1D17-dependent suppression of Fis1-mediated HIM likely promotes cell death, as deficiencies in autophagy and mitophagy has been shown to decrease cell survival (Civelek et al., 2018; Reddy et al., 2018) and Fis1 has been reported to maintain stemness through mitophagy in human lung cancer stem cells (Liu et al., 2021). The E50K mutation of the *OPTN* gene induces cell death in retinal cells involving inhibition of autophagy; TBC1D17 KD rescued cells from autophagy inhibition induced by E50K *OPTN* mutation, suggesting a crucial role for TBC1D17 in impairing autophagy and mediation of cell death in E50K mutant retinal cells (Chalasani et al., 2014). Thus, TBC1D17 likely fits into the SENP3-Fis1 pathway in regulating HIM by maintaining balance of HIM levels. The suppression of HIM levels may function to prevent excessive mitophagy. Since TBC1D17 levels decreased under hypoxia, TBC1D17-dependent HIM suppression itself would also require regulation to provide balance between cells death and survival. More investigation is needed to understand how TBC1D17 is regulated in this pathway.

In Chapter 6, we also investigated whether mitochondria-associated membranes (MAMs), the portions of ER tethered to the mitochondria considered the origin site of autophagy (Yang et al., 2020), are linked to regulation of HIM. The SNARE protein Stx17 is reported to interact with Fis1 and has roles in the MAM, autophagy and mitophagy (Hamasaki et al., 2013; Xian et al., 2019). To determine whether Stx17 is involved in regulating HIM, we knocked down Stx17 in

HeLa cells transfected with Mito-pHfluorin under hypoxia. We found that Stx17 KD significantly decreased mitophagy under both normoxia and hypoxia and abolished HIM, suggesting Stx17 regulates mitophagy. The mechanism behind this is unknown but likely linked to Stx17 promoting autophagosome maturation. This is the first time to the best of our knowledge where the role of Stx17 has been studied in HIM. There is evidence that Stx17 interacts with Fis1 to regulate Parkin-independent mitophagy (Xian et al., 2019), but there are currently no studies to our knowledge that support a link between Stx17 and the pathway we describe regarding TBC1D17 and Fis1-dependent HIM. The overexpression of Stx17 in the absence of Fis1 initiates mitophagy (Xian et al., 2019), though it is unknown how what physiological conditions *in vivo* could mimic these experimental conditions and the effect on mitophagy. One possibility is that overexpressing Stx17 causes mitochondrial damage, which the cell initiates mitophagy to clear. While both TBC1D15 and Stx17 interact with Fis1, TBC1D15 does not participate in Stx17 overexpression-mediated mitophagy (Xian et al., 2019), so it is likely TBC1D17 does not either, especially since TBC1D17 induces the opposite effect of Stx17 overexpression on mitophagy.

Lastly, we investigated whether MAM formation is regulated by SUMOylation to determine links, if any, exist between the effects of SUMOylation on MAMs and HIM regulation. Utilizing MAMtracker Green to measure the level of MAMs, we found that global SUMOylation inhibition induced by TAK-981 treatment significantly increases MAM levels in HeLa cells, whereas SENP3 KD does not significantly change MAM levels. Since inhibition of SUMOylation mimics deSUMOylation, these findings suggest that deSUMOylation affects MAM formation in addition to HIM levels. However, SENP3 does not seem to be required for MAM formation. Perhaps increased mitophagy levels through TAK-981 promote contact between the ER and mitochondria while decreasing mitophagy through SENP3 KD does not. Two additional possibilities cannot yet be discounted: 1) the remaining SENP3 in SENP knockdown cells may still deSUMO-2/3-ylate proteins and 2) other deSUMOylation enzymes such as SENP5

compensate for the SENP3-mediated deSUMO-2/3-ylation when SENP3 is depleted. In this series of MAM experiments, we have demonstrated for the first time to the best of our knowledge that MAM formation can be increased by TAK-981-mediated global SUMOylation inhibition, highlighting the critical roles of deSUMOylation in both MAMs, which are considered the site of origin for autophagy, and HIM. MAMs have been reported to be responsive to hypoxia (Wu et al., 2016; Chai et al., 2021). Unfortunately, due to technical limitations, we were unable to examine how hypoxia together with de/SUMOylation affects MAM formation with the experimental system established for this thesis. MAMtracker Green can only be used in live cell imaging, which cannot be performed due to the unavailability of confocal microscopy equipment that can be fitted inside the hypoxia workstation for observation of MAM formation dynamics.

7.2 Future Directions

The majority of the work in this thesis utilizes HeLa cells, which are easy to use and maintain for assays for autophagy and experiments investigating the fundamental molecular mechanisms underlying Parkin-independent mitophagy. Our experimental setup for quantifying levels of HIM is comprised of a hypoxia chamber, model HeLa cells, and Mito-pHfluorin probe. Immunofluorescence microscopy with this setup yielded high quality images of fixed HeLa cells with areas of mitophagy labeled in red by Mito-pHfluorin. However, we were unable to perform similar experiments surrounding HIM on living cells or track structural changes in mitochondria under hypoxia structure in a time lapse. Our hypoxia time course experiments somewhat remedy the issue of tracking the changing levels of mitophagy within HeLa cells over different lengths of exposure to hypoxia because we are able to obtain and compare the average level of mitophagy per experimental condition. Alternative imaging setups may be employed to specialize in tracking individual structural changes in mitochondria that reflect HIM levels that supplement the results of this thesis.

Additionally, since HeLa cells were the primary cell type used in this study, our findings regarding HIM may not be applicable to hypoxia response in various cell or tissue types, especially in cells expressing Parkin. Physiological oxygen levels and hypoxic stress responses vary depending on tissue type, though the average oxygen level in hypoxic tumor tissues is generally between 1-2% O_2 (Koh & Powis, 2012; Muz et al., 2015). The length of hypoxia exposure we use in our experiments (24 h) may elicit acute hypoxia response rather than chronic hypoxia response. We also did not investigate the effect of anoxia or oxygen levels above 1% on mitophagy in this study. Ideally, further work investigating HIM regulated by the SENP3-Fis1 axis and SUMOylation could be conducted in neuronal or other cancer cell lines relevant to conditions and diseases where hypoxia is implicated. SUMOylation has been increasingly shown to have relevance in cancer treatment, since the potent SUMOylation inhibitor TAK-981 is undergoing evaluation in clinical trials as an anti-tumor drug (Khattar et al., 2019; Nakamura et al., 2019; Nakamura et al., 2020; Langston et al., 2021).

Variability in mitophagy levels occurred in basal or hypoxia control conditions across independent immunofluorescence experiments. Carrier reagents such as calcium phosphate, cationic polymers or cationic lipids are commonly used in chemical transfection. The jetPRIME-mediated transfection method we utilized relies on cationic polymers as a carrier reagent to form positively charged complexes with negatively charged nucleic acids. The negative charge of the cell membrane attracts the positively charged complex, allowing the carrier reagent and nucleic acid to travels through the cell membrane via endocytosis (Damodaran et al., 2020). Cationic lipids induce autophagy in mammalian cells by increasing autophagosome formation without decreasing turnover (Man et al., 2010). Although jetPRIME transfection could potentially affect HIM levels in HeLa cells, the variation between basal mitophagy or HIM in control conditions is likely due to intra-experimental variations rather than the transfection process, since experiments

using the transfection reagent for Nsi or siRNAs do not necessarily display different mitophagy levels from those without (*i.e.*, HIM Time Course experiment, **Figure 3.18**).

A general limitation of our study is the lack of repeat data for many of our experiments. Ideally, and time permitting, repeat experiments should be performed in order to substantiate our preliminary findings presented in this thesis. In the case of Western blots performed to investigate the protein expression profile of hypoxia, improvement of blotting technique and quality would also provide clearer insights to protein expression regulated by hypoxia. As for experiments utilizing Mito-pHfluorin and immunofluorescence microscopy, more repeat experiments would account for the natural variation in mitophagy levels between individual cells in the same sample and determine whether the observed differences in mitophagy levels between experimental conditions are substantial.

Since Chapters 5 and 6 focus on the SENP3-Fis1 axis of regulation on HIM, the exact role of SENP1 in HIM remains unexplored. Our experiment exploring the effect of SENP1 KD on HIM in HeLa cells yielded unexpected results that suggested SENP1 does not regulate HIM levels. It should be noted that SENP1 is primarily responsible for deSUMOylation of SUMO-1 conjugates (Sharma et al., 2013). One possible reason for the lack of change in HIM levels in SENP1 KD cells may be redundancy in deSUMOylation of SUMO-1 conjugates by other SENP family members. To investigate this in the future, knockdown of a combination of SENP family members could be performed on HeLa cells transfected with Mito-pHfluorin to see whether overlaps in SENP SUMO-specificity resulted in a lack of change in hypoxia-induced mitophagy levels when only SENP1 was knocked down. Another possibility is that the remaining SENP1 in SENP1 KD cells is sufficient for its function in deSUMO-1-ylation. It would be ideal to investigate the role of SENP1 in HIM using SENP1 KO cells. However, it should be noted that SENP1 knockout was found to be lethal in mice embryos (Cheng et al., 2007), and SENP1 KO would affect cell viability, resulting in experimental data that are difficult to interpret. Moreover,

although SENP1 KD does not exert a lethal effect in HeLa cells, targeting multiple SENPs with overlapping SUMO-specificity could potentially affect cell viability. To overcome these technical challenges, the plasmids encoding RNAi-resistant GFP-SENP1 we generated (see **Appendix 3**) may be useful in this scenario for SENP1 rescue experiments. In the event SENP enzyme redundancy for deSUMO-1-ylation is not the cause of no change in HIM levels in SENP1 KD HeLa cells, another possibility is that SUMO-1-ylation merely does not contribute to regulation of HIM levels as strongly as SUMO-2/3-ylation. As we have shown in this thesis, the effect of global SUMOylation inhibition on HIM is more similar to that of SUMO-2/3 KD or deSUMO-2/3-ylation. This implies that global SUMOylation skews towards suppression of HIM and that SENP3 and SUMO-2/3 are more important for regulating HIM levels.

In a similar vein, SUMO proteases such as SENP5 that preferentially deSUMOylate SUMO-2/3 conjugates may compensate for the depletion of SENP3 in our experiment investigating the effect of SENP3 KD on MAM formation levels. This is another avenue to investigate with respect to overlapping SUMO specificities of SUMO proteases. Because the effect of TAK-981 treatment on HIM skews in favor of the effect of deSUMO-2/3-ylation and also appears to increase MAM formation, there is a likelihood that SUMO-2/3 and, by extension, SUMO proteases that preferentially act on SUMO-2/3 regulate MAM formation. Knocking down SENP3 in combination with SENP5 or other SUMO proteases that favor de-SUMO-2/3-ylation may reveal new information about how SUMO-2/3 regulates MAM formation. However, knockdown of multiple SENPs would likely negatively affect cell viability in this type of experiment.

Another unanswered avenue worth future investigation is whether FKBP8 definitively regulates HIM or not. Our findings contradict the study by Yoo et al. (2020), which reports FKBP8 plays a role in HIM. The depletion of FKBP8 in our study may have been incomplete. A solution to remedy incomplete RNAi-mediated depletion of FKBP8 in cells is to use CRISPR/Cas9 to

knock out FKBP8 in HeLa cells and then test whether this affects HIM with Mito-pHfluorin. FKBP8 may not regulate HIM or have a minor effect on HIM. There are no studies yet exploring how SUMOylation of FKBP8 affects cellular processes other than mitophagy.

Fis1-mediated HIM, similar to DFP-induced mitophagy, is a Parkin-independent form of mitophagy. These two forms of Parkin-independent mitophagy share a commonality in that the SUMOylation status of Fis1 are crucial in their regulation. DFP-induced mitophagy and HIM differ in their effect on SENP3 levels: DFP treatment increases SENP3 levels (Waters et al., 2022), while based on our findings, hypoxia does not significantly change SENP3 levels until after 48 h, wherein SENP3 significantly decreases. Iron chelation by DFP is reported to stabilize SENP3 through the downregulation of the E3 ubiquitin ligase CHIP, resulting in decreased global SUMO-2/3-ylation (Waters et al., 2022). Stabilization of SENP3 that occurs in DFP-induced mitophagy does not seem to manifest in HIM. SENP3 KD blocks DFP-induced increase of LC3-II expression (Waters et al., 2022) but does not affect hypoxia-induced LC3-II expression in the present study. Although DFP-induced mitophagy and HIM share similarities, further investigation is needed to understand the differences in the SENP3-Fis1 axis between these two forms Parkin-independent mitophagy.

As a continuation of this study, future protein-protein interaction assays (*i.e.*, GST Pulldown, endogenous Immunoprecipitation and Proximity Ligation Assay) would reveal if TBC1D17 interacts with Fis1 under normoxic and/or hypoxic conditions and if SUMOylation/deSUMOylation regulates the potential interaction between TBC1D17 and Fis1. This would potentially determine how TBC1D17-mediated suppression of HIM is regulated and whether this stems from interaction between Fis1 and TBC1D17. For now, as summarized in **Figure 7.1**, we propose that deSUMOylation of Fis1 correlates with decreased Fis1-TBC1D17 interaction, leading to increased HIM levels and conversely, SUMOylated Fis1 decreases HIM

levels, likely coinciding with increased Fis1-TBC1D17 interaction that promotes TBC1D17-mediated suppression of HIM.

How exactly Stx17 regulates mitophagy under normoxia and hypoxia is largely unknown. A potential experiment to determine whether Stx17 regulates HIM in a Fis1-dependent manner is to perform a Stx17 KD in Fis1 KO HeLa cells transfected with Mito-pHfluorin and CFP-Fis1, CFP-Fis1 K149R or CFP-Fis1-SUMO-2$^{\Delta GG}$ that are exposed to hypoxia and compare mitophagy levels between the conditions. If regulation of mitophagy by Stx17 is dependent on Fis1, this experiment would also explore whether SUMOylation status of Fis1 affects this regulation. Moreover, Stx17 is present in the MAM (Hamasaki et al., 2013), so Stx17 KD experiments performed in cells transfected with MAMtracker Green may show that Stx17 impacts the level of MAM formation.

Since MAMs are reported to be responsive to hypoxia (Wu et al., 2016; Chai et al., 2021), experiments that follow up on the work in this study focusing on the link between MAM and HIM may be performed. As previously mentioned, MAMtracker Green can only be used in live cells to monitor MAM levels (Sakai et al., 2021) and our hypoxia experimental setup is used for cells intended to be fixed. In order to study the MAM under hypoxic conditions, one method to overcome these technical limitations is to detect the MAM in fixed cells with alternative fluorescent probes for protein components of the MAM on the OMM and ER such as cytochrome b5 or KDEL peptide respectively and monitor the overlap of these proteins. Fis1 cannot be used as an indicator of ER-mitochondria contact points in such an experiment because it is also localized in peroxisomes in addition to the OMM (Koch et al., 2005). However, Fis1 KO HeLa cells may be used in combination with alternative fluorescent probes indicating ER-mitochondria contact points to determine whether presence of Fis1 affects MAM formation under hypoxia.

SUMOylation is emerging as a crucial regulator of tumorigenesis in various cancers (Celen & Sahin, 2020). The SUMO pathway regulates several cellular processes that contribute to tumorigenesis including cell cycle progression, angiogenesis, and hypoxic cell response (Kukkula et al., 2021). Dysregulation of SUMOylation machinery upsets the balance between deSUMOylation and SUMOylation, leading to tumorigenesis and resistance to chemotherapeutic drugs in cancer cells **(**Kukkula et al., 2021). TAK-981 is a potent inhibitor of SUMOylation, an anti-tumor drug undergoing clinical trials in cancer patients (Nakamura et al., 2019; Nakamura et al., 2020; Langston et al., 2021; Khattar et al., 2019), and as we have found in our study, a powerful inducer of mitophagy in model HeLa cells under both normoxia and hypoxia. Reduction of free SUMO levels and SUMOylation by TAK-981 treatment under hypoxic conditions in our model HeLa cells signify the importance of deSUMOylation/SUMOylation in regulating cell survival mechanisms under hypoxia. Our findings demonstrate the impact of TAK-981, and therefore also SUMOylation, on the regulation of mitophagy under normoxia and HIM, highlighting the potential of SUMOylation as a therapeutic target for health conditions where mitophagy is aberrant.

In this study, our data support the idea that HIM is regulated through a SENP3-Fis1 axis. SENP3 and Fis1 have been previously described to work in tandem to regulate mitophagy induced by iron chelation via DFP treatment (Waters et al., 2022), but to the best of our knowledge our work here is the first to uncover TBC1D17 involvement within SENP3- and Fis1-mediated regulation of Parkin-independent HIM. The relationship between TBC1D17, SENP3 and Fis1 in a regulatory pathway for HIM warrants further investigation beyond the scope of our study. Our findings provide evidence in support of these proteins as potential targets for therapeutics to modulate the balance of mitophagy in health and disease.

Our preliminary results also are the first to our knowledge to link increased MAM formation with TAK-981 treatment and global deSUMOylation, and show the role of Stx17 in

regulating HIM levels. While our examination of these processes in this study was brief, these findings may provide basis for future studies specifically focusing on MAM formation and SUMOylation or the involvement of Stx17 in HIM.

7.3 Conclusions

Various human diseases where hypoxia is implicated exhibit disturbances in mitophagy. The imbalance of mitophagy accompanying the development of these conditions can ultimately lead to cell death. Thus, research into how mitophagy is regulated under hypoxia is integral in understanding and developing treatments for diseases where mitophagy is dysfunctional. SUMOylation and its reverse process, deSUMOylation, are regulated by SUMO proteases and are crucial for the execution of HIF-1-based hypoxic cell response. In this thesis, we uncover molecular mechanisms in which the SUMO protease SENP3 regulates Parkin-independent HIM. We propose a pathway outlined in **Figure 7.1** where the SUMOylation status of Fis1 regulates the level of HIM. SENP3 but not SENP1 is likely required for the induction of mitophagy under hypoxia and deSUMOylates Fis1. Fis1 appears necessary for HIM and deSUMOylated Fis1 induces mitophagy under hypoxia, whereas Fis1 that cannot be deSUMOylated reduces HIM levels. SUMOylation on a whole, especially SUMO-2/3-ylation, appears to suppress HIM levels. The drug TAK-981, which inhibits global SUMOylation, significantly increases HIM. The Rab-GAP TBC1D17 is able to suppress HIM likely through its interaction with Fis1. However, whether the mechanism behind TBC1D17-dependent Fis1-mediated HIM involves SUMO remains unknown. In addition, this study uncovered the capability of TAK-981 in upregulating mitophagy and MAM formation, leading to the discovery of a novel form of mitophagy, SUMOylation inhibition-induced mitophagy.

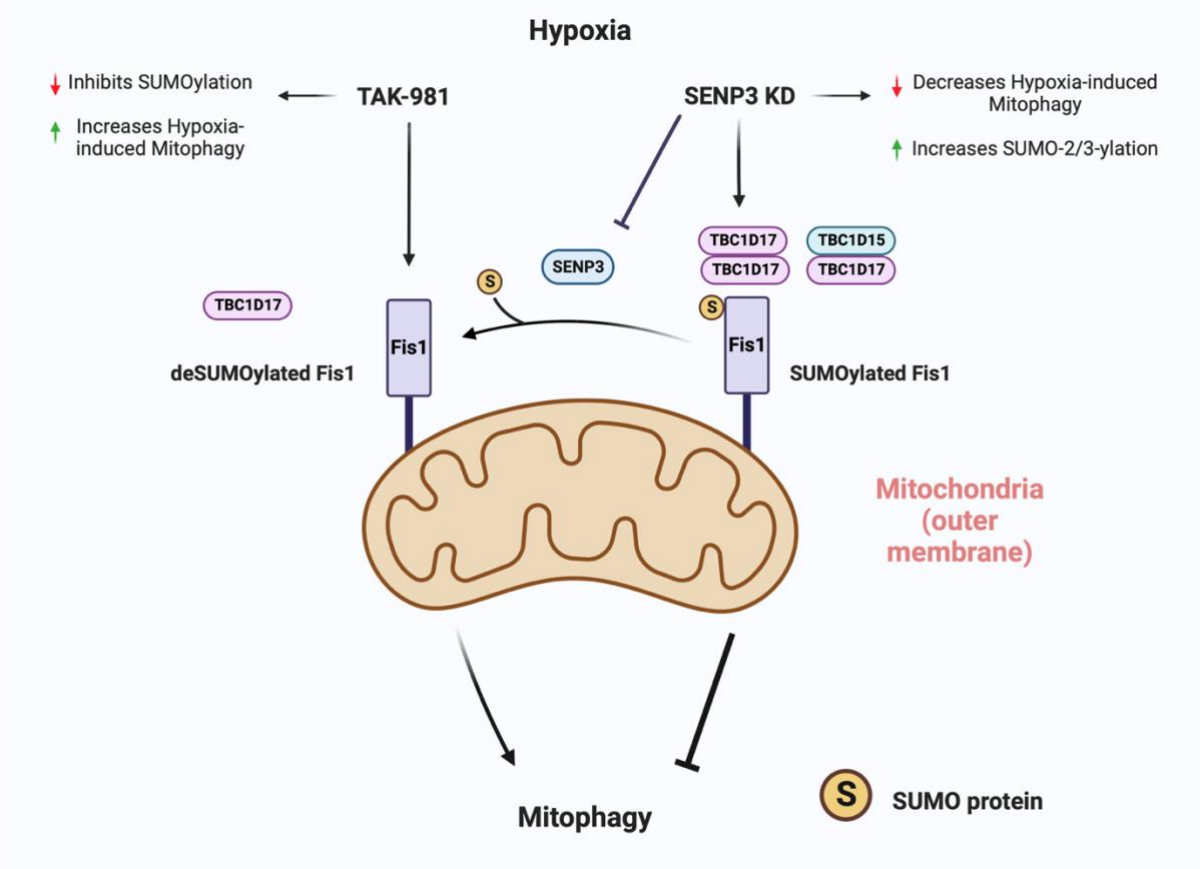

Figure 7.1: Proposed mechanistic model for SUMO-dependent Fis1-TBC1D17 interaction and regulation of hypoxia-induced mitophagy

Appendices

Appendix 1: Transfected DNA and siRNA

The DNA and siRNA used for transfection and their concentrations are listed here by chapter.

Ch 3 – 0.25 µg/well Mito-pHfluorin (Waters et al., 2022), NSi (47%, 31%, 68%; Eurofins Genomics), SENP1 siRNA (Santa Cruz sc-44449), SENP3 siRNA (Santa Cruz sc-44451)

Ch 4 – SUMO-1 siRNA (5'- CCU UCA UAU UAC C CU CUC CTT-3'), SUMO-2/3 siRNA (5'-GUC AAU GAG GCA GAU CAG ATT- 3')

Ch 5 – FKBP8 siRNA (5'-GAG UGG CUG GAC AUU CUG GTT-3'), pcDNA3 (Addgene 20011), HA-FKBP8 (Gifted from Professor Yong-Keun Jung; Yoo et al., 2020), HA-FKBP8 K335R (Forward primer: 5'-CTGAGGGCAGCCCTGA GGCTGGAACCT -3'; reverse primer: 5' AGGTTCCAGCCTCAGGG CTGCCCTCAG-3'), Fis1 siRNA (a pool of two duplexes to target two sequences, CUACCGGCUCAAGGAAUAC and GGAAUACGAGAAGGCCUUA, to silence Fis1; synthesized by Eurofins Genomics), pcDNA3-Flag-CFP (Waters et al., 2022), pcDNA3-Flag-CFP-Fis1 WT (Waters et al., 2022), pcDNA3-Flag-CFP-Fis1 K149R(Waters et al., 2022), pCDNA-Flag-CFP-Fis1-SUMO-2$^{\Delta GG}$ (Waters et al., 2022)

Ch 6 – TBC1D15 siRNA (5'-UCA ACA AGA AGA ACC AGG ATT -3'), TBC1D17 siRNA (Santa Cruz sc-97889), Stx17 siRNA (Santa Cruz, sc-92492), 0.25 µg/well MAMtracker Green (Sakai et al., 2021)

Appendix 2: Generation of RNAi-resistant GFP-SENP1

We generated plasmids encoding human GFP-SENP1 that were resistant to RNAi-mediated knockdown utilizing site-directed mutagenesis. These RNAi-resistant (RNAi-R) plasmids would be indispensable tools for future experiments involving SENP1 knockdown or overexpression due to the possibility of SENP1 siRNA off-target effects and overexpression artifacts in cells. After the introduction of three mutations to the original GFP-SENP1 WT plasmid (termed GFP-SENP1 WT RNAi-R3), Western blot analysis was performed on HeLa cells transfected with Nsi or SENP1i and GFP-SENP1 WT or GFP-SENP1 WT RNAi-R3 (**Figure S1a**). GFP-SENP1 levels in cells transfected with both SENP1i and GFP-SENP1 WT RNAi-R3 were similar to that in cells transfected with Nsi and GFP-SENP1 WT or WT RNAi-R3 (**Figure S1b**). This would suggest the SENP1 WT RNAi-R3 plasmid confers a noticeable level of RNAi-resistance. However, while these results are promising, repeat experiments are necessary to determine the consistency of RNAi-resistance the GFP-SENP1 WT RNAi-R mutant confers.

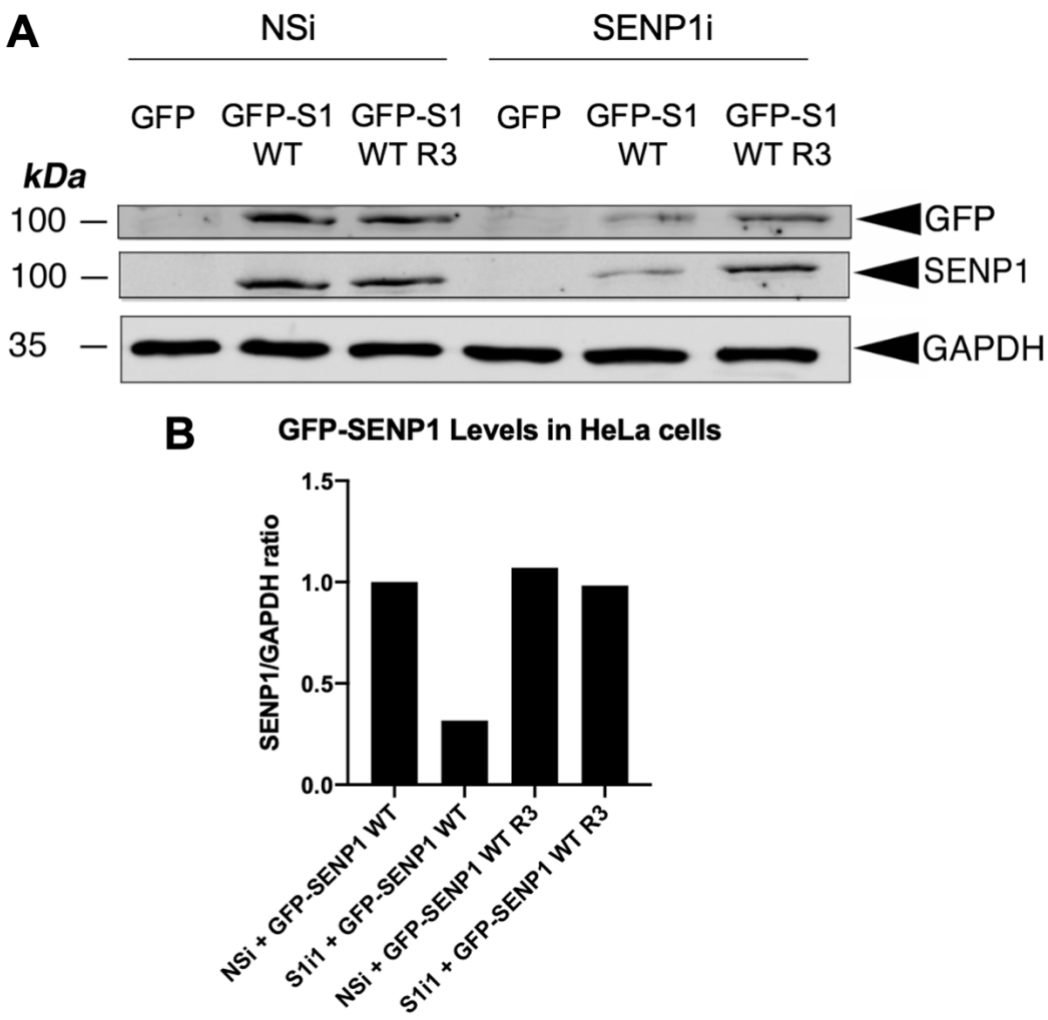

Figure S1: Generation of GFP-SENP1 WT RNAi-Resistant Mutant

Plasmids encoding RNAi-resistant human GFP-SENP1 were generated using site-directed mutagenesis. A) HeLa cells were transfected with GFP, GFP-SENP1 (S1) WT or GFP-SENP1 WT RNAi-resistant plasmid III (R3) and Nsi or SENP1-specific siRNA (SENP1i). Whole cell lysate samples were prepared and blotted as indicated. B) Histogram shows relative levels of SENP1 in HeLa cells from each experimental condition.

Appendix 3: Mito-pHfluorin Quantification Macro Program in Fiji

```
if (isOpen("Results")){
	close("Results");
}

MaxProm = getNumber("Please enter threshold value for Maxima", 1500);

//Ask user if they want to analyse another particle
while (getBoolean("Do you wish to analyse a cell?", "Yes", "No, I'm done...")==1){

	//Set the freehand tool as active
	setTool("polygon");
	//Pause and wait for user to draw a selection
	waitForUser("Draw around a cell then click OK");
	//Exit macro if no selection made
	if(selectionType() == -1){
		exit("No selection made");
	}
	run("Find Maxima...", "prominence="+MaxProm+" output=Count");
	run("Select None");
}
```

Bibliography

Agbor, T.A., Cheong, A., Comerford, K.M., Scholz, C.C., Bruning, U., Clarke, A., Cummins, E.P., Cagney, G. and Taylor, C.T. (2011). Small ubiquitin-related modifier (SUMO)-1 promotes glycolysis in hypoxia. J Biol Chem. 286(6), pp.4718-4726.

Alegre, K.O. and Reverter, D. (2011). Swapping small ubiquitin-like modifier (SUMO) isoform specificity of SUMO proteases SENP6 and SENP7. J Biol Chem. 286(41), pp.36142-36151.

Allen, G.F., Toth, R., James, J. and Ganley, I.G. (2013). Loss of iron triggers PINK1/Parkin-independent mitophagy. EMBO Rep. 14(12), pp.1127-1135.

Anding, A.L. and Baehrecke, E.H. (2017). Cleaning House: Selective Autophagy of Organelles. Developmental Cell. 41(1), pp.10-22.

Arasaki, K., Shimizu, H., Mogari, H., Nishida, N., Hirota, N., Furuno, A., Kudo, Y., Baba, M., Baba, N., Cheng, J., Fujimoto, T., Ishihara, N., Ortiz-Sandoval, C., Barlow, L.D., Raturi, A., Dohmae, N., Wakana, Y., Inoue, H., Tani, K., Dacks, J.B., Simmen, T. and Tagaya, M. (2015). A role for the ancient SNARE syntaxin 17 in regulating mitochondrial division. Dev Cell. 32(3), pp.304-317.

Avery , O.T., MacLeod , C.M. and McCarty , M. (1944). STUDIES ON THE CHEMICAL NATURE OF THE SUBSTANCE INDUCING TRANSFORMATION OF PNEUMOCOCCAL TYPES : INDUCTION OF TRANSFORMATION BY A DESOXYRIBONUCLEIC ACID FRACTION ISOLATED FROM PNEUMOCOCCUS TYPE III. Journal of Experimental Medicine. 79(2), pp.137-158.

Azad, M.B., Chen, Y. and Gibson, S.B. (2009). Regulation of autophagy by reactive oxygen species (ROS): implications for cancer progression and treatment. Antioxid Redox Signal. 11(4), pp.777-790.

Azad, M.B., Chen, Y., Henson, E.S., Cizeau, J., McMillan-Ward, E., Israels, S.J. and Gibson, S.B. (2008). Hypoxia induces autophagic cell death in apoptosis-competent cells through a mechanism involving BNIP3. Autophagy. 4(2), pp.195-204.

Azad, P., Zhao, H.W., Cabrales, P.J., Ronen, R., Zhou, D., Poulsen, O., Appenzeller, O., Hsiao, Y.H., Bafna, V. and Haddad, G.G. (2016). Senp1 drives hypoxia-induced polycythemia via GATA1 and Bcl-xL in subjects with Monge's disease. J Exp Med. 213(12), pp.2729-2744.

Bae, S.H., Jeong, J.W., Park, J.A., Kim, S.H., Bae, M.K., Choi, S.J. and Kim, K.W. (2004). Sumoylation increases HIF-1alpha stability and its transcriptional activity. Biochem Biophys Res Commun. 324(1), pp.394-400.

Baillieul, S., Chacaroun, S., Doutreleau, S., Detante, O., Pépin, J.L. and Verges, S. (2017). Hypoxic conditioning and the central nervous system: A new therapeutic opportunity for brain and spinal cord injuries? Exp Biol Med (Maywood). 242(11), pp.1198-1206.

Banasavadi-Siddegowda, Y.K., Mai, J., Fan, Y., Bhattacharya, S., Giovannucci, D.R., Sanchez, E.R., Fischer, G. and Wang, X. (2011). FKBP38 peptidylprolyl isomerase promotes the folding of cystic fibrosis transmembrane conductance regulator in the endoplasmic reticulum. J Biol Chem. 286(50), pp.43071-43080.

Bellot, G., Garcia-Medina, R., Gounon, P., Chiche, J., Roux, D., Pouyssegur, J. and Mazure, N.M. (2009). Hypoxia-induced autophagy is mediated through hypoxia-inducible factor induction of BNIP3 and BNIP3L via their BH3 domains. Mol Cell Biol. 29(10), pp.2570-2581.

Bento, C.F., Puri, C., Moreau, K. and Rubinsztein, D.C. (2013). The role of membrane-trafficking small GTPases in the regulation of autophagy. Journal of Cell Science. 126(5), pp.1059-1069.

Bento, C.F., Renna, M., Ghislat, G., Puri, C., Ashkenazi, A., Vicinanza, M., Menzies, F.M. and Rubinsztein, D.C. (2016). Mammalian Autophagy: How Does It Work? Annu Rev Biochem. 85, pp.685-713.

Bergeron, M., Yu, A.Y., Solway, K.E., Semenza, G.L. and Sharp, F.R. (1999). Induction of hypoxia-inducible factor-1 (HIF-1) and its target genes following focal ischaemia in rat brain. European Journal of Neuroscience. 11(12), pp.4159-4170.

Berk, A.J. (2005). Recent lessons in gene expression, cell cycle control, and cell biology from adenovirus. Oncogene. 24(52), pp.7673-7685.

Bernardini, J.P., Brouwer, J.M., Tan, I.K., Sandow, J.J., Huang, S., Stafford, C.A., Bankovacki, A., Riffkin, C.D., Wardak, A.Z., Czabotar, P.E., Lazarou, M. and Dewson, G. (2019). Parkin inhibits BAK and BAX apoptotic function by distinct mechanisms during mitophagy. Embo j. 38(2).

Bhujabal, Z., Birgisdottir Å, B., Sjøttem, E., Brenne, H.B., Øvervatn, A., Habisov, S., Kirkin, V., Lamark, T. and Johansen, T. (2017). FKBP8 recruits LC3A to mediate Parkin-independent mitophagy. EMBO Rep. 18(6), pp.947-961.

Bian, X., Xu, J., Zhao, H., Zheng, Q., Xiao, X., Ma, X., Li, Y., Du, X. and Liu, X. (2019). Zinc-Induced SUMOylation of Dynamin-Related Protein 1 Protects the Heart against Ischemia-Reperfusion Injury. Oxid Med Cell Longev. 2019, p1232146.

Biddlestone, J., Bandarra, D. and Rocha, S. (2015). The role of hypoxia in inflammatory disease (review). Int J Mol Med. 35(4), pp.859-869.

Biedler, J.L., Roffler-Tarlov, S., Schachner, M. and Freedman, L.S. (1978). Multiple neurotransmitter synthesis by human neuroblastoma cell lines and clones. Cancer Res. 38(11 Pt 1), pp.3751-3757.

Bjorkoy, G., Lamark, T., Brech, A., Outzen, H., Perander, M., Overvatn, A., Stenmark, H. and Johansen, T. (2005). p62/SQSTM1 forms protein aggregates degraded by autophagy and has a protective effect on huntingtin-induced cell death. J Cell Biol. 171(4), pp.603-614.

Burtscher, J., Mallet, R.T., Burtscher, M. and Millet, G.P. (2021). Hypoxia and brain aging: Neurodegeneration or neuroprotection? Ageing Research Reviews. 68, p101343.

Cai, R., Gu, J., Sun, H., Liu, X., Mei, W., Qi, Y., Xue, S., Ren, S., Rabinowitz, J.E., Wang, Y., Yeh, E.T. and Cheng, J. (2015). Induction of SENP1 in myocardium contributes to abnormities of mitochondria and cardiomyopathy. J Mol Cell Cardiol. 79, pp.115-122.

Cai, R., Yu, T., Huang, C., Xia, X., Liu, X., Gu, J., Xue, S., Yeh, E.T. and Cheng, J. (2012). SUMO-specific protease 1 regulates mitochondrial biogenesis through PGC-1alpha. J Biol Chem. 287(53), pp.44464-44470.

Callaway, E. (2013). Deal done over HeLa cell line. Nature. 500(7461), pp.132-133.

Cao, Y.-L., Meng, S., Chen, Y., Feng, J.-X., Gu, D.-D., Yu, B., Li, Y.-J., Yang, J.-Y., Liao, S., Chan, D.C. and Gao, S. (2017). MFN1 structures reveal nucleotide-triggered dimerization critical for mitochondrial fusion. Nature. 542(7641), pp.372-376.

Cappadocia, L. and Lima, C.D. (2018). Ubiquitin-like Protein Conjugation: Structures, Chemistry, and Mechanism. Chem Rev. 118(3), pp.889-918.

Carbia-Nagashima, A., Gerez, J., Perez-Castro, C., Paez-Pereda, M., Silberstein, S., Stalla, G.K., Holsboer, F. and Arzt, E. (2007). RSUME, a Small RWD-Containing Protein, Enhances SUMO Conjugation and Stabilizes HIF-1α during Hypoxia. Cell. 131(2), pp.309-323.

Celen, A.B. and Sahin, U. (2020). Sumoylation on its 25th anniversary: mechanisms, pathology, and emerging concepts. Febs j. 287(15), pp.3110-3140.

Chai, P., Cheng, Y., Hou, C., Yin, L., Zhang, D., Hu, Y., Chen, Q., Zheng, P., Teng, J. and Chen, J. (2021). USP19 promotes hypoxia-induced mitochondrial division via FUNDC1 at ER-mitochondria contact sites. Journal of Cell Biology. 220(7).

Chalasani, M.L., Kumari, A., Radha, V. and Swarup, G. (2014). E50K-OPTN-induced retinal cell death involves the Rab GTPase-activating protein, TBC1D17 mediated block in autophagy. PLoS One. 9(4), pe95758.

Chalasani, M.L., Radha, V., Gupta, V., Agarwal, N., Balasubramanian, D. and Swarup, G. (2007). A glaucoma-associated mutant of optineurin selectively induces death of retinal ganglion cells which is inhibited by antioxidants. Invest Ophthalmol Vis Sci. 48(4), pp.1607-1614.

Chen , H., Detmer , S.A., Ewald , A.J., Griffin , E.E., Fraser , S.E. and Chan , D.C. (2003). Mitofusins Mfn1 and Mfn2 coordinately regulate mitochondrial fusion and are essential for embryonic development. Journal of Cell Biology. 160(2), pp.189-200.

Chen, M., Chen, Z., Wang, Y., Tan, Z., Zhu, C., Li, Y., Han, Z., Chen, L., Gao, R., Liu, L. and Chen, Q. (2016). Mitophagy receptor FUNDC1 regulates mitochondrial dynamics and mitophagy. Autophagy. 12(4), pp.689-702.

Cheng, J., Kang, X., Zhang, S. and Yeh, E.T.H. (2007). SUMO-Specific Protease 1 Is Essential for Stabilization of HIF1α during Hypoxia. Cell. 131(3), pp.584-595.

Cieri, D., Vicario, M., Giacomello, M., Vallese, F., Filadi, R., Wagner, T., Pozzan, T., Pizzo, P., Scorrano, L., Brini, M. and Calì, T. (2018). SPLICS: a split green fluorescent protein-based contact site sensor for narrow and wide heterotypic organelle juxtaposition. Cell Death Differ. 25(6), pp.1131-1145.

Civelek, M., Mehrkens, J.-F., Carstens, N.-M., Fitzenberger, E. and Wenzel, U. (2019). Inhibition of mitophagy decreases survival of Caenorhabditis elegans by increasing protein aggregation. Molecular and Cellular Biochemistry. 452(1), pp.123-131.

Cole, A.M., Petousi, N., Cavalleri, G.L. and Robbins, P.A. (2014). Genetic variation in SENP1 and ANP32D as predictors of chronic mountain sickness. High Alt Med Biol. 15(4), pp.497-499.

Colnaghi, L., Russo, L., Natale, C., Restelli, E., Cagnotto, A., Salmona, M., Chiesa, R. and Fioriti, L. (2019). Super Resolution Microscopy of SUMO Proteins in Neurons. Front Cell Neurosci. 13, p486.

Comerford, K.M., Leonard, M.O., Karhausen, J., Carey, R., Colgan, S.P. and Taylor, C.T. (2003). Small ubiquitin-related modifier-1 modification mediates resolution of CREB-dependent responses to hypoxia. Proc Natl Acad Sci U S A. 100(3), pp.986-991.

Cui, C.P., Wong, C.C., Kai, A.K., Ho, D.W., Lau, E.Y., Tsui, Y.M., Chan, L.K., Cheung, T.T., Chok, K.S., Chan, A.C.Y., Lo, R.C., Lee, J.M., Lee, T.K. and Ng, I.O.L. (2017). SENP1 promotes hypoxia-induced cancer stemness by HIF-1alpha deSUMOylation and SENP1/HIF-1alpha positive feedback loop. Gut. 66(12), pp.2149-2159.

Damodaran, A.P., Courthéoux, T., Watrin, E. and Prigent, C. (2020). Alteration of SC35 localization by transfection reagents. Biochimica et Biophysica Acta (BBA) - Molecular Cell Research. 1867(4), p118650.

Datwyler, A.L., Lättig-Tünnemann, G., Yang, W., Paschen, W., Lee, S.L., Dirnagl, U., Endres, M. and Harms, C. (2011). SUMO2/3 conjugation is an endogenous neuroprotective mechanism. J Cereb Blood Flow Metab. 31(11), pp.2152-2159.

Delettre, C., Lenaers, G., Griffoin, J.M., Gigarel, N., Lorenzo, C., Belenguer, P., Pelloquin, L., Grosgeorge, J., Turc-Carel, C., Perret, E., Astarie-Dequeker, C., Lasquellec, L., Arnaud, B., Ducommun, B., Kaplan, J. and Hamel, C.P. (2000). Nuclear gene OPA1, encoding a mitochondrial dynamin-related protein, is mutated in dominant optic atrophy. Nat Genet. 26(2), pp.207-210.

Denison, S.R., Wang, F., Becker, N.A., Schüle, B., Kock, N., Phillips, L.A., Klein, C. and Smith, D.I. (2003). Alterations in the common fragile site gene Parkin in ovarian and other cancers. Oncogene. 22(51), pp.8370-8378.

Desterro, J.M., Rodriguez, M.S., Kemp, G.D. and Hay, R.T. (1999). Identification of the enzyme required for activation of the small ubiquitin-like protein SUMO-1. J Biol Chem. 274(15), pp.10618-10624.

Ding, W.X. and Yin, X.M. (2012). Mitophagy: mechanisms, pathophysiological roles, and analysis. Biol Chem. 393(7), pp.547-564.

Duan, C. (2016). Hypoxia-inducible factor 3 biology: complexities and emerging themes. Am J Physiol Cell Physiol. 310(4), pp.C260-269.

Edlich, F., Weiwad, M., Erdmann, F., Fanghänel, J., Jarczowski, F., Rahfeld, J.-U. and Fischer, G. (2005). Bcl-2 regulator FKBP38 is activated by Ca2+/calmodulin. The EMBO Journal. 24(14), pp.2688-2699.

Elbashir, S.M., Harborth, J., Lendeckel, W., Yalcin, A., Weber, K. and Tuschl, T. (2001). Duplexes of 21-nucleotide RNAs mediate RNA interference in cultured mammalian cells. Nature. 411(6836), pp.494-498.

Elbashir, S.M., Lendeckel, W. and Tuschl, T. (2001). RNA interference is mediated by 21- and 22-nucleotide RNAs. Genes Dev. 15(2), pp.188-200.

Epstein, A.C., Gleadle, J.M., McNeill, L.A., Hewitson, K.S., O'Rourke, J., Mole, D.R., Mukherji, M., Metzen, E., Wilson, M.I., Dhanda, A., Tian, Y.M., Masson, N., Hamilton, D.L., Jaakkola, P., Barstead, R., Hodgkin, J., Maxwell, P.H., Pugh, C.W., Schofield, C.J. and Ratcliffe, P.J. (2001). C. elegans EGL-9 and mammalian homologs define a family of dioxygenases that regulate HIF by prolyl hydroxylation. Cell. 107(1), pp.43-54.

Flotho, A. and Melchior, F. (2013). Sumoylation: a regulatory protein modification in health and disease. Annu Rev Biochem. 82, pp.357-385.

Forsythe, J.A., Jiang, B.H., Iyer, N.V., Agani, F., Leung, S.W., Koos, R.D. and Semenza, G.L. (1996). Activation of vascular endothelial growth factor gene transcription by hypoxia-inducible factor 1. Mol Cell Biol. 16(9), pp.4604-4613.

Friedman, J.R., Lackner, L.L., West, M., DiBenedetto, J.R., Nunnari, J. and Voeltz, G.K. (2011). ER tubules mark sites of mitochondrial division. Science. 334(6054), pp.358-362.

Fu, J., Yu, H.M., Chiu, S.Y., Mirando, A.J., Maruyama, E.O., Cheng, J.G. and Hsu, W. (2014). Disruption of SUMO-specific protease 2 induces mitochondria mediated neurodegeneration. PLoS Genet. 10(10), pe1004579.

Fu, Z.J., Wang, Z.Y., Xu, L., Chen, X.H., Li, X.X., Liao, W.T., Ma, H.K., Jiang, M.D., Xu, T.T., Xu, J., Shen, Y., Song, B., Gao, P.J., Han, W.Q. and Zhang, W. (2020). HIF-1α-BNIP3-mediated mitophagy in tubular cells protects against renal ischemia/reperfusion injury. Redox Biol. 36, p101671.

Fuhrmann, D.C. and Brüne, B. (2017). Mitochondrial composition and function under the control of hypoxia. Redox Biology. 12, pp.208-215.

Fukuda, R., Zhang, H., Kim, J.W., Shimoda, L., Dang, C.V. and Semenza, G.L. (2007). HIF-1 regulates cytochrome oxidase subunits to optimize efficiency of respiration in hypoxic cells. Cell. 129(1), pp.111-122.

Gallardo-Chamizo, F., Lara-Ureña, N., Correa-Vázquez, J.F., Reyes, J.C., Gauthier, B.R. and García-Domínguez, M. (2022). SENP7 overexpression protects cancer cells from oxygen and glucose deprivation and associates with poor prognosis in colon cancer. Genes Dis. 9(6), pp.1419-1422.

Gareau, J.R. and Lima, C.D. (2010). The SUMO pathway: emerging mechanisms that shape specificity, conjugation and recognition. Nat Rev Mol Cell Biol. 11(12), pp.861-871.

Gerhart-Hines, Z., Rodgers, J.T., Bare, O., Lerin, C., Kim, S.H., Mostoslavsky, R., Alt, F.W., Wu, Z. and Puigserver, P. (2007). Metabolic control of muscle mitochondrial function and fatty acid oxidation through SIRT1/PGC-1alpha. Embo j. 26(7), pp.1913-1923.

Gkikas, I., Palikaras, K. and Tavernarakis, N. (2018). The Role of Mitophagy in Innate Immunity. Front Immunol. 9, p1283.

Goonewardene, T.I., Sowter, H.M. and Harris, A.L. (2002). Hypoxia-induced pathways in breast cancer. Microsc Res Tech. 59(1), pp.41-48.

Graham, F.L., Smiley, J., Russell, W.C. and Nairn, R. (1977). Characteristics of a Human Cell Line Transformed by DNA from Human Adenovirus Type 5. Journal of General Virology. 36(1), pp.59-72.

Griffith, F. (1928). The Significance of Pneumococcal Types. Journal of Hygiene. 27(2), pp.113-159.

Gu, J., Fan, Y., Liu, X., Zhou, L., Cheng, J., Cai, R. and Xue, S. (2014). SENP1 protects against myocardial ischaemia/reperfusion injury via a HIF1alpha-dependent pathway. Cardiovasc Res. 104(1), pp.83-92.

Guo, C. and Henley, J.M. (2014). Wrestling with stress: roles of protein SUMOylation and deSUMOylation in cell stress response. IUBMB Life. 66(2), pp.71-77.

Guo, C., Hildick, K.L., Luo, J., Dearden, L., Wilkinson, K.A. and Henley, J.M. (2013). SENP3-mediated deSUMOylation of dynamin-related protein 1 promotes cell death following ischaemia. Embo j. 32(11), pp.1514-1528.

Gutierrez, M.G., Munafó, D.B., Berón, W. and Colombo, M.a.I. (2004). Rab7 is required for the normal progression of the autophagic pathway in mammalian cells. Journal of Cell Science. 117(13), pp.2687-2697.

Hamasaki, M., Furuta, N., Matsuda, A., Nezu, A., Yamamoto, A., Fujita, N., Oomori, H., Noda, T., Haraguchi, T., Hiraoka, Y., Amano, A. and Yoshimori, T. (2013). Autophagosomes form at ER–mitochondria contact sites. Nature. 495(7441), pp.389-393.

Hammond, S.M., Bernstein, E., Beach, D. and Hannon, G.J. (2000). An RNA-directed nuclease mediates post-transcriptional gene silencing in Drosophila cells. Nature. 404(6775), pp.293-296.

Han, Z.J., Feng, Y.H., Gu, B.H., Li, Y.M. and Chen, H. (2018). The post-translational modification, SUMOylation, and cancer (Review). Int J Oncol. 52(4), pp.1081-1094.

Hanahan, D., Christofori, G., Naik, P. and Arbeit, J. (1996). Transgenic mouse models of tumour angiogenesis: the angiogenic switch, its molecular controls, and prospects for preclinical therapeutic models. Eur J Cancer. 32a(14), pp.2386-2393.

Hanna, R.A., Quinsay, M.N., Orogo, A.M., Giang, K., Rikka, S. and Gustafsson, A.B. (2012). Microtubule-associated protein 1 light chain 3 (LC3) interacts with Bnip3 protein to selectively remove endoplasmic reticulum and mitochondria via autophagy. J Biol Chem. 287(23), pp.19094-19104.

He, J., Cheng, J. and Wang, T. (2020). SUMOylation-Mediated Response to Mitochondrial Stress. Int J Mol Sci. 21(16).

Hendriks, I.A., Lyon, D., Su, D., Skotte, N.H., Daniel, J.A., Jensen, L.J. and Nielsen, M.L. (2018). Site-specific characterization of endogenous SUMOylation across species and organs. Nature Communications. 9(1), p2456.

Hickey, C.M., Wilson, N.R. and Hochstrasser, M. (2012). Function and regulation of SUMO proteases. Nat Rev Mol Cell Biol. 13(12), pp.755-766.

Hirsilä, M., Koivunen, P., Günzler, V., Kivirikko, K.I. and Myllyharju, J. (2003). Characterization of the human prolyl 4-hydroxylases that modify the hypoxia-inducible factor. J Biol Chem. 278(33), pp.30772-30780.

Holmquist-Mengelbier, L., Fredlund, E., Löfstedt, T., Noguera, R., Navarro, S., Nilsson, H., Pietras, A., Vallon-Christersson, J., Borg, A., Gradin, K., Poellinger, L. and Påhlman, S. (2006). Recruitment of HIF-1alpha and HIF-2alpha to common target genes is differentially regulated in neuroblastoma: HIF-2alpha promotes an aggressive phenotype. Cancer Cell. 10(5), pp.413-423.

Huang, C., Han, Y., Wang, Y., Sun, X., Yan, S., Yeh, E.T., Chen, Y., Cang, H., Li, H., Shi, G., Cheng, J., Tang, X. and Yi, J. (2009). SENP3 is responsible for HIF-1 transactivation under mild oxidative stress via p300 de-SUMOylation. Embo j. 28(18), pp.2748-2762.

Huynh, D.T.N. and Heo, K.-S. (2021). Role of mitochondrial dynamics and mitophagy of vascular smooth muscle cell proliferation and migration in progression of atherosclerosis. Archives of Pharmacal Research. 44(12), pp.1051-1061.

ibidi. ibiTreat (Tissue Culture-Treated) Surface: Excellent Cell Adhesion. [online]. [Viewed Feb 6 2023]. Available from: https://ibidi.com/content/748-ibitreat-tissue-culture-treated-surface

Ihenacho, U.K., Meacham, K.A., Harwig, M.C., Widlansky, M.E. and Hill, R.B. (2021). Mitochondrial Fission Protein 1: Emerging Roles in Organellar Form and Function in Health and Disease. Frontiers in Endocrinology. 12.

Illingworth, C.J., Loenarz, C., Schofield, C.J. and Domene, C. (2010). Chemical basis for the selectivity of the von Hippel Lindau tumor suppressor pVHL for prolyl-hydroxylated HIF-1alpha. Biochemistry. 49(32), pp.6936-6944.

Itakura, E., Kishi-Itakura, C. and Mizushima, N. (2012). The hairpin-type tail-anchored SNARE syntaxin 17 targets to autophagosomes for fusion with endosomes/lysosomes. Cell. 151(6), pp.1256-1269.

Ivan, M., Kondo, K., Yang, H., Kim, W., Valiando, J., Ohh, M., Salic, A., Asara, J.M., Lane, W.S. and Kaelin, W.G., Jr. (2001). HIFalpha targeted for VHL-mediated destruction by proline hydroxylation: implications for O2 sensing. Science. 292(5516), pp.464-468.

Jäger, S., Bucci, C., Tanida, I., Ueno, T., Kominami, E., Saftig, P. and Eskelinen, E.-L. (2004). Role for Rab7 in maturation of late autophagic vacuoles. Journal of Cell Science. 117(20), pp.4837-4848.

Jimenez-Orgaz, A., Kvainickas, A., Nägele, H., Denner, J., Eimer, S., Dengjel, J. and Steinberg, F. (2018). Control of RAB7 activity and localization through the retromer-TBC1D5 complex enables RAB7-dependent mitophagy. Embo j. 37(2), pp.235-254.

Johnson, E.S., Schwienhorst, I., Dohmen, R.J. and Blobel, G. (1997). The ubiquitin-like protein Smt3p is activated for conjugation to other proteins by an Aos1p/Uba2p heterodimer. Embo j. 16(18), pp.5509-5519.

Juncker, M., Kim, C., Reed, R., Haas, A., Schwartzenburg, J. and Desai, S. (2021). ISG15 attenuates post-translational modifications of mitofusins and congression of damaged mitochondria in Ataxia Telangiectasia cells. Biochim Biophys Acta Mol Basis Dis. 1867(6), p166102.

Kakimoto, Y., Tashiro, S., Kojima, R., Morozumi, Y., Endo, T. and Tamura, Y. (2018). Visualizing multiple inter-organelle contact sites using the organelle-targeted split-GFP system. Sci Rep. 8(1), p6175.

Kang, R., Zeh, H.J., Lotze, M.T. and Tang, D. (2011). The Beclin 1 network regulates autophagy and apoptosis. Cell Death Differ. 18(4), pp.571-580.

Kawahara, M. and Kuroda, Y. (2000). Molecular mechanism of neurodegeneration induced by Alzheimer's beta-amyloid protein: channel formation and disruption of calcium homeostasis. Brain Res Bull. 53(4), pp.389-397.

Keith, B., Johnson, R.S. and Simon, M.C. (2011). HIF1alpha and HIF2alpha: sibling rivalry in hypoxic tumour growth and progression. Nat Rev Cancer. 12(1), pp.9-22.

Kelly, B.D., Hackett, S.F., Hirota, K., Oshima, Y., Cai, Z., Berg-Dixon, S., Rowan, A., Yan, Z., Campochiaro, P.A. and Semenza, G.L. (2003). Cell type-specific regulation of angiogenic growth factor gene expression and induction of angiogenesis in nonischemic tissue by a constitutively active form of hypoxia-inducible factor 1. Circ Res. 93(11), pp.1074-1081.

Khan, S. and Davies, I.B. (2008). Hypoxia and Alzheimer disease. Cmaj. Canada. pp.1687; author reply 1687-1688.

Khattar, M., Song, K., Grossman, S., Xega, K., He, X., Idamakanti, N. and Huszar, D. (2019). Abstract 3252: TAK-981: A first in class SUMO inhibitor in Phase 1 trials that promotes dendritic cell activation, antigen-presentation, and T cell priming. Cancer Research. 79(13_Supplement), pp.3252-3252.

Kim, C., Juncker, M., Reed, R., Haas, A., Guidry, J., Matunis, M., Yang, W.C., Schwartzenburg, J. and Desai, S. (2021). SUMOylation of mitofusins: A potential mechanism for perinuclear mitochondrial congression in cells treated with mitochondrial stressors. Biochim Biophys Acta Mol Basis Dis. 1867(6), p166104.

Kim, H., Scimia, M.C., Wilkinson, D., Trelles, R.D., Wood, M.R., Bowtell, D., Dillin, A., Mercola, M. and Ronai, Z.A. (2011). Fine-tuning of Drp1/Fis1 availability by AKAP121/Siah2 regulates mitochondrial adaptation to hypoxia. Mol Cell. 44(4), pp.532-544.

Koch, A., Yoon, Y., Bonekamp, N.A., McNiven, M.A. and Schrader, M. (2005). A role for Fis1 in both mitochondrial and peroxisomal fission in mammalian cells. Mol Biol Cell. 16(11), pp.5077-5086.

Koh, M.Y. and Powis, G. (2012). Passing the baton: the HIF switch. Trends Biochem Sci. 37(9), pp.364-372.

Koshiji, M., Kageyama, Y., Pete, E.A., Horikawa, I., Barrett, J.C. and Huang, L.E. (2004). HIF-1alpha induces cell cycle arrest by functionally counteracting Myc. Embo j. 23(9), pp.1949-1956.

Koyano, F., Okatsu, K., Kosako, H., Tamura, Y., Go, E., Kimura, M., Kimura, Y., Tsuchiya, H., Yoshihara, H., Hirokawa, T., Endo, T., Fon, E.A., Trempe, J.F., Saeki, Y., Tanaka, K. and Matsuda, N. (2014). Ubiquitin is phosphorylated by PINK1 to activate parkin. Nature. 510(7503), pp.162-166.

Kukkula, A., Ojala, V.K., Mendez, L.M., Sistonen, L., Elenius, K. and Sundvall, M. (2021). Therapeutic Potential of Targeting the SUMO Pathway in Cancer. Cancers (Basel). 13(17).

Kunz, K., Wagner, K., Mendler, L., Hölper, S., Dehne, N. and Müller, S. (2016). SUMO Signaling by Hypoxic Inactivation of SUMO-Specific Isopeptidases. Cell Rep. 16(11), pp.3075-3086.

Langston, S.P., Grossman, S., England, D., Afroze, R., Bence, N., Bowman, D., Bump, N., Chau, R., Chuang, B.C., Claiborne, C., Cohen, L., Connolly, K., Duffey, M., Durvasula, N., Freeze, S., Gallery, M., Galvin, K., Gaulin, J., Gershman, R., Greenspan, P., Grieves, J., Guo, J., Gulavita, N., Hailu, S., He, X., Hoar, K., Hu, Y., Hu, Z., Ito, M., Kim, M.S., Lane, S.W., Lok, D., Lublinsky, A., Mallender, W., McIntyre, C., Minissale, J., Mizutani, H., Mizutani, M., Molchinova, N., Ono, K., Patil, A., Qian, M., Riceberg, J., Shindi, V., Sintchak, M.D., Song, K., Soucy, T., Wang, Y., Xu, H., Yang, X., Zawadzka, A., Zhang, J. and Pulukuri, S.M. (2021). Discovery of TAK-981, a First-in-Class Inhibitor of SUMO-Activating Enzyme for the Treatment of Cancer. J Med Chem. 64(5), pp.2501-2520.

Lazarou, M., Sliter, D.A., Kane, L.A., Sarraf, S.A., Wang, C., Burman, J.L., Sideris, D.P., Fogel, A.I. and Youle, R.J. (2015). The ubiquitin kinase PINK1 recruits autophagy receptors to induce mitophagy. Nature. 524(7565), pp.309-314.

Lee, B., Oh, Y., Cho, E., DiAntonio, A., Cavalli, V., Shin, J.E., Choi, H.W. and Cho, Y. (2022). FK506-binding protein-like and FK506-binding protein 8 regulate dual leucine zipper kinase degradation and neuronal responses to axon injury. J Biol Chem. 298(3), p101647.

Lemasters, J.J. (2005). Selective mitochondrial autophagy, or mitophagy, as a targeted defense against oxidative stress, mitochondrial dysfunction, and aging. Rejuvenation Res. 8(1), pp.3-5.

Levine, B. and Klionsky, D.J. (2004). Development by self-digestion: molecular mechanisms and biological functions of autophagy. Dev Cell. 6(4), pp.463-477.

Li, M.X., Qu, Y. and Mu, D.Z. (2017). [Role of mitophagy in neonatal rats with hypoxic-ischemic brain damage]. Zhongguo Dang Dai Er Ke Za Zhi. 19(2), pp.242-249.

Li, S., Hafeez, A., Noorulla, F., Geng, X., Shao, G., Ren, C., Lu, G., Zhao, H., Ding, Y. and Ji, X. (2017). Preconditioning in neuroprotection: From hypoxia to ischemia. Prog Neurobiol. 157, pp.79-91.

Liang, C., Feng, P., Ku, B., Dotan, I., Canaani, D., Oh, B.H. and Jung, J.U. (2006). Autophagic and tumour suppressor activity of a novel Beclin1-binding protein UVRAG. Nat Cell Biol. 8(7), pp.688-699.

Liang, Y.C., Lee, C.C., Yao, Y.L., Lai, C.C., Schmitz, M.L. and Yang, W.M. (2016). SUMO5, a Novel Poly-SUMO Isoform, Regulates PML Nuclear Bodies. Sci Rep. 6, p26509.

Lim, G.G. and Lim, K.L. (2017). Parkin-independent mitophagy-FKBP8 takes the stage. EMBO Rep. 18(6), pp.864-865.

Liu, D., Sun, Z., Ye, T., Li, J., Zeng, B., Zhao, Q., Wang, J. and Xing, H.R. (2021). The mitochondrial fission factor FIS1 promotes stemness of human lung cancer stem cells via mitophagy. FEBS Open Bio. 11(7), pp.1997-2007.

Liu, K., Guo, C., Lao, Y., Yang, J., Chen, F., Zhao, Y., Yang, Y. and Yi, J. (2020). A fine-tuning mechanism underlying self-control for autophagy: deSUMOylation of BECN1 by SENP3. Autophagy. 16(6), pp.975-990.

Liu, L., Feng, D., Chen, G., Chen, M., Zheng, Q., Song, P., Ma, Q., Zhu, C., Wang, R., Qi, W., Huang, L., Xue, P., Li, B., Wang, X., Jin, H., Wang, J., Yang, F., Liu, P., Zhu, Y., Sui, S. and Chen, Q. (2012). Mitochondrial outer-membrane protein FUNDC1 mediates hypoxia-induced mitophagy in mammalian cells. Nat Cell Biol. 14(2), pp.177-185.

Liu, W.J., Ye, L., Huang, W.F., Guo, L.J., Xu, Z.G., Wu, H.L., Yang, C. and Liu, H.F. (2016). p62 links the autophagy pathway and the ubiqutin-proteasome system upon ubiquitinated protein degradation. Cell Mol Biol Lett. 21, p29.

Liu, Y.J., McIntyre, R.L., Janssens, G.E. and Houtkooper, R.H. (2020). Mitochondrial fission and fusion: A dynamic role in aging and potential target for age-related disease. Mechanisms of Ageing and Development. 186, p111212.

Lizama, B.N. and Chu, C.T. (2021). Neuronal autophagy and mitophagy in Parkinson's disease. Mol Aspects Med. 82, p100972.

Loboda, A., Jozkowicz, A. and Dulak, J. (2010). HIF-1 and HIF-2 transcription factors — Similar but not identical. Molecules and Cells. 29(5), pp.435-442.

Loftus, L.T., Gala, R., Yang, T., Jessick, V.J., Ashley, M.D., Ordonez, A.N., Thompson, S.J., Simon, R.P. and Meller, R. (2009). Sumo-2/3-ylation following in vitro modeled ischemia is reduced in delayed ischemic tolerance. Brain Res. 1272, pp.71-80.

Losón, O.C., Song, Z., Chen, H. and Chan, D.C. (2013). Fis1, Mff, MiD49, and MiD51 mediate Drp1 recruitment in mitochondrial fission. Mol Biol Cell. 24(5), pp.659-667.

Lutz, P.L. and Prentice, H.M. (2002). Sensing and Responding to Hypoxia, Molecular and Physiological Mechanisms1. Integrative and Comparative Biology. 42(3), pp.463-468.

Ma, K., Chen, G., Li, W., Kepp, O., Zhu, Y. and Chen, Q. (2020). Mitophagy, Mitochondrial Homeostasis, and Cell Fate. Frontiers in Cell and Developmental Biology. 8.

Madhu, V., Boneski, P.K., Silagi, E., Qiu, Y., Kurland, I., Guntur, A.R., Shapiro, I.M. and Risbud, M.V. (2020). Hypoxic Regulation of Mitochondrial Metabolism and Mitophagy in Nucleus Pulposus Cells Is Dependent on HIF-1α-BNIP3 Axis. J Bone Miner Res. 35(8), pp.1504-1524.

Mahajan, R., Gerace, L. and Melchior, F. (1998). Molecular characterization of the SUMO-1 modification of RanGAP1 and its role in nuclear envelope association. J Cell Biol. 140(2), pp.259-270.

Majmundar, A.J., Wong, W.J. and Simon, M.C. (2010). Hypoxia-inducible factors and the response to hypoxic stress. Mol Cell. 40(2), pp.294-309.

Malka, F., Guillery, O., Cifuentes-Diaz, C., Guillou, E., Belenguer, P., Lombès, A. and Rojo, M. (2005). Separate fusion of outer and inner mitochondrial membranes. EMBO Rep. 6(9), pp.853-859.

Man, N., Chen, Y., Zheng, F., Zhou, W. and Wen, L.-P. (2010). Induction of genuine autophagy by cationic lipids in mammalian cells. Autophagy. 6(4), pp.449-454.

Manalo, D.J., Rowan, A., Lavoie, T., Natarajan, L., Kelly, B.D., Ye, S.Q., Garcia, J.G. and Semenza, G.L. (2005). Transcriptional regulation of vascular endothelial cell responses to hypoxia by HIF-1. Blood. 105(2), pp.659-669.

Mao, K., Wang, K., Liu, X. and Klionsky, D.J. (2013). The scaffold protein Atg11 recruits fission machinery to drive selective mitochondria degradation by autophagy. Dev Cell. 26(1), pp.9-18.

Maruyama, T., Abe, Y. and Niikura, T. (2018). SENP1 and SENP2 regulate SUMOylation of amyloid precursor protein. Heliyon. 4(4), pe00601.

Matsuda, N., Sato, S., Shiba, K., Okatsu, K., Saisho, K., Gautier, C.A., Sou, Y.S., Saiki, S., Kawajiri, S., Sato, F., Kimura, M., Komatsu, M., Hattori, N. and Tanaka, K. (2010). PINK1 stabilized by mitochondrial depolarization recruits Parkin to damaged mitochondria and activates latent Parkin for mitophagy. J Cell Biol. 189(2), pp.211-221.

Matsunaga, K., Morita, E., Saitoh, T., Akira, S., Ktistakis, N.T., Izumi, T., Noda, T. and Yoshimori, T. (2010). Autophagy requires endoplasmic reticulum targeting of the PI3-kinase complex via Atg14L. J Cell Biol. 190(4), pp.511-521.

Mayfield, K.P., Hong, E.J., Carney, K.M. and D'Alecy, L.G. (1994). Potential adaptations to acute hypoxia: Hct, stress proteins, and set point for temperature regulation. Am J Physiol. 266(5 Pt 2), pp.R1615-1622.

Mazure, N.M. and Pouysségur, J. (2010). Hypoxia-induced autophagy: cell death or cell survival? Curr Opin Cell Biol. 22(2), pp.177-180.

Mendoza, H.M., Shen, L.N., Botting, C., Lewis, A., Chen, J., Ink, B. and Hay, R.T. (2003). NEDP1, a highly conserved cysteine protease that deNEDDylates Cullins. J Biol Chem. 278(28), pp.25637-25643.

Mizushima, N. (2005). The pleiotropic role of autophagy: from protein metabolism to bactericide. Cell Death Differ. 12 Suppl 2, pp.1535-1541.

Mizushima, N. (2007). Autophagy: process and function. Genes Dev. 21(22), pp.2861-2873.

Mizushima, N. and Yoshimori, T. (2007). How to interpret LC3 immunoblotting. Autophagy. 3(6), pp.542-545.

Moscat, J., Diaz-Meco, M.T., Albert, A. and Campuzano, S. (2006). Cell signaling and function organized by PB1 domain interactions. Mol Cell. 23(5), pp.631-640.

Mozdy, A.D., McCaffery, J.M. and Shaw, J.M. (2000). Dnm1p GTPase-mediated mitochondrial fission is a multi-step process requiring the novel integral membrane component Fis1p. J Cell Biol. 151(2), pp.367-380.

Mukhopadhyay, D. and Dasso, M. (2007). Modification in reverse: the SUMO proteases. Trends Biochem Sci. 32(6), pp.286-295.

Muz, B., de la Puente, P., Azab, F. and Azab, A.K. (2015). The role of hypoxia in cancer progression, angiogenesis, metastasis, and resistance to therapy. Hypoxia (Auckl). 3, pp.83-92.

Müller, S., Hoege, C., Pyrowolakis, G. and Jentsch, S. (2001). SUMO, ubiquitin's mysterious cousin. Nat Rev Mol Cell Biol. 2(3), pp.202-210.

Nakagawa, T., Shirane, M., Iemura, S., Natsume, T. and Nakayama, K.I. (2007). Anchoring of the 26S proteasome to the organellar membrane by FKBP38. Genes Cells. 12(6), pp.709-719.

Nakamura, A., Grossman, S., Song, K., Idamakanti, N., Shapiro, G. and Huszar, D. (2019). Abstract 1523: Inhibition of SUMOylation by TAK-981 induces antitumor innate immune

responses by modulating macrophage and NK cell function through Type I IFN pathway activation. Cancer Research. 79(13_Supplement), pp.1523-1523.

Nakamura, A., Song, K., Grossman, S., Xega, K., Zhang, Y., Berger, A., Shapiro, G. and Huszar, D. (2020). 552 SUMOylation inhibitor TAK-981 activates NK cells and macrophages via Type I interferon signaling and shows synergistic activity in combination with rituximab and daratumumab in preclinical models. Journal for ImmunoTherapy of Cancer. 8(Suppl 3), pp.A334-A335.

Narendra, D., Tanaka, A., Suen, D.F. and Youle, R.J. (2008). Parkin is recruited selectively to impaired mitochondria and promotes their autophagy. J Cell Biol. 183(5), pp.795-803.

Navarrete-Opazo, A. and Mitchell, G.S. (2014). Therapeutic potential of intermittent hypoxia: a matter of dose. Am J Physiol Regul Integr Comp Physiol. 307(10), pp.R1181-1197.

Onoue, K., Jofuku, A., Ban-Ishihara, R., Ishihara, T., Maeda, M., Koshiba, T., Itoh, T., Fukuda, M., Otera, H., Oka, T., Takano, H., Mizushima, N., Mihara, K. and Ishihara, N. (2013). Fis1 acts as a mitochondrial recruitment factor for TBC1D15 that is involved in regulation of mitochondrial morphology. J Cell Sci. 126(Pt 1), pp.176-185.

Owerbach, D., McKay, E.M., Yeh, E.T., Gabbay, K.H. and Bohren, K.M. (2005). A proline-90 residue unique to SUMO-4 prevents maturation and sumoylation. Biochem Biophys Res Commun. 337(2), pp.517-520.

Palikaras, K., Lionaki, E. and Tavernarakis, N. (2015). Balancing mitochondrial biogenesis and mitophagy to maintain energy metabolism homeostasis. Cell Death Differ. England. pp.1399-1401.

Palikaras, K. and Tavernarakis, N. (2012). Mitophagy in neurodegeneration and aging. Front Genet. 3, p297.

Pan, Y., Mansfield, K.D., Bertozzi, C.C., Rudenko, V., Chan, D.A., Giaccia, A.J. and Simon, M.C. (2007). Multiple factors affecting cellular redox status and energy metabolism modulate

hypoxia-inducible factor prolyl hydroxylase activity in vivo and in vitro. Mol Cell Biol. 27(3), pp.912-925.

Pankiv, S., Clausen, T.H., Lamark, T., Brech, A., Bruun, J.A., Outzen, H., Overvatn, A., Bjorkoy, G. and Johansen, T. (2007). p62/SQSTM1 binds directly to Atg8/LC3 to facilitate degradation of ubiquitinated protein aggregates by autophagy. J Biol Chem. 282(33), pp.24131-24145.

Patel, S.A. and Simon, M.C. (2008). Biology of hypoxia-inducible factor-2alpha in development and disease. Cell Death Differ. 15(4), pp.628-634.

Pichler, A., Fatouros, C., Lee, H. and Eisenhardt, N. (2017). SUMO conjugation - a mechanistic view. Biomol Concepts. 8(1), pp.13-36.

Porath, J., Carlsson, J., Olsson, I. and Belfrage, G. (1975). Metal chelate affinity chromatography, a new approach to protein fractionation. Nature. 258(5536), pp.598-599.

Porath, J. and Olin, B. (1983). Immobilized metal ion affinity adsorption and immobilized metal ion affinity chromatography of biomaterials. Serum protein affinities for gel-immobilized iron and nickel ions. Biochemistry. 22(7), pp.1621-1630.

Princz, A., Pelisch, F. and Tavernarakis, N. (2020). SUMO promotes longevity and maintains mitochondrial homeostasis during ageing in Caenorhabditis elegans. Sci Rep. 10(1), p15513.

Princz, A. and Tavernarakis, N. (2020). SUMOylation in Neurodegenerative Diseases. Gerontology. 66(2), pp.122-130.

Pursiheimo, J.P., Rantanen, K., Heikkinen, P.T., Johansen, T. and Jaakkola, P.M. (2009). Hypoxia-activated autophagy accelerates degradation of SQSTM1/p62. Oncogene. 28(3), pp.334-344.

Ratcliffe, P.J. (2007). HIF-1 and HIF-2: working alone or together in hypoxia? J Clin Invest. 117(4), pp.862-865.

Reddy, P.H., Yin, X., Manczak, M., Kumar, S., Pradeepkiran, J.A., Vijayan, M. and Reddy, A.P. (2018). Mutant APP and amyloid beta-induced defective autophagy, mitophagy, mitochondrial structural and functional changes and synaptic damage in hippocampal neurons from Alzheimer's disease. Hum Mol Genet. 27(14), pp.2502-2516.

Rizzuto, R., Pinton, P., Carrington, W., Fay, F.S., Fogarty, K.E., Lifshitz, L.M., Tuft, R.A. and Pozzan, T. (1998). Close contacts with the endoplasmic reticulum as determinants of mitochondrial Ca2+ responses. Science. 280(5370), pp.1763-1766.

Rojansky, R., Cha, M.Y. and Chan, D.C. (2016). Elimination of paternal mitochondria in mouse embryos occurs through autophagic degradation dependent on PARKIN and MUL1. Elife. 5.

Rott, R., Szargel, R., Shani, V., Hamza, H., Savyon, M., Abd Elghani, F., Bandopadhyay, R. and Engelender, S. (2017). SUMOylation and ubiquitination reciprocally regulate α-synuclein degradation and pathological aggregation. Proc Natl Acad Sci U S A. 114(50), pp.13176-13181.

Rouschop, K.M., van den Beucken, T., Dubois, L., Niessen, H., Bussink, J., Savelkouls, K., Keulers, T., Mujcic, H., Landuyt, W., Voncken, J.W., Lambin, P., van der Kogel, A.J., Koritzinsky, M. and Wouters, B.G. (2010). The unfolded protein response protects human tumor cells during hypoxia through regulation of the autophagy genes MAP1LC3B and ATG5. J Clin Invest. 120(1), pp.127-141.

Runwal, G., Stamatakou, E., Siddiqi, F.H., Puri, C., Zhu, Y. and Rubinsztein, D.C. (2019). LC3-positive structures are prominent in autophagy-deficient cells. Scientific Reports. 9(1), p10147.

Rusiñol, A.E., Cui, Z., Chen, M.H. and Vance, J.E. (1994). A unique mitochondria-associated membrane fraction from rat liver has a high capacity for lipid synthesis and contains pre-

Golgi secretory proteins including nascent lipoproteins. J Biol Chem. 269(44), pp.27494-27502.

Saitoh, H. and Hinchey, J. (2000). Functional Heterogeneity of Small Ubiquitin-related Protein Modifiers SUMO-1 versus SUMO-2/3*. Journal of Biological Chemistry. 275(9), pp.6252-6258.

Sakai, S., Watanabe, S., Komine, O., Sobue, A. and Yamanaka, K. (2021). Novel reporters of mitochondria-associated membranes (MAM), MAMtrackers, demonstrate MAM disruption as a common pathological feature in amyotrophic lateral sclerosis. Faseb j. 35(7), pe21688.

Scherer, W.F., Syverton, J.T. and Gey, G.O. (1953). Studies on the propagation in vitro of poliomyelitis viruses. IV. Viral multiplication in a stable strain of human malignant epithelial cells (strain HeLa) derived from an epidermoid carcinoma of the cervix. J Exp Med. 97(5), pp.695-710.

Schulz, S., Chachami, G., Kozaczkiewicz, L., Winter, U., Stankovic-Valentin, N., Haas, P., Hofmann, K., Urlaub, H., Ovaa, H., Wittbrodt, J., Meulmeester, E. and Melchior, F. (2012). Ubiquitin-specific protease-like 1 (USPL1) is a SUMO isopeptidase with essential, non-catalytic functions. EMBO Rep. 13(10), pp.930-938.

Scorrano, L. (2013). Keeping mitochondria in shape: a matter of life and death. European Journal of Clinical Investigation. 43(8), pp.886-893.

Sebastián, D. and Zorzano, A. (2018). Mitochondrial dynamics and metabolic homeostasis. Current Opinion in Physiology. 3, pp.34-40.

Semenza, G.L. (2000). Hypoxia, clonal selection, and the role of HIF-1 in tumor progression. Crit Rev Biochem Mol Biol. 35(2), pp.71-103.

Semenza, G.L. (2010). Vascular responses to hypoxia and ischemia. Arterioscler Thromb Vasc Biol. 30(4), pp.648-652.

Semenza, G.L., Roth, P.H., Fang, H.M. and Wang, G.L. (1994). Transcriptional regulation of genes encoding glycolytic enzymes by hypoxia-inducible factor 1. J Biol Chem. 269(38), pp.23757-23763.

Shadel, G.S. and Horvath, T.L. (2015). Mitochondrial ROS signaling in organismal homeostasis. Cell. 163(3), pp.560-569.

Shao, R., Zhang, F.P., Tian, F., Anders Friberg, P., Wang, X., Sjöland, H. and Billig, H. (2004). Increase of SUMO-1 expression in response to hypoxia: direct interaction with HIF-1alpha in adult mouse brain and heart in vivo. FEBS Lett. England. pp.293-300.

Sharma, P., Yamada, S., Lualdi, M., Dasso, M. and Kuehn, M.R. (2013). Senp1 is essential for desumoylating Sumo1-modified proteins but dispensable for Sumo2 and Sumo3 deconjugation in the mouse embryo. Cell Rep. 3(5), pp.1640-1650.

Shen, Q., Yamano, K., Head, B.P., Kawajiri, S., Cheung, J.T., Wang, C., Cho, J.H., Hattori, N., Youle, R.J. and van der Bliek, A.M. (2014). Mutations in Fis1 disrupt orderly disposal of defective mitochondria. Mol Biol Cell. 25(1), pp.145-159.

Shin, E.J., Shin, H.M., Nam, E., Kim, W.S., Kim, J.H., Oh, B.H. and Yun, Y. (2012). DeSUMOylating isopeptidase: a second class of SUMO protease. EMBO Rep. 13(4), pp.339-346.

Shiota, T., Traven, A. and Lithgow, T. (2015). Mitochondrial biogenesis: cell-cycle-dependent investment in making mitochondria. Curr Biol. 25(2), pp.R78-r80.

Shirane, M. and Nakayama, K.I. (2003). Inherent calcineurin inhibitor FKBP38 targets Bcl-2 to mitochondria and inhibits apoptosis. Nat Cell Biol. 5(1), pp.28-37.

Silveirinha, V., Stephens, G.J. and Cimarosti, H. (2013). Molecular targets underlying SUMO-mediated neuroprotection in brain ischemia. J Neurochem. 127(5), pp.580-591.

Skuli, N., Liu, L., Runge, A., Wang, T., Yuan, L., Patel, S., Iruela-Arispe, L., Simon, M.C. and Keith, B. (2009). Endothelial deletion of hypoxia-inducible factor-2alpha (HIF-2alpha) alters vascular function and tumor angiogenesis. Blood. 114(2), pp.469-477.

Solaini, G., Baracca, A., Lenaz, G. and Sgarbi, G. (2010). Hypoxia and mitochondrial oxidative metabolism. Biochimica et Biophysica Acta (BBA) - Bioenergetics. 1797(6), pp.1171-1177.

Song, Z., Ghochani, M., McCaffery, J.M., Frey, T.G. and Chan, D.C. (2009). Mitofusins and OPA1 mediate sequential steps in mitochondrial membrane fusion. Mol Biol Cell. 20(15), pp.3525-3532.

Sugo, M., Kimura, H., Arasaki, K., Amemiya, T., Hirota, N., Dohmae, N., Imai, Y., Inoshita, T., Shiba-Fukushima, K., Hattori, N., Cheng, J., Fujimoto, T., Wakana, Y., Inoue, H. and Tagaya, M. (2018). Syntaxin 17 regulates the localization and function of PGAM5 in mitochondrial division and mitophagy. Embo j. 37(21).

Sun, X., He, G., Qing, H., Zhou, W., Dobie, F., Cai, F., Staufenbiel, M., Huang, L.E. and Song, W. (2006). Hypoxia facilitates Alzheimer's disease pathogenesis by up-regulating BACE1 gene expression. Proc Natl Acad Sci U S A. 103(49), pp.18727-18732.

Takáts, S., Nagy, P., Varga, Á., Pircs, K., Kárpáti, M., Varga, K., Kovács, A.L., Hegedűs, K. and Juhász, G. (2013). Autophagosomal Syntaxin17-dependent lysosomal degradation maintains neuronal function in Drosophila. J Cell Biol. 201(4), pp.531-539.

Tang, N., Wang, L., Esko, J., Giordano, F.J., Huang, Y., Gerber, H.P., Ferrara, N. and Johnson, R.S. (2004). Loss of HIF-1alpha in endothelial cells disrupts a hypoxia-driven VEGF autocrine loop necessary for tumorigenesis. Cancer Cell. 6(5), pp.485-495.

Tang, S., Huang, G., Tong, X., Xu, L., Cai, R., Li, J., Zhou, X., Song, S., Huang, C. and Cheng, J. (2013). Role of SUMO-Specific Protease 2 in Reprogramming Cellular Glucose Metabolism. PLOS ONE. 8(5), pe63965.

Tanida, I., Ueno, T. and Kominami, E. (2004). LC3 conjugation system in mammalian autophagy. Int J Biochem Cell Biol. 36(12), pp.2503-2518.

Tanida, I., Ueno, T. and Kominami, E. (2008). LC3 and Autophagy. Methods Mol Biol. 445, pp.77-88.

Thomas, L.W. and Ashcroft, M. (2019). Exploring the molecular interface between hypoxia-inducible factor signalling and mitochondria. Cellular and Molecular Life Sciences. 76(9), pp.1759-1777.

Tirard, M., Hsiao, H.H., Nikolov, M., Urlaub, H., Melchior, F. and Brose, N. (2012). In vivo localization and identification of SUMOylated proteins in the brain of His6-HA-SUMO1 knock-in mice. Proc Natl Acad Sci U S A. 109(51), pp.21122-21127.

Tooze, S.A. and Yoshimori, T. (2010). The origin of the autophagosomal membrane. Nat Cell Biol. 12(9), pp.831-835.

Towbin, H., Staehelin, T. and Gordon, J. (1979). Electrophoretic transfer of proteins from polyacrylamide gels to nitrocellulose sheets: procedure and some applications. Proc Natl Acad Sci U S A. 76(9), pp.4350-4354.

Tran, M. and Reddy, P.H. (2020). Defective Autophagy and Mitophagy in Aging and Alzheimer's Disease. Front Neurosci. 14, p612757.

Tuschl, T., Zamore, P.D., Lehmann, R., Bartel, D.P. and Sharp, P.A. (1999). Targeted mRNA degradation by double-stranded RNA in vitro. Genes Dev. 13(24), pp.3191-3197.

Twig, G., Elorza, A., Molina, A.J., Mohamed, H., Wikstrom, J.D., Walzer, G., Stiles, L., Haigh, S.E., Katz, S., Las, G., Alroy, J., Wu, M., Py, B.F., Yuan, J., Deeney, J.T., Corkey, B.E. and Shirihai, O.S. (2008). Fission and selective fusion govern mitochondrial segregation and elimination by autophagy. Embo j. 27(2), pp.433-446.

Ulrich, H.D. (2007). SUMO Teams up with Ubiquitin to Manage Hypoxia. Cell. 131(3), pp.446-447.

Vaibhava, V., Nagabhushana, A., Chalasani, M.L., Sudhakar, C., Kumari, A. and Swarup, G. (2012). Optineurin mediates a negative regulation of Rab8 by the GTPase-activating protein TBC1D17. J Cell Sci. 125(Pt 21), pp.5026-5039.

van Vliet, A.R., Verfaillie, T. and Agostinis, P. (2014). New functions of mitochondria associated membranes in cellular signaling. Biochim Biophys Acta. 1843(10), pp.2253-2262.

Vance, J.E. (2014). MAM (mitochondria-associated membranes) in mammalian cells: lipids and beyond. Biochim Biophys Acta. 1841(4), pp.595-609.

Vara-Perez, M., Felipe-Abrio, B. and Agostinis, P. (2019). Mitophagy in Cancer: A Tale of Adaptation. Cells. 8(5).

Varuzhanyan, G., Ladinsky, M.S., Yamashita, S.I., Abe, M., Sakimura, K., Kanki, T. and Chan, D.C. (2021). Fis1 ablation in the male germline disrupts mitochondrial morphology and mitophagy, and arrests spermatid maturation. Development. 148(16).

Vaupel, P. (2004). The role of hypoxia-induced factors in tumor progression. Oncologist. 9 Suppl 5, pp.10-17.

Vaupel, P. and Harrison, L. (2004). Tumor hypoxia: causative factors, compensatory mechanisms, and cellular response. Oncologist. 9 Suppl 5, pp.4-9.

Verges, S., Chacaroun, S., Godin-Ribuot, D. and Baillieul, S. (2015). Hypoxic Conditioning as a New Therapeutic Modality. Front Pediatr. 3, p58.

Villa, E., Marchetti, S. and Ricci, J.E. (2018). No Parkin Zone: Mitophagy without Parkin. Trends Cell Biol. 28(11), pp.882-895.

Vásquez-Trincado, C., García-Carvajal, I., Pennanen, C., Parra, V., Hill, J.A., Rothermel, B.A. and Lavandero, S. (2016). Mitochondrial dynamics, mitophagy and cardiovascular disease. J Physiol. 594(3), pp.509-525.

Wai, T. and Langer, T. (2016). Mitochondrial Dynamics and Metabolic Regulation. Trends in Endocrinology & Metabolism. 27(2), pp.105-117.

Wang, B., Xiao, X., Huang, F. and Liu, R. (2019). Syntaxin-17-Dependent Mitochondrial Dynamics is Essential for Protection Against Oxidative-Stress-Induced Apoptosis. Antioxidants (Basel). 8(11).

Wang, G.L., Jiang, B.H., Rue, E.A. and Semenza, G.L. (1995). Hypoxia-inducible factor 1 is a basic-helix-loop-helix-PAS heterodimer regulated by cellular O2 tension. Proc Natl Acad Sci U S A. 92(12), pp.5510-5514.

Wang, G.L. and Semenza, G.L. (1993). Characterization of hypoxia-inducible factor 1 and regulation of DNA binding activity by hypoxia. J Biol Chem. 268(29), pp.21513-21518.

Wang, Y., Yang, J., Yang, K., Cang, H., Huang, X.Z., Li, H. and Yi, J. (2012). The biphasic redox sensing of SENP3 accounts for the HIF-1 transcriptional activity shift by oxidative stress. Acta Pharmacol Sin. 33(7), pp.953-963.

Waters, E., Wilkinson, K.A., Harding, A.L., Carmichael, R.E., Robinson, D., Colley, H.E. and Guo, C. (2022). The SUMO protease SENP3 regulates mitochondrial autophagy mediated by Fis1. EMBO Rep. 23(2), pe48754.

Wiener, C.M., Booth, G. and Semenza, G.L. (1996). In VivoExpression of mRNAs Encoding Hypoxia-Inducible Factor 1. Biochemical and Biophysical Research Communications. 225(2), pp.485-488.

Wiesener, M.S. and Maxwell, P.H. (2003). HIF and oxygen sensing; as important to life as the air we breathe? Ann Med. 35(3), pp.183-190.

Wilkinson, K.A. and Guo, C. (2022). Iron chelation promotes mitophagy through SENP3-mediated deSUMOylation of FIS1. Autophagy. 18(7), pp.1743-1745.

Wilson, E.L. and Metzakopian, E. (2021). ER-mitochondria contact sites in neurodegeneration: genetic screening approaches to investigate novel disease mechanisms. Cell Death & Differentiation. 28(6), pp.1804-1821.

Wu, W., Lin, C., Wu, K., Jiang, L., Wang, X., Li, W., Zhuang, H., Zhang, X., Chen, H., Li, S., Yang, Y., Lu, Y., Wang, J., Zhu, R., Zhang, L., Sui, S., Tan, N., Zhao, B., Zhang, J., Li, L. and Feng, D. (2016). FUNDC1 regulates mitochondrial dynamics at the ER–mitochondrial contact site under hypoxic conditions. The EMBO Journal. 35(13), pp.1368-1384.

Wu, W., Tian, W., Hu, Z., Chen, G., Huang, L., Li, W., Zhang, X., Xue, P., Zhou, C., Liu, L., Zhu, Y., Li, L., Zhang, L., Sui, S., Zhao, B. and Feng, D. (2014). ULK1 translocates to mitochondria and phosphorylates FUNDC1 to regulate mitophagy. EMBO Rep. 15(5), pp.566-575.

Xian, H., Yang, Q., Xiao, L., Shen, H.M. and Liou, Y.C. (2019). STX17 dynamically regulated by Fis1 induces mitophagy via hierarchical macroautophagic mechanism. Nat Commun. 10(1), p2059.

Xiao, H., Zhou, H., Zeng, G., Mao, Z., Zeng, J. and Gao, A. (2022). SUMOylation targeting mitophagy in cardiovascular diseases. J Mol Med (Berl). 100(11), pp.1511-1538.

Xicoy, H., Wieringa, B. and Martens, G.J.M. (2017). The SH-SY5Y cell line in Parkinson's disease research: a systematic review. Molecular Neurodegeneration. 12(1), p10.

Yamano, K., Fogel, A.I., Wang, C., van der Bliek, A.M. and Youle, R.J. (2014). Mitochondrial Rab GAPs govern autophagosome biogenesis during mitophagy. Elife. 3, pe01612.

Yan, S., Sun, X., Xiang, B., Cang, H., Kang, X., Chen, Y., Li, H., Shi, G., Yeh, E.T., Wang, B., Wang, X. and Yi, J. (2010). Redox regulation of the stability of the SUMO protease SENP3 via interactions with CHIP and Hsp90. Embo j. 29(22), pp.3773-3786.

Yang, M., Li, C., Yang, S., Xiao, Y., Xiong, X., Chen, W., Zhao, H., Zhang, Q., Han, Y. and Sun, L. (2020). Mitochondria-Associated ER Membranes – The Origin Site of Autophagy. Frontiers in Cell and Developmental Biology. 8.

Yang, S.L., Wu, C., Xiong, Z.F. and Fang, X. (2015). Progress on hypoxia-inducible factor-3: Its structure, gene regulation and biological function (Review). Mol Med Rep. 12(2), pp.2411-2416.

Yang, W., Sheng, H., Warner, D.S. and Paschen, W. (2008). Transient global cerebral ischemia induces a massive increase in protein sumoylation. J Cereb Blood Flow Metab. 28(2), pp.269-279.

Yang, Y.D., Li, M.M., Xu, G., Zhang, E.L., Chen, J., Sun, B., Chen, D.W. and Gao, Y.Q. (2019). Targeting mitochondria-associated membranes as a potential therapy against endothelial injury induced by hypoxia. J Cell Biochem. 120(11), pp.18967-18978.

Yang, Z., Zhao, X., Xu, J., Shang, W. and Tong, C. (2018). A novel fluorescent reporter detects plastic remodeling of mitochondria-ER contact sites. J Cell Sci. 131(1).

Yoo, S.-M., Yamashita, S.-i., Kim, H., Na, D., Lee, H., Kim, S.J., Cho, D.-H., Kanki, T. and Jung, Y.-K. (2020). FKBP8 LIRL-dependent mitochondrial fragmentation facilitates mitophagy under stress conditions. The FASEB Journal. 34(2), pp.2944-2957.

Yoo, S.M. and Jung, Y.K. (2018). A Molecular Approach to Mitophagy and Mitochondrial Dynamics. Mol Cells. 41(1), pp.18-26.

Yoshii, S.R., Kishi, C., Ishihara, N. and Mizushima, N. (2011). Parkin mediates proteasome-dependent protein degradation and rupture of the outer mitochondrial membrane. J Biol Chem. 286(22), pp.19630-19640.

Yu, R., Jin, S.B., Lendahl, U., Nistér, M. and Zhao, J. (2019). Human Fis1 regulates mitochondrial dynamics through inhibition of the fusion machinery. Embo j. 38(8).

Yuan, Y., Zheng, Y., Zhang, X., Chen, Y., Wu, X., Wu, J., Shen, Z., Jiang, L., Wang, L., Yang, W., Luo, J., Qin, Z., Hu, W. and Chen, Z. (2017). BNIP3L/NIX-mediated mitophagy protects against ischemic brain injury independent of PARK2. Autophagy. 13(10), pp.1754-1766.

Zhang, H., Bosch-Marce, M., Shimoda, L.A., Tan, Y.S., Baek, J.H., Wesley, J.B., Gonzalez, F.J. and Semenza, G.L. (2008). Mitochondrial autophagy is an HIF-1-dependent adaptive metabolic response to hypoxia. J Biol Chem. 283(16), pp.10892-10903.

Zhang, H., Gao, P., Fukuda, R., Kumar, G., Krishnamachary, B., Zeller, K.I., Dang, C.V. and Semenza, G.L. (2007). HIF-1 inhibits mitochondrial biogenesis and cellular respiration in VHL-deficient renal cell carcinoma by repression of C-MYC activity. Cancer Cell. 11(5), pp.407-420.

Zhao, J.F., Rodger, C.E., Allen, G.F.G., Weidlich, S. and Ganley, I.G. (2020). HIF1α-dependent mitophagy facilitates cardiomyoblast differentiation. Cell Stress. 4(5), pp.99-113.

Zhao, Q., Xie, Y., Zheng, Y., Jiang, S., Liu, W., Mu, W., Liu, Z., Zhao, Y., Xue, Y. and Ren, J. (2014). GPS-SUMO: a tool for the prediction of sumoylation sites and SUMO-interaction motifs. Nucleic Acids Res. 42(Web Server issue), pp.W325-330.

Zhou, D., Udpa, N., Ronen, R., Stobdan, T., Liang, J., Appenzeller, O., Zhao, Huiwen W., Yin, Y., Du, Y., Guo, L., Cao, R., Wang, Y., Jin, X., Huang, C., Jia, W., Cao, D., Guo, G., Gamboa, Jorge L., Villafuerte, F., Callacondo, D., Xue, J., Liu, S., Frazer, Kelly A., Li, Y., Bafna, V. and Haddad, Gabriel G. (2013). Whole-Genome Sequencing Uncovers the Genetic Basis of Chronic Mountain Sickness in Andean Highlanders. The American Journal of Human Genetics. 93(3), pp.452-462.

Zhou, H., Zhu, P., Wang, J., Zhu, H., Ren, J. and Chen, Y. (2018). Pathogenesis of cardiac ischemia reperfusion injury is associated with CK2α-disturbed mitochondrial homeostasis via suppression of FUNDC1-related mitophagy. Cell Death Differ. 25(6), pp.1080-1093.

Zhou, J., Li, X.Y., Liu, Y.J., Feng, J., Wu, Y., Shen, H.M. and Lu, G.D. (2022). Full-coverage regulations of autophagy by ROS: from induction to maturation. Autophagy. 18(6), pp.1240-1255.

Zunino, R., Schauss, A., Rippstein, P., Andrade-Navarro, M. and McBride, H.M. (2007). The SUMO protease SENP5 is required to maintain mitochondrial morphology and function. J Cell Sci. 120(Pt 7), pp.1178-1188.